Inauguraldissertation
zur Erlangung der Doktorwürde
der Naturwissenschaftlichen Fachbereiche
Biologie, Chemie und Geowissenschaften
im Fachbereich Biologie
der Justus-Liebig-Universität Giessen

Vorgelegt von

Yutong Song

M.Sc.-Virology

Biochemisches Institut
der Medizinischen Fakultät
der Justus-Liebig-Universität Giessen

Giessen, Januar 2006

Regulation of Hepatitis C Virus translation by the viral internal ribosome entry site and the 3´-untranslated region

Supervisors:

Prof. Dr. Albrecht Bindereif

Institute of Biochemistry
Faculty of Biology
Justus-Liebig-University-Giessen

HDoz. Dr. Michael Niepmann

Institute of Biochemistry
Faculty of Medicine
Justus-Liebig-University-Giessen

This work was accomplished from December 2001 to November 2005 under the supervision of HDoz. Dr. Michael Niepmann in the group of Prof. Dr. Ewald Beck in the Institute of Biochemistry, Faculty of Medicine, Justus-Liebig-University Giessen.

Acknowledgements

I would like to specially thank my direct supervisor HDoz. Dr. Michael Niepmann for his constant support, excellent guidance and creative discussions which were the key to my success on the study. Moreover, it is his encouragement and valuable suggestions that gave me motives and inspiration to make progress in my scientific research.

I would like to express my sincere thanks to Prof. Dr. Ewald Beck who has also invested a great effort in my work for his support and scientific supervision. Simultaneously, I am greatly indebted to Charlotte Beck for her personal care and kind support to my family.

Further I would like to thank Prof. Dr. Albrecht Bindereif for the co-supervision of this work and for his instructive advice and his great help on my study, as well as for his cooperation in the hnRNP L project.

I would like to thank my colleagues who create together such a nice atmosphere in the lab: Eleni Tzima, Christiane Jünemann, Barbara Preiss, Ralf Füllkrug, Michael Heimann, Pilar Hernández-Pastor, Dajana Henschker, Jochen Wiesner, Martin Hintz, René Röhrich, Nadine Englert, Hassan Jomaa and also other colleagues in the research groups of Prof. Dr. K. T. Preissner and Prof. Dr. R. Geyer at the Institute of Biochemistry. I express also my special thanks to my former colleagues Dr. Gergis Bassili and Amandus Zeller who were always ready to share their experiences with me, and often created an amicable occasion via their distinctive hearty spirit in our group. I have learned a lot from them at the beginning of my Ph.D. study. My sincere thanks also go to my former colleagues: Dr. Ann-Kristin Kollas, Dr. Boran Altincicek, and Frau Ursula Jost.

Also I want to thank Dr. Dieter Glebe, Dr. Michael Kann and Dr. Sandip Kanse who generously provided to me some mammalian cell lines (mentioned in section 2.1 Materials) and Silke Schreiner for the preparation of hnRNP L protein. I would like to thank my Chinese friends Jingyi Hui and Wenjun Ma for their kind help during my work.

I offer my thanks to the following academic programs that helped me to be in touch with life science, the Ph.D. Program (Graduiertenkolleg) "Biochemie von Nukleoproteinkomplexen" and the Sonderforschungs-bereich 535 (Collaborative Research Center) "Invasionsmechanismen und Replikationsstrategien von Krankheitserregern", which are founded by the Deutsche Forschungsgemeinschaft (DFG, German National Science Foundation) for the financial support.

I am forever indebted to my mother and my younger sister for providing me a sustained understanding and encouragement. Finally, I am forever grateful to my beloved wife for her love with great cordiality, her quietly unselfish support and her meticulous cares which are always with me whenever I need.

I Zusammenfassung

In dieser Arbeit wurde die Regulation der Translation des Hepatitis C Virus (HCV) durch die Interne Ribosomen-Eintrittsstelle (IRES) und die 3´-untranslatierte Region (3´-UTR) untersucht. Die 3´-UTR stimuliert die Translation, und einige bekannte zelluläre RNA-bindende Proteine wie auch ein neu entdecktes 210 kDa-Protein binden an die 3´-UTR und sind möglicherweise an der Regulation der Translation von HCV beteiligt.

HCV, der Erreger der non-A, non-B-Hepatitis (NANBH), ist einziger Vertreter des Genus *Hepacivirus* in der Familie *Flaviviridae*. HCV hat mehr als 170 Millionen Menschen infiziert. Etwa 80 % von ihnen sind nicht in der Lage, das Virus zu eliminieren, und tragen ein hohes Risiko, chronische Leberkrankheiten wie Zirrhose und Hepatozelluläres Karzinom zu entwickeln. Ein seit kurzem verfügbares Replikon-System hat die HCV-Forschung stark beschleunigt, aber es gibt noch kein Zellkultursystem, das einen kompletten Infektionszyklus von HCV erlaubt, ein Umstand, der die Untersuchung des viralen Lebenszyklus wie auch die Entwicklung von Impfstoffen und Medikamenten noch erheblich verlangsamt.

In dieser Arbeit wurde die Interaktion einiger bekannter zellulärer RNA-bindender Proteine, des Polypyrimidine Tract-Binding Protein (PTB), des heterogeneous nuclear Ribonucleoprotein L (hnRNP L) und des Proteins, das "upstream of *N-ras*" codiert wird (Unr), mit der HCV IRES und der 3´-UTR untersucht. PTB bindet nicht an die IRES, aber an die 3´-UTR. Im Gegensatz dazu bindet hnRNP L nur an die IRES. Darüber hinaus fördert hnRNP L die Bindung von PTB an die 3´-UTR, was darauf hindeutet, dass beide Proteine synergistisch an die HCV-RNA binden. Allerdings konnte nur eine sehr geringe Stimulation der HCV-Translation durch hnRNP L *in vitro* festgestellt werden. Auch rekombinantes Unr-Protein bindet an die HCV 3´-UTR, aber in den hier durchgeführten *in vitro*-Experimenten konnte kein signifikanter Effekt auf die Translation festgestellt werden.

Aufgrund etlicher widersprüchlicher Berichte über eine mögliche Funktion der HCV 3´-UTR bei der Translation wurde hier festgestellt, dass mehrere Aspekte der Struktur der Reporter-Konstrukte wichtige Parameter beim Test der Funktion der 3´-UTR sind. Die 3´-UTR stimuliert die Translation nur dann, wenn monocistronische Reporter-mRNAs mit einem präzisen, authentischen 3´-Ende der 3´-UTR verwendet werden. Diese Stimulation ist stärker in Zelllinien, die von Leberzellen abgeleitet sind, als in anderen Zelllinien. In der 3´-UTR sind die Variable Region, der poly(U/C)-Trakt und der am weitesten 3´-terminal gelegene Stem-Loop 1 der hoch-konservierten 3´-X-Region für die Stimulation wichtig, weniger aber die Stem-Loops 2 und 3. Die Signale für die Stimulation der Translation überlappen also zum Teil mit denen für die Initiation der RNA-Minusstrang-Synthese, so dass diese Sequenzen möglicherweise zusammen mit viralen und/oder zellulären Proteinen an einer Interaktion der 5´- und 3´-Enden des viralen Genoms und einer Umschaltung von der Translation zur RNA-Minusstrang-Synthese beteiligt sind.

Die Suche nach Proteinen, die an der Translations-Initiation von HCV beteiligt sind, ergab zunächst kein neues Protein, das an die HCV IRES bindet. Aufgrund des Befundes dieser Arbeit, dass die 3´-UTR die Translation stimuliert, wurde dann eine Regulation der Translation auch durch Proteine, die an die 3´-UTR binden, erwogen. Deshalb wurde das Design der Reporter-Konstrukte überdacht, mit dem Resultat, dass ein bisher unbekanntes Protein entdeckt wurde, das spezifisch an die HCV-RNA bindet. Dieses 210 kDa-Protein bindet an die Variable Region der 3´-UTR nur dann, wenn eine RNA mit einem authentischen 3´-Ende der 3´-UTR verwendet wird. Dies legt die Vermutung nahe, dass das 210 kDa-Protein möglicherweise im Zusammenhang mit der Termination der Translation an die HCV-RNA oder an das Ribosom bindet und an der Umschaltung von der Translation zur RNA-Minusstrang-Synthese beteiligt ist.

II Summary

In this study, the regulation of translation of Hepatitis C Virus (HCV) by the internal ribosome entry site (IRES) and the 3´-untranslated region (3´-UTR) was investigated. The 3´-UTR stimulates HCV IRES-directed translation, and some known cellular RNA-binding proteins as well as a newly discovered 210 kDa protein specifically binding to the 3´-UTR may be involved in HCV translation regulation.

HCV, the main causative agent of non-A, non-B hepatitis (NANBH), belongs to the unique genus *Hepacivirus* in the family *Flaviviridae*. HCV has infected more than 170 million people worldwide, about 80 % of whom are unable to eliminate the virus, and those are at high risk to develop chronic liver diseases including cirrhosis and hepatocellular carcinoma. The recent development of replicon systems has largely accelerated HCV research, but there is still no tissue culture system supporting a complete replication cycle of HCV, a circumstance that has slowed down studies on the basic understanding of the viral life cycle as well as drug and vaccine development.

The interactions of some known cellular RNA-binding proteins, including polypyrimidine tract-binding protein (PTB), heterogeneous nuclear ribonucleoprotein L (hnRNP L) and the protein encoded upstream of *N-ras* (Unr), with the HCV IRES and the 3´-UTR were examined. There is no direct interaction of PTB with the HCV IRES, but PTB binds specifically to the 3´-UTR. In contrast, hnRNP L binds to the IRES only. In addition, the binding of PTB to the 3´-UTR can be strengthened by hnRNP L, indicating that there is a synergistic interaction between PTB and hnRNP L. However, only a very slight positive effect of hnRNP L on HCV translation was observed *in vitro*. The recombinant Unr protein used in this work binds to the HCV 3´-UTR, but no significant effect of Unr on HCV translation could be observed *in vitro*.

Considering previous conflicting reports on a possible function of the HCV 3´-UTR in translation stimulation, it was found that reporter construct design is an important parameter in experiments testing 3´-UTR function. A translation enhancer function of the HCV 3´-UTR was detected only after transfection of monocistronic reporter RNAs and depends on a precise 3´-terminus of the HCV 3´-UTR. The 3´-UTR strongly stimulates HCV IRES-dependent translation in human hepatoma cell lines but only weakly in non-liver cell lines. Within the 3´-UTR the variable region, the poly(U/C)-tract and the most 3´-terminal stem-loop 1 of the highly conserved 3´-X region contribute significantly to translation enhancement, whereas the stem-loops 2 and 3 of the 3´-X region are involved only to minor extents. Thus, the signals for translation enhancement and the initiation of RNA minus-strand synthesis in the HCV 3´-UTR partially overlap, supporting the idea that these sequences along with viral and possibly also cellular factors may be involved in an RNA 3´-5´-end interaction and in a switch between translation and RNA replication.

In an initial attempt to search for *trans*-acting factors possibly involved in the translation initiation of HCV, no new protein was detected to bind to the HCV IRES. From the finding that the 3´-UTR stimulates translation, it was assumed that the translation initiation could be positively regulated by proteins binding to the 3´-UTR. This gave rise to a reconsideration of the experimental design of the HCV RNA constructs used for the search for new proteins, finally resulting in the discovery of a novel, yet unknown protein that binds to the HCV RNA. This unknown 210 kDa protein binds to the variable region of the HCV 3´-UTR only when a reporter RNA with exact 3´-terminus of 3´-UTR was used. This suggests that the protein may be involved in the regulation of translation stimulation by interacting, perhaps together with other yet undiscovered proteins, with the 3´-end of the HCV 3´-UTR, and the protein(s) may be involved in a switch from translation to negative-strand RNA synthesis in the life cycle of HCV.

III Abbreviations

A	Adenine
AA	amino acids
Amp^r	Ampicillin resistant
APS	Ammonium persulfate
ATP	Adenosine triphosphate
BCIP	5-Bromo-4-chloro-3-indolylphosphate
BDV	Borna disease virus
bp	base pairs
BSA	Bovine serum albumin
^oC	centigrade
C	Cytosine
CAT	chloramphenicol acetyltransferase
CMV	cytomegalovirus
CSFV	Classical swine fever virus
CTP	Cytosine triphosphate
d	deoxy-
dd	dideoxy-
ddH_2O	double distilled water
DMEM	Dulbecco's Modified Eagle's medium
DNA	deoxyribonucleic acid
DNase	deoxyribonuclease
dNTP	deoxynucleoside triphosphate
DTT	dithiothreitol
E. coli	*Escherichia coli*
EDTA	Ethylenediamine tetraacetic acid
EGTA	Ethylene glycol-bis(2-aminoethylether)-N,N,N´,N-tetraacetic acid
EMCV	Encephalomyocarditis virus
Et.Br	Ethidium bromide
eIF	eukaryotic initiation factor(s)
et al.	*et alii* (=and others)
FBS	Fetal bovin serum
FMDV	Foot-and-mouth disease virus
G	Guanine
GTP	guanosine triphosphate
HAV	Hepatitis A virus
HBV	Hepatitis B virus
HCV	Hepatitis C virus
HDV	Hepatitis delta virus
HEPES	4-(2-hydroxyethyl)piperazine-1-ethanesulfonic acid
His	histidine
hnRNP	Heterogeneous nuclear ribonucleoprotein
IFN	interferon
Ig	immunoglobulin
IRES	internal ribosome entry site
kb	kilobasepairs
kDa	kilodalton
µg	microgram
µl	microliter
µM	micromolar
mg	milligram
min	minute(s)
ml	milliliter

mM	mmol/l
M	mol/l
MOI	multiplicity of infection
mRNA	Messenger RNA
n	nano-
NBT	Nitro blue tetrazolium
NCR	noncoding region(s)
ng	nanogram
NMD	nonsense-mediated mRNA decay
NS	nonstructural protein
nt	nucleotide(s)
NTP	nucleoside triphosphate
NTR	non-translated region
OD	optical density
ORF	Open reading frame
p	pico-
PAA	polyacrylamide
PABP	poly(A)-binding protein
PAGE	polyacrylamide gel eletrophoresis
PBS	phosphate-buffered saline
PCR	polymerase chain reaction
PKR	dsRNA activated protein kinase
pmol	picomolar
PMSF	Phenyl-methyl-sulfonyl-fluoride
PTB	Polypyrimidine tract-binding protein
rpm	resolution per minute
RNA	ribonucleic acid
RNase	Ribonuclease
RNPs	ribonucleoproteins
RPA	RNase protection assay
RRM	RNA recognition domain
rNTP	ribonucleoside triphosphat
RT	room temperature
SDS	sodium dodecyl sulfate
T	Thymine
TCA	Trichloroacetic acid
Tris	tris-hydroxymethylaminomethane
tRNA	transfer ribinucleic acid
U	unit (Enzyme unit)
U	Uracil
Unr	Protein encoded upstream of *N-ras*
UTP	uridine triphosphate
UTR	untranslated region
UV	ultraviolet
vol	volume
v/v	volume/volume
w/v	weight/volume
w/w	weight/weight

Contents

Acknowledgements

I Zusammenfassung
II Summary
III Abbreviations

1 Introduction 1

1.1 The history of non-A, non-B hepatitis 1
1.2 The discovery of Hepatitis C Virus 2
1.3 The Family of *Flaviviridae* 3
1.4 The structure and genomic organization of HCV 4
1.5 The life cycle of Hepatitis C Virus 8
1.6 Translation of HCV RNA is mediated by internal ribosome entry 11
1.6.1 Eukaryotic translation initiation 11
1.6.2 Internal initiation of translation 15
1.6.2.1 General organization of viral IRES elements 16
1.6.2.2 The HCV internal ribosome entry site 17
1.6.2.2.1 The HCV 5´-untranslated region (5´-UTR) 17
1.6.2.2.2 Detection of an internal ribosome entry site element 18
1.6.2.2.3 Structural features of the HCV IRES 20
1.6.2.3 Only eIF2 and eIF3 are required for translation initiation of HCV RNA 20
1.6.2.4 Cellular *trans*-acting factors interacting with HCV IRES 22
1.6.3 The HCV 3´-untranslated region (3´-UTR) 24
1.7 Aims of this work 25

2 Materials and Methods 26

2.1 Materials 26
2.1.1 Bacterial strains and cell lines 26
2.1.1.1 Bacterial strains 26
2.1.1.2 Mammalian cell lines 26
2.1.2 Materials for bacterial growth and cell culture 26
2.1.2.1 Materials for bacterial growth 26
2.1.2.2 Materials for cell culture 27
2.1.3 Plasmids 27
2.1.4 Oligonucleotides 27
2.1.5 Enzymes 29
2.1.5.1 Restriction endonucleases 29

2.1.5.2 Modifying enzymes 29
2.1.6 Nucleotides 30
2.1.6.1 Radioactive nucleotides 30
2.1.6.2 Non-radioactive nucleotides 30
2.1.7 Size markers 30
2.1.7.1 Protein size markers 30
2.1.7.2 DNA size markers 31
2.1.8 Recombinant proteins 31
2.1.9 Chemicals and reagents 31
2.1.10 Kits 32
2.1.11 Cell culture flasks and pipets 32
2.1.12 Photo materials and X-ray films 32
2.1.13 Equipments 32
2.1.14 Buffers and solutions 33
2.1.14.1 Buffers for DNA and RNA gel electrophoresis 33
2.1.14.2 Buffers for protein gel electrophoresis 33
2.1.14.3 Buffers for molecular biological methods 34
2.1.14.4 Buffer for plasmid DNA preparations 34
2.1.14.5 Buffers and solutions for DNA purification with affinity columns 35
2.1.14.6 Buffers for immunological methods 35
2.1.14.7 Protein-RNA interaction buffers 36
2.1.14.8 Buffers for preparation of S10 lysate of HeLa or Huh-7 cells 36
2.1.14.9 Immunoprecipitation buffers 37
2.1.14.10 Buffers for *in vitro* translation 37
2.15.4.11 Buffers for purification of His_6-tagged proteins under native conditions (Ni-NTA) 38
2.1.14.12 Buffers for RNase Protection Assay (RPA) 38

2.2 Methods 39
2.2.1 Microbiolobical methods 39
2.2.1.1 Preparation of competent bacterial cells -- Classical $CaCl_2$ method 39
2.2.1.2 Transformation of competent cells 39
2.2.2 Molecular biological methods 39
2.2.2.1 Preparation of plasmid DNA 39
2.2.2.2 Enzymatic modifications of DNA 41
2.2.2.3 Proteinase K digestion 42
2.2.2.4 The polymerase chain reaction (PCR) 42
2.2.3 *In vitro* transcription and translation 43
2.2.3.1 Preparation of DNA templates for *in vitro* RNA transcription 43
2.2.3.2 *In vitro* transcription with T7- or SP6-RNA polymerase 43
2.2.3.3 *In vitro* transcription of radio-labelled RNA 44
2.2.3.4 *In vitro* translation 44
2.2.4 Capping and poly(A) tailing of *in vitro* transcribed RNA 45

2.2.4.1 Capping of *in vitro* transcribed RNA 45
2.2.4.2 Poly(A) tailing of *in vitro* transcribed RNA 45
2.2.5 Detection of reporter gene 46
2.2.5.1 Detection of *Firefly* luciferase (FLuc) reporter gene 46
2.2.5.2 Detection of *Renilla* luciferase (RLuc) reporter gene 47
2.2.6 RNA-protein interactions 47
2.2.6.1 UV cross-linking reaction 47
2.2.6.2 Electrophoretic mobility shift assay (EMSA) 48
2.2.7 Biochemical methods 49
2.2.7.1 Purification of recombinant proteins by Ni-NTA-His-tag-protein 49
2.2.7.2 Depletion of PTB from rabbit reticulocyte lysate (RRL) 49
2.2.7.3 Preparation of S10 cytoplasmic lysates from HeLa or Huh-7 cells 49
2.2.8 Immunological methods 50
2.2.8.1 Western blot 50
2.2.8.2 Immunoprecipitation (IP) 50
2.2.9 Gel electrophoresis 51
2.2.9.1 Agarose gel electrophoresis and recovery of DNA fragments from agarose gels 51
2.2.9.2 Denaturing polyacrylamide gel electrophoresis 51
2.2.9.3 SDS polyacrylamide gel electrophoresis (SDS-PAGE) 52
2.2.9.4 Coomassie brilliant blue staining 52
2.2.9.5 Autoradiography 52
2.2.10 Cell culture methods 52
2.2.10.1 Subculture protocol of adherent cell lines 52
2.2.10.2 Freezing protocol of mammalian cells 53
2.2.10.3 Resuscitation of frozen cells 53
2.2.11 Transfection of nucleic acids into mammalian cell cultures 53
2.2.11.1 Transfection with DNA (Lipofectamine 2000 method) 53
2.2.11.2 Transfection with RNA 53
2.2.12 Ribonuclease protection assay (RPA) 54
2.2.12.1 Synthesis of [α-^{32}P]-labelled RNA probe and purification of the probe 54
2.2.12.2 Preparation of sample RNA 55
2.2.12.3 Hybridization and RNase digestion of probe and sample RNA 55
2.2.12.4 Separation and detection of protected fragments 55

3 Results 56

3.1 Part I: The search for unknown cellular proteins which interact with the Hepatitis C Virus 5´- and 3´-untranslated region 56
3.1.1 Optimization of protein binding to the HCV IRES RNA 57
3.1.2 Analysis of the interaction of proteins from cellular lysates with the HCV IRES and its deletion mutants 59
3.1.3 The HCV RNA constructs used for the protein-searching study 62

3.1.4 Choice of the optimal radioactive-labelling ribonucleotide for the detection of proteins binding to the HCV RNA 63
3.1.5 Optimization of protein binding specificity 65
3.1.6 Detection of proteins in ammonium sulfate precipitation fractions 68
3.1.7 Conclusions 70

3.2 Part II: Synergetic interaction of known cellular proteins – PTB, hnRNP L and Unr – with the Hepatitis C Virus RNA 71
3.2.1 Interaction of polypyrimidine tract-binding protein (PTB) with HCV RNAs 71
3.2.1.1 Interaction of recombinant and cellular PTB with different HCV RNAs analyzed by UV cross-linking assay 71
3.2.1.2 Effect of PTB on HCV translation in reticulocyte lysate 73
3.2.2 Interaction of heterogeneous nuclear ribonucleoprotein L (hnRNP L) with HCV RNAs 77
3.2.2.1 Detection of the interaction of hnRNP L with different HCV RNAs by shifts and UV cross-linking assay 78
3.2.2.2 Effect of recombinant hnRNP L on HCV translation 81
3.2.3 Interaction of the protein encoded upstream of *N-ras* (Unr) with HCV RNAs 82
3.2.3.1 Interaction of recombinant Unr with different HCV RNAs by gel shift assay and UV cross-linking assay 83
3.2.3.2 Effect of recombinant Unr on HCV translation 85
3.2.4 Interaction of PTB, hnRNP L and Unr with HCV RNAs 85
3.2.4.1 Interaction of PTB, hnRNP L and Unr in concert with the HCV RNAs 86
3.2.4.1.1 PTB and hnRNP L 86
3.2.4.1.2 Unr and hnRNP L 88
3.2.4.1.3 PTB and Unr 89
3.2.4.1.4 PTB, hnRNP L and Unr 90
3.2.4.2 Effects of PTB, hnRNP L and Unr on the HCV translation 91
3.2.5 Conclusions 92

3.3 Part III: The Hepatitis C Virus RNA 3´-untranslated region strongly enhances translation directed by its internal ribosomal entry site 93
3.3.1 The reporter construct used to analyze the possible influence of the HCV 3´-UTR on translation 93
3.3.2 Optimization of *in vitro* translation conditions 94
3.3.3 Effect of the HCV 3´-UTR on IRES-mediated translation in rabbit reticulocyte lysate 96
3.3.4 Influence of reporter construct design and transfection protocol details detection of translation enhancement by the 3´-UTR 97
3.3.5 Expression differences are not due to differences in RNA stability or transfection efficiency 99
3.3.6 Additional nucleotides at the 3´ end of 3´-UTR disable stimulation 102

3.3.7 The HCV 3´-UTR enhances IRES-dependent translation preferentially in human liver-derived cell lines 103
3.3.8 Interaction of the protein encoded upstream of *N-ras* (Unr) with HCV RNAs 104
3.3.9 Conclusions 106

3.4 Part IV: An unknown protein of about 210 kDa binds to the HCV RNA only in the presence of both 5´- and 3´-UTR 107
3.4.1 Redesigning the HCV RNA constructs used for the protein research 107
3.4.2 Detection of an unknown protein binding to the HCV RNA with a precise end of the 3´-UTR 108
3.4.3 The unknown protein interacts with the variable region of the HCV 3´-UTR 112
3.4.4 Conclusions 115

4 Discussion 116

4.1 Interaction of cellular proteins with the HCV RNA untranslated regions and their effects 116
4.1.1 PTB 116
4.1.2 hnRNP L protein 119
4.1.3 Unr protein 121
4.2 The HCV 3´-UTR strongly enhances the IRES-dependent translation 122
4.3 Regulation of HCV translation by a novel, as yet unknown 210 kDa protein? 128

5 References 131

Appendices 147
pHCV wt clone map 147
Interaction of FSAP with HCV RNA 148
Publications 151

1 Introduction

Viruses (from the latin "virus", meaning "poison") are small infectious particles that consist of proteins and only one type of nucleic acids, either DNA or RNA, which is packaged in a protein capsid. In 1898, Friedrich Loeffler and Paul Frosch found that the causative agent of foot-and-mouth disease in livestock is an infectious particle smaller than any bacterium. This was the first clue to the nature of the viruses (Loeffler & Frosch, 1964). In order to replicate, viruses must infect a suitable host cell since they lack most of the internal structure and machinery which characterize "life", including the biosynthetic machinery that is necessary for reproduction. Viruses infect bacteria (then the virus is called a bacteriophage), plants, animals and humans, and they are the cause of a very wide range of human diseases like the common cold, hepatitis, AIDS, smallpox, flu, poliomyelitis, the lethal haemorrhagic disease caused by ebolaviruses, and the latest disease of severe acute respiratory syndrome (SARS) which was first recognized in March 2003 and subsequently found to be caused by a new type of coronavirus (SARS-CoV) (WHO data).

The present study focuses on the internal initiation of translation, a characteristic mechanism of translation used by Hepatitis C Virus (Family: *Flaviviridae*, Genus: *Hepacivirus*) and foot-and-mouth disease virus (Family: *Picornaviridae*) to initiate their own polyprotein synthesis. Some *cis*- and *trans*-acting factors possibly involved in the process of HCV translation were principally highlighted.

1.1 The history of non-A, non-B hepatitis

The first evidence for the existence of a non-A, non-B (NANB) hepatitis agent came from studies of multiple attacks of viral hepatitis in narcotic addicts in the 1950s (Havens, 1956). The existence of two forms of hepatitis, ‘infectious’ (type A) and ‘serum’ (type B), had been recognized in the 1940s and further reports revealed that no patient had more than one attack of either form of hepatitis. In a study of 30 episodes of acute viral hepatitis in patients, two of 30 (7 %) were found to be caused by hepatitis A, and 12 (40 %) by hepatitis B (Mosley et al., 1977). Thus there were 16 cases (53 %) not attributable to either of the two known hepatitis viruses. Exclusion of Epstein-Barr virus (EBV) and cytomegalovirus (CMV) in these patients strengthened the argument for the existence of NANB hepatitis agents.

The discovery of "Australia antigen" in 1964, by Blumberg, and its association with viral hepatitis led to detailed studies of post-transfusion hepatitis (PTH) (Blumberg, 1964). The first studies were carried out in the 1960s, prior to the screening of blood for hepatitis B surface antigen (HBsAg), when approximately 50 % of multiply transfused patients developed PTH in the USA. Most of the available blood at that time came from commercial blood donors and the equivalent rate for PTH from voluntary blood donors was much lower with one study reporting that none of 28 patients receiving volunteer blood developed hepatitis (Walsh et al., 1970). The introduction of screening and exclusion of commercial blood donors led to a dramatic fall in PTH from 30.6 cases/1000 units to 3.7 cases/1000 units of blood transfused (Alter et al., 1972). Although it was not possible to estimate the individual effects, it was generally thought that the exclusion of the commercial donor was the most significant determinant in the decrease in PTH. However, the findings that PTH had not been eradicated by these

measures, as well as evidence that the presence of "Australia" (HBsAg) antigen could not prevent PTH (Holland et al., 1969), led to the search for alternative hepatitis agents. In one study in the early 1970s the majority of cases of PTH following cardiac surgery were not caused by HBV, and could not be explained by infection with EBV or CMV viruses (Purcell et al., 1971). Another study revealed that 12 of 108 (11 %) prospectively followed multiply transfused cardiac surgery patients developed PTH, despite receiving volunteer blood tested for HBsAg (Alter et al., 1975). Four of these 12 patients developed hepatitis B virus (HBV) infection. The other eight cases of PTH were shown not to be related to HBV, hepatitis A virus (HAV), EBV or CMV, suggesting that NANB hepatitis was the major cause of PTH in this group of patients. Studies of hepatitis in drug addicts also identified a separate type of hepatitis, which was characterized by the absence of HBsAg and of high levels of immunoglobulin M (IgM), suggestive of HAV infection (Iwarson et al., 1973).

By the late 1970s, 7-10 % of blood transfusion recipients still developed hepatitis. Serological tests failed to implicate hepatitis A or B in 90 % of these patients and the term "non-A, non-B (NANB) hepatitis" was used to describe this condition. The tendency for this condition to become chronic with progression to cirrhosis was soon recognized (Realdi et al., 1982; Dienstag, 1983). Both infectious and non-infectious causes of NANB hepatitis had to be excluded and, in the late 1970s, transmission of the agent from humans to chimpanzees was reported (Alter et al., 1978; Tabor et al., 1978). The NANB agent appeared to be present at low levels in humans and led to chronic infection in about 50 % of chimpanzees, causing distinctive histological appearances in their livers. This agent was shown to be sensitive to organic solvents, and to pass through filters of 80 nm pore-size, suggesting that it was a small enveloped virus (Bradley et al., 1983; Bradley et al., 1985).

In the 1980s the exclusion of donors with abnormal liver function tests (LFTs) or with antibody to hepatitis B core antigen (HBcAb), two surrogate markers of NANB post-transfusion hepatitis, almost halved the rate of PTH. Despite the knowledge of a distinct PTH syndrome and evidence to show successful serial transmission of these agents, by the mid 1980s the agent responsible for NANB hepatitis remained frustratingly elusive.

1.2 The discovery of Hepatitis C Virus

Most of the early studies on NANB hepatitis had focused on chimpanzee transmission investigations, showing that the putative agent was present in most patients with NANB hepatitis at a low titre of 10^2-10^3 chimpanzee infectious doses per ml ($CID \cdot ml^{-1}$). The agent was known to cause the appearance of distinctive, membranous tubules within the hepatocytes of experimentally infected chimpanzees. Buoyant density studies with the tubule-forming agent suggested that it is a small enveloped RNA virus because transmission to chimpanzees could be prevented by heat, β-propiolactone, and formalin or by organic solvent inactivation of the infectious fraction (Bradley et al., 1985).

Initial studies by Choo and his colleagues at the Chiron Corporation were hampered by the inability to extract sufficiently concentrated nucleic acids from infectious material. Therefore, plasma was pooled from infected animals and, by titrating infectivity in other animals, a plasma pool was obtained with a titre of approximately 10^6 $CID \cdot ml^{-1}$. Following ultracentrifugation, total nucleic acid was extracted, rendered single-stranded and then both RNA and DNA were reverse transcribed using random primers. A cDNA expression library was created by cloning the random fragments into the vector λgt11, and this was then screened with serum derived from patients diagnosed with chronic NANB hepatitis. After screening more than a million clones, one (5-1-1) was found to react with serum from several NANB hepatitis patients and also with serum from experimentally infected

chimpanzees following the onset of hepatitis (Choo et al., 1989). Three further overlapping clones were isolated by using the 5-1-1 cDNA as a hybridization probe to screen the original library and a 1089 nucleotide continuous open-reading frame (ORF) was reconstructed. The antigen (C100-3) used in the first-generation enzyme-linked immunosorbent assay (ELISA) was prepared by expressing this ORF as a fusion polypeptide with human superoxide dismutase in yeast (Kuo et al., 1989). Most cases of NANB hepatitis were found to be associated with C100-3 antibody and this response was used to define infection with a new virus, hepatitis C virus (HCV) (Alter et al., 1989; Bruix et al., 1989; Colombo et al., 1989). Although the virus was first cloned in 1989, it was not before 1994 that there have been claims of visualization of the virus by immunoelectron microscopy (Kaito et al., 1994).

Up to date, Hepatitis C virus is the first virus detected before its viral particle is found through electron microscopy. Furthermore, the discovery of HCV is the first example achieved by way of an unprecedented use of modern molecular cloning techniques, which came to the world in the late of 1980s, rather than by the conventional method of virus isolation (Choo et al., 1989).

1.3 The Family of *Flaviviridae*

Based on the phylogenetic sequence comparisons, HCV appears to be more closely related to pestiviruses than to the flaviviruses. For instance, both HCV and pestiviruses contain a relatively long 5′-untranslated region (5′-UTR), or also called 5′-nontranslated region (5′-NTR), with several AUG codons, whereas flaviviruses contain a short 5′-UTR of about 95-132 nucleotides in length without an AUG (except tick-borne encephalitis virus) (Rice et al., 1986; Collett et al., 1988b; Pletnev et al., 1990). Like pestiviruses, HCV does not have a cap-structure at the 5′ terminus of the genomic RNA (Collett et al., 1989; Brock et al., 1992; Tsukiyama-Kohara et al., 1992). The translation of flaviviral RNAs is mediated by a cap-dependent scanning mechanism, and usually initiated at the 5′ end proximal AUG triplet (Chambers et al., 1990). In contrast to flaviviruses, multiple AUG triplets have been found in the long 5′-UTR of HCV and pestiviruses. The methyltransferase gene found in the flavivirus NS5 region has not been found in the HCV genome. Several experimental approaches have failed to detect a cap structure at the 5′ end of pestivirus genomic RNA (Collett et al., 1988b; Brock et al., 1992). By analogy to pestiviruses, it is likely that the HCV genomic RNA is uncapped. While several AUG codons are located upstream of the translation initiation site of the HCV polyprotein, they do not appear to function as alternative start sites (Tsukiyama-Kohara et al., 1992).

Genus	Number of serotypes	Members
Flavivirus	10	12(79)
Pestivirus	1	3(12)
Hepacivirus	6	1(10)

Table 1: Classification of Flaviviruses. The numbers in brackets represent the tentative strains and isolates. (Source: International Committee Taxonomy of Viruses, 2002)

In the end, on the basis of several criteria including genomic organization, molecular features, and biochemical properties, HCV has been classified as the sole member of a distinct genus called *Hepacivirus* in the family *Flaviviridae,* which includes the flaviviruses and the animal pathogenic pestiviruses (Kato et al., 1990; Choo et al., 1991; Inchauspe et al., 1991; Okamoto et al., 1991; Takamizawa et al., 1991). Table 1 shows some fundamental information on the family of *Flaviviridae*.

Flaviviral virions are spherical, 40-50 nm in diameter. They are with a lipid envelope and fine peplomers that do not show any structure or symmetry. The genome consists of a single molecule of linear, positive-sense, single-stranded RNA, 10.7 kb (flaviviruses), 12.5 kb (pestiviruses), or 9.6 kb (hepatitis C virus) in size. The pestiviruses and HCV do not have cap structure at 5′-end of RNA genome, whereas the 5′-end structure of the RNA of flaviviruses consists of a type 1 cap. A type 1 cap structure (m^7GpppA^mp) has been found at the 5′ end of flavivirus RNA (Chambers et al., 1990) which may have resulted from the action of the proposed methyltransferase activity in the flaviviral NS5 protein (Koonin & Dolja, 1993). Except for some tick-borne flaviviruses, the RNA does not contain a 3′-terminal poly (A) tail. Virons contain two or three membrane-associated proteins, a core protein, lipids derived from host cell membranes, and carbohydrates in the form of glycolipids and glycoproteins as well.

There are about 70 recognized diseases caused by members of the *Flaviviridae* family. 13 cause disease in humans, such as Yellow Fever, Dengue, and Japanese Encephalitis. Common manifestations are febrile illnesses, encephalitis, hemorraging, and hepatitis. Most of theses viruses are transmitted by mosquitoes. However, Hepatitis C is transmitted by sexual contact and blood contact like other Hepatitis B virus. It has a very narrow host range, and infects only human and chimpanzee. However, it is obviously different from the diseases of hepatitis A or hepatitis B. That is the reason why it was called non-A, non-B hepatitis (NANBH) before 1989 when Hepatitis C Virus was isolated and named. So far, HCV infects more than 170 million people worldwide and causes rising rates of liver diseases such as chronic hepatitis, liver cirrhosis and hepatocellular carcinoma. The only therapy currently available is combination treatment with a high dose of interferon-α (IFN-α) and the nucleoside analogue ribavirin. However, only ~ 40% of all patients benefit from this treatment and develop a sustained response. For this reason, HCV has become a focus of intensive research worldwide since the 1990s.

1.4 The structure and genomic organization of HCV

Morphologically, the HCV viral particle has a spherical shape which is about 40-80 nm in diameter, with fine spike-like surface projections and an inner core measuring 30 to 35 nm in diameter. It consists of an envelope derived from host membranes into which are inserted the virally encoded glycoproteins surrounding an icosahedral nucleocapsid and a single-stranded RNA genome (Fig. 1). The viral capsid gives the hepatitis C virus characteristic shape and size, and protects the infectious viral RNA from ribonucleases in the environment. Unlike picornaviruses carrying a small viral protein (virion protein genome-linked; VPg) which is attached to the 5′-end through a phosphodiester linkage, HCV does not contain such a special protein. The VPg appears to play an important role in initiation of picornaviral RNA synthesis, and it is believed that this protein is cleaved off by cellular proteinases soon after the entry into infected cell. The VPg is not essential for infectivity, since full-length *in vitro* synthesized RNA (without VPg) is still infectious. As every enveloped virus, HCV is sensitive to detergents and dehydration.

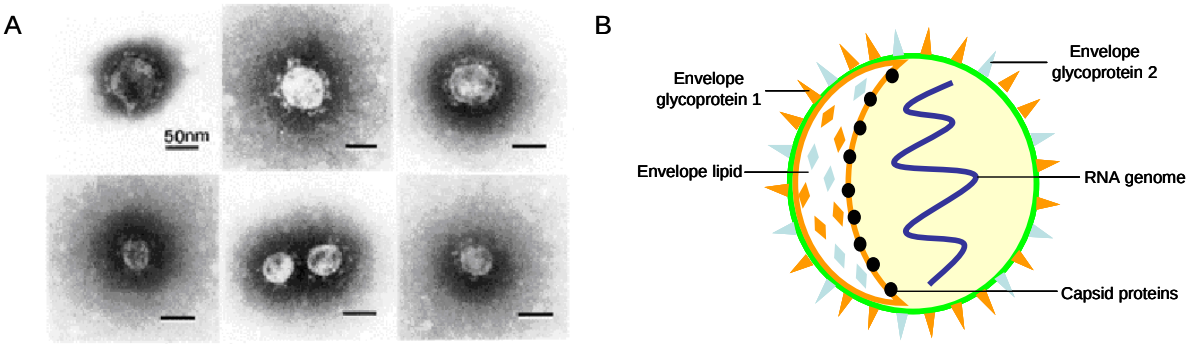

Fig. 1: Electron microscope morphology of HCV associated particles and model structure of HCV. (A) EM photos of HCV particle. Top panels: 60-70 nm virions; lower panels: 30-40 nm putative defective interfering particles. **(B)** Model structure of HCV. The left side of the illustration shows the viral surface of envelope lipids and glycoproteins; the right side shows the RNA genome encased by capsid proteins.

The viral genome of HCV is represented as a single-stranded RNA molecule with positive polarity, composed of about 9600 nucleotides that are flanked by non-translated regions at the 5´- and 3´-end, respectively. The viral RNA contains only one single large open reading frame (ORF) encoding a polyprotein of 3010-3033 amino acids that is processed into individual viral proteins by both viral and cellular proteases (Fig. 2) (Selby et al., 1993; Hijikata et al., 1993b; Grakoui et al., 1993c; Bartenschlager & Lohmann, 2000a). Besides the polyprotein, the expression of a novel HCV protein has been reported (Walewski et al., 2001; Xu et al., 2001; Boulant et al., 2003). Translation of this additional viral gene product also initiates at the core gene AUG start codon, but ribosomes shift into an alternative reading frame in the vicinity of the 11th codon. The resulting 17-kDa protein is therefore called the frameshift (F) or alternative reading frame (ARF) protein (Varaklioti et al., 2002). However, the exact role of the F protein remains to be defined (Bartenschlager et al., 2004).

The HCV polyprotein is cleaved co- and post-translationally by cellular and viral proteinases into eleven different products, with the structural proteins located in the amino-terminal one-third and the non-structural replicative proteins in the remainder (Fig. 2). The first cleavage product of the polyprotein is the highly basic core protein, forming the major constituent of the nucleocapsid (Yasui et al., 1998). In addition, a number of other functions like modulation of several cellular processes or induction of hepatocellular carcinoma in transgenic mice have been attributed to the core protein (Chen et al., 1997; Matsumoto et al., 1997; Chang et al., 1998; Moriya et al., 1998). Envelope proteins (E1 and E2) are highly glycosylated type 1 transmembrane proteins, forming two types of stable heterodimeric complexes: a disulfide-linked form representing misfolded aggregates and a non-covalently linked heterodimer corresponding most likely to the pre-budding complex (Deleersnyder et al., 1997). In addition, E2 was shown to interact with the IFN-induced double-stranded RNA-activated protein kinase PKR. Upon induction by IFN-α, this enzyme reduces protein synthesis via phosphorylation of translation initiation factor eIF2-α, but in cells containing E2, PKR is inhibited, allowing continuation of translation in the presence of IFN (Taylor et al., 1999).

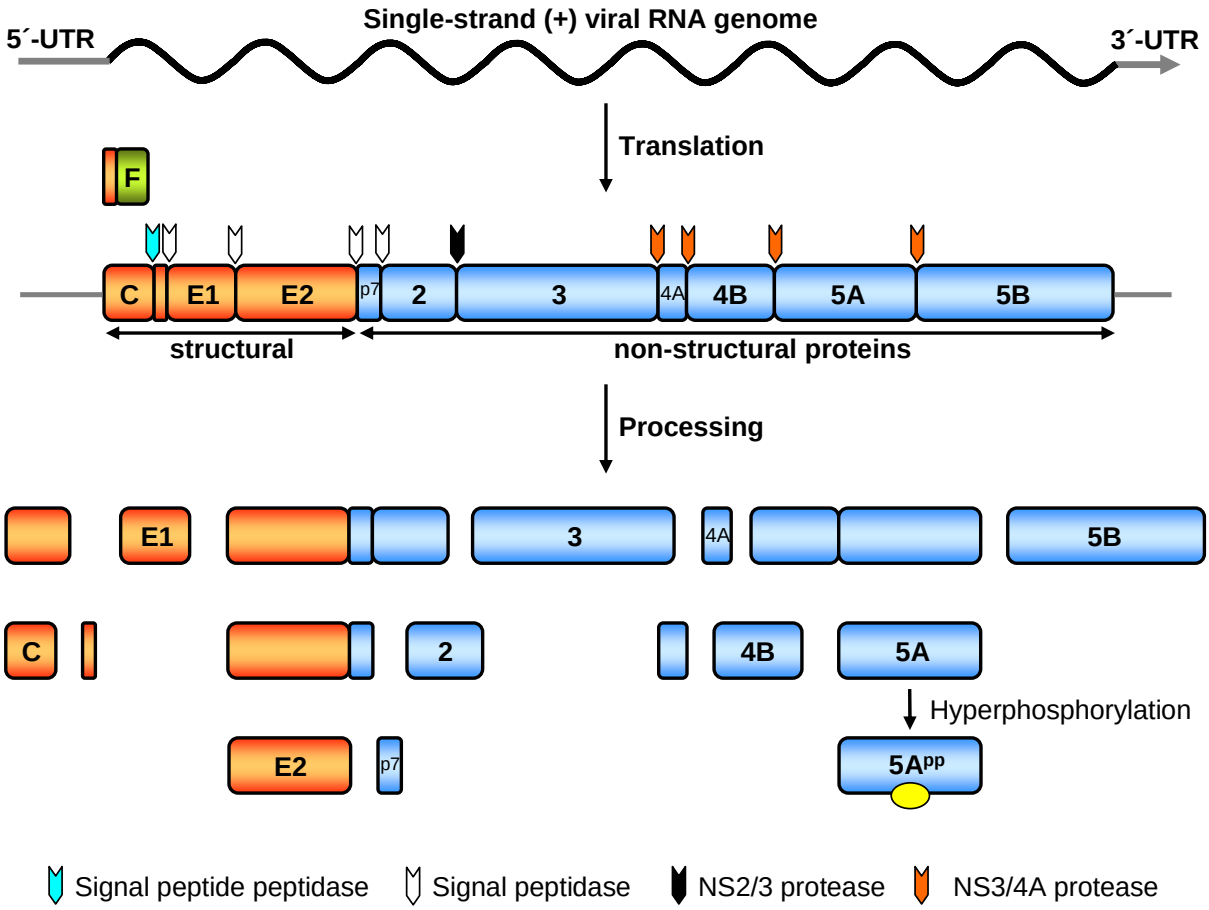

Fig. 2: Genomic organization of HCV and processing pathways of the polyprotein. A schematic representation of the HCV genome with the 5´- and 3´-UTR is shown in the top, the translation products are given below. Proteinases involved in processing of the polyprotein are indicated by arrows that are specified in the bottom of the figure. The major cleavage pathways leading to distinct processing intermediates, most notably E2-p7-NS2 and NS4B-5A are indicated. The hyperphosphorylation of NS5A probably occurs after full proteolytic cleavage. The F protein generated by ribosomal frameshifting is depicted above the polyprotein.

Downstream of the structural region there is a small integral membrane protein, p7, a highly hydrophobic polypeptide, which seems to function as an ion channel located at the carboxy terminus of E2 (Griffin et al., 2003; Pavlovic et al., 2003). Most of the non-structural (NS) proteins, NS2, NS3, NS4A, NS4B, NS5A and NS5B, are required for replication of the viral RNA (Lohmann et al., 1999). NS2 and the amino-terminal domain of NS3 constitute the NS2–3 proteinase, catalysing cleavage at the NS2/3 site (Hirowatari et al., 1993; Grakoui et al., 1993a; Hijikata et al., 1993a). NS3 is a bifunctional molecule carrying, in the amino-terminal ~180 residues, a serine-type proteinase responsible for cleavage at the NS3/4A, NS4A/B, NS4B/5A and NS5A/B sites and, in the carboxy-terminal remainder, NTPase/helicase activities essential for translation and replication of the HCV genome (Eckart et al., 1993; Suzich et al., 1993; Tomei et al., 1993; Bartenschlager et al., 1993b; Grakoui et al., 1993b; Kim et al., 1995; Gwack et al., 1996; Hong et al., 1996; Tai et al., 1996; Kolykhalov et al., 2000). In addition, NS3 may have other properties involved in interference with host cell functions like inhibition of protein kinase A-mediated signal transduction or cell transformation (Sakamuro et al., 1995; Borowski et al.,

1996a). NS4A is an essential cofactor of the NS3/4A proteinase and is required for efficient polyprotein processing (Bartenschlager et al., 1994; Failla et al., 1994; Lin et al., 1994b; Tanji et al., 1995a). The function of the hydrophobic NS4B is so far unknown. The transmembranous structure of NS4B and the absence of enzymatic activities suggest that this protein might play a noncatalytic role. Presumably, its main function is the induction of membranous vesicles or membrane invaginations that may serves as scaffolds for the assembly of the HCV replication complex (Egger et al., 2002; Bartenschlager et al., 2004).

HCV proteins	Molecular weight (kDa)	Function
F/ARF protein	17	?
Core	23 (precursor), 21(mature)	RNA binding; nucleocapsid
E1	31-35	Envelope protein; fusion domain?
E2	70	Envelope protein; receptor binding
p7	7	Viroporin (ion channel?)
NS2	21	Component of NS2-3 proteinase
NS3	69	Component of NS2-3 and NS3/4A proteinase (N-terminal domain); NTPase/helicase (C-terminal domain); Interference with IRF-3
NS4A	6	NS3/4A proteinase cofactor
NS4B	27	Induction of membranous vesicles
NS5A	56 and 58 (basal and hyperphosphorylated form, respectively)	IFN-α resistance? RNA replication?
NS5B	68	RNA-dependent RNA polymerase

Table 2: HCV proteins and their presumed functions in the viral life cycle (Cited from Bartenschlager et al., 2004).

NS5A is a fascinating protein. Many cellular proteins interact with NS5A, although their functional relevance is largely unclear (He & Katze, 2002; Tellinghuisen & Rice, 2002; Macdonald & Harris, 2004). NS5A is phosphorylated on multiple serine residues by cellular kinases and can be found in hypophosphorylated (56 kDa) and hyperphosphorylated (58 kDa) forms. Major phosphorylation sites have been determined for a few HCV isolates (Reed & Rice, 1999; Katze et al., 2000), and kinases capable of phosphorylating NS5A have been identified. These include AKT, p70S6K, MEK1, MKK6, cAMP-dependent protein kinase A-α and casein kinase II (Ide et al., 1997; Reed et al., 1997; Kim et al., 1999; Coito et al., 2004). It is not yet clear which kinases are involved in generating the different phosphoforms of NS5A, or which phosphorylation sites are functionally relevant, and the role of NS5A phosphorylation remains an area of intense interest. For the HCV-H isolate the major phosphorylation site has been mapped to serine residue 2321 of the polyprotein and the proline-rich nature of the flanking sequence suggests that a proline-directed kinase is responsible for NS5A phosphorylation (Reed & Rice, 1999). The role that NS5A might play in RNA replication is so far not known, but based on analogy with other RNA viruses where phosphoproteins are important regulators of replication, one could assume that NS5A plays a similar role. Apart from such a function, NS5A appears to be involved in resistance of the infected cell to

the antiviral effect of IFN. At least for some HCV isolates NS5A is able to bind to PKR, blocking inhibition of translation in the IFN-treated cell (Gale et al., 1997; Gale et al., 1998c).

NS5B is the workhorse of the HCV RNA replication machinery, which has been identified as the RNA-dependent RNA polymerase (RdRp) (Behrens et al., 1996; Lohmann et al., 1997; Yuan et al., 1997; Al et al., 1998; Yamashita et al., 1998). NS5B has a typical 'right hand' polymerase structure, with catalytic sites in the base of the palm domain, surrounded by thumb and finger domains (Penin et al., 2004). The overall structure of NS5B is remarkably similar to the RdRP of bacteriophage Φ6 (Butcher et al., 2001). NS5B also has a low-affinity GTP-binding site, distal from the active site, which is thought to be involved in allosteric regulation of the finger–thumb interaction (Bressanelli et al., 2002). A brief summary of the individual protein products and their main function(s) is given in Table 2.

1.5 The life cycle of Hepatitis C Virus

The human liver is the main site of HCV replication, but there is strong evidence that it can also replicate in peripheral blood mononuclear cells (PBMCs) or in experimentally infected B- and T-cell lines (Esteban et al., 1998), in epithelial cells in the gut (Deforges et al., 2004) and in the central nervous system (Forton et al., 2004). Studies of viral dynamics in patients treated with IFN-alpha revealed a virion half-life of 3-5 hours and a clearance and production rate of 10^{-12} particles per day (Neumann et al., 1998; Zeuzem et al., 1998; Ramratnam et al., 1999). Another feature of HCV replication is the rapid generation of virus variants, primarily due to the high error rate of the viral RNA dependent RNA polymerase (RdRp) that, based on analogies with RdRps of other plus-stranded RNA viruses, is expected to be in the range of 10^{-4}. Indeed, HCV strains isolated from the same individual over time (as well as from different individuals) show different biological, serological and molecular characteristics, with a significant fraction of defective virus genomes, some of which may yield defective interfering particles. Within the host, viral genomes are found as heterogeneous populations termed "quasispecies". Owing to the lack of an animal model or a cell culture system able to support efficient virus replication, our understanding of the molecular mechanisms of HCV replication comes from the study of closely related flavi- and pestiviruses. These viruses enter cells by receptor-mediated endocytosis and low-pH mediated membrane fusion in lysosomes. An idealized HCV life cycle is illustrated in Fig. 3.

Attachment and entry. The first step in a virus life cycle is the attachment of the infectious particle to the host cell, for which a specific interaction between a receptor on the cell surface and a viral attachment protein on the surface of the particle is required. Although the mechanism of HCV entry into cells is still unknown, the E2 glycoprotein is thought to play a major role in virus attachment to the target cell. CD81, a member of the tetraspanin superfamily of cell surface molecules and expressed on virtually all cells, is the putative receptor for HCV entry into the host cell, since this molecule strongly interacts with E2 as well as virus particles *in vitro* (Pileri et al., 1998). Additionally, the virus may also be able to enter the cell by binding to low-density lipoprotein (LDL) receptors (Monazahian et al., 1999). But whether interaction with the LDL receptor or CD81 leads to internalization and a productive infection remains to be determined. Based on comparison with fusion peptides of paramyxoviruses, E1 may be involved in membrane fusion (Flint et al., 1999c). The low pH within the endosomal compartment may induce a major structural rearrangement of the E1, resulting in exposure of a fusion peptide which destabilizes membranes, leading to membrane fusion and particle entry into the cytoplasm.

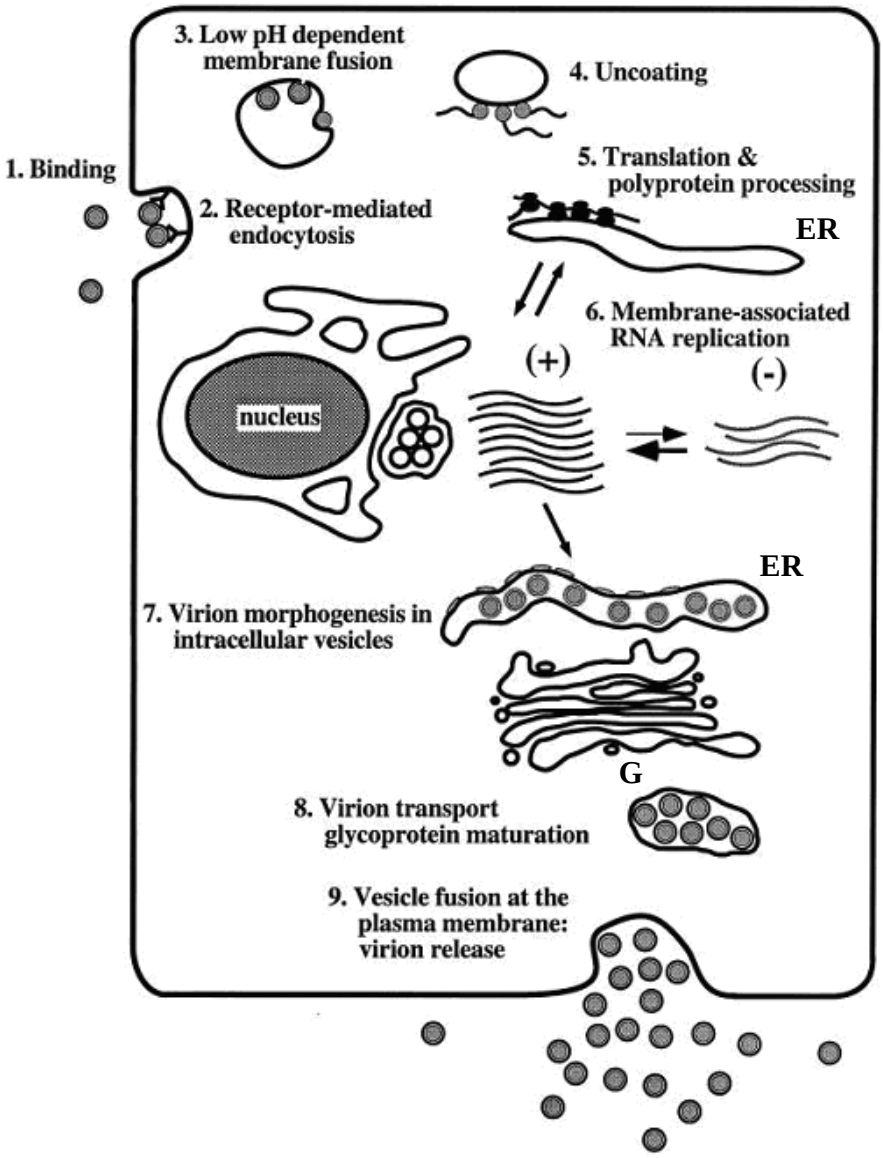

Fig. 3: Hypothetical model of the HCV life cycle. Upon infection of the host cell, the plus-strand RNA genome (+) is liberated into the cytoplasm and translated. The polyprotein is processed and viral proteins remain tightly associated with membranes of the endoplasmic reticulum (ER). Minus-strand RNA (–) is synthesized by the replicase composed of NS3 - 5B and serves as template for production of excess amounts of plus-strand RNA. Via interaction with the structural proteins plus-strand RNA is encapsidated. Particles are enveloped by budding into the lumen of the ER and virus particles are exported via transit through the Golgi (G) complex.

Polyprotein translation and processing. Following decapsidation, the genomic RNA is directly translated in the cytoplasm. Since the genome is not capped, translation is mediated by an internal ribosome entry site (IRES) element rather than by a cap-dependent mechanism employed by most eukaryotic and cellular mRNA (this issue will be described in detail in the following part). This activity does not seem to require most of the canonical eukaryotic initiation factors (eIFs) (Pestova et al., 1998b). The very 3´ end of the HCV genome as well as several cellular factors (polypyrimidine tract-binding protein, La autoantigen, heterogeneous nuclear ribonucleoprotein L and other unidentified proteins) interact with the HCV IRES and may be also involved in translation, but this

is still enigmatic (Ali & Siddiqui, 1995; Hahm et al., 1998b; Ito & Lai, 1999; Ali et al., 2000; Lu et al., 2004). This stimulation by host factors implies that cellular proteins that vary in abundance or activity during the cell cycle might in part regulate HCV translation (Honda et al., 2000).

Directed by the IRES, the polyprotein is translated at the rough endoplasmic reticulum (rER) and cleaved co- and post-translationally by host and viral proteinases. The individual HCV proteins form a stable replicase complex associated with intracellular membranes (Tanji et al., 1995a; Wölk et al., 2000). This allows the tight coupling of different viral functions as well as the production of viral proteins and RNA in a distinct compartment. The proteinase cofactor NS4A further contributes to efficient polyprotein cleavage and replication by increasing the metabolic stability of NS3 which is rapidly degraded in its absence, and by anchoring NS3 to intracellular membranes so that the enzyme and its substrate are concentrated in very close proximity (Hijikata et al., 1993b; Lin et al., 1997; Ishido et al., 1998; Koch & Bartenschlager, 1999; Neddermann et al., 1999).

RNA replication. The positive strand RNA genome of HCV is copied into a minus strand intermediate that serves for synthesis of new genomic plus strands. However, the individual steps underlying RNA replication are largely unknown, even though the establishment of a tissue culture system for subgenomic replicons now facilitates the related studies (Lohmann et al., 1999). *In vitro*, the RNA dependent RNA polymerase (RdRp) initiates replication by elongation of a primer hybridized to an RNA homopolymer or via a "copy-back" mechanism (Behrens et al., 1996; Lohmann et al., 1997; Yuan et al., 1997; Al et al., 1998; Yamashita et al., 1998; Ferrari et al., 1999). In this latter case, sequences at the 3´ end fold back intramolecularly and hybridize, generating a 3´ end that can be used for elongation, resulting in a product about twice the length of the input template. However, in the presence of high GTP or ATP concentration, RdRp can initiate RNA synthesis *de novo*, and this probably occurs *in vivo* (Kao et al., 1999; Oh et al., 1999; Luo et al., 2000; Zhong et al., 2000a). Concerning the template specificity, NS5B seems to bind preferentially to a sequence in its own 3´ coding region (Cheng et al., 1999). Alternatively, the template specificity may be accomplished by the high local concentration of both NS5B and the viral RNA within the replicase complex (Lohmann et al., 1997). Efficient RNA replication very likely depends on additional viral and cellular factors, like the NS3 helicase which unwinds stable RNA structures or the phosphoprotein NS5A (Lohmann et al., 1997).

In addition to viral proteins, cellular components are probably involved in RNA synthesis as well. One candidate is PTB, found to specifically interact with sequences in the 3´-UTR (Ito & Lai, 1997; Tsuchihara et al., 1997; Chung & Kaplan, 1999). Another candidate is glyceraldehyde-3-phosphate dehydrogenase (GAPDH), binding to the poly(U)-sequence in the 3´-UTR (Petrik et al., 1999). Finally, cellular proteins provisionally called p87 and p130 were identified by UV-cross linking experiments with the X-tail sequence, but the nature of these proteins remains to be determined (Inoue et al., 1998a).

Proteins from other viruses may also affect HCV replication. For example, in most cases, the cell lines co-infected with other viruses like human T-lymphotropic virus type I (in the case of the MT2 T-cell line), a murine retrovirus (in the case of the MOLT4-Ma T-cell line) or Epstein–Barr virus (EBV) (in the case of the Daudi B-cell line) support HCV replication (Sugawara et al., 1999). Furthermore, Sugawara et al. observed that HCV-positive patients with a hepatocellular carcinoma frequently have a high EBV load, and presented evidence that the enhancement of HCV replication is mediated by EBV nuclear antigen 1 (Sugawara et al., 1999).

Virion assembly and release. In the absence of systems allowing the production of sufficiently high amounts of virus particles, the assembly of HCV cannot be studied in detail. Particle formation may be initiated by the interaction of the core protein with the 5´ half of the RNA genome (Shimoike et al., 1999). Such binding of the core protein represses translation from the IRES, suggesting a potential mechanism to switch from translation

and replication to assembly (Zhang et al., 2002). Whether the core protein forms a distinct nucleocapsid structure or a rather non-structured ribonucleoprotein complex with the HCV genome is unknown, but the core protein is able to interact with itself (Matsumoto et al., 1996). Viral capsids acquire their envelope by budding through ER membranes, where the E1 and E2 protein are inserted (Sato et al., 1993; Dubuisson et al., 1994; Duvet et al., 1998; Cocquerel et al., 1999). Then, the virions are supposed to be exported via the constitutive secretory pathway.

1.6 Translation of HCV RNA is mediated by internal ribosome entry

Most eukaryotic and cellular mRNAs are functionally monocistronic and contain a 5´-terminal m^7GpppN (where N can be any nucleotide) cap structure on which the initiation of translation strongly depends. The initiation codon used as the start site for protein synthesis is preceded by a 5´-UTR in which the length, nucleotide composition, and structure can determine the efficiency and the mechanism by which a given mRNA is translated (Hershey & Merrick, 2000). For the most part, the factors that influence the binding of 40S subunits to the mRNA provide the limiting step in translation initiation.

In eukaryotic cells, transcription and translation are separated in space and time. Before translation occurs in the cytoplasm, the primary transcript is modified and processed immediately in the nucleus by capping, splicing and addition of about 50 to 200 adenylic residues (poly A) at the 3´end of the mRNA. The cap structure is a 7-methylguanosine residue which is attached to the first nucleotide at the 5´end of the mRNA by an unusual 5´-to-5´ triphosphate linkage. This cap structure is essential for efficient protein synthesis, and, in addition, it contributes to the stability of the mRNA by protecting the 5´ end from phosphatases and nucleases (Palmer et al., 1993; Gunnery & Mathews, 1995). Cellular mRNAs contain a relatively short 5´-UTR of about 50 to 100 nucleotides long located between the cap structure and the open reading frame (ORF) that usually contains the authentic initiation codon (AUG). The poly (A) tail at the 3´ terminus influences both mRNA stability and translation efficiency.

1.6.1 Eukaryotic translation initiation

The translation in eukaryotes is divided into three phases: initiation, elongation and termination. The reactions in each step are promoted by soluble protein factors. The rate-limiting step of translation usually occurs during the initiation phase.

The initiation phase of translation is a complex process leading to assembly of a ribosomal 80S complex at the initiation codon of an mRNA. This process is promoted by several proteins called eukaryotic initiation factors (eIFs) (see Tables 3 and 4). Prior to initiation of translation, the 80S ribosome must dissociate into its 40S and 60S subunits. This process is facilitated by eIF3 and eIF1A which help to maintain a pool of dissociated subunits probably by an allosteric effect due to a change in the structure of the 40S subunit upon eIF3 binding (Benne & Hershey, 1976; Srivastava et al., 1992).

eukaryotic initiation factor	Molecular weight (kDa)	Function
eIF1	12.6	AUG recognition
eIF1A	16.5	Met-tRNA$_i$ binding to 40S subunit
eIF2α	36.2	affects eIF2B binding by phosphorylation
eIF2β	39.0	binds to eIF2B, eIF5
eIF2γ	51.8	binds GTP, Met-tRNA$_i$, GTPase
eIF2Bα	33.7	nonessential, helps to recognize phosphorylated eIF2
eIF2Bβ	39.0	binds GTP, helps to recognize phosphorylated eIF2
eIF2Bγ	50.4	Guanine nucleotide exchange activity
eIF2Bδ	57.8	binds ATP, helps to recognize phosphorylated eIF2
eIF2ε	80.2	Guanine nucleotide exchange activity
eIF3 (see table 4)	~ 700.0	ribosomal dissociation; promotes binding of mRNA and Met-tRNA$_i$ to 40S subunit
eIF4A I / II	44.4 / 46.3	ATP dependent RNA helicase
eIF4B	69.2	binds RNA, stimulates helicase
eIF4E	25.1	binds m^{7}G-cap of mRNA
eIF4G I / II	171.6 / 176.5	binds eIF4E, eIF4A, eIF3, PABP · RNA
eIF5	48.9	stimulates GTPase activity of eIF2
eIF5B	139	GTPase, promotes subunit joining reaction

Table 3: Overview of the mammalian translation initiation factors (Modified from Hershey & Merrick, 2000 and Hellen & Sarnow, 2001)**.**

Mammalian eIF3 is the largest and most complex eukaryotic translation initiation factor with an apparent molecular weight of about 700 kDa. It has been first isolated and purified from rabbit reticulocyte lysate on the bases of its ability to stimulate the translation of globin mRNA (Benne & Hershey, 1976; Safer et al., 1976). Latest results show that human eIF3 consists of at least twelve non-identical subunits (Table 4). Until now, the cDNAs encoding the subunits, p170, p116, p110, p66, p48, p47, p44, p40, p36 and p35 have been cloned and sequenced (Asano et al., 1997; Chaudhuri et al., 1997; Johnson et al., 1997; Méthot et al.,o 1997 ; Block et al., 1998). p69 that was found in 2001 has been identified as an eIF3-associated protein (Morris-Desbois et al., 2001). Yeast eIF3 contains only five subunits, TiF32, NIP1, PRT1, TIF34 and TIF35(Danaie et al., 1995; Asano et al., 1998; Phan et al., 1998; Hanachi et al., 1999) that are homologous to the human eIF3 subunits p170, p116, 110, p36 and p44, respectively(Asano et al., 1997).

The first stage in translation initiation is binding of the ternary complex eIF2·GTP·Met-tRNA$_i$ to the 40S ribosomal subunit bound with eIF3 and eIF1A to form the 43S-preinitiation complex (Benne et al., 1978). eIF2 selects the initiator tRNA from a pool of elongator tRNAs by recognizing the methionyl residue and the A-U base pair at the end of the acceptor stem (Fig. 4).

Human		*Arabidopsis*		Yeast			Comments
Name	Mass	Name	Mass	Name	Gene	Mass	
p170	166.5	eIF3a	114.3	p110		111.1	binds RNA
p116	98.9	eIF3b	81.9	p93	*PRT1*	88.1	RRM, binds eIF1, eIF5
p110	105.3	eIF3c	103.0	p90	*NIP1*	93.4	
p66	64.0	eIF3d	66.2				RRM, binds RNA
p48	52.2	eIF3e	51.8				
p47	37.6	eIF3f	31.9				
p44	35.4	eIF3g	32.7	p36	*TIF35*	30.5	RRM, binds RNA, eIF4B
p40	39.9	eIF3h	38.4				
p36	36.5	eIF3i	36.4	p39	*TIF34*	38.8	
p35	29.0				*HCR1*	29.6	
p28	25.1	eIF3k	25.7				
p69	69.0						cell growth controlling
		eIF3l	56				
				p135		145.2	(also called *CLUI*)

Table 4: eIF3 subunits from mammalian, plant and yeast cells. The human subunits are named according to their apparent masses as determined by SDS-PAGE. The human p69 was reported recently to be an eIF3-associated protein (Morris-Desbois et al., 2001). The yeast p135 is associated with eIF3 but has not definitely been characterized as a subunit of eIF3 (Vornlocher et al., 1999) (Modified from Hershey, 2000).

The second stage is the binding of 43S-preinitiation complex to the m^7G cap structure at the 5′ end of mRNA. The cap structure is recognized by the cap binding protein (eIF4E), a subunit of eukaryotic translation initiation factor 4F (eIF4F). Mammalian eIF4F is a heterotrimeric protein complex of 250 kDa composed of eIF4E, eIF4G and eIF4A which plays the key role in recruiting the mRNA to the 43S initiation complex (Hershey & Merrick, 2000). eIF4G is an adaptor protein which binds eIF4E, eIF4A, eIF3, and the 40S ribosome (Hentze, 1997; Sachs et al., 1997). eIF4A exhibits RNA-dependent ATPase activity (Grifo et al., 1983) and a bidirectional RNA helicase activity which is stimulated by eIF4B and eIF4H (Rozen et al., 1990; Rogers et al., 1999). The binding of eIF4F to mRNA further recruits eIF4B and eIF4H. The entire complex in conjunction with the hydrolysis of ATP is thought to melt the secondary structures near the 5′ end of the mRNA that would otherwise impair ribosome movement from the 5′ proximal region to the AUG codon (Rozen et al., 1990; Rogers et al., 1999).

Following recognition of the cap structure and unwinding of the secondary structure in the 5′-UTR, the 43S preinitiation complex binds to the cap proximal region of the mRNA. This ribosomal binding is thought to be mediated by interactions of eIF4G and eIF4B with eIF3-bound 40S subunit (Lamphear et al., 1995; Méthot et al., 1996). The 40S ribosomal subunit with associated initiation factors then migrates along the 5′-UTR in 5′-3′ direction probably in a linear scanning mode until it encounters the initiation codon to form the 48S preinitiation complex (Jackson, 2000). Selection of the initiation codon most probably occurs by codon-anticodon base pairing with the Met-$tRNA_i$. However, a few nucleotides flanking the initiation codon (–3 and +4 relative to the A of AUG) are also important for the selection process. Purines in the context A/GCCAUGA/G are optimal for initiation. This special sequence is well-known as “Kozak sequence” (Kozak, 1989a). Both eIF1 and eIF1A

participate in the selection of the initiation codon. In their absence, the ribosome binds to the cap structure but is not able to reach the initiation codon (Pestova et al., 1998b).

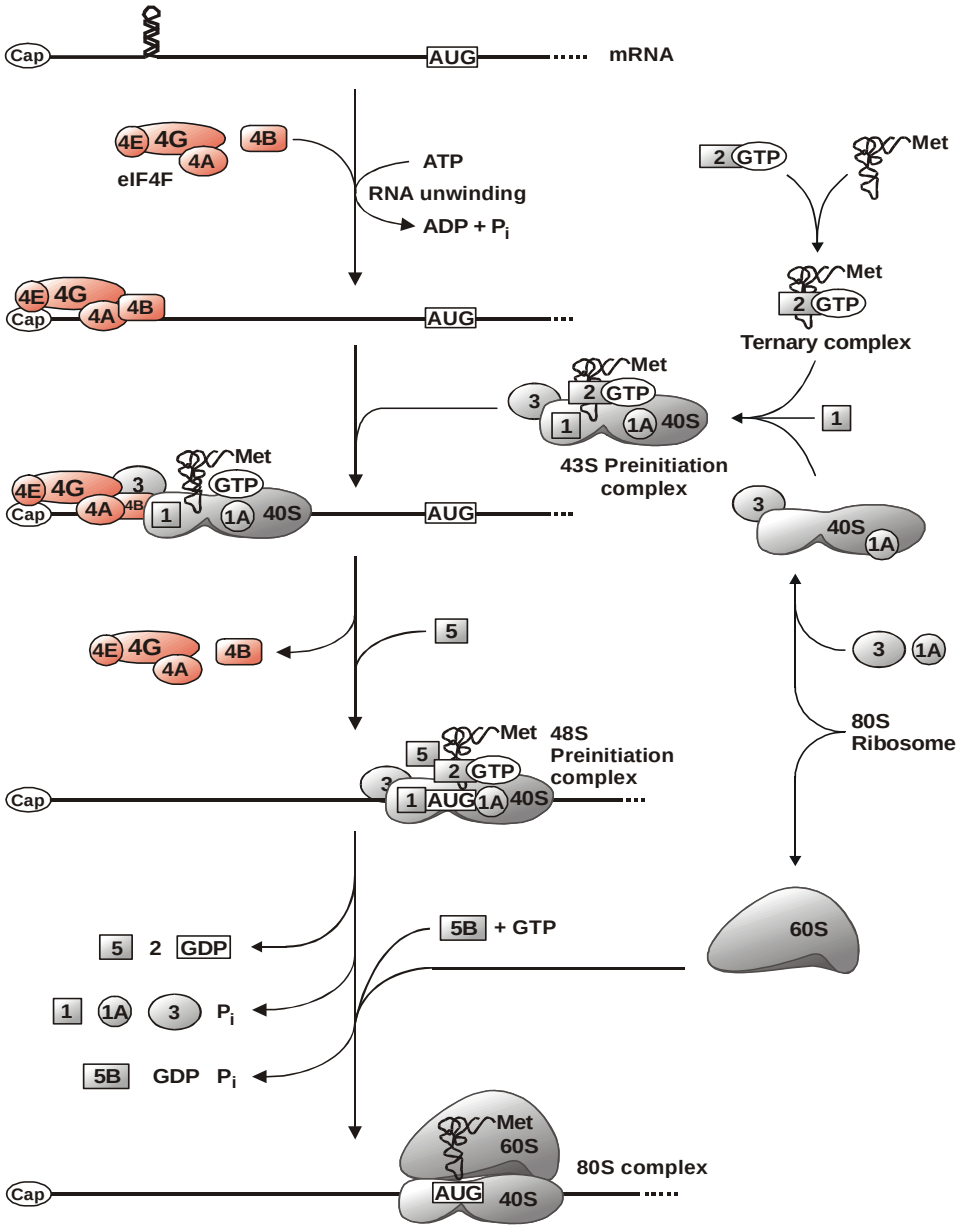

Fig. 4: Schematic representation of the translation initiation pathway in eukaryotic cells (Modified from Hershey & Merrick, 2000).

The last stage of translation initiation is the displacement of initiation factors from the 48S complex and the joining of the 60S subunit in a way that the Met-tRNA$_i$ is positioned in the P site of the ribosome to form an 80S complex at the initiation codon ready to commence the translation of the coding sequence. This step is aided by eIF5 and eIF5B (Hershey & Merrick, 2000; Pestova et al., 2000). eIF5 promotes the hydrolysis of the GTP-bound eIF2 in the presence of the 40S subunit. The binary complex of GDP-bound eIF2 is released from the ribosome together with other initiation factors. The continuity of initiation events requires the regeneration of GTP-bound eIF2, which is stimulated by the guanine-nucleotide exchange factor (GEF), eIF2B. Liberated

initiation factors are then recycled for another cycle of initiation when the translating 80S ribosome encounters a termination codon (UAG, UAA or UGA). The termination codon is recognized by release factors eRF1 and eRF3 which mediate the release of the peptide chain from the bound tRNA by hydrolysis. Once termination has occurred, the 40S subunit is free to continue scanning the mRNA or to leave it. Molecular details of this mechanism have not been fully elucidated. However, evidence for ribosomal scanning comes from observations that initiation is strongly inhibited by insertion of additional AUG triplets or of stable secondary structures between the 5´ end and the initiation codon (Kozak, 1989b).

1.6.2 Internal initiation of translation

More than twenty years ago, it was reported that prokaryotic, but not eukaryotic, ribosomes could bind circular RNA molecules, suggesting that eukaryotic ribosomes enter mRNAs exclusively via their free 5´ ends (Kozak, 1979; Konarska et al., 1981). However, it was known that RNA genomes of picornaviruses have properties that are incompatible with initiation by 5´end-dependent scanning. Therefore, translation of several eukaryotic mRNAs, for example, in picornaviruses, cannot be accounted for by the canonical scanning model mentioned above. An alternative mechanism plays a key role for the initiation of viral polyprotein synthesis, which is significantly different from the 5´ cap-dependent translation. Translation of the picornaviral RNA is initiated cap-independently and occurs by direct ribosomal attachment to a *cis*-acting element which is known as the internal ribosome entry site (IRES) located downstream from the 5´ end of the viral RNA. Internal initiation was first discovered in the picornaviruses such as encephalomyocarditis virus (EMCV) and poliovirus (Jang et al., 1988; Pelletier & Sonenberg, 1988d), and has since been extended to other RNA viruses and a few cellular mRNAs (Hellen & Sarnow, 2001; Martinez-Salas et al., 2001). So far, all picornaviral mRNAs have been found to contain IRES elements. Table 5 provides a list of RNA viruses and one DNA virus, Karposi´s sarcoma-associated herpesvirus, whose genomes contain IRES elements. In principle, initiation at internal AUG triplets can also occur as a result of leaky scanning or of reinitiation (Hellen & Sarnow, 2001).

Virus	**reference**
Poliovirus (PV)	Pelletier and Sonenberg, 1988d
Rhinovirus (RV)	Borman and Jackson, 1992
Encephalomyocarditis virus (EMCV)	Jang et al., 1988
Foot-and-mouth disease virus (FMDV)	Kühn et al., 1990
Hepatitis C Virus	Tsukiyama-Kohara et al., 1992
Bovine virai diarrhea virus (BVDV)	Poole et al., 1995
Friend murine leukemia virus *gag* mRNA	Berlioz and Darlix, 1995
Moloney murine leukemia virus *gag* mRNA	Vagner et al., 1995b
Classic Swine Fever Virus (CSFV)	Rijnbrand et al., 1997
Rous sarcoma virus	Deffaud and Darlix, 2000a
Human immunodeficiency virus *env* mRNA	Buck et al., 2001
Plautia stali intestine virus	Sasaki and Nakashima, 1999
Rhopalosiphum padi virus	Domier et al., 2000
Cricket paralysis virus	Wilson et al., 2000b
Karposi´s sarcoma-associated herpesvirus	Grundhoff and Ganem, 2001

Table 5: Internal ribosome entry sites in viral genomes (Cited from Hellen & Sarnow, 2001).

1.6.2.1 General organization of viral IRES elements

The IRES elements of the related picornaviruses can be classified into three groups on the bases of their primary sequences, predicted secondary structures, and requirements for efficient translation initiation (Jackson & Kaminski, 1995) (Fig. 5). First, the entero- and rhinovirus group (type I IRES, e.g., poliovirus, human rhinovirus and coxackievirus); second, the cardio- and aphthovirus group (type II IRES, including encephalomyocarditis virus (EMCV), theiler's murine encephalomyelitis virus (TMEV) and foot-and-mouth disease virus (FMDV) and third the hepatoviruses (hepatitis A virus). The IRES elements of HCV and pestiviruses which are members of the *Flaviviridiae* family comprise the fourth group of viral IRES elements (Reynolds et al., 1995) (Fig. 5). Also several cellular mRNAs that contain IRES elements have been identified including mRNAs that encode the immunoglobulin heavy chain binding protein Bip (Macejak & Sarnow, 1991), the human insulin-like growth factor II (Teerink et al., 1995), the fibroblast growth factor 2 "FGF-2" (Vagner et al., 1995) and the transcription factor c-Myc (Stoneley et al., 2000).

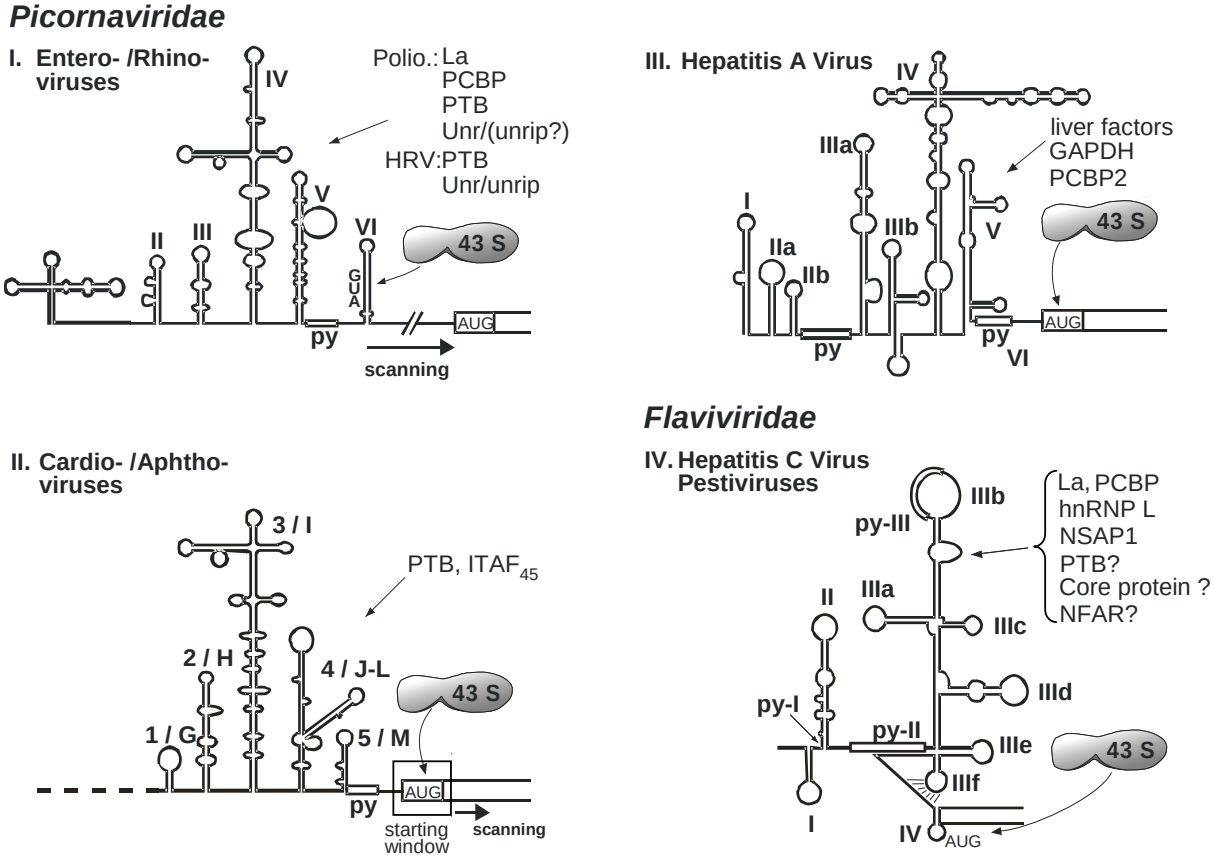

Fig. 5: Organization of viral IRES elements. Schematic representation of the IRES elements of entero-/rhinoviruses (e.g., poliovirus), cardio-/aphthoviruses (e.g., FMDV and EMCV), hepatitis A virus and hepatitis C virus. The major domains are indicated according to Niepmann 1999. Pyrimidine-rich sequence elements (Py) are shown as solid rectangles, AUG denotes the position of the translation codon (modified from Niepmann, 1999).

The overall structure of picornavirus IRES elements appears to be roughly similar. They contain a large central domain consisting of a long stem and a cross-shaped upper part (Fig. 5, groups I, II, and III). Upstream of this large central domain, there are different numbers of smaller domains with structures that differ among the picornavirus groups. A mid-size domain is located downstream of the central domain. It consists of a domain with bulges in the upper part in entero- and rhinoviruses and hepatitis A virus (HAV), or a characteristic Y-shaped structure in cardio- and aphthoviruses. In contrast, in the HCV and pestivirus IRES elements, one large domain appears to replace the central domain and the downstream domains of the picornavirus IRES elements. Within each group of picornaviruses, there is strong conservation of the IRES secondary structure but a lower degree of conservation of the primary sequence.

The 5´-UTRs of HCV and the related classical swine fever virus (CSFV), bovine viral diarrhea virus (BVDV), and GB virus B (GBV-B) contain IRESes that are ~ 330-390 nucleotides in length and have related structures, even though their sequences differ significantly from one another (Lemon, 1997). Sequence differences between the IRESes of different genotypes of any one of these viruses consist mostly of compensatory nucleotide changes within structural elements that serve to maintain base pairing (Smith et al., 1995). As in the picornaviral IRESes, mutations that disrupt helical regions in HCV-like IRESes can substantially reduce their initiation activity, but this can be restored by compensatory second-site mutations (Rijnbrand et al., 2000a). These observations are consistent with a model for IRES function in which helices form a structural scaffold to orient conserved unpaired regions that act as binding sites for factors and ribosomes so that they can assemble functional initiation complexes.

1.6.2.2 The HCV internal ribosome entry site

1.6.2.2.1 The HCV 5´-untranslated region (5´-UTR)

HCV is now classified as a distinct genus of *Hepacivirus*, with at least six major genotypes that differ from each other in nucleotide sequence by up to 35 %. The viral RNA genome of HCV contains a relative long 5´-untranslated region (5´-UTR). While remarkable nucleotide diversity exists among HCV subgroups, the 5´-UTR maintains a very high degree of nucleotide conservation (> 93 %) (Okamoto et al., 1991). The 5´-UTR varies in length from 332 to 341 nucleotides depending on the HCV subtype (Han et al., 1991; Takamizawa et al., 1991; Chen et al., 1992; Tanaka et al., 1992). Only the 5´-UTR and the adjacent core protein-encoding sequences are highly conserved (Simmonds et al., 1993b; Simmonds, 1995). Sequences from the 5´-UTRs of even the most distantly related HCV subtypes do not differ by more than 10 % and are usually much more similar. The HCV 5´-UTR is longer than that of flaviviruses, but closely resembles the 5´-UTRs of pestiviruses such as bovine viral diarrhoea virus (BVDV), border disease virus (BDV) and classical swine fever virus (CSFV) in terms of length, sequence and secondary structure (Abastado et al., 1991; Brown et al., 1992; Wang et al., 1995a; Becher et al., 1997; Becher et al., 1998). The BVDV, BDV and CSFV 5´-UTRs are 385, 372 and 372 nucleotides long, respectively, and like the HCV 5´-UTR, contain several AUG triplets upstream of the initiation codon and form extensive secondary structures. Although the HCV 5´-UTR differs from those of BVDV and CSFV at over 50 % of base positions, many of these nucleotide differences are covariant substitutions, indicative of conserved secondary and/or tertiary structure.

The HCV 5´-UTR consists of four major structural domains, designated I to IV in the 5´- to 3´- direction, and a pseudoknot upstream of the authentic initiation codon (Fig. 6). Support for the existence of these structures has come from phylogenetic comparison (Wang et al., 1995a; Bayliss & Smith, 1996), mutational analyses and from the results of chemical and enzymatic probing (Brown et al., 1992; Wang et al., 1995a; Honda et al., 1996a). BVDV and CSFV 5´-UTRs have similar structures except that residues equivalent to domain IV are unstructured (Wang et al., 1995a; Bayliss & Smith, 1996; Sizova et al., 1998).

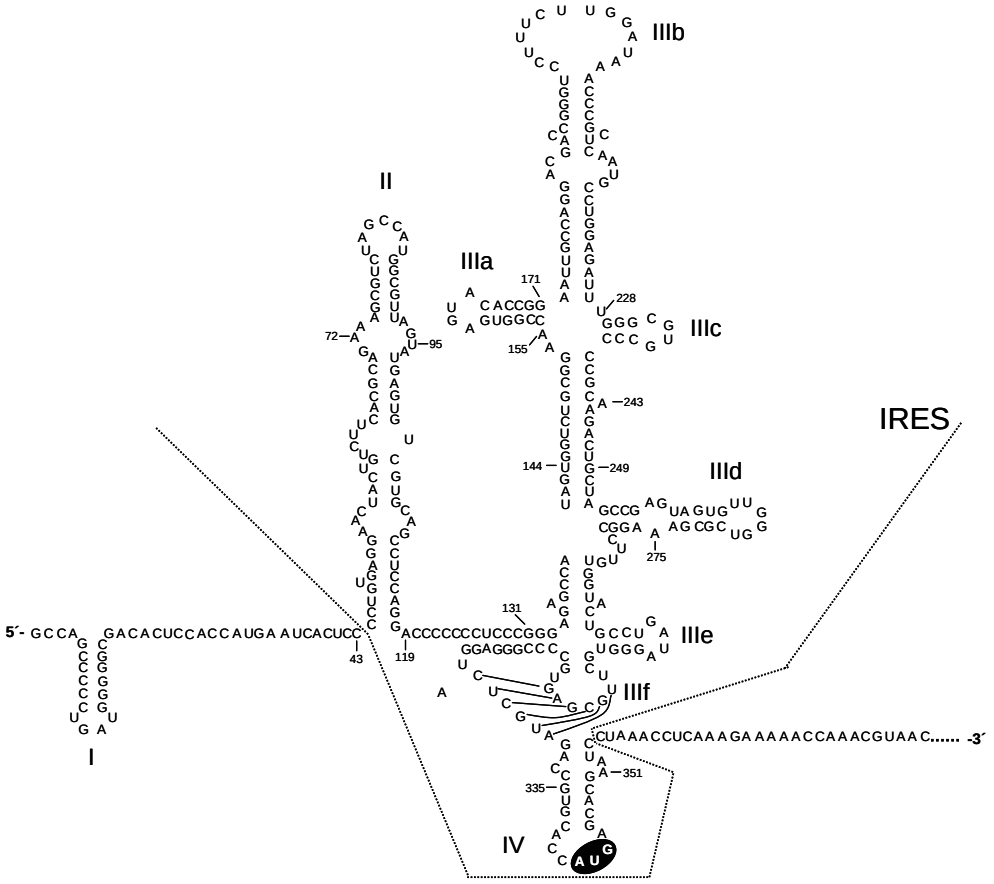

Fig. 6: The secondary and tertiary RNA structure of the complete HCV 5´-untranslated region (5´-UTR) followed by the viral open reading frame. The Roman numbers represent the four major domains and six subdomains (followed by small English letters). The region comprising the IRES (to be described later) extends from domain II to domain IV and thus also includes a short stretch of upstream core protein-encoding sequence. The initiator AUG codon is highlighted (Modified from Honda, 1999).

1.6.2.2.2 Detection of an internal ribosome entry site element

The most conclusive proof to verify the mechanism of "internal initiation" is the experimental observation that insertion of a putative IRES element into the intercistronic spacer of a dicistronic construct with two protein-coding ORFs promotes efficient translation of the downstream cistron (Fig. 7b). Insertion of a heterologous "spacer" at the same position permits leaky scanning and reinitiation but does not promote efficient translation of the downstream cistron by internal ribosomal entry (Fig. 7a). Three further approaches show that initiation of

translation of the downstream cistron is not simply a consequence of reinitiation after translation of the first cistron. First, insertion of a stable hairpin near the 5´ end of the mRNA prevents translation of the upstream cistron without affecting IRES-mediated translation of the downstream cistron (Fig. 7e). Second, poliovirus encodes a protease 2A that cleaves the eIF4G subunit of eIF4F, thereby abrogating its essential function in cap-mediated translation initiation of the upstream cistron without affecting IRES-mediated initiation of the downstream cistron (Fig. 7c). Third, the size and structure of different IRES elements vary considerably, but a common property that distinguishes them from the 5´-UTRs of conventional capped mRNAs is that their activity is often impaired by minor sequence changes, including deletions, insertions and substitutions (e.g., Fig. 7d).

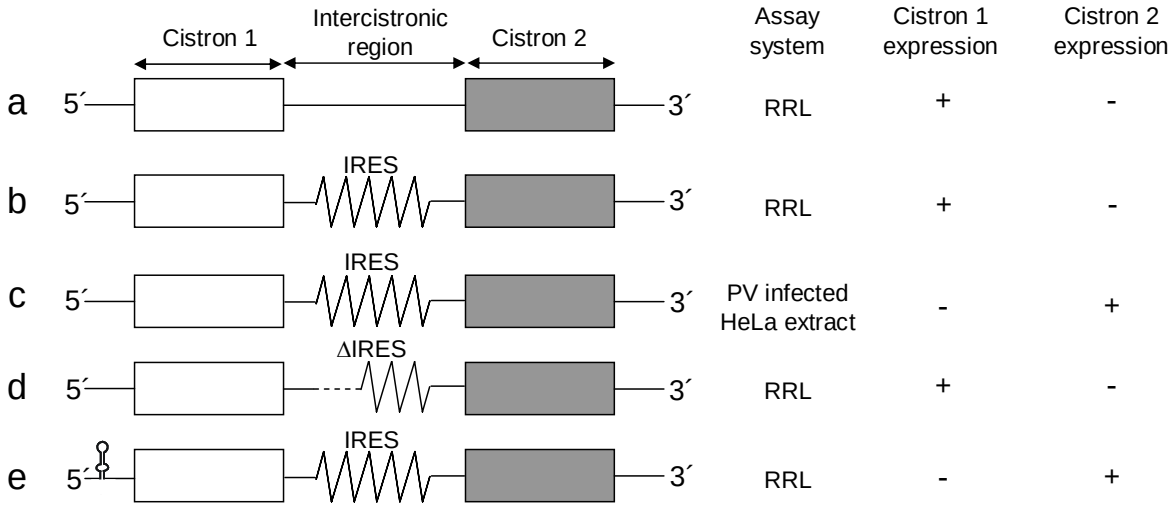

Fig. 7: Schematic structure of dicistronic mRNAs used for the proof of IRES function by *in vitro* translation, and the pattern of expression of upstream and downstream cistrons. Encoding regions are boxed and non-coding regions are shown as lines, except that segments of the hepatitis C virus internal ribosomal entry site (IRES) in the intercistronic area are drawn as zig-zag lines. Expression of cistron 1 and 2 is as indicated and is based on the results of previous reports for HCV (Tsukiyama-Kohara et al., 1992; Wang et al., 1993; Poole et al., 1995; Reynolds et al., 1995; Rijnbrand et al., 1997). PV, poliovirus; RRL, rabbit reticulocyte lysate (modified from Hellen & Pestova, 1999).

Using these different assays mentioned above, the first line of evidence in demonstrating the presence of an internal ribosome entry site (IRES) element within the 5´-UTR of HCV genome came from *in vitro* translation studies by Tsukiyama-Kohara and his colleagues (Tsukiyama-Kohara et al., 1992). In support of the *in vitro* analysis of the translational regulation of the HCV RNA, experiments carried out in another group had employed an *in vivo* system by introducing *in vitro* synthesized RNA into HepG2, a hepatoblastoma cell line. The 5´-UTR of HCV was inserted between two reporter genes, chloramphenicol acetyl transferase (CAT) and *Firefly* luciferase (FLuc). Their results obtained from *in vitro* and *in vivo* experiments provided the unequivocal evidence for the presence of an IRES element within the HCV 5´-UTR.

Together with the results obtained from the investigations with other flaviviruses, it has shown unambiguously that HCV, together with BVDV and CSFV, all contain an IRES element in their 5´-UTRs (Tsukiyama-Kohara et al., 1992; Wang et al., 1993; Poole et al., 1995; Rijnbrand et al., 1996).

1.6.2.2.3 Structural features of the HCV IRES

Mutagenesis studies together with biochemical probing analysis revealed that the HCV IRES consists of three major structural domains (II, III, and IV) radiating from a complex pseudoknot (Fig. 6). Reconstructions of the IRES at ~20 Å resolution produced by cryo-electron microscopy have shown that these domains form an extended structure in which the pseudoknot and domain IV are centrally located (Spahn et al., 2001).

Domain I comprises the extreme 5′ end of the 5′-UTR and is not part of the IRES, but is required for the viral replication. Domain II contributes significantly to IRES function, but deletion of this domain does not lead to complete loss of translation activity, and domain II is also involved in replication (Reynolds et al., 1996; Kolupaeva et al., 2000a, 2000b). Domain III contains several essential elements, including a large four-way junction (IIIabc) and two smaller stem-loop structures (IIId and IIIe). The structures of IIId and IIIe have been solved by NMR spectroscopy (Klinck et al., 2000; Lukavsky et al., 2000). Domain IV contains the initiation codon and is base-paired in the HCV and GBV-B IRESes, but not in those from BVDV or CSFV. HCV coding sequences per se are not essential for internal initiation, because they can be replaced completely by heterologous sequences (Tsukiyama-Kohara et al., 1992; Wang et al., 1993). However, there has been some controversy as to whether HCV sequences located downstream from the initiation codon influence the efficiency of IRES-mediated initiation (Reynolds et al., 1995; Lu & Wimmer, 1996). If one considers that ribosomal entry occurs at the initiation codon without prior scanning (Reynolds et al., 1996; Rijnbrand et al., 1997), and that mutations in the IRES that stabilize structures containing the initiation codon inhibit ribosomal attachment and consequently IRES-mediated initiation (Honda et al., 1996b; Myers et al., 2001), it then seems likely that the negative influence of some heterologous coding sequences on IRES function may be because they interfere sterically with ribosomal attachment.

1.6.2.3 Only eIF2 and eIF3 are required for translation initiation of HCV RNA

Biochemical reconstitution of the initiation process on the HCV IRES has revealed that the 40S subunit can bind specifically and stably to the HCV IRES without any requirement for initiation factors (Fig. 8) in such a way that the initiation codon is placed in the immediate proximity of the ribosomal P site (Pestova et al., 1998b). This ribosomal attachment does not require any initiation factors, including those (eIFs 4A, 4B, 4F) that are required for ribosomal attachment to capped mRNA and to the picornavirus RNA such as EMCV and FMDV (Pestova et al., 1996; Saleh et al., 2001). 43S complexes bind the HCV IRES directly to form 48S complexes in which the initiation codon and the anticodon of initiator tRNA are base-paired. These 48S complexes are competent to complete the remaining stages in initiation. Assembly of 48S complexes is enhanced by (but does not require) eIF3, so eIF2 is the only essential initiation factor up to this stage. In the final stage of initiation, eIF3 is absolutely required for subsequent joining of the 60S subunit to the 48S complex to form an 80S ribosome capable of polypeptide synthesis (Pestova et al., 1998b). Fig. 8 also shows IRES binding can induce a profound conformational change in the 40S subunit (indicated with an asterisk in Fig. 8B) and close the mRNA binding cleft (Spahn et al., 2001), and subsequent addition of the ternary eIF2/GTP/initiator-tRNA complex to IRES/40S subunit complexes is necessary and sufficient for formation of 48S complexes.

Direct ribosomal attachment to eukaryotic mRNAs without a requirement for initiation factors is unprecedented in eukaryotes but is characteristic of translation in prokaryotes. Prokaryotic mRNAs bind to small (30S) ribosomal subunits as a result of base pairing between the Shine-Dalgarno (SD) sequence and complementary anti-SD sequences in the 16S rRNA (Shine & Dalgarno, 1974). The sequences in the HCV IRES that are recognized by the 40S ribosomal subunit have not yet been identified. However, nucleotides 1-39, 26-67, 172-227, 229-238 and 332-341 of the HCV 5′-UTR and all of the coding sequences can be deleted without preventing binary [40S subunit-IRES] complex formation, so these sequences do not contain primary determinants of ribosomal binding. Binding of the IRES to the 40S subunit therefore appears to require the base of the stem-loop III including subunit IIId through IIIf and the stem-loop IV. HCV IRES-mediated initiation appears to involve sequential IRES-40S subunit interactions: a primary binding step is followed by interaction(s) that promote entry and accurate orientation of the initiation codon and flanking sequences in the mRNA-binding cleft. In contrast to attachment of prokaryotic ribosomes to the linear SD sequence, attachment of eukaryotic ribosomes to the HCV IRES is therefore likely to involve interactions with multiple discontinuous sites on this highly structured RNA.

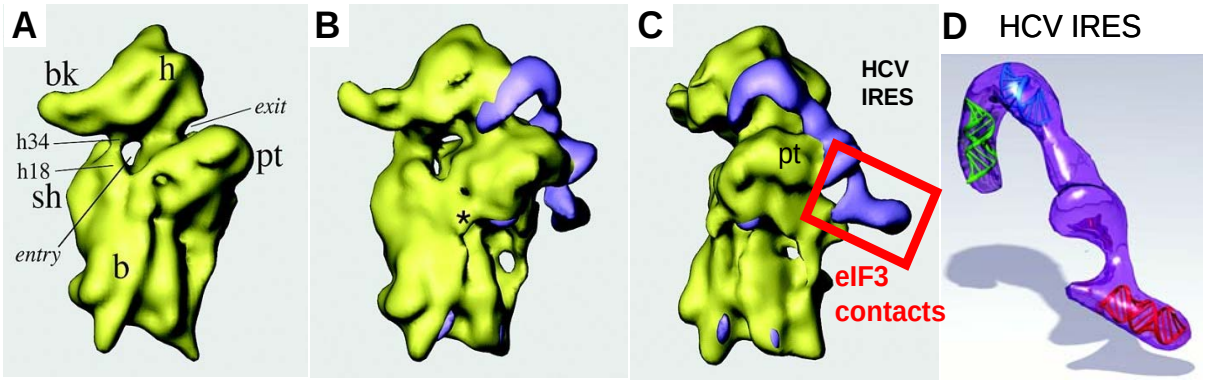

Fig. 8: The HCV IRES recruiting the 40S ribosomal subunit, visualized by cryo-electron microscopy. (A) Surface representation of the vacant 40S ribosomal subunit. Some landmarks of the 40S subunit are indicated: b, body of 40S subunit; bk, beak; h, head; pt, platform; sh, shoulder. "Entry" and "exit" label the proposed entry and exit path, respectively, of the mRNA. h18 and h34 indicate the positions of helices 18 and 34, respectively, of the 18S rRNA as identified by comparison with a cryo-EM map of the 80*S* ribosome from yeast. **(B)** The 40S subunit in complex with the HCV IRES RNA viewed from the 60S side of the 40S subunit, and from the platform (pt) side **(C)**, respectively. The cryo-EM maps are shown in yellow. The map corresponding to the full-length HCV IRES RNA is superposed and shown in purple. The conformation change in the IRES-40S subunit complex is indicated with an asterisk in **(B)**. The contacting point of eIF3 with the HCV IRES is squared. **(D)** The full-length HCV IRES RNA helix (Modified from Spahn et al., 2001).

eIF3 is stoichiometrically associated with free 40S ribosomal subunits in the cytoplasm and is therefore effectively a constitutive component of native 40S subunits (Sundkvist & Staehelin, 1975). eIF3 binds specifically to BVDV, CSFV and HCV IRESes (Pestova et al., 1998b), and chemical and enzymatic foot-printing has localized its binding site to an internal bulge between subdomain IIIa and IIIb of the HCV IRES, and to an identical position in the CSFV IRES (Sizova et al., 1998). Mutations in the HCV IRES that impair

binding of eIF3 all reduce the activity of the IRES (Buratti et al., 1998; Sizova et al., 1998; Pestova et al., 1998b).

The affinity of 40S subunit and of eIF3 for distinct structural elements in HCV IRES may enhance binding of native 40S subunits to the viral RNA in the cytoplasm where it competes with cellular mRNAs for the translation apparatus. The presence of binding sites for two different components of native 40S subunits on the IRES is also likely to promote ribosomal attachment to them in an orientation that promotes entry of the initiation codon into the ribosomal P site.

The binding site for eIF3 has been mapped by using cross-linking, toe- and foot-printing to the apical half of domain III (Buratti et al., 1998; Sizova et al., 1998; Pestova et al., 1998b; Pestova & Hellen, 1999; Odreman-Macchioli et al., 2000; Kieft et al., 2001). Although eIF3 is not needed for 48S complex formation, it binds specifically to the IRES and is likely to be a constituent of 40S/IRES complexes *in vivo*. UV cross-linking of eIF3 to [α-^{32}P]-UTP labelled HCV and CSFV IRES elements resulted in strong labelling of four (p170, p116/110, p66, p47) of the twelve subunits of eIF3 (Buratti et al., 1998; Sizova et al., 1998; Ji et al., 2004), but it is not yet known which subunit(s) are primary determinants of this interaction. Presumably, eIF3 may destabilize incorrectly assembled 48S complexes (Kolupaeva et al., 2000b) and play a role in stages of initiation after 48S complex formation (Pestova et al., 1998b). The independent interaction of eIF3 and eIF2/GTP/initiator-tRNA/40S subunit complex with the HCV-like IRESes is likely to enhance the affinity and specificity of binding and to stabilize the resulting 48S IRES/mRNA complexes.

1.6.2.4 Cellular *trans*-acting factors interacting with the HCV IRES

In addition to eIF3, the HCV IRES element also recruits additional cellular host RNA-binding proteins that are not involved in normal cellular cap-dependent translation to commence efficient internal translation initiation (Niepmann, 1999; Belsham & Sonenberg, 2000). Up to present knowledge, these cellular proteins include:

(1) Human La autoantigen (52 kDa), an RNA-binding protein that belongs to the RNA recognition motif superfamily, which is involved in initiation and termination of RNA polymerase III transcription (Gottlieb & Steitz, 1989; Maraia et al., 1994; Maraia, 1996). In poliovirus translation, La was the first cellular factor identified to bind the IRES in close proximity of the conserved AUG codon (Meerovitch et al., 1989). Addition of La protein to rabbit reticulocyte lysate (RRL) greatly enhances the translation of poliovirus mRNA at the correct initiation site and inhibits translation initiation at incorrect sites (Meerovitch et al., 1993; Svitkin et al., 1994).

(2) The polypyrimidine tract-binding protein (PTB, 57 kDa) is one of the most studied non-standard cellular factors which plays a role in translation initiation of most picornaviruses. It was initially characterized as a component of splicing complexes (Garçia-Blanco et al., 1989) that is involved in the differential splice site selections with various cellular mRNAs (Valcárcel & Gebauer, 1997). PTB binds the IRES elements of most picornaviruses (Table 6) like EMCV (Jang & Wimmer, 1990), FMDV (Luz & Beck, 1990), Poliovirus (Hellen et al., 1994) and rhinovirus (Borman et al., 1993). By the use of depletion and reconstitution systems it has been shown that PTB stimulates the translation of EMCV (Borovjagin et al., 1994; Kaminski et al., 1995), FMDV (Niepmann, 1996; Niepmann et al., 1997) and rhinovirus (Hunt & Jackson, 1999b). PTB binds to two separate regions in the FMDV IRES RNA, the domain 2 near the 5´ end of the IRES and a second binding region including the polypyrimidine tract and the domain 4 in the 3´ part of the IRES. Moreover, it has been

demonstrated that PTB is a component of both 48S and 80S ribosomal initiation complexes formed with FMDV IRES RNA (Niepmann et al., 1997). Very recently, PTB has been proven to a monomer rather than a dimer which challenges the previous concept of PTB dimerization (Simpson et al., 2004; Amir-Ahmady et al., 2005; Song et al., 2005). The actual mode of function of PTB in picornavirus translation is not yet understood. However, the influence of PTB on EMCV translation varies with the sequence context of the IRES (Kaminski & Jackson, 1998). This leads to the idea that PTB may act as an "RNA chaperone" that aids to maintain an appropriate tertiary structure of the IRES. In the case of HCV IRES element, it is still controversial if PTB binds to the HCV IRES element or not (Ali & Siddiqui, 1995; Kaminski et al., 1995; Ito & Lai, 1999).

(3) Heterogeneous nuclear ribonucleoprotein L (hnRNP L, 68 kDa) binds to a region about nucleotides between the authentic HCV AUG codon at position 342 and 402 in the HCV core protein-encoding sequence, i.e., directly downstream of the binding site for La mentioned above (Hahm et al., 1998b). This sequence partially represents the 3´ border of the IRES and contributes to IRES function. Binding of hnRNP L to this sequence correlates with IRES activity, suggesting that hnRNP L might also be involved in the regulation of HCV IRES activity. The close vicinity of the binding sites for La and hnRNP L points to a possible interaction between these two proteins in HCV translation, and even hnRNP L and PTB may interact each other since the N-terminal RRM domain of PTB was shown to bind to hnRNP L (Hahm et al., 1998a).

(4) The Poly(rC) binding protein (PCBP, 39 kDa), also known as hnRNP E, is another cellular protein, which binds specifically to the poliovirus (Blyn et al., 1996; Gamarnik & Andino, 1997; Parsley et al., 1997) and the hepatitis A virus IRES RNA (Graff et al., 1998). PCBP exists in two isoforms, PCBP1 and PCBP2. Both isoforms of PCBP specifically interact with two domains of the poliovirus 5´-UTR, the 5´-terminal cloverleaf structure of the viral plus-strand RNA and the domain IV of the IRES. Depletion of PCBPs from HeLa cell extracts inhibits the IRES activity to support the translation of poliovirus, rhinovirus and coxsackie B virus, but translation of EMCV and FMDV was not affected. Recombinant PCBP2 but not the closely related PCBP1 (> 80 % amino acid identity) restored the activity of entero-/rhinovirus IRES elements (Blyn et al., 1997; Walter et al., 1999). In the case of HCV, PCBP-1 and PCBP-2 were found to bind specifically to the HCV 5´-untranslated region (Spangberg & Schwartz, 1999b). However, no functional involvement of PCBP in HCV IRES function was reported so far.

IRES	**Translation initiation factors**	**Trans-acting cellular factors**
EMCV	eIF4G-Ct, eIF4A, eIF3, eIF2	PTB, La
FMDV	eIF4B, eIF4G-Ct, eIF4A, eIF2, eIF3	PTB, $ITAF_{45}$
Poliovirus	eIF4B, eIF3, eIF4G-Ct	PTB, PCBP2, La, Unr
Rhinovirus	not investigated	PTB, PCBP2, La, Unr, Unrip
HCV	eIF2 and eIF3 only	PTB (controversial), La, hnRNP L, PCBP1 and 2, NSAP1

Table 6: Functional RNA-protein interactions in viral IRES elements. (Ct, C-terminal)

Also, other cellular RNA-proteins were reported to interact with HCV IRES element, such as ribosomal proteins (Fukushi et al., 1999; Fukushi et al., 2001; Otto et al., 2002), the proteasome subunit PSMA7 (Krüger et al., 2001), nucleolin (Izumi et al., 2001), NS1-associated protein 1 (NSAP1) (Kim et al., 2004) and some other

proteins that were only qualitatively observed but not yet further confirmed (Lu et al., 2004). These considerations suggest that the role of these RNA-binding proteins, which bind at multiple sites, may somehow stabilize the complex secondary and tertiary structure of the IRES to allow the conserved motifs to interact with the cellular translation machinery.

1.6.3 The HCV 3´-untranslated region (3´-UTR)

Unlike most of the viruses carrying a poly (A) tail at the 3´ terminal end of their RNA genomes, the HCV genome contains an unusual specific untranslated region at the 3´ end. This is a very characteristic region in the HCV RNA genome. The length of it is usually shorter, about 221-225 nucleotides, than that of the 5´-UTR. This 3´UTR also contains significantly ordered RNA structures with three distinct regions: (1) an upstream variable region (VR) within which substantial sequence diversity is evident between different genotypes of HCV; (2) a poly(U)-poly(UC) [poly-(U/UC)] tract; and (3) a very highly conserved, 98-nucleotide 3´ terminal segment (called 3´X-region or X-tail) which putatively forms three stem-loop structures (designated SL1, SL2 and SL3, in the 3´- to 5´- direction) (Fig. 9) (Tanaka et al., 1995; Kolykhalov et al., 1996; Ito & Lai, 1997). The poly-(U/UC) tract and the downstream 3´-X are both required for infectivity of synthetic, genome-length RNA inoculated into chimpanzees (Morita et al., 1999; Kolykhalov et al., 2000).

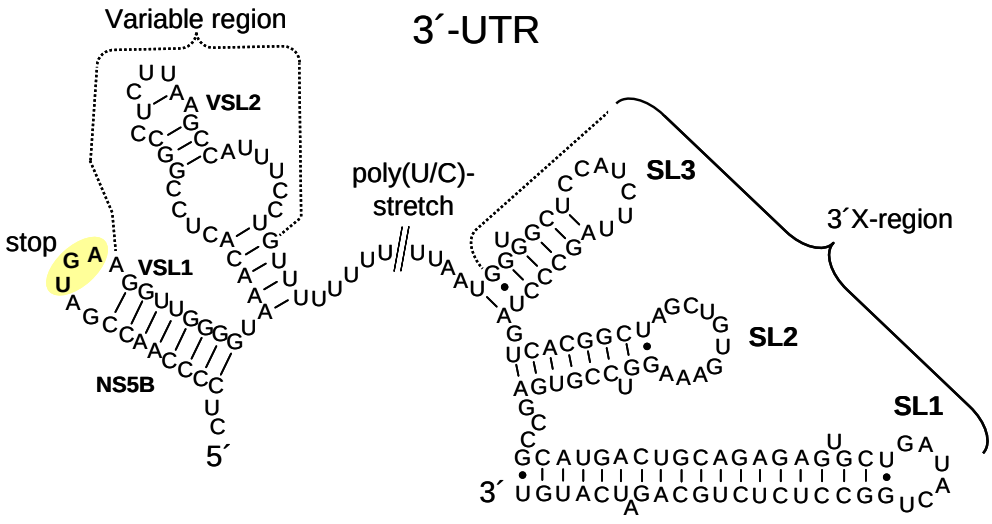

Fig. 9: Potential secondary structure of the 3´-UTR of the HCV genotype 1a. Modified from the references (Blight & Rice, 1997) and (Kolykhalov et al., 2000) with the two stem-loops in the variable region (VSL1 and VSL2) and the other two domains as described in the text. The VSL1 includes the very 3´-end sequences of NS5B coding sequence and the very beginning part of variable region sequences. The stop codon of the polyprotein ORF is highlighted in bold.

In addition, the VR segment also contributes to efficient RNA replication, shown by using subgenomic replicons derived from the Con1 strain of HCV (Friebe & Bartenschlager, 2002; Yi & Lemon, 2003a). In a recently published paper, Friebe and co-workers have shown that a nucleotide sequence complementarity between the

upper loop of the non-structural protein NS5B and the loop region of SL2 in the 3´ X-region, which is called a pseudoknot (kissing-loop) structure, is essential for the replication (Lee et al., 2004; You et al., 2004; Friebe et al., 2005). Furthermore, the 3´-UTR of HCV was also reported to play putatively a stimulating role in the HCV RNA translation activity although some conflicting data have been reported (Ito et al., 1998; Ito & Lai, 1999; Fang & Moyer, 2000; Michel et al., 2001; Murakami et al., 2001; Friebe & Bartenschlager, 2002; Kong & Sarnow, 2002; McCaffrey et al., 2002; Imbert et al., 2003). In this work, the 3´-UTR has been found to play a very important role in the HCV translation, which will be described in the third part of the Results section.

1.7 Aims of this work

In the work presented in this thesis, the functional interactions of several known cellular factors with the Hepatitis C Virus and FMDV internal ribosome entry site elements and the possible role of the 3´-UTR of HCV in the IRES-dependent translation have been studied in detail.

The aim of the first part of this work was to attempt to search for some other cellular proteins that might bind specifically to the IRES of HCV in order to achieve a better understanding of the translation initiation pathway directed by HCV internal ribosome entry sites. Using a combination of several techniques such as electrophoretic mobility shift assay (EMSA), UV cross-linking assay and western blot, the interaction of several proteins with HCV IRES RNA has been investigated. The possible binding sites for those unknown proteins that may bind to the HCV IRES element were tentatively determined as well.

The main goal of the present study was to address whether and how the 3´-UTR of HCV RNA influences the HCV translation activity directed by the HCV internal ribosome entry site, either *in vitro* or *in vivo*, since many conflicting effects of the HCV 3´-UTR on the HCV translation have been reported previously. Besides, the effects of HCV mutants introduced into the 3´-UTR structure on the HCV translation efficiency were also determined.

In the last part of this work, promoted by the profound positive results derived from the translation stimulation by the HCV 3´-UTR, a very promising observation - the binding of a novel, but as yet not known protein of about 210 kDa - has been detected by using a new HCV clone. This 210 kDa protein binds specifically to the 3´-UTR of HCV and may be involved in the stimulation of translation by the 3´-UTR.

2 Materials and Methods

2.1 Materials

2.1.1 Bacterial strains and cell lines

2.1.1.1 Bacterial strains

BL21-CodonPlus-RIL

BL21-CodonPlus-RIL (*E. coli B F*$^-$, *ompT*, *hsdS*(r_B^- m_B^-), *dcm*$^+$, *Tet*^{r}, *gal*, *endA*, *Hte*, (*argU*, *ileY*, *leuW*, *Cam*^{r})). This strain, a derivative of *E. coli* B, is a general protein expression strain that lacks both the Lon protease and the O*mp* T protease which can degrade proteins during the purification process.

***E. coli* DH5 α**

E. coli DH5 α is highly transformable and usually used for large-scale production of plasmid DNAs. This strain also generates low endonucleases during incubation.

***E. coli* XL1-Blue**

E. coli XL1-Blue (*F*$^-$*::Tn10*, *proA*$^+$*B*$^+$*lac*^{9}, (*lacZ*), *M15/recA1end*, *A1gyrA96*, (*Nal*^{r})*thi*, *hsdR17* (r_k^- m_k^-), *supE44*, *relA1lac*), is a strain with the EndA$^-$ phenotype that allows the production of large amounts of DNA with a high quality.

2.1.1.2 Mammalian cell lines

The following four cell lines were kindly provided by Dr. D. Glebe, Dr. M. Kann and Dr. S. Kanse, respectively:

Huh-7	(Human hepatocellular carcinoma cells)
Hep G2	(Human caucasian hepatocyte carcinoma cells)
HeLa	(Human negroid cervix epitheloid carcinoma cells)
BHK-21	(Baby hamster kidney cells)

2.1.2 Materials for bacterial growth and cell culture

2.1.2.1 Materials for bacterial growth

Standard I medium (Merck, Darmstadt)

- with 25 µg/ml Kanamycin and/or 150 µg/ml Ampicillin
- with 5 µg/ml Tetracycline and/or 150 µg/ml Ampicilli

Luria-Broth (LB) medium

- 0.5 % (w/v) Extract of yeast powder
- 1 % (w/v) Peptone from meat, trypsin-digested
- 1 % (w/v) NaCl

adjusted to pH 7.5, autoclaved

LB plates

- 1.5 % (w/v) Bacto Agar (Difco, Augsburg) high-gel strength in LB medium, autoclaved

Antibiotic plates

- Standard I plates with 25 µg/ml Kanamycin and/or 150 µg/ml Ampicillin
- Standard I plates with 5 µg/ml Tetracycline and/or 150 µg/ml Ampicillin

2.1.2.2 Materials for cell culture

Dulbecco's Modified Eagle's Medium (DMEM)	Invitrogen, USA
Fetal Bovine Serum (FBS)	Invitrogen, Germany
100× Penicillin-streptomycin solution (10,000 U/ml penicillin and 10,000 µg/ml streptomycin)	Invitrogen, Germany
10× Trypsin-EDTA (0.5 g/L Trypsin, 0.2 g/L EDTA)	Invitrogen, Germany
Tissue culture petri dishes	BD Labware, USA
Tissue culture flasks	TPP, Germany
6-, 12- and 24-well microplates	TPP, Germany

2.1.3 Plasmids

pHCV-FL-1b	Kindly provided by Prof. Dr. R. Bartenschlager, University of Heidelberg.
pHCV-1a	Kindly provided by Dr. S-E. Behrens, modified by M. Niepmann and Y. Song. For plasmid details, see Appendix -- pHCV wt clone map.
pHCV-FL-1a+1b	Modified and constructed by M. Niepmann and Y. Song.
pHCV Δ1, Δ2	Constructed by Dr. S-E. Behrens, modified by M. Niepmann and Y. Song
All HCV deletion mutants used in this study	Constructed by Y. Song
pM12	Constructed by K. Ochs (Ochs et al., 1999)
pM12+HCV 3´UTR	Constructed by Y. Song
pMPolio	Constructed by K. Ochs (Ochs et al., 2002)

2.1.4 Oligonucleotides

All oligonucleotides used in this work were obtained from Carl Roth GmbH, Karlsruhe.

Description	Length	Sequence (5´ - 3´)
HCMV_4986_for	27	CCA ATA GGC CGA AAT CGG CAA AAT CCC
HCMV_Luc_rev	23	TTC ACA ATT TGG ACT TTC CGC CC
HCV_3X_rev	22	ACA TGA TCT GCA GAG AGG CCA G
LD_forward	21	CGA TTT AGA GCT TGA CGG GGA
HCV_439_rev	21	CAC CAA CGA TCT GAC CAC CGC
Luz_rev	20	GTT CCA TCC TCT AGA GGA TA
H2099_for	24	GAC ATA GCT TAC TGG GAC GAA GAC
H3030_rev	21	CGA ACG ACC GAG CGC AGC GAG
PBS_172_for	24	CGT GGA CTC CAA CGT CAA AGG GCG
HCV_D3_rev	26	TAT CAG GCC CCG GGA GGG GGG GTC CT
HCV_D3_for	23	CTC CCG GGG CCT GAT AGG GTG CT
HCV_D3a_rev	23	GGC AAT TCG TTC CGC AGA CCA CT

Description	Length	Sequence (5´ - 3´)
HCV_D3a_for	23	TGC GGA ACG AAT TGC CAG GAT GA
HCV_D3b_rev	26	ACG CCC AAT CCG GTG TAC TCA CCG GT
HCV_D3b_for	26	ACA CCG GAT TGG GCG TGC CCC CGC GA
HCV_D3c_rev	23	CTC GCG GGC AAA TCT CCA GGC AT
HCV_D3c_for	23	GAG ATT TGC CCG CGA GAC TGC TA
HCV_D3d_rev	28	CCA CAA GGC TAG CAG TCT CGC GGG GGC A
HCV_D3d_for	23	ACT GCT AGC CTT GTG GTA CTG CC
HCV_D3e_rev	26	TCG CAA GCA GTA CCA CAA GGC CTT TC
HCV_D3e_for	26	GTG GTA CTG CTT GCG AGT GCC CCG GG
HCV_D3f_rev	23	TCC CGG GGC ACC CTA TCA GGC AG
HCV_D3f_for	23	ATA GGG TGC CCC GGG AGG TCT CG
HCV_aug_rev	29	GAG GTT TAG GCT ACG AGA CCT CCC GGG GC
HCV_aug_for	23	TCT CGT AGC CTA AAC CTC AAA GA
3X_Gen_for	21	GGG CGT GGA TAG CGG TTT GAC
3X_Gen_rev	22	CGC AGC GAG TCA GTG AGC GAG G
D3SL1_rev	21	GGC TCA CGG ACC TTT CTC TGC
D3SL2_rev	23	CAT GCG GCC TAG GGC TAA GAT GG
D3SL2_for	23	AGC CCT AGG CCG CAT GAC TGC AG
D3SL1+2_rev	22	CTA GGG CTA AGA TGG AGC CAC C
D3SL3_rev	25	GCC GTG ACT TAA AGA AGG GAA AAA G
D3SL3_for	24	TTC TTT AAG TCA CGG CTA GCT GTG
D3VR_rev	24	CCG GGA AAT GGT CAC AAT TTG GAC
D3VR_for	26	CCA AAT TGT GAC CAT TTC CCG GTT TT
D3UC_rev	20	AGC CAC CAC CGG GAA ATG GC
D3UC_for	21	TTT CCC GGT GGT GGC TCC ATC
D3VUC_rev	26	GAG CCA CCT TCA CAA TTT GGA CTT TC
D3VUC_for	26	ATT GTG AAG GTG GCT CCA TCT TAG CC
D3UCX_rev	24	CCG GGA AAT GGC TTA AGA GGC CGG
D3SL2+3_rev	25	CAT GCG GCT TAA AGA AGG GAA AAA G
D3SL2+3_for	23	TTC TTT AAG CCG CAT GAC TGC AG
FL_RD15_rev	33	ACA TAA CAA ATC TAA TCA CAA TTT GGA CTT TCC
HCMV_Dcore_rev	22	ATC TGC ATG ACG TCC TGT GGG C
HCMV_Dcore_for	23	AGG ACG TCA TGC AGA TCT TCA TG
Up_kpn_for	25	GTC AGA TCT ACG GGG CCT GTT ACT C
Dn_kpn_rev	23	ACC CCA ACC TTC ATC GGT TGG GG
Up_spe_for	28	AAC CGA TGA AGG TTG GGG TAA ACA CTC C
Af_spe_rev	27	GGC GAC TAG TAC ATG ATC TGC AGA GAG
Up_afl_for	22	GAC CCC GCT GGT TCA TGT GGT G
Dn_afl_rev	24	ATG CCG GCC ACA TGA TCT GCA GAG
Up_hdv_for	22	GAT CAT GTG GCC GGC ATG GTC C
Dn_spe_rev	21	GGT TCC GCG CAC ATT TCC CCG
5B_rev	21	ATG CCG GCC TCA TCG GTT GGG
Hdv_for	22	AAC CGA TGA GGC CGG CAT GGT C
Seq_spe_rev	21	ATT TCC CCG AAA AGT GCC ACC
Seq_kpn_for	23	ATG TAT GCG CCC ACC TTG TGG GC

2.1.5 Enzymes

2.1.5.1 Restriction endonucleases

All restriction enzymes used in this work were provided from Fermentas (MBI), Luckenwalde; New England Biolabs (Bio), Schwalbach; Boehringer Mannheim (Boehringer), Mannheim and Promega (Pro), Heidelberg. Reactions were performed according to protocols provided by the suppliers. Arrows indicate the cleavage site.

Enzyme	U/µl	Buffer	Supplier	Recognition Sequence
Aat II	20	NEB-4	Bio	GACGT$^{\downarrow}$C
Afl II(BspT I)	2	NEB-2	Bio	C$^{\downarrow}$TTAAG
Bam HI	20	NEB-2	Bio	G$^{\downarrow}$GATCC
Bgl I	10	NEB-3	Boehringer	GCC(N_4)$^{\downarrow}$NGGC
Bgl II	10	NEB-3	Pro	A$^{\downarrow}$GATCT
BsiW I	15	NEB-3	Bio	C$^{\downarrow}$GTACG
Bsm I	5	NEB-2	Bio	GAATG$^{\downarrow}$CN
Bst XI	10	NEB-3	Bio	CCA$N_5^{\downarrow}$NTGG
EcoN I	15	NEB-4	Bio	CCTNN$^{\downarrow}$NNNAGG
EcoR I	20	spec. NEB-buffer	Bio	G$^{\downarrow}$AATTC
EcoR V	20	spec. NEB-buffer	Bio	GAT$^{\downarrow}$ATC
Hind III	20	NEB-2	Bio	A$^{\downarrow}$AGCTT
Kpn I	10	NEB-1	Bio	GGTAC$^{\downarrow}$C
Nco I	5	NEB-4	Bio	C$^{\downarrow}$CATGG
Nde I	20	50 mM NaCl	Bio	CA$^{\downarrow}$TATG
NgoM IV	10	NEB-4	Bio	G$^{\downarrow}$CCGGC
Nhe I	10	50 mM NaCl	Boehringer	G$^{\downarrow}$CTAGC
Pst I	20	NEB-3	Bio	CTGCA$^{\downarrow}$G
Sac I	10	NEB-Sac	Bio	AGT$^{\downarrow}$ACT
Sal I	20	Buffer H	Bio	G$^{\downarrow}$TCGAC
Sma I	10	NEB-4	Bio	CCC$^{\downarrow}$GGG
Spe I	10	NEB-2	Bio	A$^{\downarrow}$CTAGT
Van 91I	10	MBI-red	Fermentas	CCA$N_4^{\downarrow}$NTGG
Xba I	60	NEB-2	Bio	T$^{\downarrow}$CTAGA
Xho I	20	NEB-2	Bio	C$^{\downarrow}$TCGAG

2.1.5.2 Modifying enzymes

Enzyme	U/µl	Supplier
Alkline Phosphatase, Shrimp (SAP)	1	Roche, Mannheim
DNA-Polymerase (Klenow-fragment)	2	Boehringer, Mannheim
DNase I (RNase free)	10	Boehringer, Mannheim
Guanylyltransferase	5	Ambion
Poly(A) polymerase	750	USB Corporation, USA
Polynucleotide kinase (T4)	10	Biolabs, Schwalbach
Proteinase K (10 mg/ml)	10 µg/µl	Merck, Darmstadt
RNase A	10 µg/µl	Boehringer, Mannheim
SP6 RNA Polymerase	25	Fermentas, Oldendorf

Enzyme	U/µl	Supplier
Taq DNA Polymerase	5	Promega, Heidelberg
T3 RNA Polymerase	1.6	AGS, Heidelberg
T_4 DNA Ligase	6 Weiss Units	Biolabs, Schwalbach
T7 RNA-Polymerase	20	Fermentas, Oldendorf

* 1 Weiss Unit = 66.6 New England Biolabs Units.

2.1.6 Nucleotides

2.1.6.1 Radioactive nucleotides

All radiochemicals used in this study were obtained from Amersham Biosciences, Freiburg.

[α-^{32}P]-rATP: > 400 Ci/mmol, 10 mCi/ml
[α-^{32}P]-rCTP: > 400 Ci/mmol, 10 mCi/ml
[α-^{32}P]-rGTP: > 400 Ci/mmol, 10 mCi/ml
[α-^{32}P]-UTP: > 400 Ci/mmol, 10 mCi/ml
^{35}S-Met: > 600 Ci/mmol, 15 mCi/ml
[^{14}C]-Protein Marker, 5 µCi/ml

2.1.6.2 Non-radioactive nucleotides

Ribonucleoside triphosphates (rNTPs): Pharmacia LKB GmbH, Freiburg
Deoxyribonucleoside triphosphates (dNTPs), Boehringer, Mannheim

2.1.7 Size markers

2.1.7.1 Protein size markers

Protein	**(^{14}C)-methylated proteins (kDa)** (Amersham)
Myosin	220.0
Phosphorylase B (rabbit muscle)	97.4
Bovine serum albumin	66.0
Ovalbumin	45.0
Carboanhydrase	30.0
Lysozyme (hen egg white)	14.3

10 kDa protein ladder, Invitrogen, USA

Protein	**Prestained (kDa)** (New England Biolabs)
MBP-β-Galactosidase	175.0
MBP-Paramyosine	83.0
Glutamine dehydrogenase	62.0
Aldolase	47.0
Triosephosphate isomerase	32.0
β-Lactoglobuline A	25.0
Aprotinin	6.0

2.1.7.2 DNA size markers

DNA ladder marker: (BioLine)	10 kbp, 8000 bp, 6000 bp, 5000 bp, 4000 bp, 3000 bp, 2500 bp, 2000 bp, 1500 bp, 1000 bp, 800 bp, 600 bp, 400 bp, 200 bp.

Another DNA marker was obtained from R. Füllkrug, Gießen: pSP64 is cleaved with *Hind* III, *Dra* I and *Hinf* I, (a mixture with 1:2:4 of corresponding restricted plasmid was used).
DNA fragments: 2999 bp, 2288 bp, 1198 bp, 692 bp, 517 bp, 396 bp, 354 bp, 218 bp, 176 bp, 75 bp, 65 bp.

2.1.8 Recombinant proteins

--Human PTB fused to $(His)_6$ at N-terminus (59.1 kDa)	Kindly provided by Dr. M. Niepmann, Giessen
--His-Unr protein	Kindly provided by Dr. H. Jacquemin-Sablon, Bordeaux, France
--GST-hnRNP L protein	Kindly provided by Prof. A. Bindereif, Giessen

2.1.9 Chemicals and reagents

Acrylamide solution (40 %)	Roth
Ammonium persulfate (APS)	Serva
Bovine serum albumin (BSA)	Merck
5-Bromo-4-chloro-3-indolyl-phosphate (BCIP)	GERBU
Bromophenol blue (RNase free)	Sigma-Aldrich
Collagen	Sigma-Aldrich
Coomassie brilliant blue R-250	Serva
Dimethyl sulfoxide (DMSO)	Merck
Dithiothreitol (DTT) (RNase free)	Biozyme
Ethylene diamine tetra acetic acid (EDTA)	Merck
Ethidium bromide	Fluka
Formamide	Gibco-BRL
Glycerol	Roth
L-Glutathione (reduced form)	Serva
Glutathione sepharose 4B	Pharmacia
HEPES (N-[2-Hydroxyethyl]piperazine- N´-[2-ethanesulfonic acid])	Roth
Imidazole	Sigma
MOPS	Serva
Ni-NTA agarose	Qiagen
Nitro blue tetrazolium (NBT)	GERBU
N,N,N´,N´-Tetra methyl ethylene diamine (TEMED)	Sigma-Aldrich
Poly(U)-sepharose	Pharmacia
Phenylmethylsulfonylfluoride (PMSF)	Boehringer
D(+)-Sucrose	Roth
TALON	CloneTech
Transfer-RNA (tRNA)	Sigma
Tris (Hydroxymethyl)-aminomethan	Roth
Tween 20 (Polyoxyethylenesorbitan monolaurate)	Sigma

Other inorganic chemicals, organic substances and solvents were purchased from Sigma-Aldrich, Merck, Boehringer Mannheim GmbH, Serva, Difco and ICN Biochemicals GmbH.

2.1.10 Kits

Easy pure DNA purification kit, Biozyme, Oldendorf
GFX *Micro* Plasmid Prep Kit, Amersham Biosciences
GFX PCR DNA and Gel Band Purification Kit, Amersham Biosciences
Materials for DNA affinity purification of plasmid DNA, Nucleobond, Macherey-Nagel GmbH & Co KG
Materials for DNA affinity purification of plasmid DNA, Jetstar, Genomed GmbH, Bad Oeynhausen
Plasmid purification midi kit, Qiagen
Poly(A) tailing kit, USB Corporation
RNA Capping kit, Ambion
RNA TransMessenger® transfection Kit, Qiagen
RNeasy Purification kit, Qiagen

2.1.11 Cell culture flasks and pipets

T-50 cell culture flasks, Greiner
5-ml plastic pipets, Falco
10-ml plastic pipets, Falco

2.1.12 Photo materials and X-ray films

Cronex MD-Developer, Du Pont, Bad Homburg
Cronex MF-E Fixer, Du Pont, Bad Homburg
Film Cassettes Cronex Lightning Plus, Du Pont, Boston, USA
Kodak Biomax BMS X-ray film, Eastman Kodak, Rochester, NY, USA
Kodak Biomax BMR 1 X-ray film, Eastman Kodak, Rochester, NY, USA
Kodak X-omat XAR5 X-ray film, Eastman Kodak, Rochester, NY, USA
Polaroid 667 Professional, Polaroid Corporation, Cambridge, MA, USA

2.1.13 Equipments

All equipments needed for this work are listed as following:

Centrifuges
Low speed centrifuge: J2-21 with rotors JA 10, JA 14, JA 17, JA 20, Beckman Instruments, Summerset, USA
Table centrifuge: Eppendorf centrifuge 54156.
Ultracentrifuge: Optima LE-80K with SW41 Ti rotor, Beckman Instruments, Summerset, USA

Gel-electrophoresis systems
Horizontal minigel-system, AGS, Heidelberg
Mini-gel chamber, Keutz, Reiskirchen
Power supply, EPS 500/400, Pharmacia LBK, Freiburg

Shakers
Diffusions-Destain apparature, Desaga, Heidelberg
Mixer 54322, Eppendorf, Hamburg

Mixer, Ikamag Ret, Ika-Werk, Staufen i.Br.
Vortex Genie2, Scientific Industries Bohemia, New York

Other equipments

Fast-Blot-Apparatur, Biometra, Göttingen
Luminometer (Lumat LB9507), Berthold, Germany
PCR instrument, Biometra GmbH, Göttingen
Polaroid MP-4 Land Camera, Polaroid Corporation, Cambridge, USA
Robocycler, Stratagen, Gebouw, California
Transilluminator, Herolab GmbH, Wiesloch
TRI-CARB 1500, Liquid Scintillation Analyser, PACKARD, A Canberra Company
Ultraviolett light (hand lamp) Konrad Benda, Wiesloch

2.1.14 Buffers and solutions

For all buffers, the final concentrations are given and stock solutions are indicated in brackets.

2.1.14.1 Buffers for DNA and RNA gel electrophoresis

TAE-buffer (E-buffer)	40.0	mM	Tris-OH, pH 8.0
(20× stock solution)	40.0	mM	Sodium acetate
	2.0	mM	EDTA
TBE-buffer	90.0	mM	Tris-borate, pH 8.3
(10× stock solution)	2.5	mM	EDTA
Gel-loading buffer (FM), native	75.0	% (v/v)	Glycerol
Stock solution	0.1	mM	EDTA
	0.1	%	Bromophenol blue
	0.1	%	Xylene cyanol FF
Gel-loading buffer (FA), denaturing	80.0	%	Formamide
Stock solution	1.0	mM	EDTA
	0.1	% (w/v)	Bromophenol blue
	0.1	% (w/v)	Xylene cyanol FF
Staining solution	2.0	µg/ml	Ethidium bromide in TAE buffer
(5,000× stock solution)			

2.1.14.2 Buffers for protein gel electrophoresis

Acrylamide solution (40:1)	30.0	% (w/v)	Acrylamide
	0.75	% (w/v)	Bisacrylamide
Stacking gel buffer	125.0	mM	Tris-HCl, pH 6,8
(4× stock solution)	0.1	% (w/v)	SDS
Seperating gel buffer	375.0	mM	Tris-HCl, pH 8.8
(4× stock solution)	0.1	% (w/v)	SDS

Loading buffer	125.0	mM	Tris-HCl, pH 6.8
	20.0	%	Glycerol
	10.0	%	ß-Mercaptoethanol (added freshly)
	4.0	% (w/v)	SDS
	0.02	% (w/v)	Bromophenol blue
Loading buffer with urea	125.0	mM	Tris-HCl, pH 6,8
	7.0	M	Urea
	20.0	%	Glycerol
	10.0	%	ß-Mercaptoethanol (added freshly)
	4.0	% (w/v)	SDS
	0.02	% (w/v)	Bromophenol blue
Running buffer (TG)	25.0	mM	Tris-OH, pH 8.3
(10× stock solution)	192.0	mM	Glycine
	0.1	% (w/v)	SDS
Coomassie blue staining solution	50.0	%	Ethanol
	10.0	%	Acetic acid
	0.1	% (w/v)	Coomassie brilliant blue R-250
Destaining solution	7.5	%	Acetic acid
	5.0	%	Ethanol

2.1.14.3 Buffers for molecular biological methods

Ligase buffer	20.0	mM	Tris-HCl, pH 7.5
(10× stock solution)	5.0	mM	$MgCl_2$
	5.0	mM	DTT
	50.0	µg/ml	BSA
	0.5	mM	ATP (added separately)
Transcription buffer	50.0	mM	Tris-HCl, pH 7.5
(5× stock solution)	10.0	mM	$MgCl_2$
	10.0	mM	Spermidine
Alkaline phosphatase-(SAP) buffer	50.0	mM	Tris-HCl, pH 8.5
(10× stock solution)	0.1	mM	EDTA
Proteinase K buffer	50.0	mM	Tris-HCl, pH 7.5
(10× stock solution)	10.0	mM	$CaCl_2$
	0.5	% (w/v)	SDS

2.1.14.4 Buffer for plasmid DNA preparations

Phenol buffer	80.0	% (w/v)	Phenol
	50.0	mM	Tris-OH
	0.1	%	Hydroxy chinoline

TE-buffer	10.0	mM	Tris-HCl, pH 8.0
	0.1	mM	EDTA
TELT buffer	50.0	mM	Tris-HCl, pH 7.5
	62.5	mM	EDTA
	2.5	M	Lithium chloride
	0.4	%	Triton-X-100

2.1.14.5 Buffers and solutions for DNA purification with affinity columns

Sol A	5.0	mM	Tris-HCl, pH 8.0
	10.0	mM	EDTA
	50.0	mM	Glucose
	10.0	µg/ml	RNase A (added freshly before use)
Sol B	0.2	M	NaOH
	1.0	%	SDS
Sol C	3.0	M	Sodium acetate
	2.0	M	Acetic acid
QBT	50.0	mM	MOPS, pH 7.0
	750.0	mM	NaCl
	15.0	%	Ethanol
	0.15	%	Triton X-100
Wash buffer	50.0	mM	MOPS, pH 7.0
	1.0	M	NaCl
	15.0	%	Ethanol
Elution buffer	50.0	mM	MOPS, pH 8.2
	1.25	M	NaCl

2.1.14.6 Buffers for immunological methods

TBST 150-buffer	10.0	mM	Tris-HCl, pH 8.0
(20× stock solution)	150.0	mM	NaCl
	0.05	%	Tween-20
TBST 500-buffer	10.0	mM	Tris-HCl, pH 8.0
(20× stock solution)	500.0	mM	NaCl
	0.05	%	Tween-20
Block-buffer	10.0	mM	Tris-HCl, pH 8.0
(TBST 150 + BSA)	150.0	mM	NaCl
	3.0	%	BSA (added freshly, stir well)
	0.05	%	Tween-20
Transfer buffer	25.0	mM	Tris-OH, pH 8.3
(10× stock solution)	192.0	mM	Glycine
	10.0	%	Ethanol
	0.1	% (w/v)	SDS (only for large proteins)

Alkaline phosphatase buffer	100.0	mM	Tris-HCl, pH 9.5
	100.0	mM	NaCl
	5.0	mM	$MgCl_2$
Stop Mix	10.0	mM	Tris-HCl, pH 8.0
	1.0	mM	EDTA

2.1.14.7 Protein-RNA interaction buffers

Cross-linking buffer (for FMDV)	10.0	mM	HEPES, pH 7.9
(5× stock solution)	1.0	mM	DTT
	2.0	mM	$MgCl_2$
	1.0	µg/µl	tRNA
	10	%	Glycerol
	0.05	%	NP-40
	1.0	mM	ATP (added separately)
EMSA binding buffer (5×)	25.0	mM	HEPES, pH 7.4
	125.0	mM	KCl
	10.0	mM	$MgCl_2$
	10.0	mM	DTT
	0.5	mM	EDTA
	19.0	%	Glycerol
EMSA running buffer (1×)	45.0	mM	Tris-borate, pH 8.3
	1.25	mM	EDTA

2.1.14.8 Buffers for preparation of S10 lysate of HeLa or Huh-7 cells

Isotonic buffer (1×)	35.0	mM	Hepes, pH 7.4
	146.0	mM	NaCl
	11.0	mM	Glucose
Hypotonic buffer (1×)	20.0	mM	Hepes, pH 7.4
	10.0	mM	KCl
	1.5	mM	$MgCl_2$
	1.0	mM	DTT
	0.5	mM	PMSF
	0.1	mM	EDTA
	0.1	mM	EGTA
S10 buffer (10×)	200.0	mM	Hepes, pH 7.4
	1.2	M	KCl
	40.0	mM	$MgCl_2$
	50.0	µg/ml	DTT
Phosphate-buffered saline (PBS)	4.3	mM	Na_2HPO_4
(10× stock solution)	1.4	mM	KH_2PO_4
	137.0	mM	NaCl
	2.7	mM	KCl

2.1.14.9 Immunoprecipitation buffers

Binding buffer	20.0	mM	Tris HCl, pH7.5
	200.0	mM	NaCl
	10.0	µg/µl	BSA
Wash buffer A	50.0	mM	Tris-HCl, pH 7.5
	500.0	mM	NaCl
	1.0	mM	Imidazole
	100.0	µg/ml	tRNA
	50.0	µg/ml	BSA
Wash buffer B	50.0	mM	Tris-HCl, pH 7.5
	500.0	mM	NaCl
	1.0	mM	Imidazole
	100.0	µg/ml	tRNA
	100.0	µg/ml	BSA
	0.25	%	Tween-20
	0.25	%	NP-40
Phosphate-buffered saline (PBS)	8.0	mM	Na_2HPO_4
(10× stock solution)	2.0	mM	NaH_2PO_4
	140.0	mM	NaCl

2.1.14.10 Buffers for *in vitro* translation

Firefly Luciferase-assay reagent	20.0	mM	Tricine
(Promega)	1.07	mM	$(MgCO_3)_4Mg(OH)_2$ x 5 H_20
	2.67	mM	$MgSO_4$
	0.1	mM	EDTA
	33.3	mM	DTT
	270.0	µM	Coenzyme A
	470.0	µM	Luciferin
	530.0	µM	rATP
			pH 7.8
Dilution buffer for *Firefly* luciferase reagents			
	25.0	mM	Glycylglycine, pH 7.8
	15.0	mM	$MgSO_4$
	0.1	mM	EDTA
	33.3	mM	DTT
	1.0	mM	rATP
Renilla Luciferase-assay reagent	1.0	mg/ml	Coelenterazine in Methanol
(Roche)			
Dilution buffer for *Renilla* luciferase reagents			
	0.1	M	Potassium Phosphate, pH 7.4
	0.5	M	NaCl
	1.0	mM	EDTA

2.1.14.11 Buffers for purification of His_6-tag proteins under native conditions (Ni-NTA)

Lysis buffer	50.0	mM	NaH_2PO_4
	300.0	mM	NaCl
	10.0	mM	Imidazole
			adjust to pH 8.0 using NaOH
Wash buffer	50.0	mM	NaH_2PO_4
	300.0	mM	NaCl
	20.0	mM	Imidazole
			adjust to pH 8.0 using NaOH
Elution buffer	50.0	mM	NaH_2PO_4
	300.0	mM	NaCl
	250.0	mM	Imidazole
			adjust to pH 8.0 using NaOH
Dialysis buffer	10.0	mM	Tris-Cl, pH 7.5
(set up freshly)	0.1	mM	DTT
	10.0	mM	NaCl
	3.0	%	Glycerol

2.1.14.12 Buffers for RNase Protection Assay (RPA)

Hybridization buffer	80.0	%	Formamide
	40.0	mM	Tris-Cl, pH 7.5
	400.0	mM	NaCl
	1.0	mM	EDTA
RNase digestion buffer	10.0	mM	Tris-Cl, pH 7.5
	5.0	mM	EDTA
	300.0	mM	NaCl
	40.0	µg/ml	RNase A (added freshly)
	2.0	µg/ml	RNase T_1(added freshly, if needed)

2.2 Methods

2.2.1 Microbiological methods

2.2.1.1 Preparation of competent bacterial cells -- Classical $CaCl_2$ method

Preparation of competent bacterial cells using the $CaCl_2$ procedure is performed according to (Sambrook et al., 1989). The cells from an overnight culture are diluted in 1:50 or 1:100 with standard–I or LB medium containing appropriate antibiotics, and incubated further for 90 to 120 min at 37°C with vigorous shaking until the density of 1~2 × 10^8 cell/ml (or OD = 0.8 ~ 1) is reached. The culture is centrifuged at 5,000 rpm for 10 min at 4°C, cell pellets are resuspended gently in $^1/_5$ volume (based on the original culture volume) of ice-cold 30 mM $CaCl_2$ and incubated on ice for 30 min. Bacterial cells are recovered by centrifugation for 10 min at 5000 rpm at 4°C and resuspended in $^1/_{20}$ volume (based on the original culture volume) of ice-cold 30 mM $CaCl_2$. The competent cells are either used immediately for transformation or are prepared for freezing at -80°C by adding a certain volume of glycerol stock solution (final concentration of glycerol in cell suspension is 20 %). This procedure is less efficient but commonly used for transformation of supercoiled plasmid DNA or ligation solution.

2.2.1.2 Transformation of competent cells

For the transformation, 0.01-0.001 pmol of plasmid-DNA or ligation reaction (0.05-0.1 pmol) are added to 100 µl of competent cells and incubated on ice for 30 min. Cells are heat-shocked for 60-90 seconds at 42°C. After cooling for 3-5 min on ice, 900 µl of pre-warmed standard-I-medium or LB medium are added and incubated at 37°C for at least 1 hr. Transformed bacterial cells are pelleted by centrifugation and plated on selective antibiotics-containing plates.

2.2.2 Molecular biological methods

2.2.2.1 Preparation of plasmid DNA

Small-scale preparation of plasmid DNA

Plasmid DNA mini-preparation is usually done according to the following protocol: A single plasmid-containing bacterial colony is inoculated into 2-3 ml of LB medium containing corresponding amount of antibiotics (ampicillin, tetracyclin, kanamycin, etc) in a loosely capped 10 ml glass test-tube. The tube is incubated overnight at 37°C on shaking-bed. These cultures are collected by centrifugation at maximum speed for 20 sec. Supernatants (medium) are removed and cell pellets are completely resuspended in 300 µl of solution I by vigorous vortexing, until the pellets are completely dispersed. Then 300 µl of solution II (containing SDS and NaOH; SDS denatures bacterial proteins, and NaOH denatures chromosomal and plasmid DNA) is added. The content is mixed by inverting the tube a few times. After incubation for < 5 min at room temperature, the mixture is then neutralized by treatment with 600 µl of solution III (the plasmids then remain in solution containing potassium acetate, which causes the covalently closed plasmid DNA to reanneal rapidly to its supercoiled structure, while the bacterial chromosome and other components aggregate). The tube is inverted gently for 10-30 seconds until the precipitate is evenly dispersed. The tube is centrifuged at 13,000 rpm for 5 min at room temperature in a microcentrifuge (Heraeus, Germany). After centrifugation, the supernatant is transferred by

gentle aspiration to a GFX-column placed in a collection tube, and incubated at room temperature for 1-2 minutes. Then this column is centrifuged at full speed for 1 min. and the flow-through is discarded. Another 400 µl of wash buffer is loaded on the column and spun at 13,000 rpm for 1 min. The column with plasmid DNA is dried and then placed in a new microcentrifuge tube. Then the plasmid DNA is eluted by centrifugation for 1 min after incubation with a desired volume of TE buffer (pH 8.0) or sterilized double-distilled H_2O and stored at -20 °C.

Large-scale preparation of plasmid DNA

Large quantities of high quality plasmid DNA are purified from bacterial cultures by using Nucleobond® AX 100-affinity cartridges (Macherey-Nagel GmbH & CoKG, Düren). Bacterial cells from 100 ml of overnight plasmid-bearing bacterial cell cultures are harvested by centrifugation at 4,000 rpm for 10 min at 4°C.

The supernatants are discarded and bacterial cell pellets are resuspended carefully with 4 ml of buffer S1. Bacterial cells are lysed by addition of 4 ml of buffer S2, the suspensions are mixed gently by inverting the tube 4 to 6 times. Vigorous mixing should be avoided to prevent shearing of bacterial genomic DNA and subsequent contamination of plasmid DNA. After incubation for ≤ 5 min at room temperature, 4 ml of pre-cooled buffer S3 are added. This results in a precipitate containing chromosomal DNA and other cellular compounds. The suspension is gently mixed by inverting the tube 4 to 6 times until a homogeneous suspension is formed. The mixture is then incubated on ice for 5 min. Plasmid DNA is separated from SDS-protein complexes and chromosomal DNA by centrifugation at 14,000 rpm for 20 min at 4°C. The supernatant is removed carefully from the precipitate and further clarified by filtration using a Nucleobond® filter moisted with water. Clarified flow-through is loaded directly onto a Nucleobond® AX 100 affinity cartridge pre-equilibrated with buffer N2. The cartridge is washed three times with buffer N3. Finally, the plasmid DNA is eluted with 5 ml of buffer N5. Purified plasmid DNA is precipitated with 0.7 volume of isopropanol at room temperature. The DNA is pelleted by centrifugation for 30 min (13,000 rpm) at 4°C, pellets are washed two times with 80 % ethanol, air dried and redissolved in 100-120 µl of ddH_2O or TE buffer.

Extraction of plasmid DNA from agarose gel

For the elution of plasmid DNA from agarose gel, the easy pure DNA purification kit (Biozyme) is used. The desired DNA band is excised from ethidium bromide stained gel under long-wave length UV light. The approximate volume of the gel slice is determined by weight estimation of the agarose slice (100 µg is equal approximately to 100 µl binding buffer). The slice is then transferred to an eppendorf tube. The agarose gel slice is incubated for 5 min at 55°C with three volumes of "Salt Buffer" solution until the agarose gel is completely dissolved. DNA from the solution is allowed to bind to "Bind Matrix" at room temperature for 5 min with gentle rocking. For 1.5 µg of expected DNA, 1.5 µl of "Bind Matrix" is added. The matrix (with the bound DNA) is recovered by centrifugation for 5 seconds at 14,000 rpm. To wash the DNA, the matrix is resuspended in 1 ml of "Wash buffer" and centrifuged for a few seconds (this step is repeated two times). The rest of "Wash buffer" is discarded, and the matrix is dried by leaving the tube for 5 to 10 min at room temperature. The DNA is eluted using TE buffer. The supernatant containing eluted DNA is carefully removed, placed in a new eppendorf tube and stored at -20°C.

Phenol-chloroform extraction and ethanol precipitation

This protocol is used to purify and concentrate the DNA and RNA preparations. An equal volume of equilibrated phenol is added to the nucleic acid containing solution, vortexed vigorously and centrifuged at maximum speed for 5 min. The upper (aqueous) phase, which contains the nucleic acid, is placed into another centrifuge tube and

extracted with an equal volume of phenol : chloroform (1:1). The rest of phenol is removed by extraction with another equal volume of chloroform. Nucleic acids are precipitated by addition of 0.1 volume of 3 M sodium acetate pH 5.2 and of 2.5 volume of ice-cold 100 % ethanol (calculated after salt addition). After incubation for 0.5-1 hr on ice or at -20°C, nucleic acids are pelleted by centrifugation for 30 min at 13,000 rpm (4°C). Pellets are washed two times with 80 % ethanol, air dried, resuspended in a desired volume of ddH_2O or TE buffer (pH 8.0) and stored at -20°C.

2.2.2.2 Enzymatic modifications of DNA

Digestion of DNA with restriction endonucleases

Digestion of DNA with restriction endonucleases is performed according to the standard protocols as described by (Sambrook et al., 1989). For each restriction endonuclease, the optimal reaction conditions are chosen as recommended by the manufacturer. The amount of enzyme and DNA varies depending upon the specific application.
For most analytical purposes, 1 µg of DNA is digested with 1 unit of endonuclease enzyme in 25 µl reaction mixture. After incubation, aliquots of the digested DNA are tested on agarose gels. Digestion reactions are terminated by extraction with phenol : chloroform, and cleaved DNA is then ethanol precipitated.

Dephosphorylation of linearized DNA

The terminal 5´-phosphate can be removed from the termini of the linear DNA by treatment with shrimp alkaline phosphatase (SAP) (Roche Applied Corp.). This strategy is used to suppress self-ligation and re-circularization of the linear vector. To the restriction reaction, 0.1 volume of 10× SAP buffer and an appropriate amount of SAP (1 Unit SAP/1 pmol DNA end) are added. The reaction mixture is then incubated for 10 min (for sticky ends) or 1 hr (for blunt ends) at 37°C and 15 min at 65°C. At the end of the dephosphorylation reaction, SAP is removed by digestion with a small amount of proteinase K and the dephosphorylated DNA is then purified by the GFX PCR DNA and Gel Band Purification Kit.

Filling in a 5´-overhang with *Klenow*-fragment enzyme

Following a restriction enzyme digestion that generates 5´-overhang ends, the *Klenow* fragment of *E. coli* DNA polymerase I that possesses a 3´-5´ polymerase activity is used to fill 5´-overhang ends with deoxynucleotides (dNTPs). To the restriction reaction, 2.5 mM (final concentration) of dNTPs plus 100 U/ml *Klenow* enzyme are added and the reaction mixture is incubated for 30 min at 25°C. The DNA is extracted with phenol : chloroform and ethanol precipitated. DNA pellets are air dried and resuspended in ddH_2O.

Ligation reaction

Ligation of a segment of foreign DNA to a linearized plasmid vector is carried out using the ligase kit (Biolabs). To 0.03-0.05 pmol of dephosphorylated vector an appropriate amount of insert DNA is added in a molar excess of 3:1 or 5:1 with 1 µl of ligase buffer in a final volume of 10 µl ligation reaction. The ligation is performed at 12-14°C overnight after addition of 0.5 U T_4-DNA ligase.

Standard ligation reaction

1.0	µl	10× Ligase buffer
1.0	µl	5 mM ATP (for blunt ends) / 10 mM ATP (for sticky ends)
	µl	Vector (0.03 – 0.05 pmol)
	µl	Fragment (insert)
0.5	U	T_4-DNA ligase
	µl	Sterile ddH_2O
Σ = 10	µl	Final volume

The ligation reaction is incubated overnight at 12-14°C. Following the ligation reaction, ligated DNA is transformed into competent cells of an appropriate host strain.

2.2.2.3 Proteinase K digestion

Proteinase K is a highly active protease that is used to remove DNA-binding proteins and enzymes such as CIP that must be completely removed from DNA preparations if the subsequent ligations should work efficiently. To a mixture of dephosphorylated DNA reaction, SDS and EDTA (pH 8.0) are added to the final concentration of 0.5 % and 5 mM, respectively. After mixing, the reaction mixture is supplemented with 50 µg/ml of proteinase K and incubated for minimum 30 min at 56°C or overnight at 37°C. The DNA is recovered by centrifugation, phenol : chloroform extracted, ethanol precipitated and resuspended in TE buffer or ddH_2O.

2.2.2.4 The polymerase chain reaction (PCR)

The polymerase chain reaction is used to amplify *in vitro* a segment of DNA that lies between two regions of known sequence. The PCR simply entails mixing template DNA, two appropriate synthesized DNA oligonucleotide primers, thermostable Taq DNA-polymerase, deoxyribonucleotides (dNTPs), and buffer. Once assembled, the mixture is cycled many times through temperatures that permit denaturation, annealing, and synthesis to exponentially amplify a product of specific size and sequence.

The initial step in a PCR cycle denatures the target DNA by heating it to 94°C or higher for 15 sec to 2 min. In this denaturation process, the two intertwined strands of the DNA double helix separate from one another, producing the necessary single-stranded DNA template for the thermostable DNA polymerase. The next step of the cycle reduces the temperature to 40-65°C. At this temperature the oligonucleotide primers can anneal with the separate target DNA strands and serve as primers for DNA synthesis by the thermostable DNA polymerase. Finally, the synthesis of new DNA begins when the reaction temperature raises to 72°C. Extension of the primer by the polymerase lasts approximately 1 to 2 min. This cycle will be repeated 20 to 40 times. The amplified DNA is then analysed by gel electrophoresis and may be used for cloning.

Preparative PCR

The preparative PCR is performed to amplify DNA fragments for cloning. For preparative PCR, the high-fidelity *Taq* polymerase (Combizyme) is used. The reaction mixtures are prepared as follows:

Standard PCR reaction mixture

x	µl	Template DNA (final amount of DNA is 1 ng/µl)
1.0	µl	10× *Taq*-buffer
1.0	µl	25 mM $MgCl_2$
1.0	µl	2.5 mM dNTPs
0.5	µl	10 µM Oligonucleotide A
0.5	µl	10 µM Oligonucleotide B
0.15	µl	*Taq* DNA-polymerase (5 U/µl)
y	µl	Sterile ddH_2O
Σ = 10	µl	Final volume

The reaction components are mixed in a thin-walled 0.5 ml reaction tube. The PCR reaction mixture is placed in a thermal cycler. The PCR machine is basically programmed as follows:

30 Seconds, 94°C	Denaturation of the DNA template
45 Seconds, 55-60°C	Annealing (Hybridization, the exact temperature was decided according to the T_m of the two primers)
60 Seconds, 72°C	Elongation (extension of primer in 5´→3´ direction by the DNA–polymerase)

This cycle is repeated 19-24 times. The time for the last extension step is extended to 3-5 min to ensure that all the PCR products are full length. The amplified PCR product with the desired sequences is then purified by agarose gel electrophoresis. The recovered PCR product is digested with two selected restriction endonucleases, gel purified, and ligated to the vector previously cleaved with the same endonucleases.

2.2.3 *In vitro* transcription and translation

2.2.3.1 Preparation of DNA templates for *in vitro* RNA transcription

Plasmid DNA with either SP6 or T7 promoter is either linearized with an appropriate restriction endonuclease or amplified through standard PCR to generate appropriate RNA templates for *in vitro* transcription to produce RNA of defined length. Linearized DNA or PCR DNA fragments are then extracted with phenol : chloroform and ethanol precipitated.

2.2.3.2 *In vitro* transcription with T7- or SP6-RNA polymerase

The protocol for *in vitro* RNA transcription is based on the RNA synthesis by bacteriophage SP6 polymerase using a vector that contains SP6 promoter sequence as described (Melton et al., 1984). The reaction components should be kept at room temperature during the addition of each successive component to prevent the precipitation of DNA, since DNA can precipitate in the presence of spermidine at lower temperature. The transcription components are mixed in the order listed below:

Standard transcription reaction

x	µl	Sterile ddH_2O
2.0	µl	5× transcription-buffer (including DTT)
1.0	µl	2.5 mM rNTPs (Pharmacia)
	µl	Linearized or PCR DNA template (final concentration 20-40 ng/µl)
0.5	µl	T7 or SP6-RNA polymerase (20 U/µl)
Σ = 10	µl	Final volume (the volume of this reaction may be scaled up)

The reaction mixture is incubated for 60 min at 37°C (for T7 polymerase) or 40°C (for SP6 polymerase). An aliquot of the RNA transcript is examined for integrity of the synthesized RNA by 1 % agarose gel electrophoresis. The RNA is then extracted with phenol : chloroform and precipitated by addition of 2.5 volumes of ice cold 96 % ethanol after addition of 0.1 volume of 3 M sodium acetate pH 5.2. Following centrifugation (13,000 rpm) for 30 min at 4°C, the precipitate is washed two times with 80 % ethanol, air dried and resuspended in a desired volume of RNase-free H_2O.

2.2.3.3 *In vitro* transcription of radio-labelled RNA

Internally radio-labelled RNA is synthesized in a 10 µl reaction volume. As example, for transcription of [α-^{32}P] UTP labelled RNA, 50 µCi [α-^{32}P]-UTP (400 Ci/mmol, 10 mCi/ml) is used, and the concentration of the non-radio-labelled UTP is adjusted to 12.5 µM. The final concentrations of the three unlabelled nucleoside triphosphates (rATP, rCTP, rGTP) are adjusted to 250 µM.

Standard transcription reaction for the synthesis of radio-labelled RNA

x	µl	Sterile ddH_2O
2.0	µl	5× transcription-buffer (Biozyme)
1.0	µl	10 mM DTT
1.0	µl	2.5 mM rATP, rGTP, rCTP
1.0	µl	100 µM unlabelled UTP
1.0	µl	[α-^{32}P]-UTP (400 Ci/mmol, 10 mCi/ml) (final concentration = 2.5 µM)
		Linearized or PCR DNA template (20-40 ng/µl)
0. 5	µl	T7- or SP6-RNA Polymerase
Σ = 10	µl	Final volume

The transcription reaction is incubated at 37°C (for T7 RNA polymerase) or 40°C (for SP6 RNA polymerase) for 60-90 min. An aliquot of the RNA transcript is examined for the integrity of the synthesized RNA with denaturing 6 % polyacrylamide gel electrophoresis containing 7 M urea. Subsequently, the reaction mixture is phenol : chloroform extracted, and the RNA is precipitated by addition of 2.5 volumes of ice cold 100 % ethanol after addition of 0.1 volume of 3 M sodium acetate pH 5.2. The precipitate is washed two times with 80 % ethanol, air dried and resuspended in RNase-free H_2O. The RNA is separated from unincorporated nucleotides by gel filtration on Sephadex G-50 column (Pharmacia), ethanol precipitated, and redissolved in a desired volume of RNase-free H_2O.

2.2.3.4 *In vitro* translation

Unlabelled RNA is synthesized in the presence of 250 µM unlabelled nucleotides. Translation reactions contain 0.20 µg of RNA in a 10 µl reaction including 50 % rabbit reticulocyte lysate (Promega).

Standard reaction for *in vitro* translation

4.4	µl	Rabbit reticulocyte lysate (Promega)
0.85	µl	1 M KCl
0.2	µg	RNA (directly from *in vitro* transcription)
		Sterile ddH_2O
Σ = 10	µl	Final volume

RNAs (ca. 0.20 µg) are translated in RRL as described above in 10 µl reaction volume. The final concentration of K^+ in the reaction system should usually be adjusted to the physiological salt concentration (~135 mM K^+). The reaction mixtures are incubated for 60 min at 30°C and reactions are terminated by transferring the reaction mixture directly on ice. Aliquots of translation reactions are then used for measuring the translation efficiency.

2.2.4 Capping and poly(A) tailing of *in vitro* transcribed RNA

2.2.4.1 Capping of *in vitro* transcribed RNA

Mammalian mRNAs contain a 5′ terminal structure m^7GpppX found to be involved in many aspects of a cellular mRNA′s life cycle, including mRNA stability, mRNA transport and mRNA translation. Placing a 5′-cap analog onto an *in vitro* synthesized RNA transcript can be performed in vitro using cap analog and a phage RNA polymerase. The enzyme incorporates the cap analog onto the 5′-end of the RNA as it is being transcribed. However, a native 5′-cap can be added to an RNA transcript using the endogenous enzyme, guanylyltransferase. This reaction has the benefits of allowing researchers to specifically label their mRNA at the 5′-end so that they can study the translational efficiency using this modified mRNA transcript.

Guanylyltransferase, the vaccinia virus capping enzyme, is composed of two components, the D1 component (95 kDa) and the D12 component (33 kDa). It transfers GMP from GTP to RNA processing a di- or triphosphate terminus. The enzyme has three activities: (1) a 5′ RNA triphosphatase activity removes the 5′-terminal phosphate of a 5′-triphosphate RNA; (2) a guanylyltransferase activity transfers GTP to the 5′-end of the RNA in 3′→5′ orientation producing a 5′-5′ bond; and (3) a guanine-7-methyltransferase activity transfers the methyl group from a donor SAM (S-Adenosyl Methionine) to the 7 position of guanosine. The resulting capped RNA is said to have a cap 0 (zero) structure.

The reaction condition is listed as follows:

x	µl	RNA substrate (final concentration is 5-10 pmol/µl)
1	µl	10× capping buffer
1	µl	S-Adenosyl Methionine (Ado-Met)
1	µl	Guanylyltransferase (usually the final concentration is 0.05 U/µl)
3	µl	rGTP or [α-^{32}P]-rGTP (400 Ci/mmol, 10 mCi/ml)
		Nuclease-free H_2O
Σ =	10 µl	Final volume

The reaction mixture is incubated for 60 min at 37°C (alternatively, 1 U/µl RNase inhibitor could be also added if necessary). The reaction product is then purified by Qiagen RNeasy Kit for the next step.

2.2.4.2 Poly(A) tailing of *in vitro* transcribed RNA

Poly(A) polymerase catalyzes the incorporation of adenine residues into the 3′-termini of various kinds of polyribonucleotides. Its salt optimum is high as seen by its maximum activity at 300-400 mM NaCl. This enzyme uses various kinds of single-stranded RNA as a primer. However, double-strand RNA, synthetic polyribonucleotides and short oligonucleotides are not recommended for use as primers, and DNA cannot be used as a primer. This enzyme incorporates adenine residues and uses ATP as its only substrate. ADP and dADP cannot be used as substrates. The incorporation of CTP and UTP is less 5 % than that of ATP, and the enzyme cannot incorporate GTP into the 3′-termini of polyribonucleotides. This enzyme requires Mg^{2+} or Mn^{2+} for reaction, and the activity becomes maximal when both are present (2.5 mM Mn^{2+}, 10 mM Mg^{2+}).

The standard protocol of adding poly(A) tailing to RNA is as follows:

	2 µl	5× Poly(A) tailing reaction buffer
		RNA substrate (final concentration is ~ 0.008 pmol)
	1 µl	10 mM rATP
		Poly(A) Polymerase (final concentration is 25U/µl reaction)
		RNase-free H_2O
Σ =	10 µl	Final volume

The mixture is incubated at 37°C for 20 min. The reaction is terminated by heating at 65°C for 10-15 min. Then the poly(A) tailing RNA is purified by RNeasy kit and redissolved in a desired volume of RNase-free H_2O for immediate use or stored at -20°C.

2.2.5 Detection of reporter gene

2.2.5.1 Detection of *Firefly* luciferase (FLuc) reporter gene

In this work, the efficiency of internal translation initiation directed by the complete HCV IRES or deletion mutants was measured using a monocistronic reporter system that contains the *Firefly* luciferase (Fluc) reporter gene detecting the IRES-dependent translation. The luciferase gene is derived from the coding sequence of the luc gene cloned from the *Firefly* Photinus pyralis. The luciferase is an enzyme that catalyzes the oxidation of D-luciferin in the presence of ATP, Mg^{2+} and coenzyme A to generate the light emission (De Wet et al., 1987). The light output from the luciferase reaction is quantitated using a luminometer. The total amount of light measured is proportional to the amount of luciferase reporter activity in the sample. *Firefly* luciferase is widely used as a reporter gene for studying gene regulation and function, and for pharmaceutical screening. It is a very sensitive genetic reporter due to the lack of any endogenous luciferase activity in mammalian cells or tissues and the very nature of bioluminescence (Wood et al., 1984; Wood, 1991). *Firefly* luciferase is a 62,000 Da protein which is active as a monomer and does not require subsequent processing for its activity. The enzyme catalyzes ATP-dependent D-luciferin oxidation by oxygen into oxyluciferin with emission of light centred on 560 nm. As with many enzymes, *Firefly* luciferase follows Michaelis-Menten kinetics, and as a result maximum light output is not achieved until the substrates and co-factor are present in large excess. When assayed under these conditions, light emitted from the reaction is directly proportional to the number of luciferase enzyme molecules. For *in vitro* translation, luciferase activity is measured directly after reaction by addition of 4 µl of the translation reaction mixture to 100 µl of substrate solution (25 mM glycylglycine pH 7.8, 15 mM $MgSO_4$, 0.1 mM EDTA, 33 mM DTT, 1 mM rATP, 85 µM coenzyme A, 120 µM beetle luciferin) at room temperature and measuring the emitted light intensity for 20 sec in a Berthold Lumat 9507 luminometer. A similar translation reaction mixture without RNA is used as a blank.

For *in vivo* translation, the transfected cells are harvested and washed once with 1x PBS. Then about 150 µl of pre-cooled 1× Passive Lysis Buffer (PLB) is added onto the cells and incubated on a shaker for 10-15 min. at room temperature. The cytoplasmic lysate is transferred to a microcentrifuge tube and spun at 13,000 rpm for 1 min. at 4°C. The supernatant is transferred to another new microcentrifuge tube. Then the luciferase activity is measured by addition of 15-20 µl of the translation lysate to 100 µl of substrate solution (mentioned above) at room temperature and measuring the emitted light intensity for 20 sec in a Berthold Lumat 9507 luminometer. A similar translation lysate without RNA is used as a blank.

2.2.5.2 Detection of *Renilla* luciferase (RLuc) reporter gene

Renilla luciferase has been used as a reporter gene for studying gene regulation and function *in vitro* and *in vivo*. Recently, *Renilla* luciferase has been widely used in multiplex transcriptional reporter assays or as a normalizing transfection control for *Firefly* luciferase assay. *Renilla* luciferase, a monomeric 36,000 Da protein, catalyzes coelenterazine oxidation by oxygen to produce light. The enzyme does not require post-translational modification for its activity and may function as a genetic reporter immediately following translation. Coelenterazine (native) is the natural substrate for *Renilla* luciferase. However, over a dozen of coelenterazine analogs have been synthesized, many of which are now commercially available. These coelenterazine analogs all function as substrates for *Renilla* luciferase with different properties in terms of emission wavelength, cell membrane permeability and quantum efficiency. Coelenterazine also emits light from enzyme-independent oxidation, a process known as autoluminescence. The autoluminescence is enhanced by superoxide anion and peroxynitrite in cells and tissues.

For *in vivo* translation, the transfected cells are harvested and washed once with 1x PBS. Then about 150 µl of pre-cooled 1× Passive Lysis Buffer (PLB) is added onto the cells and incubated on a shaker for 10-15 min. at room temperature. The cytoplasmic lysate is transferred to a microcentrifuge tube and spun at 13,000 rpm for 1 min. at 4°C. The supernatant is transferred to another new microcentrifuge tube. Then the luciferase activity is measured by addition of 15-20 µl of the cytosol lysate to 100 µl of substrate solution (Coelenterazine substrate is diluted in 1:100 in RLuc buffer) at room temperature and measuring the emitted light intensity for 20 sec in a Berthold Lumat 9507 luminometer. A similar translation lysate without RNA is used as a blank.

2.2.6 RNA-protein interactions

2.2.6.1 UV cross-linking reaction

The UV cross-linking assay is performed essentially as described previously (Pelletier & Sonenberg, 1985b). The idea of the UV cross-linking assay is to specifically transfer the radioactive label from a RNA binding site to the binding protein. Irradiation of RNA with UV light produces purine and pyrimidine free radicals. If a protein molecule is in close proximity to the free radical, a covalent bond can be formed, cross-linking the protein to the RNA.

Standard reaction for cross-linking of proteins to radio-labelled IRES RNA:

	x	µl	Sterile ddH_2O
	2.0	µl	5× cross-linking buffer or nothing
	y	µl	1 M KCl (adjusting the final concentration of potassium to about 130 mM)
	4.0	µl	Rabbit reticulocyte lysate (Promega) or cytoplasmic extract of Huh-7 cells
	z	µl	Internally radio-labelled IRES RNA (ca. 0.06 pmol)
Σ =	10	µl	Final volume (the volume of this reaction may be scaled up)

Internally radio-labelled RNA (ca. 0.06 pmol) is incubated for 10 min at 30°C with 4 µl of micrococcus nuclease-treated rabbit reticulocyte lysate (RRL; Promega) or cytoplasmic extract of Huh-7 cells (S10 lysate) in 10 µl total volume. The endogenous potassium acetate in the RRL or extract of Huh-7 cells (S10 lysate) results in a final K^+ concentration of 38 mM or 54 mM, respectively. Reaction mixtures are irradiated at 254 nm on ice at the distance of 2 cm with an 8 W UV-hand lamp for 30 min in an eppendorf microcentrifuge tube or in a 96-well microtiter plate. Excess RNA is then digested for 60-90 min at 37°C with 10 mg/ml of RNase A, leaving fragments of radio-labelled RNAs cross-linked to the polypeptides. Protein samples are boiled for 5-10 min with 5 µl of electrophoresis sample buffer. Proteins are resolved on SDS-8 % polyacrylamide gels depending on the

size of the proteins of interest. The gel is fixed with Coomassie destaining solution three times each for 15 min to remove the free radioactive nucleotides, then the gel is dried, and proteins that were radio-labelled by covalently bound RNA oligonucleotides are detected by autoradiography.

For cross-linking cellular proteins or any other proteins to radio-labelled HCV IRES RNA, the reaction components are mixed as follows:

		Sterile ddH_2O
3.3	µl	Rabbit reticulocyte lysate (Promega) or 4 µl Huh-7 S10 lysate
0.85	µl	1 M KCl
		[α-^{32}P]-UTP labelled HCV IRES RNA (ca. 0.06 pmol)
Σ = 10	µl	Final volume

The UV cross-linking is performed either in the presence or in the absence of the proteins in a final volume of 10 µl (or as otherwise indicated). Proteins cross-linked to radio-labelled HCV or FMDV IRES RNA are separated on 8 % or 10 % SDS-polyacrylamide gel electrophoresis, the gel is dried, and proteins are detected by autoradiography.

2.2.6.2 Electrophoretic mobility shift assay (EMSA)

The electrophoretic mobility shift assay (EMSA) or band shift is based on the observation that stable peptide•RNA/DNA complexes migrate through polyacrylamide gels more slowly than free RNA/DNA fragments. The assay allows us to determine the amount of RNA/DNA bound by the peptide as a function of the peptide concentration. This in turn allows the equilibrium dissociation constant (K_d) to be estimated.

In addition to measuring peptide•RNA/DNA interactions, the band shift method can also be used to study complexes between peptides and RNA, RNA and DNA, and RNA and RNA. The only requirement is that the species involved form discrete complexes that are stable under the electrophoretic conditions being used. Attaining discrete bands often involves varying the gel parameters. Conditions that are easily varied include: gel temperature, running buffer, percentage of acrylamide, ratio of bis-acrylamide (the cross-linking agent) to acrylamide, reaction buffer and reactant concentrations.

The reaction components in EMSA with RNA were mixed as follows:

1 µl		[α-^{32}P]-UTP labelled RNA substrate (~ 0.003-0.006 pmol/10 µl)
2 µl		5× binding buffer
1 µl		10 µg/µl tRNA (final concentration is 1 µg/µl)
		RNase-free H_2O
Σ = 10 µl		Final volume

The mixture solution is incubated at 30°C for 10 min. Then heparin is added to stop the reaction and incubated for another 10 min at 30°C. 4-5 µl of 50 % glycerol is added to each sample for loading on the native polyacrylamide-TBE gel.

The gel system used for the EMSA usually is a 4 % polyacrylamide gel without any detergent such as SDS, providing native conditions for the RNA-protein complexes also during the gel run.

The composition of the native gel is listed as follows:

4 %	Acrylamide/bisacrylamide (30:0.75)
5 % (v/v)	Glycerol
0.5 ×	TBE (autoclaved)
0.1 %	TEMED
0.1 %	APS
	Sterile ddH_2O

The gel should be pre-run about half an hour at the working current before the samples are loaded. The running buffer is 1/2 TBE buffer. The loading buffer is only RNase-free glycerol (the final concentration of glycerol in the sample is about 12.5 %). The indicator is also RNase-free and loaded on one or both side(s) of the gel. The current during gel-running is usually less than 30 mA/gel, voltage is 100 V. The gel run should be performed at 4°C. After electrophoresis, the gel is fixed in destaining buffer for 30-40 min, and then dried. The protein-RNA complexes are detected by autoradiography.

2.2.7 Biochemical methods

2.2.7.1 Purification of recombinant proteins by Ni-NTA His-tag-protein

Purification method: Ni-NTA His-tag-Protein

The purification procedure is performed according to the manufacturer's instructions (Qiagen).

2.2.7.2 Depletion of PTB from rabbit reticulocyte lysate (RRL)

Endogenous PTB is removed from rabbit reticulocyte lysate (Promega) essentially as described (Niepmann et al., 1997). Briefly, 1 ml of RRL is adjusted to 250 mM potassium acetate and incubated with 75 µl of poly(U)-Sepharose, and then centrifuged, the supernatant is saved carefully and stored in liquid nitrogen. Aliquots from the poly(U)-Sepharose-treated lysate are tested and compared with untreated Poly(U)-Sepharose lysate for the presence of traces of PTB by the cross-linking assay with the FMDV IRES.

2.2.7.3 Preparation of S10 cytoplasmic lysates from HeLa or Huh-7 cells

Monolayer cells are washed once with 10 ml PBS/20 cm cell culture Petri dish. Cells are harvested in 2 ml PBS by treatment with Trypsin-EDTA buffer and collected in 15 or 50 ml Falcon tube (depending on the volume of the cells). Cell suspension is centrifuged 5 min at 1,000 rpm, 4°C. The volume of the cell pellet (= Packed Cell Volume, PCV) is estimated and resuspended in 10 times PCV of isotonic buffer, mixed well and incubated for 5-10 min on ice. After centrifugation at 1,250 rpm for 5 min, 0°C, the cell pellets are washed two times again with isotonic buffer. After the last wash, cells are resuspended in 1.5 times PCV hypotonic buffer, mixed well and rotated on a rotater for 10-15 min at 4°C (cold room). An aliquot of the cell suspension is checked under the microscope during time. When ~ 90 % of the cells are broken, this cell suspension is transferred into a Douncer. The cells are broken by 10 to 15 strokes using a tight pestle. Then the broken cells are transferred to the original tube and add 1/10 cell suspension volume of S10 10× buffer, mixed well and aliquoted to 2 ml microcentrifuge tube. Cell debris are removed by centrifugation at 2,000 rpm, 4°C. The supernatant is transferred to another microcentrifuge tube and centrifuged again at 10,000 rpm for 10 min, 4°C. The supernatant is aspirated to a new tube and stored in liquid nitrogen as quickly as possible. This lysate can be used for UV cross-linking assays.

2.2.8 Immunological methods

2.2.8.1 Western blot

Immunoblotting provides a reliable method to check any sample for the presence of a protein antigen. The idea behind this technique is to separate protein antigens by gel electrophoresis and then transfer the proteins out of the gel onto a membrane such as nitrocellulose (Burnette, 1981). The antigen is then characterized on the basis of both its interaction with a specific antibody and its relative molecular weight.

For the identification of initiation factors, protein samples are separated by SDS-polyacrylamide gel electrophoresis and then electrophoretically transferred for 3 hrs at 400 mA to a pre-wet nitrocellulose membrane with transfer buffer using a Biometra-Fast blot apparatus. After transfer, the gel is stained with Coomassie blue to verify transfer efficiency.

To block non-specific protein binding sites, the membrane is immersed overnight in block-buffer (TBST-150, 3 % BSA). The binding of primary antibody diluted with block-buffer (1:250, 1:20 for mouse anti-eIF4G and mAb 324; mouse IgM-hybridoma tissue culture supernatant, respectively) is performed for 1 hr at RT. The blot is washed four times for 10 min with TBST-500 and then exposed for 1 hr at RT to (1:1000) blocking buffer diluted AP-conjugated secondary antibody directed against the primary antibody (AP-conjugated goat anti-mouse IgG is directed against mouse anti-eIF4G, and AP-conjugated goat anti-mouse IgM is directed against mAb 324-mouse IgM). After washing the membrane (4×, for 10 min.) with TBST-500, the membrane is transferred to a freshly prepared staining substrate solution of BCIP/NBT. For preparation of 50 ml of this solution, 150 µl of BCIP solution (50 mg/ml 5-Bromo-4-Chloro-3-Indolylphosphate in 100 % Dimethylformamid) and 150 µl of NBT solution (50 mg/ml Nitroblue tetrazolium in 70 % Dimethylformamid) are mixed with 50 ml of alkaline phosphatase buffer. The staining is stopped by washing the membrane in stop solution when the bands have reached the desired intensity.

2.2.8.2 Immunoprecipitation (IP)

The identification of proteins that are covalently bound to radio-labelled RNA in the UV cross-linking assay is further verified by immunoprecipitation. First antibody-antigen complexes are allowed to form, then the complexes are collected and purified by using protein A-coated Sepharose beads. Protein A specifically interacts with conserved regions of the antibodies, thus forming an immobilized antibody-antigen complex bound to the beads. Unspecific binding of molecules from the starting solution is prevented by washing the beads. The purified antigens are then analyzed by SDS-polyacrylamide gel electrophoresis.

Protein A-coated Sepharose beads (Pharmacia) are swollen for 1 hr at 4°C in phosphate buffered saline (PBS; 8 mM Na_2HPO_4, 2 mM NaH_2PO_4, 140 mM NaCl) plus 0.1 µg/µl BSA and 0.1 µg/ml of tRNA. Then, 600 µl of standard cross-linking reaction are prepared as below:

Standard cross-linking reaction

120.0	µl	Cross-linking buffer (5×)
3.0	µl	rATP (100 mM)
198.0	µl	Rabbit Reticulocyte lysate (Promega)
		Internally radio-labelled wild type HCV IRES RNA (1.5-2.5 pmol)
		Sterile ddH_2O
∑ = 600.0	µl	Final volume

After the binding reaction and UV irradiation, excess RNA is removed with 15 µl of 3 mg/ml RNase A and 4.0 µl of 2 mg/ml RNase T1 for 1 hr at 37°C.

Half of the UV cross-linking reaction is incubated for 1 hr on ice with 20 µl of sheep anti-eIF3 antibody in binding buffer (20 mM Tris-HCl pH 7.5, 200 mM NaCl, 10 mg/ml BSA) in a final reaction volume of 500 µl, whereas 20 µl of preimmune serum is added to the other half of the UV cross-linking reaction.

Next, 15 µl of pre-swollen protein A-coated Sepharose beads (Fluka) are added to either the immunoprecipitation reaction with anti-eIF3 or to the reaction with preimmune serum. Antibody-antigen complexes are allowed to bind to the protein A coated beads 15 min at 4°C. The antibody-antigen complexes bound to protein A beads are then recovered by centrifugation. The beads are washed two times for 10 min at 4°C with wash buffer A and three times for 30 min at 4°C with wash buffer B (wash buffer A, 0.25 % Tween, 0.25 % NP-40). After each wash the beads are transferred to a new eppendorf tube. The final wash is performed with PBS for 10 min at 4°C. Detergents are omitted from the final rinse as a precaution against the generation of abnormal SDS-PAGE migration patterns.

Finally, the beads are resuspended in protein sample buffer containing 7 M urea to release the radio-labelled polypeptides. The protein A beads are removed by centrifugation and the solubilized radio-labelled proteins are analyzed by separation on a SDS-8 % polyacrylamide gel and visualized by autoradiography.

2.2.9 Gel electrophoresis

2.2.9.1 Agarose gel electrophoresis and recovery of DNA fragments from agarose gels

To analyze or separate nucleic acid fragments, agarose gel electrophoresis is performed according to a standard protocol (Sambrook et al., 1989). Depending on the size of DNA fragments to be separated, 1 to 2 % agarose gels are prepared in 1× TAE buffer. Before loading the gel, the nucleic acid samples are mixed with 1/5 volume of FM-agarose gel loading buffer (75 % Glycerol, 0.1 mM EDTA, 0.1 % bromophenol blue, 0.1 % xylene cyanol FF). The electrophoresis is performed at ca. 2 to 5 Volts/cm, and stopped when the bromophenol blue tracking dye has migrated at least 2 cm from the wells. The gel is then soaked in ethidium bromide solution, a fluorescent intercalating dye, in a concentration of 0.5 µg/ml for 20-30 min.

For analytical gels, the electrophoresis result is illuminated with ultraviolet light (λ = 254 nm) and photographed with a Polaroid MP-4 Land camera. For preparative gels, the band(s) of interest is located with ultraviolet light, cut out, and extracted with the GFX PCR DNA and Gel Band Purification Kit (Amersham) according to the description of the manufacturer. To control the efficiency of the elution, an aliquot of the recovered DNA is analyzed again on an agarose gel.

When agarose gel electrophoresis is used to analyze the integrity of the full length non-radio-labelled *in vitro* transcribed RNAs, great care should be taken to avoid accidental contamination with RNases. The gel electrophoresis apparatus is cleaned carefully, autoclaved agarose and buffers are used.

2.2.9.2 Denaturing polyacrylamide gel electrophoresis

To analyze or separate ribonucleic acids, denaturing 6-12 % polyacrylamide gels are used. Electrophoresis is performed under denaturing conditions (containing 7 M urea). Autoclaved 1× TBE buffer is used as running buffer. First, pre-electrophoresis is performed for 15 min under normal electrophoresis conditions to flush out the impurities in the gel (and to create a higher temperature throughout the gel). Before loading, the ribonucleic acid samples are mixed with an equal volume of FA-gel loading buffer (80 % formamide, 0.1 mM EDTA, 0.1 % bromophenol blue, 0.1 % xylene cyanol FF) and denatured for 2 min at 70 °C. The gel is illuminated with UV light after staining with ethidium bromide.

To determine the percent incorporation and integrity of *in vitro* synthesized radio-labelled RNAs, radio-labelled transcripts are mixed with an equal volume of FA-gel loading buffer and denatured for 3 min at 80°C, then

loaded to denaturing 6 % polyacrylamide gel with 7 M urea. Autoclaved 1× TBE is used as running buffer. The electrophoresis is performed at 30 mA for 8-9 min, the running is stopped when the bromophenol blue tracking dye has reached the middle of the gel. Radio-labelled RNAs are located by autoradiography. The gel is covered with plastic wrap and exposed directly to Kodak X-ray film for 3 to 5 min.

2.2.9.3 SDS-polyacrylamide gel electrophoresis (SDS-PAGE)

For the analytical and preparative separation of proteins under SDS-denaturing conditions, the discontinuous gel system is utilized (Laemmli, 1970). The gels are composed of 8 to 12 % poly-acrylamide separating gel and 6 % polyacrylamide stacking gel. Before loading, the protein samples are mixed with an equal volume of 4 × SDS gel loading buffer and denatured by heating for 5 min at 95°C. The electrophoresis is performed with a vertical gel chamber in 1×Tris-glycine buffer. After electrophoresis, the gel is fixed and stained immediately with Coomassie blue solution for 30 min, and then dried after destaining.

For the analysis of radio-labelled proteins: after electrophoresis, the gel is fixed with destaining solution (5 % ethanol, 7.5 % acetic acid) for 15 min with gentle agitation. After destaining, the gel is covered with plastic wrap, placed on two moistened Whatman® blot papers, and then dried under vacuum on a gel-dryer. Autoradiography is subsequently performed.

Stacking gel:		**Separating gel:**	
6.0 %	Acrylamide/bisacrylamide (30:0.75)	8-12 %	Acrylamide/bisacrylamide (30:0.75)
125.0	mM Tris-HCl, pH 6.8	375.0	mM Tris-HCl, pH 8.8
0.1 %	(w/v) SDS	0.1 %	(w/v) SDS
0.1 %	(w/v) APS	0.1 %	(w/v) APS
0.1 %	(v/v) TEMED	0.1 %	(v/v) TEMED

2.2.9.4 Coomassie brilliant blue staining

Coomassie brilliant blue R-250 binds non-specifically to almost all proteins, which allows detection of essentially all protein bands in polyacrylamide gels. The gels to be stained and fixed are incubated for 30 min with gentle agitation in staining solution (0.12 % Coomassie brilliant blue R-250, 50 % ethanol, 10 % acetic acid). After staining, gels are destained several times with fresh destaining solution until a clear background appears.

2.2.9.5 Autoradiography

This is a technique used to visualize and quantitate radio-labelled RNA-protein complexes by direct exposure of the dried gel to Kodak X-ray film for 1 to 3 days at room temperature so as to generate sharper bands with lower background (direct autoradiography), or at -70°C using an intensifying screen to generate stronger bands (indirect autoradiography). Additionally, the wet gel is covered with plastic wrap and exposed directly to Kodak film for 5 to 15 min at room temperature to locate *in vitro* synthesized radio-labelled RNAs,.

2.2.10 Cell culture methods

2.2.10.1 Subculture protocol of adherent cell lines

Cells are maintained in a 37°C, 5 % CO_2 humidified incubator (Heraeus, Germany). Every 4-5 days (depending on the different type of cells), cells are first washed with 1× PBS, then trypsinized by 1× Trypsin-EDTA for 5-10

min at 37°C. The fresh DMEM is added to stop the reaction. The suspended cells are finally split and reseeded into new dishes or flasks.

Preparation of working medium:

450 ml	1× DMEM
50 ml	FBS
5 ml	Antibiotics (100× penicillin-streptomycin solution)

The mixture is mixed well before using.

2.2.10.2 Freezing protocol of mammalian cells

The fresh freezing medium (6 ml D-MEM, 2 ml FBS, 2 ml high purity DMSO) should be made in advance. Cells grow until they have reached at least 80 % confluence for freezing preservation. The cells are prepared as described above. The cell suspension is pipetted into a sterilized centrifugation tube and centrifuged for 5 min at 550 rpm at 4°C. The supernatant is discarded and the tube is placed on ice. 1 ml of ice-cold D-MEM/DMSO is added and leaving the tube on ice for 10 min. Cells are aliquoted in pre-cooled (4°C) freezing vials (1 ml of cells/vial) and immediately placed into a –70°C freezer overnight. The next day, the vials are transferred in a liquid nitrogen tank.

2.2.10.3 Resuscitation of frozen cells

A vial of frozen cells is thawed quickly in a 37°C water-bath. When the last ice has molten, the cells are pipetted immediately in a flask containing 5 ml of pre-warmed working DMEM. After 4-6 hours, the medium must be changed to remove dead cells.

2.2.11 Transfection of nucleic acids into mammalian cell cultures

2.2.11.1 Transfection with DNA (Lipofectamine® 2000 method)

Cells are seeded in each well of a microtiter plate (6-, 12- or 24-well) in an appropriate growth medium containing serum and antibiotics at least 24 hr before transfection. The cells in each well should be up to at least 70-80 % confluence for transfection. Circular plasmid DNA or PCR fragment DNA (1 µg) is diluted in 100 µl 1× DMEM (without serum and antibiotics) in a microcentrifuge tube. 10 µl of Plus Reagent is added into the mixture, mixed by pipetting and incubated at room temperature for 15 min. 2 µl of Lipofectamine® Reagent is diluted into 100 µl 1× DMEM (without serum and antibiotics) in a second microcentrifuge tube and mixed by pipetting. The diluted Lipofectamine® Reagent is added into the tube containing pre-complexed DNA and Plus Reagent. This complex solution is mixed well and incubated for 15 min at room temperature. While complexes are forming, the medium in the wells is replaced with 0.5-1 ml 1× DMEM (without serum and antibiotics). The DNA-Plus-Lipofectamine® Reagent complexes (200 µl volume in total) are added into each well containing fresh medium. The complexes are mixed into the medium gently and incubated at 37°C, 5 % CO_2 for 24-48 h for assay.

Preparation of cell lysate: cells are harvested by addition of 1× Passive Lysis Buffer (Promega) after removal of the old medium and once wash with 1× PBS buffer in each well. The plate is placed on a shaker fro 15 min at room temperature until all cells were nearly detached. This raw cell suspension is transferred into a new microcentrifuge tube and spun at full speed by centrifugation. The supernatant is transferred to another new microcentrifuge tube and 15-20 µl is taken for assay on luminometer.

2.2.11.2 Transfection with RNA

TransMessenger transfection reagent is designed to efficiently transfect eukaryotic cells with RNA. This reagent is based on a lipid formulation and is used in conjunction with a specific RNA-condensing reagent (Enhancer R) and an RNA-condensing buffer (Buffer EC-R). In the first step of TransMessenger-RNA complex formation, the RNA is condensed by interaction with Enhancer R in a defined buffer. In the second step, TransMessenger transfection reagent is added to the condensed RNA to produce TransMessenger-RNA complexes. The TransMessenger-RNA complexes are then mixed with serum-free medium and added directly to cells.

For transfection of adherent cells using single-strand RNA in one well of a 24-well plate, the protocol is as follows: at least 24 hrs before transfection, 8-10 × 10^4 cells are seeded into each well of a 24-well plate in 0.5 ml appropriate growth medium containing serum and antibiotics. The cells are incubated at normal growth condition (generally at 37°C and 5 % CO_2). On the day of transfection (cells should be 80-90 % confluent), 1.6 µl of Enhancer R is diluted in buffer EC-R. 0.8 µg of RNA is added and mixed by pipetting a few times. The final volume should be 100 µl (always mix Enhancer R with Buffer EC-R before addition of RNA) and incubated at room temperature for 5 min. 4 µl of TransMessenger transfection reagents is added to the RNA-Enhancer R mixture. The mixture is pipetted up and down a few times. The samples are incubated for 10 min at room temperature to allow transfection-complex formation. While complex formation takes place, the growth medium is gently aspirated from the plate, and the cells are carefully washed once with sterile PBS buffer using 1.5-2 times the volume of medium used for cell seeding. 100 µl of growth medium without serum or antibiotics is added to the tube containing the transfection complexes. Mixing by pipetting up and down a few times, then the transfection complexes are immediately added drop-wise onto the wells (204 µl/well). The plate is gently swirled to ensure distribution of the transfection complexes. Cells are incubated with the transfection complexes for 3-4 hrs under normal growth conditions. If needed, the complexes are removed from the cells, cells are washed once with PBS, then 0.5 ml fresh medium containing serum and antibiotics is added to the cells and incubated under normal growth conditions to allow for protein expression. Incubation time is determined by the assay and RNA used.

Preparation of cell lysate: the same as that of DNA transfection (**2.2.11.1**)

2.2.12 Ribonuclease protection assay (RPA)

The ribonuclease protection assay is an extremely sensitive technique for the quantitation of specific RNAs in solution. The ribonuclease protection assay can be performed on total cellular RNA or poly(A)-selected mRNA as a target. The sensitivity of the ribonuclease protection assay derives from the use of a complementary *in vitro* transcript which is radio-labelled to high specific activity. The probe and target RNA are hybridized in solution, after which the mixture is diluted and treated with ribonuclease (RNase) to degrade all remaining single-stranded RNA. The hybridized portion of the probe will be protected from digestion and can, after removal of the RNase, be visualized via electrophoresis of the mixture on a denaturing polyacrylamide gel followed by autoradiography. Since the protected fragments are analyzed by high resolution polyacrylamide gel electrophoresis, the ribonuclease protection assay can be employed to accurately map mRNA features such as initiation and termination sites. If the probe is hybridized at a molar excess with respect to the target RNA, then the resulting signal will be directly proportional to the amount of complementary RNA in the sample.

The purification protocol of all RNA solution during this assay was performed by using RNeasy kits from Qiagen Company.

2.2.12.1 Synthesis of [α-^{32}P]-labelled RNA probe and purification of the probe

In order to perform the RPA, the [α-^{32}P]-labelled anti-sense RNA probe is synthesized by T3 or T7 RNA polymerase *in vitro* transcription. Firstly, the anti-sense plasmid DNA is linearized by relevant restriction

enzyme and purified as mentioned before (Method **2.2.2.1**). Then the linearized plasmid is transcribed according to the standard transcription protocol to generate the anti-sense probe. Then the following reagents are added to digest the DNA templates:

RNA solution (~ 1 µg/µl)	adjusted to 90 µl
RNase-free DNase I (10 U/µl)	1 µl
RNase-free H_2O	8 µl
1 M $MgCl_2$ (RNase-free)	1 µl
Final volume	100 µl

The mixture is incubated at 37°C for 15 min. Then this RNA mixture is purified by RNeasy Kit (Qiagen) according to the manufacturer's instruction. The probe is redissolved in a desired volume of RNase-free H_2O and stored at -20°C or -40°C.

2.2.12.2 Preparation of sample RNA

About 0.8 µg of purified RNA sample is transfected into Huh-7 cells according to the supplier's manual. After four hours of transfection, the cell lysate is prepared as quickly as possible from the transfected cells with PLB (Promega) procedure. After centrifugation at full speed for 1 min, the supernatant is transferred to a new microcentrifuge tube containing 1 % SDS and 10 µg of tRNA. Then, $CaCl_2$ (RNase-free) is added to a final concentration of 1 mM, 30 µg of proteinase K are also added, and the sample mixture is incubate at 50°C for 1 hr. After digestion, the lysate is extracted with phenol : chloroform and precipitated with ethanol. Finally, the re-isolated RNA is dissolved in a certain volume of hybridization buffer and used for the next step or stored at -20°C for future use.

2.2.12.3 Hybridization and RNase digestion of probe and sample RNA

About 30 µl of the purified RNA from **2.2.11.2** is taken into a new microcentrifuge tube containing 3-4 µl of probe RNA, mixed well and incubated for 5 min. at 85°C to denature RNAs. The sample is spun briefly and rapidly transferred to a 42°C water-bath to incubate overnight for hybridization (in order to obtain optimal hybridization, the hybridization time should be at least 14 hr).

The fresh RNase digestion buffer containing 40 µg/ml RNase A is prepared before the hybridization procedure is finished. 300 µl of freshly-made RNase digestion buffer (10-fold volume of hybridization buffer used for last step) is added and incubated for 90 min. at 30°C. 16.5 µl of 10 % SDS is added (final is 0.5 %), and subsequently, 1 µl of 10 µg/µl tRNA (as carrier) , 11 µl of 30 mM $CaCl_2$ as well as 100 µg of proteinase K are added. This mixture is incubated at 37°C for 30 min. to inactivate RNase A. Subsequently, the mixture is extracted with phenol : chloroform, precipitated with ethanol in the presence of NaCl (but not sodium acetate). The RNA pellet is washed three times with 80 % ethanol and dried at room temperature.

2.2.12.4 Separation and detection of protected fragments

After hybridization and RNase digestion, the precipitated sample is resuspended in 4 µl FA buffer and incubated for 5 min at 95°C to denature the RNA. The samples are loaded into wells of a denaturing polyacrylamide-TBE gel (gel percentage depending on the size of probe). Gels are run at about 30 mA constant current for 8-10 min. Then, the gel is fixed in fixer for 30-40 min., dried on a gel-drier for at least 1 hr. Finally, the dried gel is exposed to X-ray film. An appropriate time is determined for exposures until an optimal image is obtained.

3 Results

3.1 Part I: The search for unknown cellular proteins which interact with the Hepatitis C Virus 5´- and 3´-untranslated regions

The main goal of this first part of the study was to investigate the interaction of proteins from extracts of liver-derived cell lines with the HCV IRES RNA or the HCV IRES plus the 3´-UTR, aiming at the possible discovery of as yet unknown proteins which may regulate HCV translation in a tissue-specific manner.

As described in the "Introduction" section, the initiation of translation occurs either by cap-dependent scanning or by direct binding of a ribosome to a specialized RNA element called an internal ribosome entry site (IRES) (Hellen & Sarnow, 2001). Although canonical translation initiation factors are involved in translation initiation directed by most IRES elements, in particular those of the picornaviruses which are distantly related to HCV, many other RNA-binding proteins have also been shown to play important roles. For instance, host cell proteins such as polypyrimidine tract-binding protein (PTB), the La autoantigen, poly(rC)-binding proteins (PCBP) and the protein encoded upstream of *N-ras* (Unr) bind directly to IRESes and enhance the translation of picornaviral mRNAs. Also, translational initiation of hepatitis C virus (HCV) RNA is initiated by internal entry of ribosome at an IRES in the 5´-untranslated region (5´-UTR). Curiously, while most IRESes require only 5´-UTR sequences for full activity, the HCV IRES was shown to include a short stretch of protein-encoding sequences downstream of the initiating AUG (Reynolds et al., 1995; Lu & Wimmer, 1996), according to the fact that the AUG is embedded in an RNA secondary structure, the stem-loop IV which is part of the functional HCV internal ribosome entry site (see Fig. 6). However, other reports have suggested that the core-encoding sequence is not strictly essential for HCV IRES activity (Tsukiyama-Kohara et al., 1992; Wang et al., 1993; Rijnbrand et al., 2001). Thus, the molecular basis of translational activation by the HCV core-encoding sequence is not yet completely understood.

In the past ten years, except for the involvement of eIF3 (Buratti et al., 1998; Sizova et al., 1998), several other proteins such as La, PTB, PCBP, hnRNP C and L, and some ribosomal proteins are found to interact with the HCV IRES or with the 3´-UTR (Ali & Siddiqui, 1995, 1997; Ito & Lai, 1997; Tsuchihara et al., 1997; Hahm et al., 1998b; Chung & Kaplan, 1999; Fukushi et al., 1999; Gontarek et al., 1999; Luo, 1999; Spangberg et al., 1999a; Fukushi et al., 2001; Otto et al., 2002), but some of them are not essential for 48S complex formation *in vitro*. Moreover, the proteasome subunit PSMA7 (Krüger et al., 2001), nucleolin (Izumi et al., 2001), the NS1-associated protein 1 (NSAP1) (Kim et al., 2004) and some other proteins were also reported to bind HCV IRES RNA (Lu et al., 2004). However, none of these proteins could be linked to a possible tissue-specific stimulation of HCV translation.

In this part of this study, the possible interaction of yet unknown cellular proteins with the HCV RNA was examined, either in the absence or in the presence, respectively, of 3´-UTR sequences, to search for proteins that bind synergistically in the presence of both the 5´-UTR and the 3´-UTR, and thus can be assumed to be involved in HCV RNA genome circularization and translation stimulation, and possibly confer tissue-specific translation regulation of HCV.

3.1.1 Optimization of protein binding to the HCV IRES RNA

In this part of the study, the UV cross-linking assay (see Materials and Methods **2.2.6.1**) was used as the major technique to search for new proteins, including cellular proteins or canonical translation initiation factors, which might be involved in the internal translation initiation of HCV RNA.

One crucial feature of this method is that RNA-protein interactions can be detected in their natural conformation since no additional linker ligands which may disrupt the secondary structure of the RNA are introduced. Irradiation of radio-labelled RNA with UV light at 254 nm produces purine and pyrimidine free radicals. When a protein molecule is in close contact to the RNA, a covalent bond may be formed between a nucleotide free radical and a reactive amino acid of the protein, resulting in transfer of the radioactive label from RNA to the RNA-binding protein. The detection of a given protein in the UV cross-linking depends on several parameters like temperature, the time of incubation with the RNA, concentration of different mono-valent and divalent ions, buffer conditions as well as the type of the α-^{32}P radio-labelled ribonucleotide used for internal labelling of the RNA molecule. The major disadvantage of this method is that not every protein that binds to the RNA may necessarily be cross-linked and detected. It has been shown that mainly 10 amino acids including cysteine, tyrosine, phenylalanine, histidine, arginine, lysine, serine, methionine, threonine and tryptophan can form a covalent bond with uracil or cytosine upon UV irradiation with different intensities (Smith, 1976).

For this purpose, one HCV RNA template – the HCV IRES only – was obtained by linearization of the monocistronic HCV wild-type reporter plasmid with *Aat* II (Fig. 10A). Then in the first experiment, different UV cross-linking buffers were tested to find satisfying conditions for the binding of proteins to the [α-^{32}P]-UTP labelled HCV IRES RNA in UV cross-linking reactions with cellular lysates (rabbit reticulocyte lysate, RRL, and cytoplasmic extract of Huh-7 cells, a hepatoma cell line). The result obtained with the reaction including double-distilled H_2O only was almost the same as that obtained with the reaction including different buffers (data not shown). Accordingly, in all further experiments, no additional buffer was supplemented to the UV cross-linking reaction with the HCV IRES RNA except for the addition of potassium acetate or chloride to adjust the final potassium concentration to physiological conditions (~135 mM).

In order to possibly improve the binding of proteins to the HCV IRES RNA, it was examined whether addition of various detergents or reducing agents such as dithiothreitol (DTT) would influence protein binding and UV cross-linking efficiency. Fig. 10B and C show a series of UV cross-linking assays performed with different concentrations of DMSO, glycerol, CHAPS, NP-40, Tween-20, Triton-X-100, DTT and β-mercaptoethanol in the reactions. The results show that increasing amounts of any detergent did not exhibit any stimulatory effect on the binding of the detected proteins to the [α-^{32}P]-UTP labelled HCV IRES RNA (Fig. 10B). The binding of the proteins including p170, p116/110 to the HCV IRES did hardly change in all cases. According to these observations, no additional detergent was added to the reactions in all following UV cross-linking assays.

Moreover, the influence of increasing amounts of DTT and β-mercaptoethanol on the binding of proteins to the labelled HCV IRES RNA was also examined (Fig. 10C). The result shows that both DTT and β-mercaptoethanol did also not exhibit any stimulatory effect on the cross-linking efficiency of any protein bound to the HCV IRES.

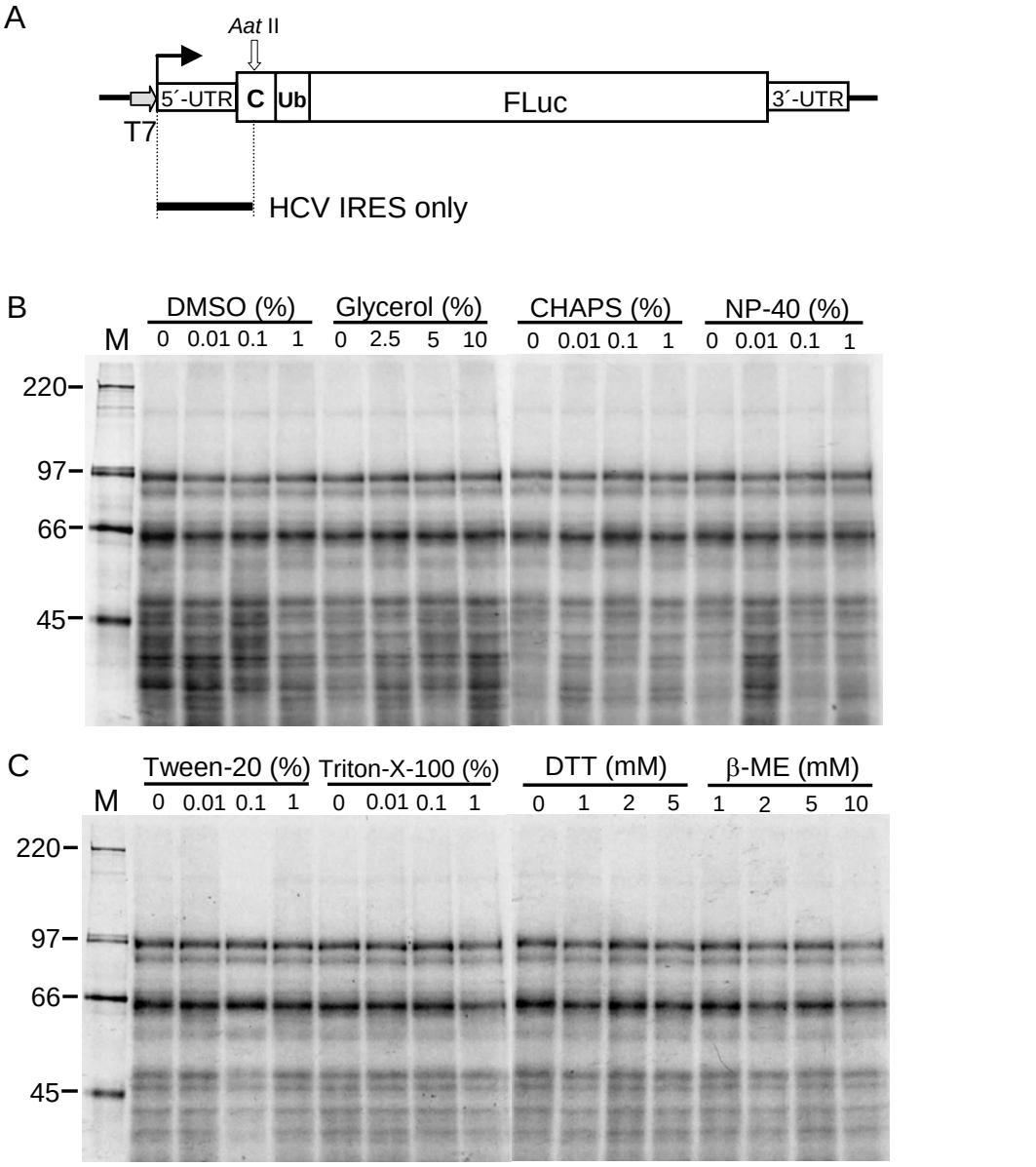

Fig. 10: Effects of some additives on the cross-linking results with [α-^{32}P]-UTP labelled HCV IRES RNA in reticulocyte lysate. (A) Schematic diagram of the HCV wild-type (wt) construct and HCV IRES only RNA. The very beginning part of the core protein-encoding sequences is included in the "HCV IRES only" RNA (solid line). *Aat* II was used for generating the "HCV IRES only" RNA template. T7, T7 RNA polymerase promoter; UTR, untranslated region; C, partial core protein-encoding sequences; Ub, ubiquitin sequences; FLuc, *Firefly* luciferase reporter gene. **(B, C)** UV cross-linking was performed in 10 µl reaction volume with 4.4 µl of RRL and 0.06 pmol of HCV IRES RNA internally labelled with [α-^{32}P]-UTP. Reaction mixtures were incubated for 10 min at 30°C to allow the binding of proteins from the RRL to the HCV RNA in the presence of 135 mM potassium and then UV irradiated at 254 nm on ice for 30 min. Excess RNA was digested by incubation with 3 mg/ml RNase A for 60 min at 37°C. Proteins were separated on SDS-8 % polyacrylamide gels and visualized by autoradiography. All detergents as well as DTT, β-mercaptoethanol (β-ME) and their concentrations are indicated above the gels. The molecular masses of ^{14}C labelled proteins marker (M) are given in kDa and indicated at the left side of the gels.

Based on these observations, none of the tested reagents was used in the following UV cross-linking experiments.

3.1.2 Analysis of the interaction of proteins from cellular lysates with the HCV IRES and its deletion mutants

According to the results obtained from the previous experiment, UV cross-linking assays with the HCV IRES and deletion mutants were performed. For this purpose, a series of deletion mutant plasmids was cloned from the basic monocistronic HCV wild-type construct as shown in Fig. 10A by PCR mutagenesis. All these deletions are shown in Fig. 11.

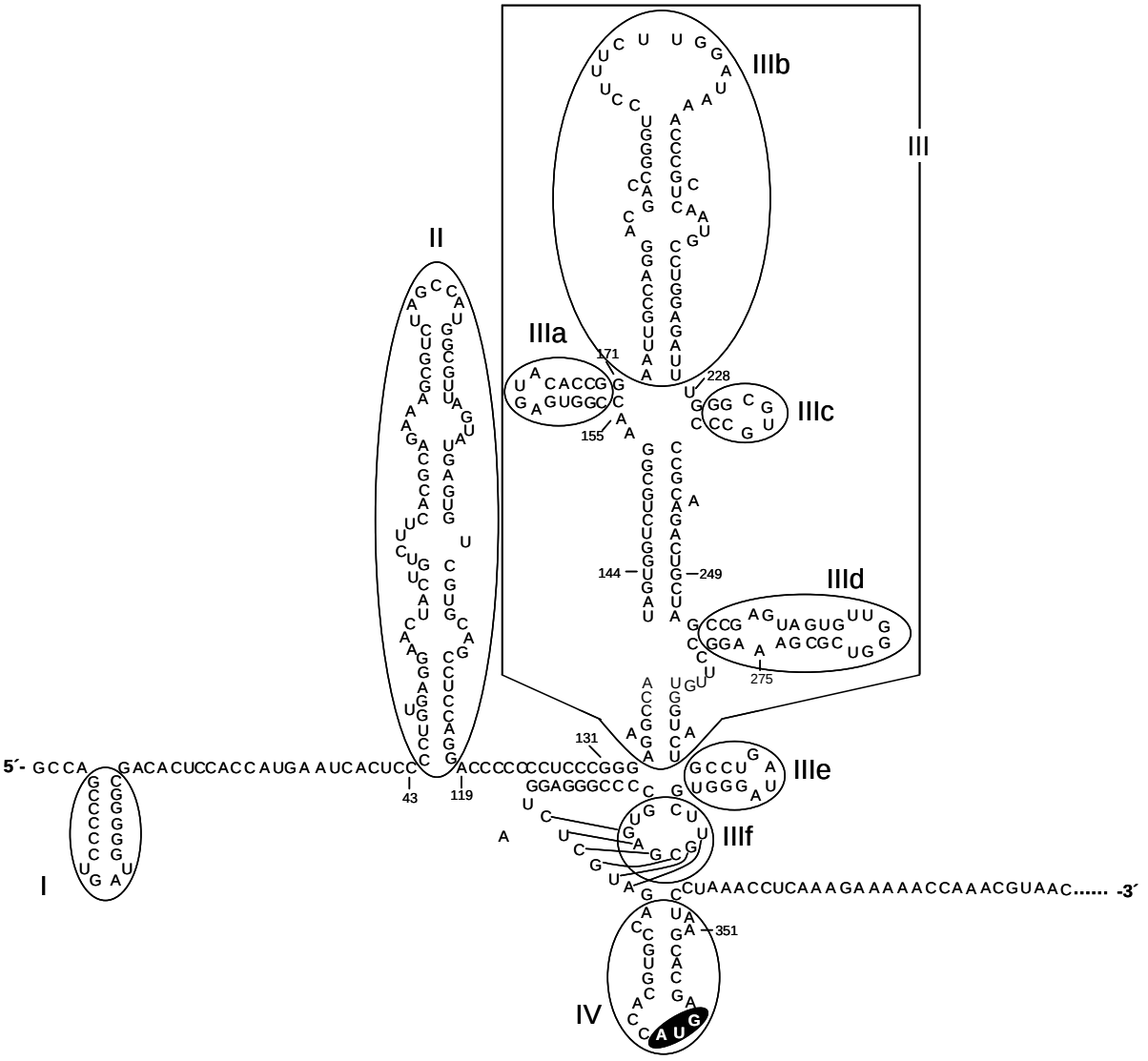

Fig. 11: Deletion mutations introduced into the HCV 5´-UTR sequence. The circled areas represent the deleted sequences. The big boxed area represents the large deletion of domain III within the 5´-UTR. The highlighted AUG represents the authentic start codon (modified from Honda et al., 1999).

All these plasmids including the wild-type 5´-UTR and the deletion mutants were linearized with *Aat* II located in nucleotides downstream of the HCV core start codon AUG. The corresponding RNA molecules were *in vitro* transcribed by T7 RNA polymerase in the presence of [α-^{32}P]-UTP. UV cross-linking assays with these RNA molecules were carried out under the optimized conditions described above. The results (Fig. 12) show that, unfortunately, no novel protein was detected with either RRL (Fig. 12A) or Huh-7 cytoplasmic extract (Fig. 12B). Only subunits of eIF3 such as p170, p116/110 and p64 which bind to the HCV IRES wild-type were detected. However, with several deletion mutant RNAs proteins appear in addition to those obtained with the wild-type IRES, reflecting a situation in which the loss of specific binding of certain proteins (like eIF3) leaves RNA regions free for the binding of other proteins that would not bind to the wild-type IRES.

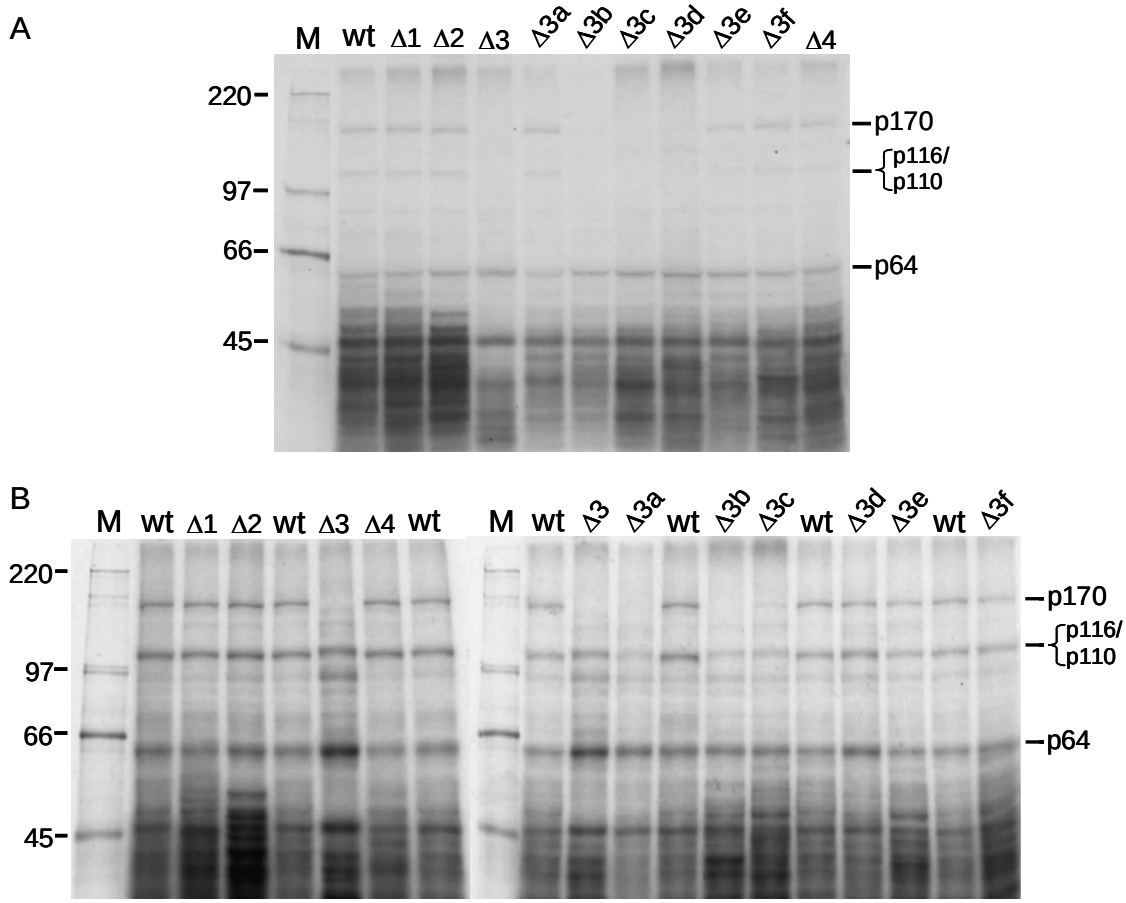

Fig. 12: Interaction of proteins from RRL (A) and Huh-7 lysate (B) with HCV IRES and its deletion mutants by UV cross-linking assay. The HCV RNA molecules were *in vitro* transcribed from the corresponding templates of the HCV IRES and the deletion mutants shown in Fig. 11. The reactions were performed as described in Fig. 10 with RRL and cytoplasmic lysate of Huh-7 cells. Proteins were separated on SDS-8 % polyacrylamide gels and visualized by autoradiography. The molecular masses of ^{14}C labelled proteins marker (M) are given in kDa and the positions of the subunits of eIF3 (p170, p116/110 and p64) are indicated at the right side of the gel. wt, wild-type of HCV IRES; Δ1, Δ2, Δ3, Δ4 etc. represent the different mutants in which major domains or subdomains of the HCV 5´-UTR had been deleted. The protein sample UV cross-linked to each deletion mutant was run side by side with the wt reaction to allow a better comparison of the labelled protein patterns in **(B)**.

The stem-loop 3, more accurately to say, the sub-domains 3a, 3b and 3c of the stem-loop 3, have been further confirmed in this experiment as the major binding site for eIF3 subunits (p170, p116/110). However, no new protein was found to bind to the HCV IRES RNA under these experimental conditions.

Until now, very little is known about the components of the ribosome that contact the HCV IRES. On the one hand, many proteins with low molecular weight have been detected to be cross-linked to the HCV IRES as observed in Fig. 12. On the other hand, eukaryotic 40S ribosomal subunit consists of about 33 different low-molecular weight proteins (called ribosomal protein small, "RpS"). Thus, it is a reasonable assumption that many small proteins found to bind to the HCV IRES are 40S ribosomal proteins. Previous experiments have shown that the small ribosomal subunit proteins S9 and S5 can bind to the HCV IRES (Fukushi et al., 1999; Fukushi et al., 2001). Another 7 small ribosomal subunit proteins have also been reported to be cross-linked to the HCV IRES. These are RpS2, RpS3, RpS6, RpS10, RpS15, RpS27 and RpS16 or RpS18 (Otto et al., 2002).

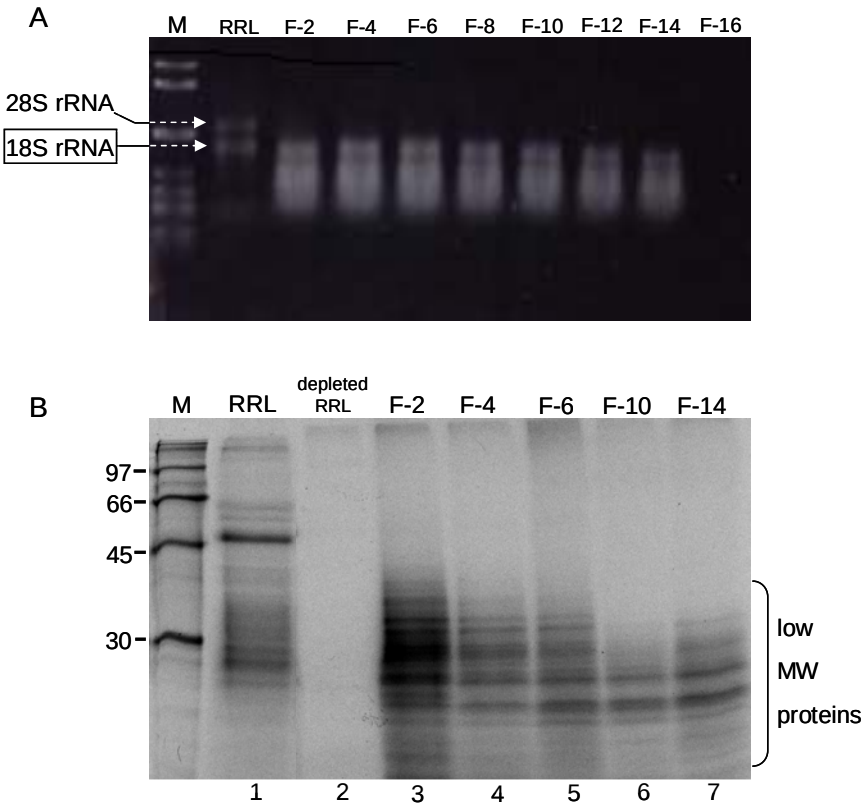

Fig. 13: Interaction of ribosomal proteins from RRL with [α-^{32}P]-UTP labelled HCV IRES RNA by UV cross-linking assay. (A) Agarose gel for detection of 18S rRNA from different fractionates (F-2 to F-16) after sucrose gradient centrifugation of ribosomal 40S subunits. F-number, fraction numbers. All fractions were extracted by Phenol/chloroform and precipitated with ethanol prior to gel-loading. **(B)** UV cross-linking assays with different fraction lysates. Lane 1, normal RRL; Lane 2, RRL without ribosomes and eIF3; Lane 3-7, purified 40S ribosomal subunit from fraction numbers corresponding to (A) after sucrose gradient centrifugation. Assays were performed as described in Fig. 10. Proteins were separated on SDS-14 % polyacrylamide gels and visualized by autoradiography. The molecular masses of ^{14}C labelled proteins marker (M) are given in kDa. The low molecular weight (MW) proteins related to 40S ribosomal subunit are indicated at the right side of the gel.

To confirm that the small proteins detected in Fig. 12 are mainly proteins of the small ribosomal subunit, 40S ribosomal subunits were isolated by sucrose gradient centrifugation from rabbit reticulocyte lysate according to a method described previously (Kieft et al., 2001). Although the peak of 40S ribosomal subunit in the gradient profile appeared to be not clear and sharp (data not shown), 18S rRNA, the only RNA inside the 40S ribosomal subunit, was readily detected in the bottom fractions recovered by fractionation of the gradient, which indicates that the 40S ribosomal subunits were sufficiently pure and at least did not contain any contaminating 60S subunits which would contain 28S rRNA (Fig. 13A). The result of the UV cross-linking assay with the purified 40S subunits and HCV RNA (Fig. 13B) shows that indeed the low molecular weight proteins binding to the HCV IRES are proteins of the small ribosomal subunit.

3.1.3 The HCV RNA constructs used for the protein-searching study

Since no novel protein was found using the UV cross-linking assays with the HCV IRES only RNA, two additional RNA constructs were considered to be used in the further experiments.

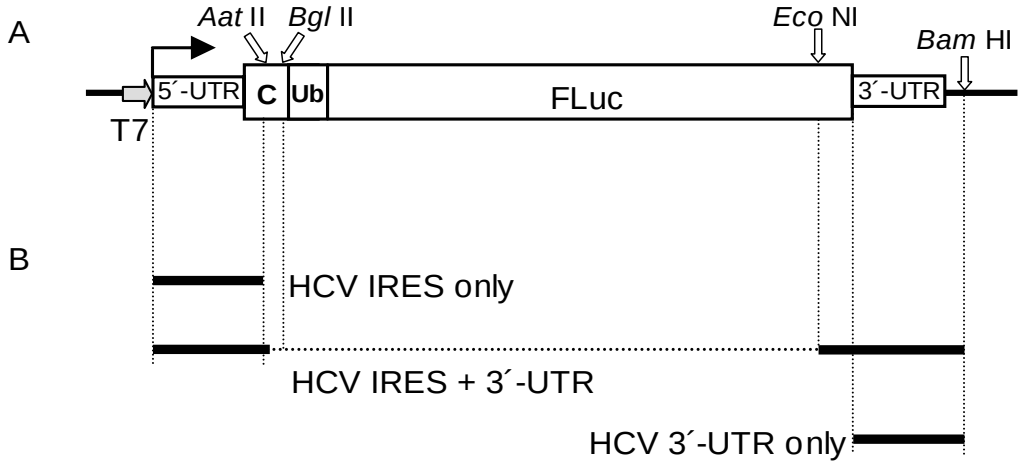

Fig. 14: Schematic diagram of the HCV wide-type (wt) construct (A) and three corresponding RNAs (B). The very beginning part of the core protein-encoding sequences is included in the "HCV IRES only" RNA and the "HCV IRES + 3´-UTR" RNA. *Aat* II and *Bam* HI were used for generating the "HCV IRES only" RNA template and the other two RNA templates, respectively. The solid lines represent the RNA molecules and the horizontal dotted line represents the part deleted from the original HCV wt plasmid in the IRES + 3´-UTR combination construct. T7, T7 RNA polymerase promoter; UTR, untranslated region; C, partial core protein-encoding sequences; Ub, ubiquitin sequences; FLuc, *Firefly* luciferase reporter gene.

These two additional HCV RNAs are: (1) the combination of HCV IRES and 3´-UTR - firstly, a intermediate plasmid was generated by religation of the HCV wt construct after double-digestion with *Bgl* II and *Eco* NI followed by treatment with *Klenow* fragment; this intermediate plasmid was secondly double-digested with *Aat* II and *Bgl* II followed by *Klenow* fragment and religation. Then *Bam* HI was used to linearize this new plasmid to produce the corresponding template; (2) the HCV 3´-UTR only. This was produced in two steps: firstly, the

construct generated in (1) was double-digested with *Bam* HI and *Bgl* II; then the small fragment containing the HCV 3´-UTR was ligated into another vector derived from pM12 (see Appendix) double-digested with the same enzymes. The recovered *Bam* HI recognition sequence was then used to generate the linearized RNA template. The HCV RNAs were synthesized using T7 (for HCV IRES or IRES+3´-UTR) or SP6 (for HCV 3´-UTR only) RNA polymerase in the presence of [α-^{32}P]-labelled ribonucleotides *in vitro* according to standard protocols.

The idea of using the HCV IRES plus 3´-UTR combination RNA was to search for proteins that are possibly involved in HCV genome circularization; thus, such proteins could be assumed to bind strongly only in the presence of both the 5´- and the 3´-end of the genomic RNA.

3.1.4 Choice of the optimal radioactive-labelling ribonucleotide for the detection of proteins binding to the HCV RNA

The three HCV RNAs - IRES only, IRES plus 3´-UTR, and 3´-UTR only - were internally labelled with four different nucleotides; [α-^{32}P]-ATP, -CTP, -GTP or -UTP, respectively. Rabbit reticulocyte lysate (RRL, purchased from Promega) which is competent for FMDV translation (Kühn et al., 1990) and also good for HCV RNA translation (data are shown later), as well as cytoplasmic lysate of human Huh-7 hepatoma cells were used as the source of IRES-binding proteins. UV cross-linking assays were then carried out using the radioactively-labelled RNAs as described above and the two different lysates.

Several proteins binding to the complete HCV IRES or the 3´-UTR were detected in the UV cross-linking assays with [α-^{32}P]-ATP, -CTP, -GTP, and -UTP-labelled RNAs (Fig. 15). A strongly labelled protein band migrating at about 57 kDa in the presence of [α-^{32}P]-CTP and -UTP, but only with the HCV IRES + 3´-UTR and the HCV 3´-UTR only RNAs, is identical to polypyrimidine-tract binding protein (PTB) (Tsuchihara et al., 1997; Luo, 1999). Two other bands appeared between 220 and 97 kDa with different intensities. These two proteins are supposed to be the 170 kDa and 116 or 110 kDa subunits of eIF3 (Buratti et al., 1998; Sizova et al., 1998). Obviously, all these detectable bands appeared more evidently in cytoplasmic Huh-7 lysate (Fig. 15B) than in RRL (Fig. 15A). In addition, in Huh-7 lysate, many proteins migrating near 66 kDa were detected to be cross-linked to the HCV IRES only and IRES + 3´-UTR RNAs, but not to the HCV 3´-UTR only RNA. Many distinctly strong bands below 66 kDa were also observed when the HCV 3´-UTR RNA was internally labelled with [α-^{32}P]-UTP. In RRL, only very faint bands below 66 kDa were found with some HCV RNAs, but again [α-^{32}P]-UTP labelled RNAs generated a good binding pattern.

Another polypeptide of about 66 kDa was also detected with [α-^{32}P]-UTP labelled HCV RNAs especially in the Huh-7 lysate. This protein is supposed to be one of the subunits of eukaryotic translation initiation factor eIF3 (Sizova et al., 1998). In addition, the UV cross-linking assay with [α-^{32}P]-GTP labelled RNAs showed also strong labelling of proteins with the HCV IRES RNA in both RRL and Huh-7 lysate. Therefore, [α-^{32}P]-UTP and -GTP labelled HCV RNAs were used for further detection of proteins in the UV cross-linking assay.

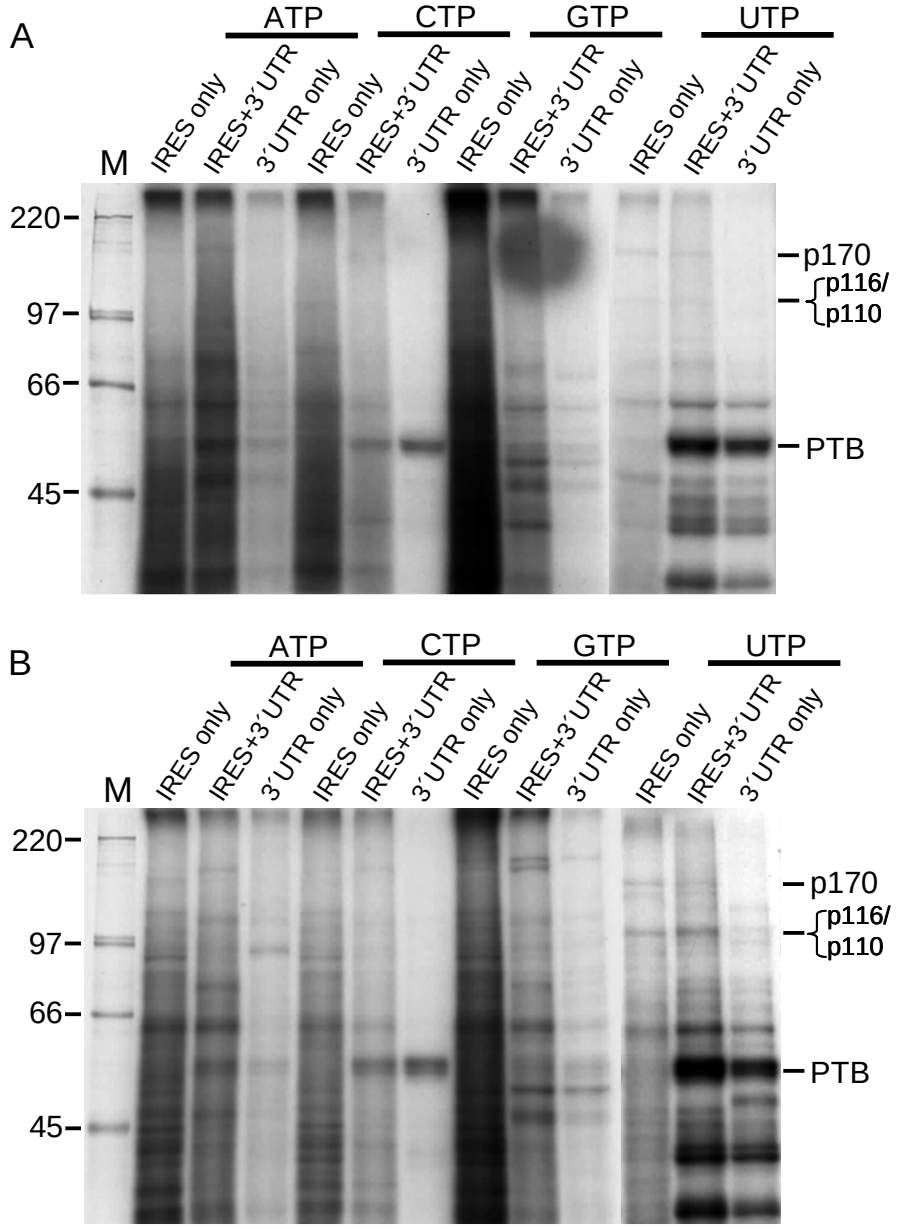

Fig. 15: Detection of proteins in RRL (A) and cytoplasmic extract of Huh-7 cells (B) using different HCV RNAs labelled with different nucleotides. The three HCV RNAs were *in vitro* transcribed from corresponding templates as shown in Fig. 14. UV cross-linking assays were carried out in 10 µl total volume with 4.4 µl of RRL or 4 µl of cytoplasmic extract of Huh-7 cells and 0.06 pmol of HCV RNAs internally labelled with either [α-^{32}P]-ATP, -CTP, -GTP or -UTP as indicated. Reaction mixtures were incubated for 10 min at 30°C to allow the binding of proteins from the RRL or Huh-7 cytoplasmic lysate to the HCV RNAs in the presence of 135 mM potassium and then UV irradiated at 254 nm on ice for 30 min. Excess RNA was digested by incubation with 3 mg/ml RNase A for 60 min at 37°C. Proteins were separated on SDS-8 % polyacrylamide gels and visualized by autoradiography. The molecular masses of ^{14}C labelled proteins marker (M) are given in kDa and the positions of the subunits of eIF3 (p170 and p116/110) and PTB are indicated at the right side of the gels.

Fig. 16 shows a similar experiment using the three HCV RNAs labelled only with [α-^{32}P]-UTP and -GTP performed in RRL and Huh-7 lysate. Again, very clear binding signals of the three proteins described above - p170, p116/110 and PTB - were observed in both lysates, but they appeared stronger with the cytoplasmic extract of Huh-7 (Fig. 16B) than with RRL (Fig. 16A). In the case of Huh-7 lysate, these three bands could be detected more evidently with [α-^{32}P]-UTP labelled RNAs (Fig. 16, lanes 4-6 and 10-12) than with [α-^{32}P]-GTP labelled RNAs (Fig. 16, lanes 1-3 and 7-9).

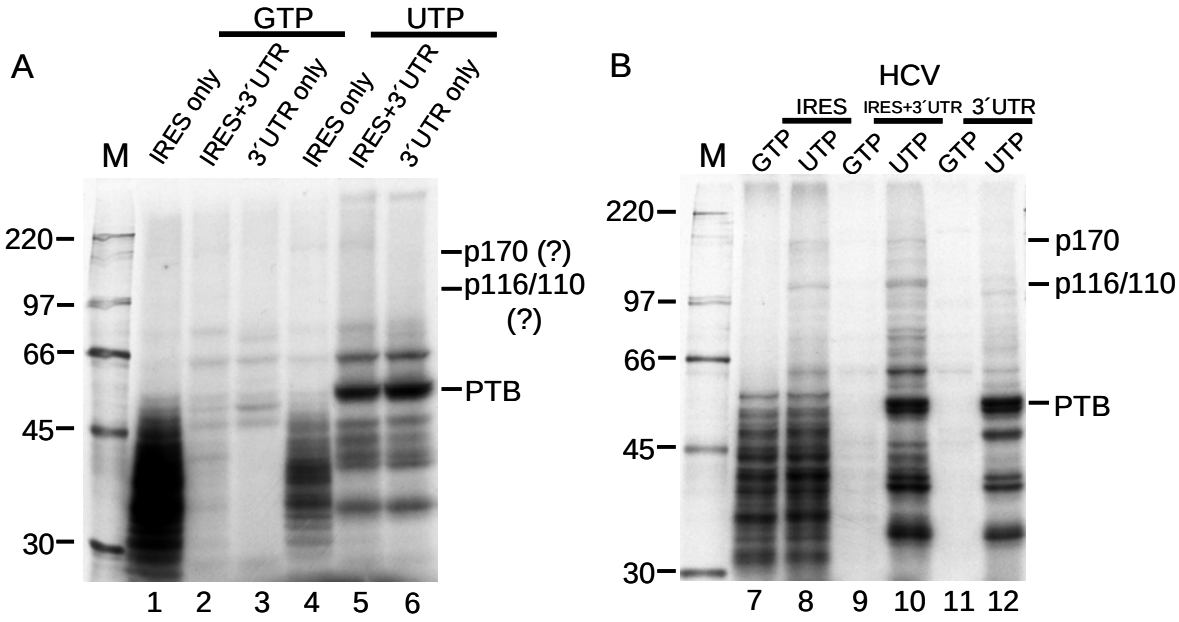

Fig. 16: UV cross-linking assay with [α-^{32}P]-GTP and -UTP labeled HCV RNAs in RRL (A) and Huh 7 lysate (B). The three HCV RNAs were *in vitro* transcribed from corresponding templates as shown in Fig. 14. UV cross-linking assays were performed as described in Fig. 10. Proteins were separated on SDS-8 % polyacrylamide gels and visualized by autoradiography. The molecular masses of ^{14}C labelled proteins marker (M) are given in kDa and the positions of the subunits of eIF3 (p170 and p116/110) and PTB are indicated at the right side of the gels.

According to these results, [α-^{32}P]-UTP labelled HCV RNAs were finally chosen for all following UV cross-linking experiments.

3.1.5 Optimization of protein binding specificity

In order to optimize the conditions for binding of proteins from RRL and Huh-7 lysate to the [α-^{32}P]-UTP labelled HCV IRES, IRES plus 3´-UTR and 3´-UTR RNAs, the effects of various parameters on the efficiency of the UV cross-linking assay were examined.

In order to reduce unspecific binding of proteins, transfer RNA (tRNA) was added as an unspecific competitor to the reactions. The results (Fig. 17) show that addition of tRNA resulted in efficient reduction of some unspecific

background (for example, the band marked with arrows in Fig. 17). However, too high concentrations of tRNA (2.5 µg/µl or 5 µg/µl) in the reactions even abolished binding of eIF3 subunits. Thus, a final concentration of 1 µg/µl tRNA was used in all following experiments.

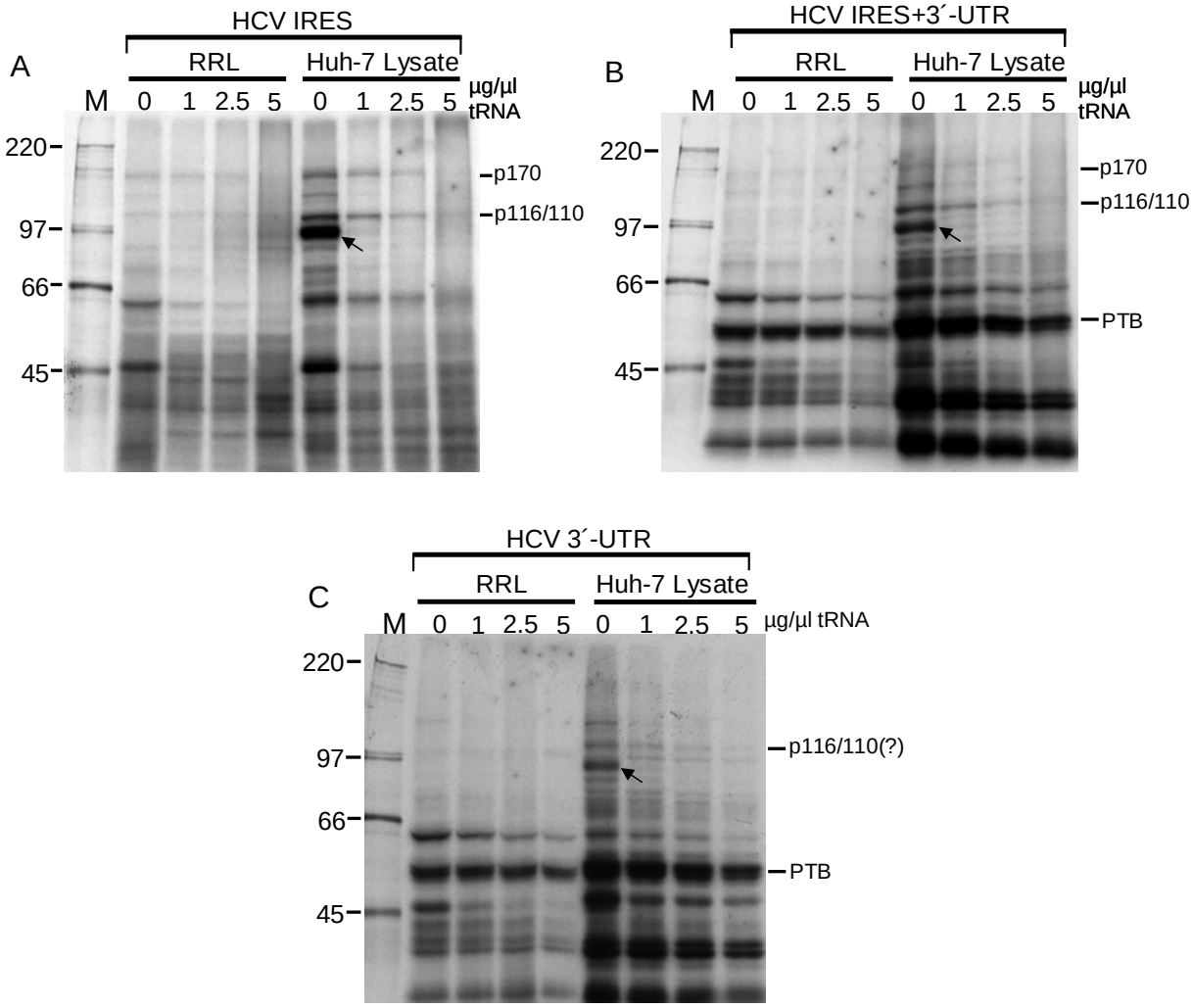

Fig. 17: UV cross-linking assays with HCV IRES only RNA (A), HCV IRES plus 3´-UTR RNA (B) and HCV 3´-UTR only RNA (C) in the absence or presence of tRNA in both RRL and Huh-7 lysate. The three HCV RNAs were *in vitro* transcribed from corresponding templates as shown in Fig. 14. The reactions were all performed as described in Fig. 10 under the same conditions in standard RRL and cytoplasmic lysate of Huh-7 cells, respectively. The final amounts of tRNA added to the reactions are indicated above the gels. Proteins were separated on SDS-8 % polyacrylamide gels and visualized by autoradiography. The molecular masses of ^{14}C labelled proteins marker (M) are given in kDa and the positions of the subunits of eIF3 (p170 and p116/110) and PTB are indicated.

In the experiments described above, the binding signals obtained with all three different HCV RNAs were usually clearer with cytoplasmic extract of Huh-7 cells than with rabbit reticulocyte lysate, especially for PTB (Fig. 17B and C) and the subunits of eIF3 (Fig. 17A and B). Interestingly, it was unexpectedly observed that one of the subunits of eIF3 (p116/110) obviously also binds to the HCV 3´-UTR RNA (Fig. 17C). However, this

binding was not studied further at this time since this part of the study aimed at the detection of proteins that bind synergistically to both the 5´-UTR and the 3´-UTR.

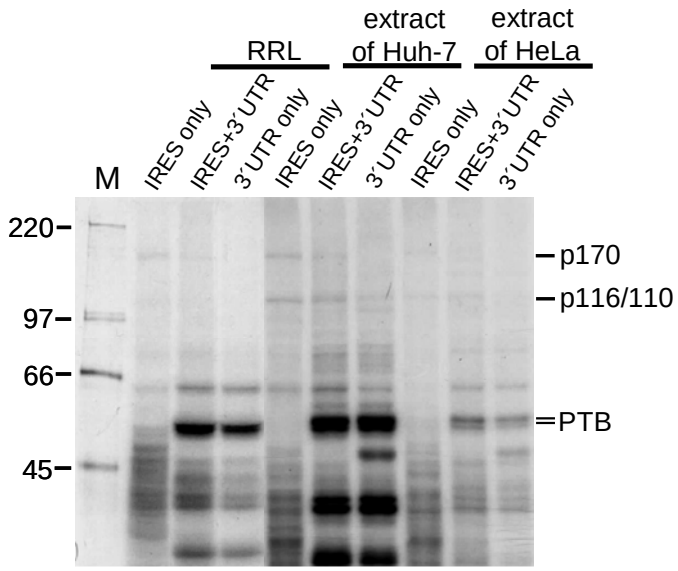

Fig. 18: Comparison of different cellular lysates in UV cross-linking assay with three HCV IRES RNAs. The three HCV RNAs were *in vitro* transcribed from corresponding templates as shown in Fig. 14. The reactions were all performed as described in Fig. 10. Proteins were separated on a SDS-8 % polyacrylamide gel and visualized by autoradiography. The molecular masses of ^{14}C labelled proteins marker (M) are given in kDa and the positions of the subunits of eIF3 (p170 and p116/110) and PTB are indicated.

In addition to RRL and Huh-7 lysate, cytoplasmic lysate of HeLa cells was also tested with the three HCV RNAs since it had been reported that HCV IRES-directed translation is similarly efficient both in hepatocytic cells such as Hep G2 and Huh-7 and in non-hepatocytic cells such as HeLa cell (Tsukiyama-Kohara et al., 1992; Reynolds et al., 1995; Kamoshita et al., 1997). The result shown in Fig. 18 demonstrates that the protein binding patterns derived from the HeLa lysate were almost similar to that observed with RRL and Huh-7 lysate. However, the labelling intensities of those proteins binding to the HCV RNAs such as p170, p116/110 and PTB are clearly weaker in HeLa lysate, and even weaker than in RRL (e.g., the PTB band).

Next, different preparations of cytoplasmic lysate of Huh-7 were also tested in order to confirm that the observed pattern of proteins is reproducible from batch to batch. The result shows that two different Huh-7 lysates prepared at different times generated almost the same labelling pattern in the UV cross-linking assay (Fig. 19), also regarding the binding signals of PTB and eIF3. Thus, the procedure of Huh-7 lysate preparation was proven to be reproducible. Furthermore, the final potassium concentration in the reaction with Huh-7 lysate was tested as well (data not shown) and then always adjusted to ~135 mM which is consistent with the physiological conditions inside living cells.

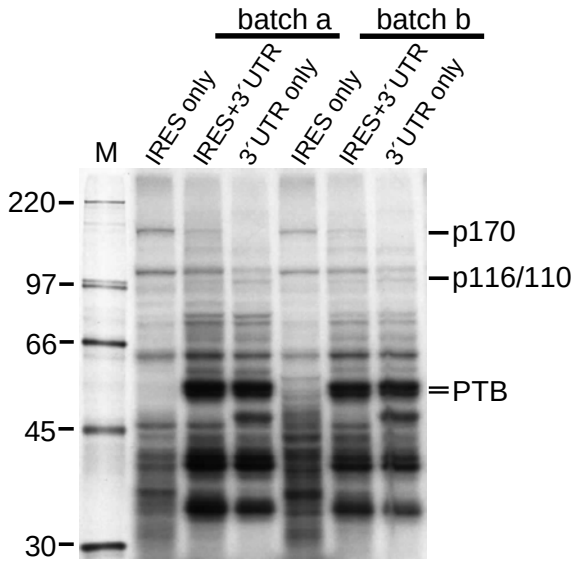

Fig. 19: Comparison of different batches of Huh-7 lysate in the UV cross-linking assay with three HCV RNAs. The three HCV RNAs were *in vitro* transcribed from corresponding templates shown in Fig. 14. All reactions were performed as described in Fig. 15. Proteins were separated on a SDS-8 % polyacrylamide gel and visualized by autoradiography. The molecular masses of ^{14}C labelled proteins marker (M) are given in kDa and the positions of the subunits of eIF3 (p170 and p116/110) and PTB are indicated.

3.1.6 Detection of proteins in ammonium sulfate precipitation fractions

In the cytoplasmic lysate of Huh-7 cells, many proteins were found to be cross-linked to the HCV RNA by UV irradiation. In order to investigate these binding proteins in more detail, ammonium sulfate precipitation was used to separate the proteins into different fractions.

According to a Coomassie stain of the ammonium sulfate fractions analysed on a protein gel (Fig. 20A), most proteins are precipitated in the range of 20-80 % ammonium sulfate saturation, and the patterns of the individual fractions appear to be significantly different. Each fraction was then used for UV cross-linking assays with the three HCV RNAs. The result (Fig. 20B) shows that most proteins binding to the HCV RNAs are mainly present in the 20-40 % and 40-60 % ammonium sulfate fractions. Also, some proteins yielded very clear binding signals in other fractions. For example, PTB is present preferentially in the 20-40 % fraction, a little weaker in the 40-60 % fraction and even much weaker in the 0-20 % fraction (Fig. 20B, lanes 5-6, 8-9, 11-12). Subunits of eIF3 mainly binding to the HCV IRES are much more evident in the 20-40 % saturation fraction than in any other fraction (Fig. 20B, lanes 4, 7, 10, 13, 16). In addition, some new proteins binding to HCV RNAs (Fig. 20B, lanes 12-17) or to the HCV 3´-UTR RNA (Fig. 20B, lane 18) were observed at 60-80 % and 80-100 % of ammonium sulfate saturation (marked with arrows), but they were not detected when complete Huh-7 lysate was used (Fig. 20B, lanes 1-3). By the way, this experiment further confirmed that PTB does not bind to the HCV IRES in the UV cross-linking assay even though there are three polypyrimidine-rich tracts within the HCV IRES region (see Fig. 6 for reference and Fig. 20B, lanes 1, 4, 7, 10).

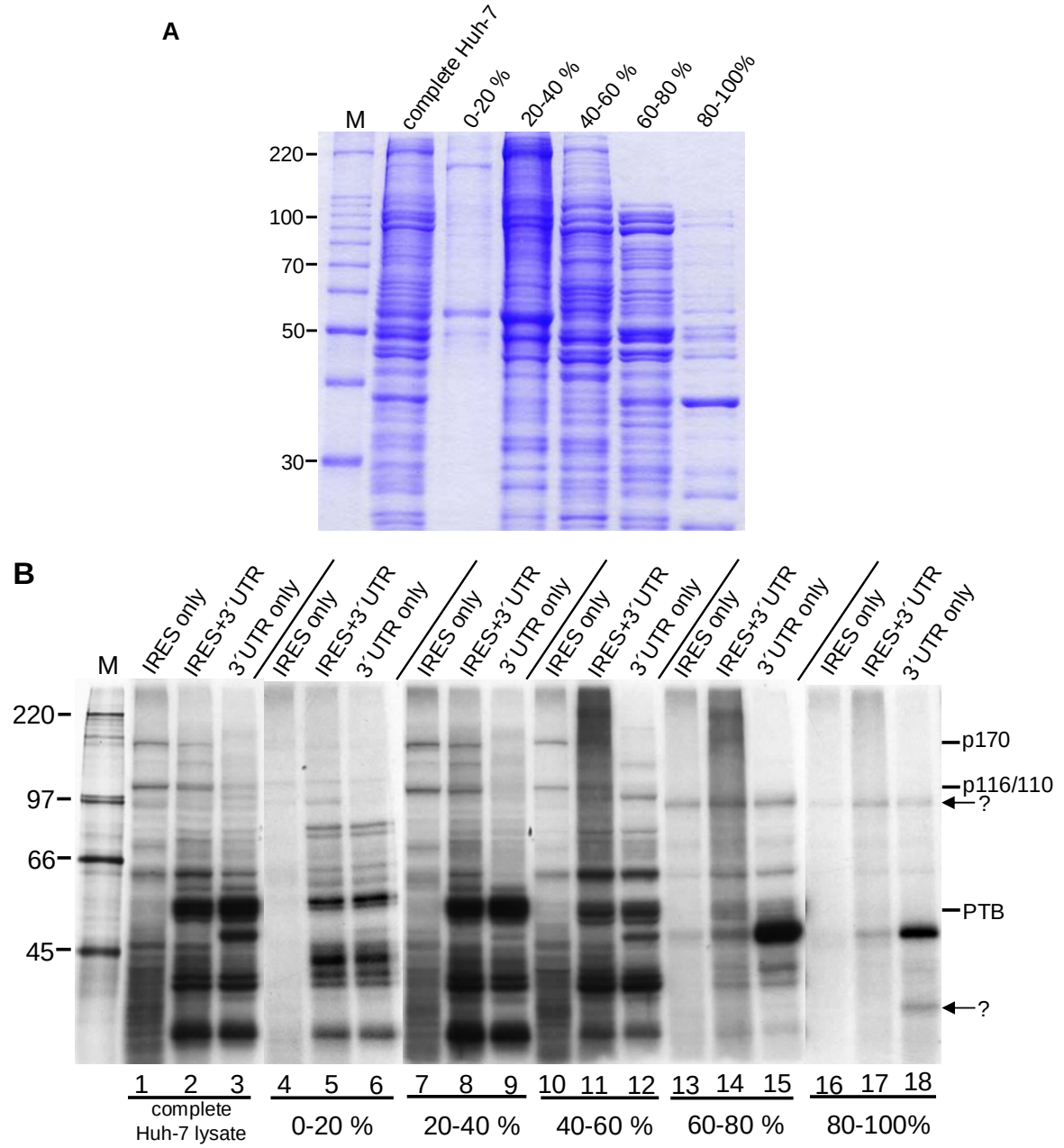

Fig. 20: Analysis of interaction of proteins from ammonium sulfate saturations with HCV RNAs in Huh-7 cytoplasmic lysate. (A) Proteins present in Huh-7 cytoplasmic fractions after ammonium sulfate precipitation. Proteins were separated on a 10 % SDS-PAGE gel and stained with Coomassie brilliant blue. The molecular masses of marker proteins (M, Invitrogen) are indicated in kDa at the left side of the gel. **(B)** UV crosslink assay with [α-^{32}P]-UTP labelled HCV RNAs and complete Huh-7 lysate or ammonium sulfate fractions. The three HCV RNAs used are shown in Fig. 14. Proteins were separated on a SDS-8 % PAGE gel and visualized by autoradiography. The molecular masses of ^{14}C labelled proteins marker (M) are given in kDa, and the positions of the subunits of eIF3 (p170 and p116/110) and PTB are indicated. Some unknown binding proteins discussed in the text are indicated with arrows and question marks.

However, no new proteins could be detected to bind exclusively to the IRES plus 3′-UTR combination RNA but the IRES alone or the 3′-UTR alone, which could be assumed to be possibly involved in genome circularization and translation stimulation.

3.1.7 Conclusions

Unfortunately, except for some known cellular proteins (such as PTB and several subunits of eIF3) reported to bind to either the HCV 3′-UTR or the IRES RNA, no novel cellular protein which may bind to the HCV IRES RNA was detected, even in the presence of the 3′-UTR which might provide synergistically possible binding chance for proteins present in the cellular lysate like RRL and cytoplasmic extract of Huh-7 cells, under the binding systems presented here. Further attempts should concentrate on revising the HCV RNA construct used for this protein-seeking programme. In a later part of this study, re-designed RNA constructs were used, resulting in the discovery of a novel protein (see Results, Part **IV**).

3.2 Part II: Synergetic interaction of known cellular proteins – PTB, hnRNP L and Unr – with the Hepatitis C Virus RNA

The aim of the second part of this study was to analyze the interaction of a limited set of well-known *trans*-acting cellular proteins with the HCV RNA including the IRES or the 3´-UTR or a combination of both IRES and 3´-UTR.

As described in the first part of the Results section, several well-characterized cellular factors have already been reported to bind to the HCV RNA including the IRES or the 3´-UTR and to possibly affect the HCV IRES-mediated translation. These factors include the human La autoantigen (Ali & Siddiqui, 1997; Isoyama et al., 1999), PTB (Ali & Siddiqui, 1995; Tsuchihara et al., 1997; Luo, 1999), some ribosomal proteins (Fukushi et al., 1999; Fukushi et al., 2001; Otto et al., 2002), poly(C)-binding proteins (PCBPs, Spangberg & Schwartz, 1999b), hnRNP L (Hahm et al., 1998b), eIF3 (Buratti et al., 1998; Sizova et al., 1998), NS1-associated protein 1 (NSAP1, Kim et al., 2004), the proteasome subunit PSMA7 (Krüger et al., 2001), nucleolin (Izumi et al., 2001) and some other proteins including Unr (Lu et al., 2004). Among these, the interaction of PTB, which has been shown to play important roles in the translation of picornaviruses, with the HCV IRES and its exact role in HCV IRES-mediated translation are controversial (Ali & Siddiqui, 1995; Kaminski et al., 1995; Ito & Lai, 1999; Gosert et al., 2000; Tischendorf, 2004). This part will first focus on studying the interaction of PTB with the HCV RNA to examine whether PTB actually binds to the HCV IRES RNA or not.

In addition, the possible influence of interactions between these RNA-binding proteins (such as PTB and hnRNP L, PTB and Unr, Unr and hnRNP L) on HCV IRES-dependent translation was investigated as well, since PTB and hnRNP L interact tightly (both of them belong to the hnRNPs family, (Hahm et al., 1998a), and PTB and Unr act synergistically in efficient Apaf-1 IRES function (Mitchell et al., 2001; Mitchell et al., 2003).

3.2.1 Interaction of polypyrimidine tract-binding protein (PTB) with HCV RNAs

3.2.1.1 Interaction of recombinant and cellular PTB with different HCV RNAs analyzed by UV cross-linking assay

In the HCV 5´-UTR, there are three pyrimidine-rich tract motifs which could, in principle, serve as binding sites for the polypyrimidine tract-binding protein (PTB). They are located at nucleotides 40 to 46 (Py-I), 120 to 130 (Py-II), and 191 to 199 (Py-III). The Py-I and Py-III sequences are part of single-stranded regions, but Py-II sequences are partially base-paired with nucleotides 318 to 323 (Fig. 6 in Introduction section). Some conflicting observations have been reported on the interaction of PTB with the HCV IRES (Ali & Siddiqui, 1995; Kaminski et al., 1995; Beales et al., 2001). In order to analyze the binding of PTB to the HCV IRES, the interaction of recombinant PTB as well as cellular PTB with different HCV RNA constructs was investigated by the UV cross-linking assay. These RNA constructs were generated from the corresponding monocistronic HCV plasmid construct shown in Fig. 14 in the first part of the Results section.

Two HCV RNAs were synthesized using T7 (HCV IRES only) or SP6 (HCV 3´-UTR only) RNA polymerase in the presence of [α-^{32}P]-UTP. The radioactively labelled HCV IRES and 3´-UTR RNAs were incubated in a UV cross-linking reaction with purified recombinant His_6-PTB at various protein concentrations without addition of any other protein. tRNA was added simultaneously to the reaction mixtures as a competitor to eliminate possible unspecific binding.

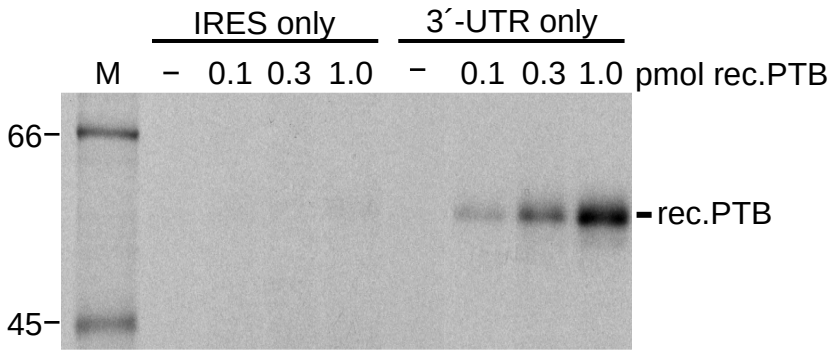

Fig. 21: Interaction of recombinant PTB with the HCV IRES and 3´-UTR RNAs in the absence of cellular lysate. UV cross-linking assays were performed in 10 µl volumes in the presence of 1 µg/µl tRNA and analyzed on an 8 % SDS-PAGE. The amount of recombinant PTB (rec. PTB) added to the reactions is indicated on the top of the gel. The molecular masses of ^{14}C labelled proteins marker (M) are given in kDa. The position of rec. PTB (59 kDa) is indicated at the right side of the gel.

The reaction mixtures were subsequently UV-irradiated on ice for 30 min, and then digested with RNase A prior to analysis by SDS-PAGE and autoradiography. Only very weak PTB bands were found to be cross-linked to the HCV 5´-UTR RNA, whereas the HCV 3´-UTR which is known to be bound effectively by PTB (Tsuchihara et al., 1997) showed very strong PTB binding (Fig. 21). In conclusion, the recombinant PTB does obviously not interact with the HCV 5´-UTR.

The PTB binding experiment described above was carried out with a PTB protein expressed in *E. coli*. To analyze the possible interaction of PTB from cell lysate with the HCV IRES and 3´-UTR RNAs, rabbit reticulocyte lysate (RRL) purchased from Promega and Huh-7 S10 cytoplasmic lysate prepared from cultured Huh-7 hepatoma cells were used. Two or three closely migrating proteins with an average molecular mass of 57 kDa were observed as major bands in the HCV 3´-UTR RNAs, but these proteins were not found with the HCV IRES RNA (Fig. 22). These two or three bands in the range of 57 kDa may represent isomers of PTB as reported by other groups (Garçia-Blanco et al., 1989; Bothwell et al., 1991; Patton et al., 1991).

In conclusion, the cellular 57 kDa PTB protein interacts directly with the HCV 3´-UTR, but not with the HCV IRES. Even though PTB is required for the internal translation directed by some picornavirus IRESes such as the FMDV IRES and the EMCV IRES (Hellen et al., 1993; Witherell et al., 1993; Niepmann et al., 1997), the results shown here indicate that PTB does not bind the HCV IRES. This finding is in accordance with a previous report by another group which shows that PTB is not required for translation directed by the HCV IRES in a reporter construct which does not contain the HCV 3´-UTR (Kaminski et al., 1995).

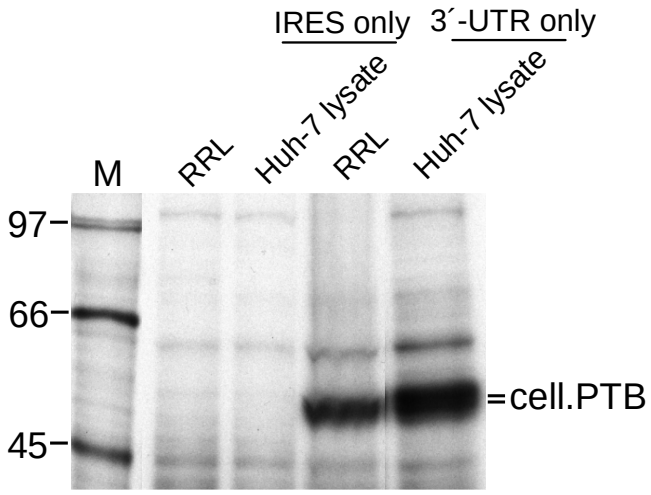

Fig. 22: Interaction of the endogenous PTB contained in RRL and Huh-7 lysate with the HCV IRES and 3´-UTR RNAs. UV cross-linking assays were performed in 10 µl volumes with [α-^{32}P]-UTP labelled HCV RNAs. Proteins are analyzed by 8 % SDS-PAGE and visualized by autoradiography. The molecular masses of ^{14}C labelled proteins marker (M) are given in kDa, and the position of cellular PTB (cell. PTB) is indicated at the right side of the gel.

3.2.1.2 Effect of PTB on HCV translation in reticulocyte lysate

The results of the PTB binding experiments presented above have shown that neither recombinant PTB nor cellular PTB can be effectively UV cross-linked to the HCV IRES RNA, which means that translation initiation of the HCV RNA does not require PTB.

It has been shown that the HCV RNA genome possesses a unique highly conserved region at the 3´-end of the genome. The 3´-UTR of HCV consists of three elements: a 30- to 40-nucleotide (nt) variable region, followed by a 20- to 200-nt poly-(U/C) stretch and, at the very 3´-end, a highly conserved 98-nt sequence termed the 3´X region (Tanaka et al., 1995; Tanaka et al., 1996). Tsuchihara and co-workers have reported that PTB can specifically bind to the HCV 3´-UTR (Tsuchihara et al., 1997). These authors suggested that a 3´UTR-PTB interaction is involved in the specific initiation of HCV genome replication. However, they did not show if PTB-binding is functional or not. It will be shown in the third part of the Results section that translation of HCV can be stimulated by the HCV 3´-UTR. Therefore, the following experiments were carried out to investigate whether there is a functional role of PTB in HCV translation through the interaction with the 3´-UTR.

For this purpose, two different monocistronic reporter RNAs were used (Fig. 23). They both contain the entire HCV 5´-UTR sequence plus partial core protein-encoding sequences, a ubiquitin sequence and the entire *Firefly* luciferase (FLuc) reporter gene, either ending exactly at the 3´-end of the FLuc coding sequence, or additionally including the complete HCV 3´-UTR. The upstream part of the core protein-encoding sequence was included since the 5´-region of the core protein-encoding sequence was required for efficient internal initiation of HCV (Reynolds et al., 1995; Rijnbrand et al., 1995).

The two monocistronic reporter RNAs were *in vitro*-transcribed from PCR-generated templates. *In vitro*-translation experiments using these RNAs were then performed in rabbit reticulocyte lysate (RRL) in the

presence of 130 mM potassium chloride, which is close to the physiological potassium concentration of 140 mM. The efficiency of translation was then analyzed by measuring *Firefly* luciferase (FLuc) activity.

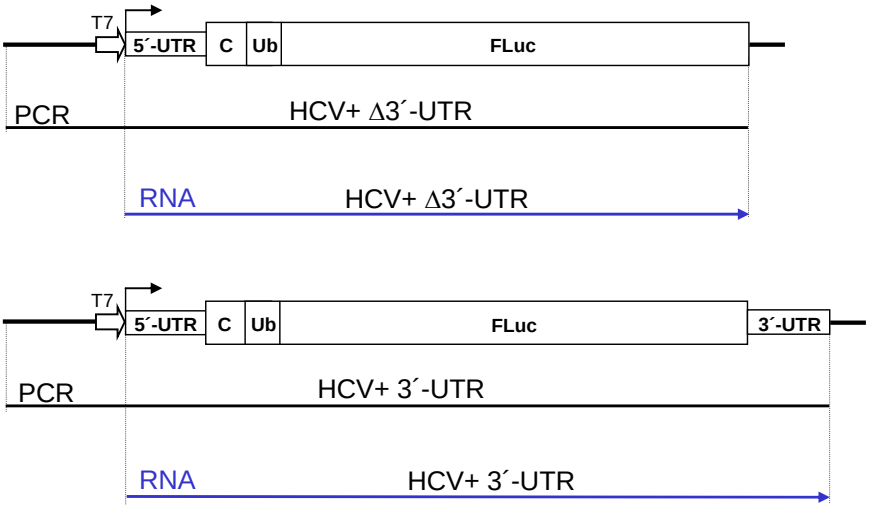

Fig. 23: Schematic representation of the HCV plasmids, PCR templates for transcription and reporter RNAs. T7, T7 RNA polymerase promoter; UTR, untranslated region; C, partial core protein-encoding sequences; Ub, ubiquitin sequences; FLuc, *Firefly* luciferase reporter gene.

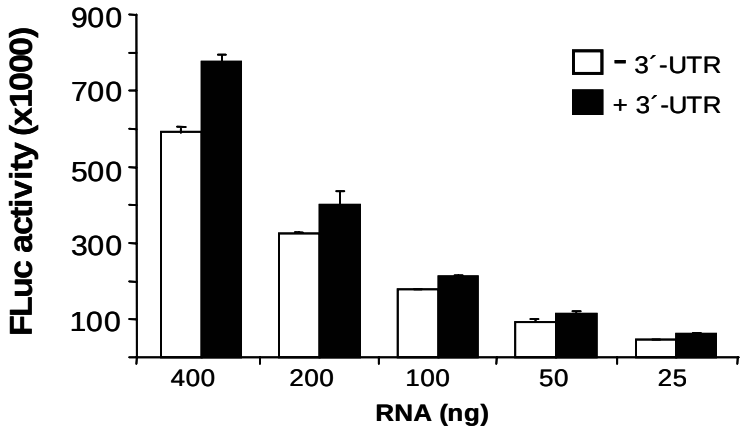

Fig. 24: Effect of the presence of the HCV 3´-UTR on HCV IRES-mediated translation in rabbit reticulocyte lysate. *Firefly* luciferase (FLuc) activities from various amounts of RNA expressed by *in vitro*-translation performed in standard rabbit reticulocyte lysates (RRL). The columns and bars represent the means and standard deviations of at least three independent experiments.

The results demonstrate that the activity of the *Firefly* luciferase translated from different transcripts in reticulocyte lysate at different amount of RNA did not show any difference, irrespective if the 3´UTR was included or not (Fig. 24).

In addition, a possible role of PTB in the HCV IRES-driven translation was further investigated by using an *in vitro* translation system described previously, the PTB-depleted RRL (Niepmann, 1996; Niepmann et al., 1997).

The endogenous PTB was removed from normal RRL using RNA (EMCV IRES domain 1)-affinity beads (see Materials and Methods). The amount of PTB remaining in the lysate was monitored by a UV cross-link assay using radioactively labelled FMDV IRES RNA (Fig. 25). After treatment with the RNA-affinity beads, the amount of PTB in RRL was largely, but not completely, reduced. Some proteins seemed not to be affected dramatically, whereas others were influenced seriously (Fig. 25, lane 2). For instance, eIF4G was still present in PTB-depleted RRL, but the labelling intensity of eIF4B appeared much weaker in depleted RRL than in normal RRL. Nevertheless, it was shown that PTB can stimulate binding of eIF4G to the FMDV IRES when added to this PTB-depleted reticulocyte lysate (Song et al., 2005), which proved that this PTB-depleted lysate is suitable for testing a possible influence of PTB on HCV translation.

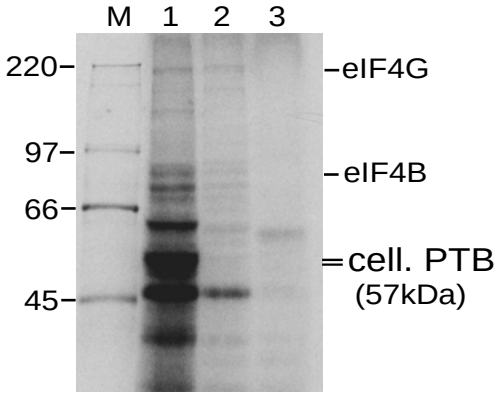

Fig. 25: Comparison of PTB-depleted and normal RRLs by UV cross-linking assay with radioactively labelled FMDV IRES RNA. UV cross-linking assays were performed in 10 µl volumes in normal RRL (lane 1) or PTB-depleted RRL (lane 2), respectively. Proteins were analyzed on 8 % SDS-PAGE and visualized by autoradiography. The molecular masses of ^{14}C labelled proteins marker (M) are given in kDa. The position of cellular PTB (cell. PTB, 57 kDa) is indicated on the right side of the gel. eIF4G, eukaryotic initiation factor 4G; eIF4B, eukaryotic initiation factor 4B.

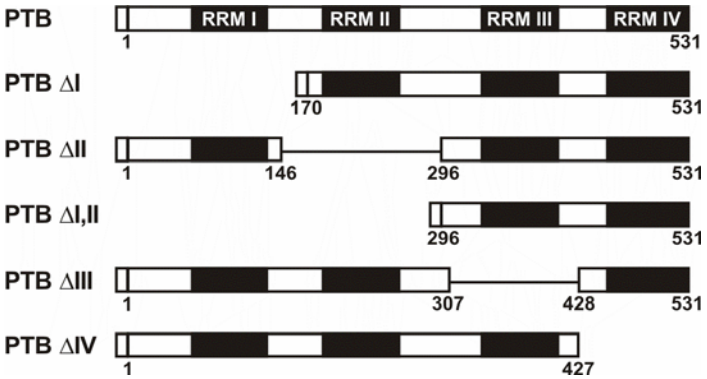

Fig. 26: The wild-type PTB protein and its deletion mutants used for the translation stimulation assay. Mutants are shown with amino acid numbers flanking the deletions (Song et al., 2005). The small N-terminal box represents the His_6-tag.

To examine if the PTB-depleted lysate functionally responds to the addition of recombinant PTB, test experiments (Fig. 27) were performed with the foot-and-mouth disease virus (FMDV) IRES and PTB as well with domain deletion mutants of PTB (see Fig. 26).

PTB has four RNA-recognition motifs (RRM) or ribonucleoprotein (RNP) domains (Gil et al., 1991; Kenan et al., 1991; Patton et al., 1991). PTB ΔI was even more active than wild-type PTB in the stimulation of IRES activity. Thus, PTB domain I is not required for FMDV translation stimulation. With PTB ΔII, a slightly lower efficiency of FMDV translation stimulation was observed. At the highest concentration of 240 nM, still 85 % stimulation was achieved.

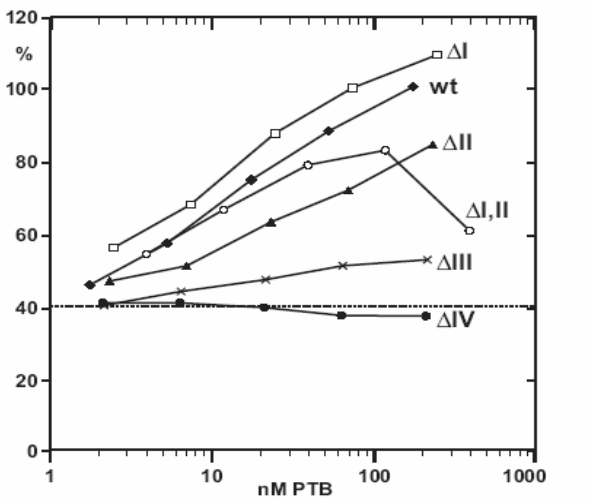

Fig. 27: Test of the PTB-depleted lysate: stimulation of FMDV IRES dependent translation by wild-type PTB and PTB deletion mutants. The dotted line indicates the basal translation efficiency of 40.6 % obtained with PTB-depleted RRL in the absence of supplemented PTB. To the PTB-depleted RRL, either wild-type PTB (wt) or the corresponding mutants PTBΔI, ΔII, ΔI,II, ΔIII or ΔIV (see Fig. 26), respectively, were added before translation. The X-axis indicates the final concentrations of added PTB protein in the reaction. Readings show the efficiency of translation of the IRES dependent luciferase gene (pM12 RNA), standardized by setting the reaction with 100 ng wild-type PTB as 100%. All curves originate from the same value at about 40% stimulation (lines not shown due to the logarithmic scale on the X-axis).

A stimulation of IRES-driven translation was also obtained with PTB ΔI,II. In contrast, PTB ΔIII caused only a very slight increase in translation efficiency, whereas no stimulation was detected with PTB ΔIV (Song et al., 2005). In conclusion, stimulation of FMDV IRES-driven translation can be achieved with a PTB protein that only contains the two RNA-binding domains III and IV, and the PTB-depleted RRL can be regarded as a test system suitable for the analysis of the role of PTB in *in vitro*-translation reactions.

This PTB-depleted RRL was then used to analyze the effect of added purified recombinant His_6-PTB on the HCV translation. The results show that the HCV IRES-directed translation could not be stimulated by addition of exogenous PTB to the PTB-depleted RRL (Fig. 28). However, *Firefly* luciferase expression was considerably reduced in the PTB-depleted RRL compared with normal RRL, indicating that some other factors required for HCV IRES-mediated translation might have been depleted together with PTB during the depletion procedure.

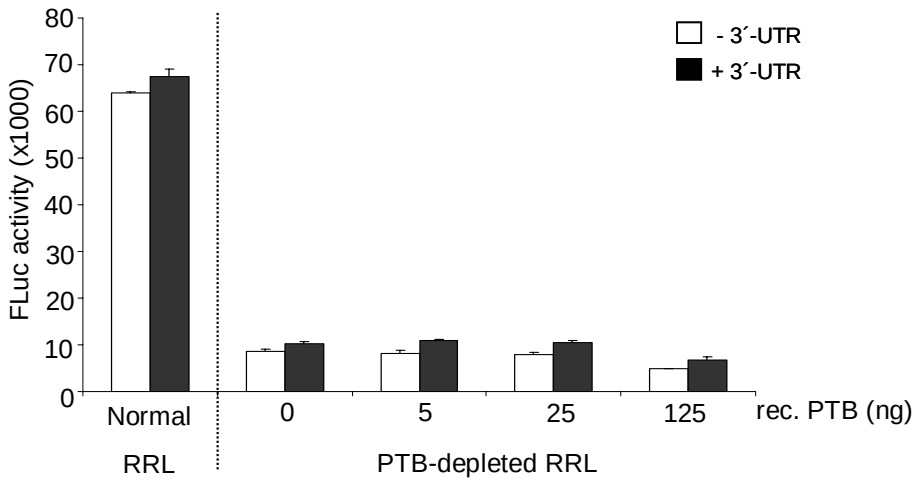

Fig. 28: Effect of PTB on HCV translation performed *in vitro* in PTB-depleted RRL. The amounts of recombinant PTB (rec. PTB) added in the reactions are indicated. *Firefly* luciferase (FLuc) activities of the translational products from HCV RNAs were measured in PTB-depleted RRL with increasing amount of recombinant PTB. The columns and bars represent the means and standard deviations of duplicate experiments.

Taken together with the results above, it is concluded that PTB, although specifically binding to the HCV 3´-UTR, has no detectable effect on the efficiency of translation of the HCV RNA in this *in vitro*-translation system.

3.2.2 Interaction of heterogeneous nuclear ribonucleoprotein L (hnRNP L) with HCV RNAs

Heterogeneous nuclear ribonucleoproteins (hnRNPs) are abundant nucleoplasmic pre-mRNA-binding proteins which play important roles in the biogenesis of mRNA (Dreyfuss et al., 1993). hnRNPs are, by definition, nuclear proteins that interact with heterogeneous nuclear RNAs (hnRNAs). Several functions have been suggested for hnRNPs. They mostly relate to RNA functions such as pre-mRNA processing, mRNA translocation from the nucleus to the cytoplasm, and translation (Dreyfuss et al., 1993). The last two functions are attributed to a group of hnRNPs that shuttle between the nucleus and the cytoplasm. Several hnRNPs were reported to play roles in translation. PTB (hnRNP I) was shown to enhance IRES-dependent translation of encephalomyocarditis virus (EMCV) and foot-and-mouth disease virus (FMDV) mRNAs (Kaminski et al., 1995; Niepmann, 1996). hnRNP E2, which is also known as PCBP2, was required for the efficient translation of poliovirus RNA in HeLa cells (Blyn et al., 1997). On the other hand, hnRNP K and E1 inhibit translation of erythroid 15-lipoxygenase mRNA by binding to the 3´-UTR of the mRNA (Ostareck et al., 1997). Therefore, it would not be surprising to discover other hnRNPs which may be involved in the process of translation.

hnRNP L was reported to be localized mainly in the nucleus (Pinol Roma et al., 1989). Interestingly, hnRNP L was found in the cytoplasm as well as in the nucleus when transcription of cellular mRNA was blocked by poliovirus infection or treatment with actinomycin D (Hahm et al., 1998b). These findings suggest that hnRNP L

may shuttle between the nucleus and the cytoplasm in a transcription-sensitive manner similar to that of some other hnRNP proteins, for example, hnRNP A1, E, and I (Michael et al., 1995). Therefore, hnRNP L may facilitate translation of some mRNAs while it stays in the cytoplasm. The following experiments were launched on the basis of the evidence that this 68 kDa hnRNP L protein can specifically interact with the 3´ border of the HCV IRES including part of the core protein-encoding sequence (Hahm et al., 1998b).

3.2.2.1 Detection of the interaction of hnRNP L with different HCV RNAs by shifts and UV cross-linking assay

In the following experiments, the electrophoretic mobility shift assay (EMSA), or band shift, and the standard UV cross-link assay were used to detect the binding of hnRNP L or other recombinant proteins to the HCV RNAs. The EMSA is based on the observation that protein-RNA complexes migrate through polyacrylamide gels more slowly than free RNA fragments.

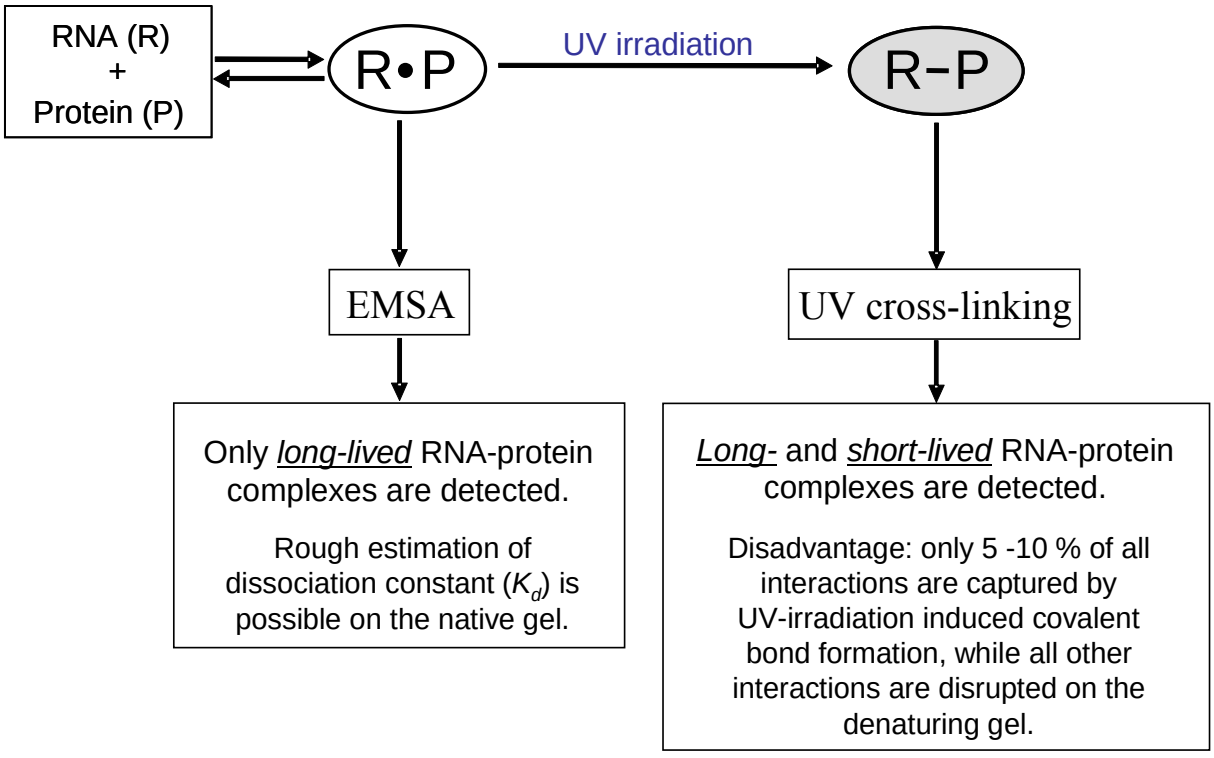

Fig. 29: Schematic diagram of differences between shift and UV cross-linking assays. EMSA, electrophoretic mobility shift assay; R•P, non-covlant RNA-protein complex; R-P, covalently fixed RNA-protein complex.

Both the electrophoretic mobility shift assay (EMSA) and the UV cross-link assay detect direct interactions between native protein and native RNA, but each assay has particular advantages and disadvantages. In the shift

assay, the protein-RNA interaction is monitored approximately quantitatively and allows a rough estimation of dissociation constants (K_d). However, successful detection requires that the interaction of a given protein molecule with a given RNA molecule is stable enough to withstand both the incubation step and the gel-electrophoresis. In contrast, in the UV-crosslink assay even very short-lived binding events are captured by UV-induced covalent bonds between protein and RNA. However, only 5 to 10 % of the interactions are covalently fixed by the UV-light, while all other interactions are disrupted when loading the samples to a denaturing protein gel.

Thus, the major difference between these two methods, as shown in Fig. 28, is that both long- and short-lived RNA-protein complexes can be detected after UV irradiation, whereas only long-lived RNA-protein complexes can be detected in the EMSA. Based on this difference, different binding results were often obtained using the different methods, even if the binding reactions were exactly the same.

hnRNP L can specifically bind to sequences at the 3´-border of the HCV IRES (Hahm et al., 1998b). However, it remains unclear how this binding may be influenced by the presence of the 3´-UTR. In order to answer this question, low amounts of recombinant GST-fused hnRNP L (kindly provided by Prof. A. Bindereif, Giessen) were used in the shift assay with the three HCV RNA constructs shown in Fig. 14. The result shown in Fig. 30A demonstrates that GST-hnRNP L interacts directly with the HCV IRES RNA but not with the HCV 3´-UTR RNA.

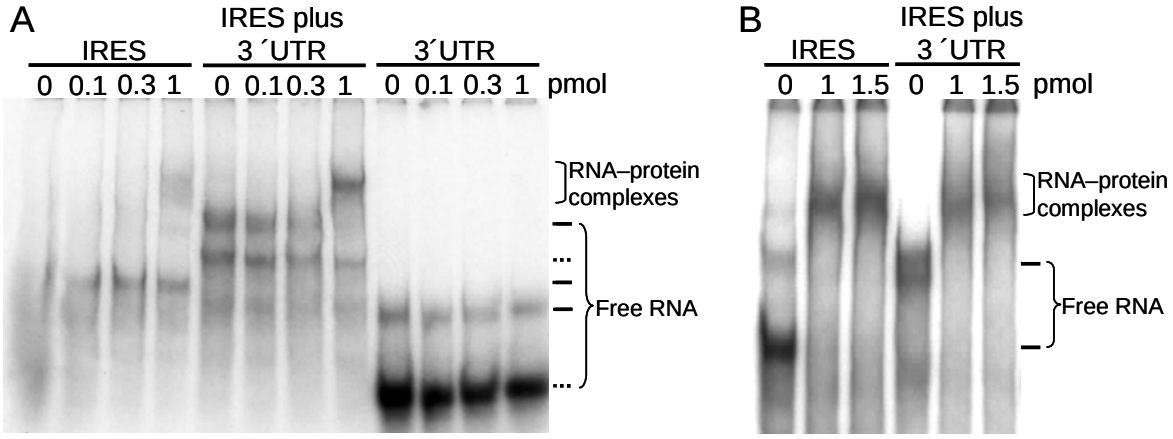

Fig. 30: Interaction of GST-fused hnRNP L with HCV RNAs analyzed by EMSA. (A) Interaction of GST-hnRNP L with transcripts that had not been gel-purified. The solid bars on the right side mark the authentic RNAs of the desired length, and the dotted bars represent the short transcripts prematurely terminating within the poly-(U/C) stretch in the HCV 3´-UTR. **(B)** Interaction of GST-hnRNP L with gel-purified HCV transcripts. The HCV RNAs used in the assay are shown in Fig. 14. Shifts were performed using [α-^{32}P]-UTP labelled HCV RNAs. Samples were analyzed on 4 % non-denaturing polyacrylamide-TBE gels and visualized by autoradiography. The amounts of hnRNP L added to the reactions are indicated on the top of the gels. The positions of free RNA and RNA-protein complexes are indicated.

It should be noted that the small RNA fragments observed below the authentic HCV IRES plus 3´UTR and the 3´-UTR RNA fragments (dotted bars in Fig. 30A) resulted from incomplete transcription through the long poly-

(U/C) stretch within the 3´-UTR during *in vitro* transcription. Therefore, the EMSA experiment was repeated with gel-purified transcripts, with essentially the same result (Fig. 30B).

In the experiment shown above, hnRNP L is shown to bind clearly to the HCV IRES in a binding system without any other protein. Then, it was reasonable to investigate if this binding was still detectable when the cellular lysates such as RRL and cytoplasmic extract of Huh-7 were used in the binding assay, and if this binding of hnRNP L to the HCV IRES might play a role in *in vitro*-translation assay. hnRNP L was reported to be localized mainly in the nucleus (Pinol Roma et al., 1989). To make sure that recombinant GST-hnRNP L protein supplemented to cellular extracts such as reticulocyte lysate or Huh-7 cell extract for functional assays would result in a considerable increase in the hnRNP L concentration in these reactions, the presence of the hnRNP L in these extracts was tested by western-blotting using anti-hnRNP L antibody (kindly provided by Prof. A. Bindereif, Giessen).

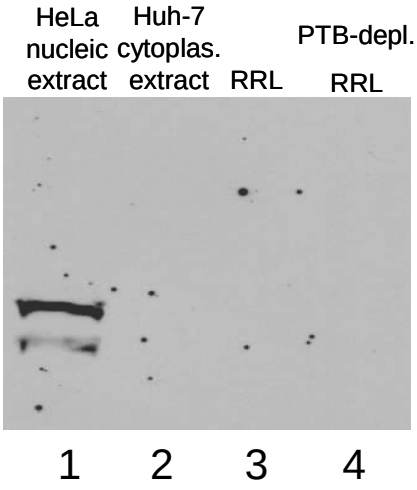

Fig. 31: Detection of endogenous hnRNP L in RRL and cytoplasmic extract of Huh-7 cells. HeLa nuclear extract was used as a positive control. PTB-depleted RRL was also tested.

The result demonstrates that there is no detectable hnRNP L in either RRL or Huh-7 S10 lysate (Fig. 31, lanes 2-4), whereas hnRNP L can be detected in HeLa nuclear extract in considerable amounts (lane 1).

Then, UV cross-link assays were carried out using the same three HCV RNA molecules together with the recombinant GST-fused hnRNP L. The results shown in Fig. 32 clearly demonstrate that hnRNP L can specifically bind to the HCV IRES in the absence of lysate (Fig. 32, lanes 2 and 6). However, this binding was competed when GST-hnRNP L protein was mixed with either RRL or Huh-7 lysate (Fig. 31, lanes 3, 4, 7 and 8). In addition, the HCV 3´ -UTR was confirmed not to bind hnRNP L in the UV cross-linking assay (Fig. 31, lane 10). This result is in accordance with the results of the shift assays shown in Fig. 30.

Taken together, these results indicate that hnRNP L weakly interacts with HCV IRES RNA, but not with the HCV 3´-UTR.

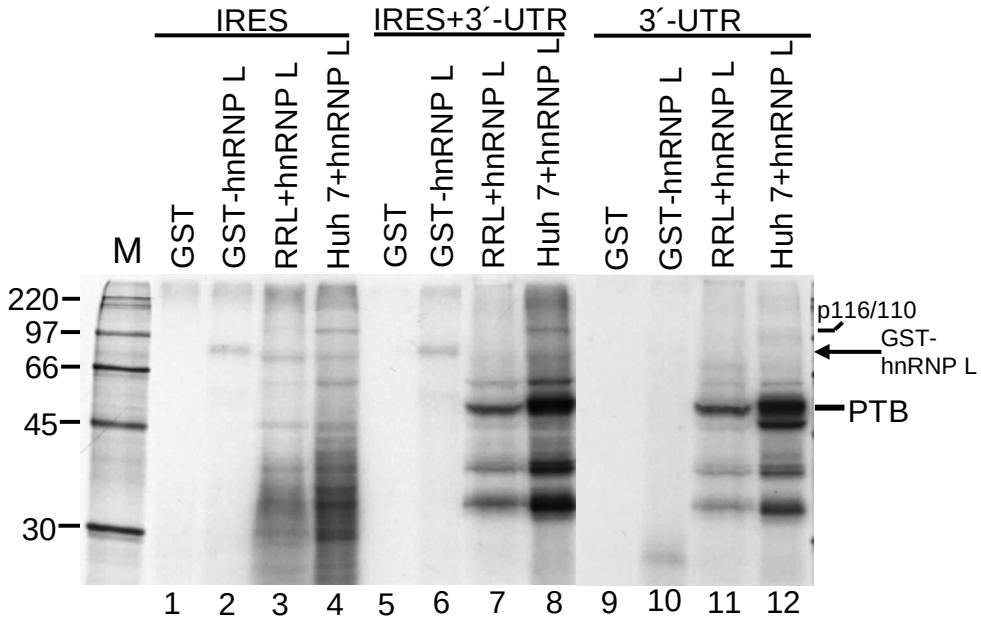

Fig. 32: Interaction of GST-fused hnRNP L with HCV RNAs analyzed by UV cross-linking assays. The reactions were performed with [α-^{32}P]-UTP labelled HCV RNAs in the presence of 1 pmol of GST (lanes 1, 5 and 9) or GST-hnRNP L (lanes 2, 6 and 10), with GST-hnRNP L-supplemented RRL (lanes 3, 7 and 11) or with GST-hnRNP L-supplemented Huh-7 lysate (lanes 4, 8 and 12). The amount of GST-hnRNP L added to both lysates was 1 pmol. The HCV RNAs used in this assay are shown in Fig. 14. Proteins were separated by 12 % SDS-PAGE and visualized by autoradiography. The position of GST-hnRNP L (~94 kDa) is indicated with an arrow at the right side of the gel. The molecular masses of ^{14}C labelled proteins marker (M) are given in kDa.

3.2.2.2 Effect of recombinant hnRNP L on HCV translation

In the western blot described above, no endogenous hnRNP L was detected in the reticulocyte lysate, rendering the lysate possibly suitable as an *in vitro* test system for the detection of a possible function of added recombinant hnRNP L on HCV translation. Using the monocistronic HCV RNA constructs with or without an exact end of the HCV 3´-UTR (Fig. 23), *in vitro* translations were carried out at a physiological potassium concentration (~130 mM) in normal RRL.

The results show that the HCV IRES-directed translation is not sufficiently enhanced in both RRL and PTB-depleted RRL in the presence of hnRNP L, irrespective if the 3´-UTR is present or not (Fig. 33). Addition of 0.1 pmol (equivalent to ~10 nM) of GST-hnRNP L caused a slight stimulation of *Firefly* luciferase expression, increasing about 20 % in normal RRL and 31 % in PTB-depleted RRL only when the HCV RNAs containing the 3´-UTR were used (Fig. 33A and B). However, the observation that the translation efficiencies decreased at high amounts of hnRNP L in both cases implicates that the role of hnRNP L in the HCV IRES-directed translation might be somehow dose-dependent.

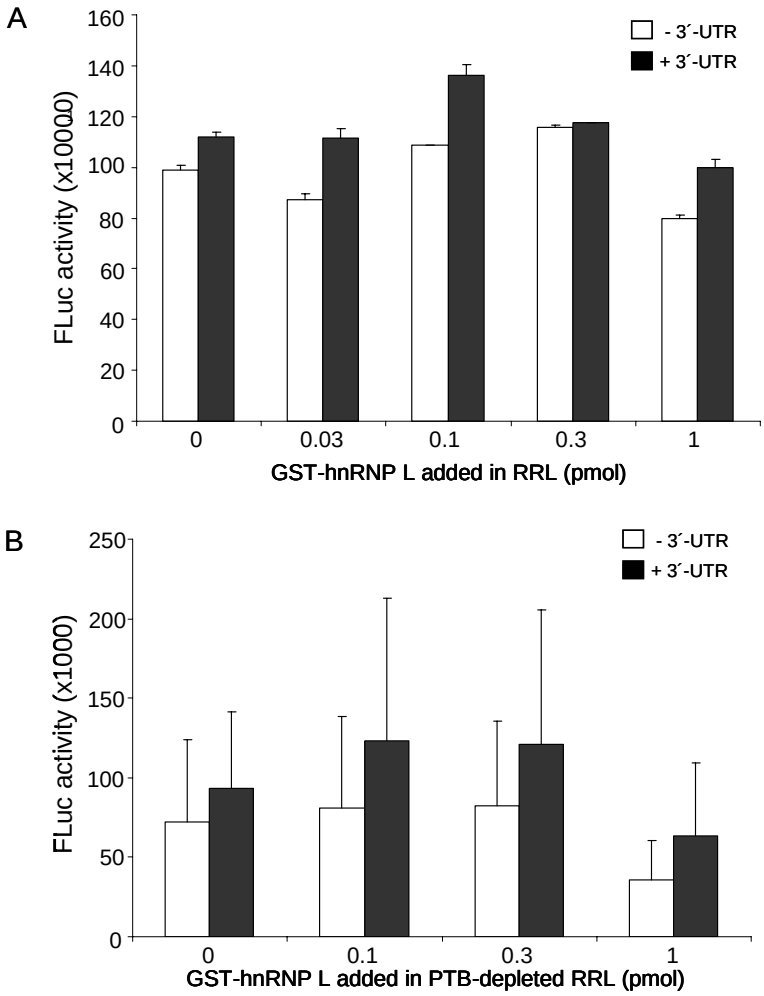

Fig. 33: Effect of hnRNP L on HCV translation in normal RRL (A) and PTB-depleted RRL (B). *Firefly* luciferase (FLuc) activities were determined after 60 min. incubation of the reporter RNAs (Fig. 23) at 30°C together with the amounts of recombinant hnRNP L indicated at the bottom of the graphs. The columns and bars represent the means and standard deviations of duplicate experiments.

Since PTB is present in normal RRL and hnRNP L interacts with PTB (Hahm et al., 1998a), possible changes in translation activity might be induced by the interactions among HCV RNA, hnRNP L and PTB (the corresponding explanation will be considered in the Discussion section).

3.2.3 Interaction of the protein encoded upstream of *N-ras* (Unr) with HCV RNAs

The Unr gene (upstream of *N-ras*) was identified as a transcription unit located immediately upstream of the *N-ras* gene in the genome of several mammalian species: guinea pig (Doniger & DiPaolo, 1988), rat (Jeffers et al., 1990), mouse and human (Nicolaiew et al., 1991). Unr is ubiquitously expressed and codes for an 85 kDa protein. It is an essential gene: the homozygous knockout is lethal in mice at the stage of embryo development at day 10, which implies that Unr is not essential for general cell viability and cell division, but must be essential

for certain stages in differentiation (Boussadia et al., 1997). It has a broad tissue and cell-type distribution (Lopez Fernandez et al., 1995) and is largely cytoplasmic (Jacquemin Sablon et al., 1994). There are two known isoforms differing by the inclusion or exclusion of the optional exon 5 (Boussadia et al., 1993) with a 10 : 1 ratio in abundance of the smaller versus the larger isoform. Unr is a member of the cold-shock family of single-stranded nucleic acid-binding proteins (Doniger et al., 1992). However, it is exceptional amongst this family in that it has five copies of the cold-shock domain (CSD), each of which has an unusual amino acid sequence signature motif, FFH, at its RNA-binding surface, whereas all other members of the family have FVH at this position (Doniger et al., 1992). The occurrence of this unusual motif in all five CSDs implies that Unr arose by repeated duplication of a protein that originally had just one domain.

Unr has been identified as one of two proteins which bind to the human rhinovirus-2 (HRV-2) 5´-UTR and stimulate translation from HRV-2 IRES, the second protein is PTB (Hunt & Jackson, 1999b). All five cold-shock domains of Unr have been reported to be required for stimulation of human rhinovirus RNA translation (Brown & Jackson, 2004).

3.2.3.1 Interaction of recombinant Unr with different HCV RNAs by gel shift assay and UV cross-linking assay

It has been shown that Unr can be UV cross-linked to the human rhinovirus (HRV) IRES RNA (Hunt et al., 1999a). To determine whether Unr interacts directly with the three HCV RNAs shown in Fig. 14, EMSA and UV cross-linking assays using [α-^{32}P]-UTP labelled RNAs and purified recombinant His-Unr protein (kindly provided by Dr. H. Jacquemin-Sablon, Bordeaux) were carried out.

Initially, only HCV IRES RNA was used for the UV cross-linking assay in normal RRL. However, no binding of Unr to the HCV IRES was detected, even in the absence of tRNA which may function as a competitor to reduce unspecific binding (Fig. 34A). Then, the other two RNAs were taken into account for the following experiments. First, high concentrations of [α-^{32}P]-UTP labelled HCV RNAs (about 0.12-0.14 pmol) were used for the shift assay under the standard conditions reported for the EMSA (Konarska & Sharp, 1986). However, no shifted bands were detected with all three different RNAs (data not shown). Only when lower concentrations of RNAs (about 6-7 nmol) were used in the shift assay, protein-RNA complexes were found with the HCV 3´-UTR RNA at the concentration of 10 nM Unr. With the other two RNAs (IRES and IRES plus 3´-UTR), RNA-protein complexes could be detected only at a high concentration of Unr (100 nM) (Fig. 34B). These results indicate that: (1) Unr may not interact directly with the HCV IRES; (2) Unr binds to the HCV 3´-UTR; and (3) the presence of the HCV IRES somehow inhibits the binding of Unr to the 3´UTR.

In contrast, in the UV cross-linking assay, Unr interacts with all three HCV RNAs (Fig. 35A) in the absence of any other protein. All binding signals were still detectable even in the presence of tRNA, but became significantly weaker, especially in the case of HCV IRES RNA (Fig. 35A). However, in the presence of other proteins derived from Huh-7 lysate, the binding of Unr to the HCV RNAs was not detectable any more (Fig. 35B).

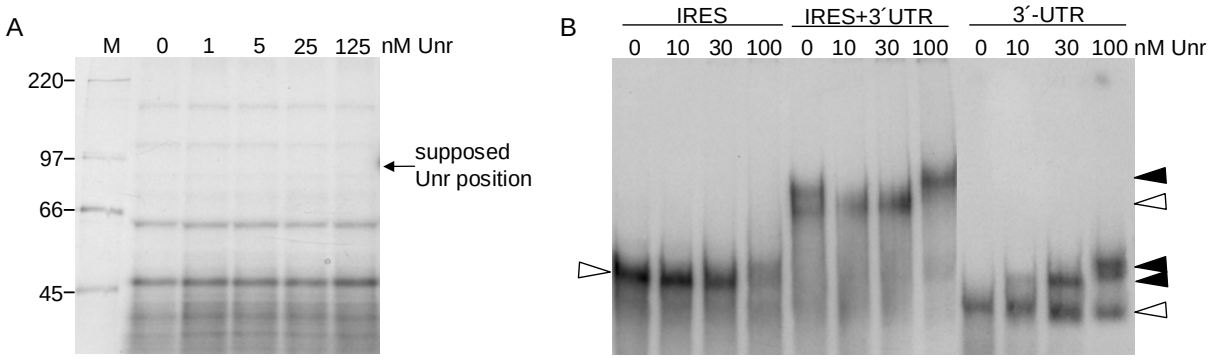

Fig. 34: Binding of recombinant Unr to the HCV RNAs. (A) UV cross-linking assay with HCV IRES RNA with [α-^{32}P]-UTP labelled HCV IRES RNA in RRL. The final concentrations of Unr added in each reaction are indicated on the top of the gel. The samples were analyzed by 8 % SDS-PAGE and autoradiography. The molecular masses of ^{14}C labelled proteins marker (M) are given in kDa. The expected position of Unr (~94 kDa) is marked with an arrow. **(B)** Binding of Unr to the gel-purified HCV RNAs in the shift assay. No tRNA and no heparin were used in this assay. Samples were analyzed on 4 % nondenaturing polyacrylamide gels and visualized by autoradiography. The white arrows represent free RNAs, and black arrows represent RNA-protein complexes.

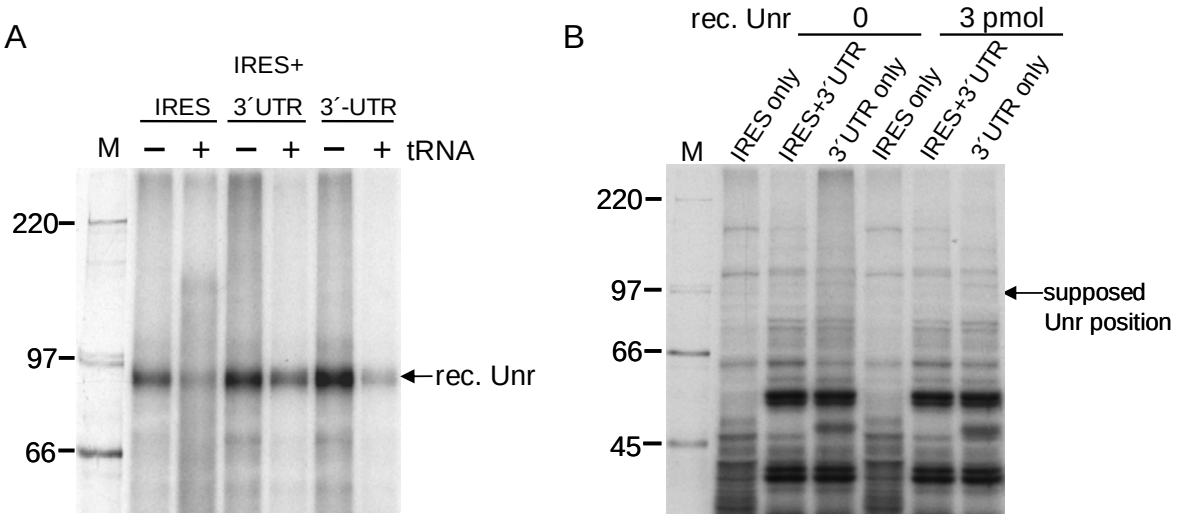

Fig. 35: Binding of Unr to [α-^{32}P]-UTP labelled HCV RNAs analyzed by the UV cross-linking assay. (A) Assays performed in the absence or presence of tRNA without any other protein. The amount of recombinant Unr (rec. Unr) added to each reaction was 1.3 pmol (equivalent to ~130 nM). The final concentration of tRNA in the reaction is 1 µg/µl. The position of rec. Unr (~94 kDa) is indicated. **(B)** Assays performed in Huh-7 lysate in the absence or presence of rec. Unr, in the presence of 1 µg/µl tRNA. Samples were separated by 8 % SDS-PAGE and visualized by autoradiography. The molecular masses of ^{14}C labelled proteins marker (M) are given in kDa. The expected position of Unr is indicated.

In conclusion, Unr binds only weakly to the HCV 3´-UTR, and its binding can be competed by other proteins in the cell lysate.

3.2.3.2 Effect of recombinant Unr on HCV translation

To address the question whether Unr plays a functional role in the translation of HCV RNAs with or without the 3´-UTR region (Fig. 23), *in vitro*-translation assays were performed with the HCV RNAs in normal RRL (Fig. 36).

The results show that addition of recombinant Unr protein to the reticulocyte lysate leads to a decrease in translation efficiency. Moreover, these data imply that the translation level of HCV RNA could be relieved to a certain extent by the presence of the HCV 3´-UTR. Similar results were also found in PTB-depleted RRL (data not shown).

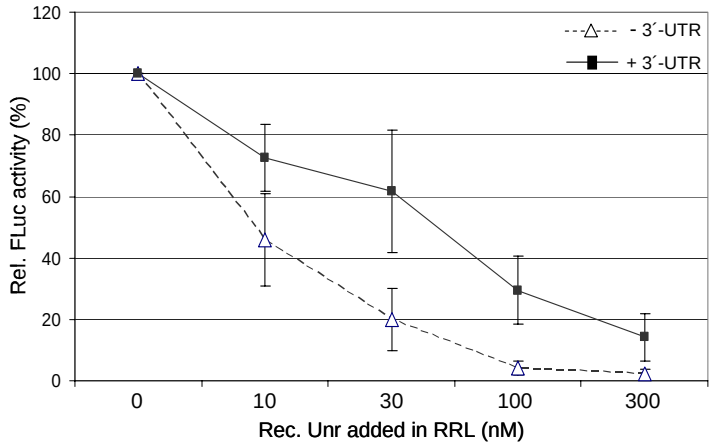

Fig. 36: Effect of recombinant Unr on HCV translation in normal RRL. The amounts of increasing recombinant Unr (Rec. Unr) added to the reactions are indicated at the bottom of the graph. Relative *Firefly* luciferase (Rel. FLuc) activities in the lysates were measured after assay. The Fluc values expressed from HCV RNA with or without 3´-UTR are set to 100 %. The bars represent standard deviations of three independent experiments.

Taken together, these data suggest that the recombinant Unr protein used here inhibits the translation efficiency of the HCV RNA. The reasons for this observation are not known yet. However, it can be speculated that the status of the Unr protein preparation may play a role, since the recombinant Unr protein had been purified from *E.coli* under denaturing conditions and was renatured after purification. Thus, it is not known that which portion of the protein is in the authentic native conformation and if misfolded proteins inhibit the translation reaction.

3.2.4 Interaction of PTB, hnRNP L and Unr with HCV RNAs

The results presented above show that the interactions of different cellular proteins individually with HCV RNAs are quite different: PTB and Unr bind clearly to the HCV 3´-UTR but not to the HCV IRES RNA alone, whereas hnRNP L binds to the HCV IRES only. With respect to the HCV IRES-mediated translation, the roles they play

are different. PTB and Unr both exhibit down-regulatory effects with different degrees on HCV translation, whereas hnRNP L shows a slightly stimulating effect at a certain concentration. It is known that PTB and hnRNP L interact with each other, and they are possibly involved in functions like pre-mRNA processing and mRNA translocation from the nucleus to the cytoplasm (Dreyfuss et al., 1993; Hahm et al., 1998a). Moreover, the presence of both Unr and PTB is required for the formation of an RNA structure in Apaf-1 IRES that has the correct conformation for binding of the 40S ribosomal subunit to initiate translation efficiently (Mitchell et al., 2003). Therefore, it was interesting to investigate if these *trans*-acting factors interact with one another and whether they may act synergistically in the translation of the HCV RNA, which is the main goal of the following part of the work.

3.2.4.1 Interaction of PTB, hnRNP L and Unr in concert with the HCV RNAs

3.2.4.1.1 PTB and hnRNP L

The results in the previous section show that PTB can bind specifically to the HCV 3´-UTR irrespective if cellular proteins are present or not (Fig. 21 and 22), and hnRNP L clearly binds to the HCV IRES (Fig. 30 and 32). In order to check a possible interaction of PTB and hnRNP L in concert with the HCV RNA in the shift assay, the following experiment was designed. The HCV IRES plus 3´-UTR RNA labelled with [α-^{32}P]-UTP was selected for the shift assays and incubated with increasing amounts of GST-hnRNP L in the absence or presence of a constant amount of recombinant PTB.

The result shown in Fig. 37 demonstrates unambiguously that PTB and hnRNP L not only bind independently of each other to the HCV IRES plus 3´-UTR RNA (Fig. 37, lanes 2, 6 and 7), but they also bind together to the same HCV RNA as seen by the position of the higher shifted bands marked with arrows (Fig. 37, lanes 3-5).

Then, UV cross-linking assays were performed with the three HCV RNAs in the presence of both PTB and hnRNP L. Interestingly, it was found that PTB binding to the HCV RNAs is clearly strengthened by the presence of hnRNP L. With increasing amounts of hnRNP L, binding of PTB to the RNA was gradually increased, especially in the case of the RNAs including 3´-UTR portion (Fig. 38, lanes 5-12).

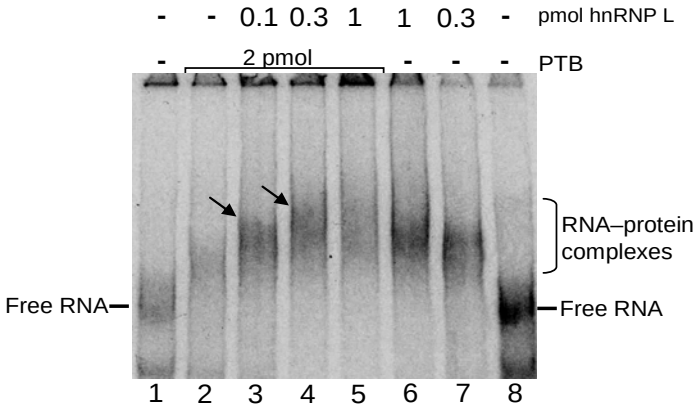

Fig. 37: Binding of PTB and hnRNP L to the HCV IRES plus 3´-UTR RNA in a supershift assay. The final concentration of tRNA added to each shift reaction was 1 µg/µl. All samples were analyzed on a 4 % nondenaturing polyacrylamide gel and visualized by autoradiography. The final amounts of hnRNP L added to the reactions are indicated on the top of the gel. The position of the free RNA and of RNA-protein complexes are indicated on the right side of the gel.

In contrast, when the hnRNP L concentration was kept constant and PTB added in variable amounts, no corresponding stimulation of hnRNP L binding by increasing amounts of PTB was detected (data not shown).

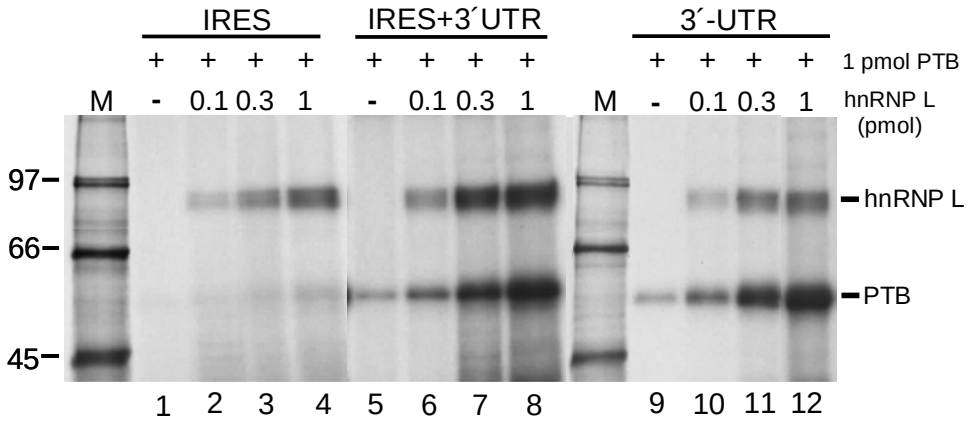

Fig. 38: Stimulation of PTB binding to the HCV RNAs by hnRNP L analyzed by the UV cross-linking assay. Three HCV RNAs labelled with [α-^{32}P]-UTP were used (see Fig. 10). Assays were performed in the presence of 1 µg/µl tRNA without any other protein. The amounts of GST-hnRNP L added to the reactions are indicated on the top. The final concentration of PTB added to each reaction is 1 pmol (equivalent to a final concentration of ~100 nM). All samples were separated by an 8 % SDS-PAGE and visualized by autoradiography. The molecular masses of ^{14}C labelled proteins marker (M) are given in kDa. The positions of PTB and GST-hnRNP L are indicated on the right side of the gel.

At the same time, two unexpected observations were obtained in this assay. One is that the HCV 3´-UTR, shown previously not to interact with hnRNP L, is bound by hnRNP L in the presence of PTB. The other finding is that PTB can bind to the HCV IRES RNA in the presence of hnRNP L, although the labelling intensity is very weak. These observations are quite contrary to the results of the former experiments when PTB or hnRNP L were examined individually with corresponding HCV RNAs. Presumably, these binding signals are due to possible protein-protein interactions between PTB and hnRNP L in combination with the HCV RNA. However, the mechanism behind this observation remains unclear.

Next, UV cross-linking assays were performed under the same condition with all PTB deletion mutants (Fig. 26) present in constant amounts and variable amounts of hnRNP L, but this time, only the HCV IRES plus 3´-UTR RNA was used. The results shown in Fig. 39 not only confirm that hnRNP L stimulates the binding of PTB to the HCV RNA (see Fig. 38), but also verify that PTB ΔI,II strongly interacts with the HCV IRES plus 3´-UTR RNA. In contrast, neither PTB ΔIII (46.5 kDa) nor ΔIV (47.6 kDa) protein can bind to the HCV IRES plus 3´-UTR RNA in the UV cross-linkING assays (lanes 9-16). These observations show that not only in the interaction of PTB with the FMDV IRES, but also in the interaction with the HCV RNA, the PTB domains III and IV are much more important than the domain I and II.

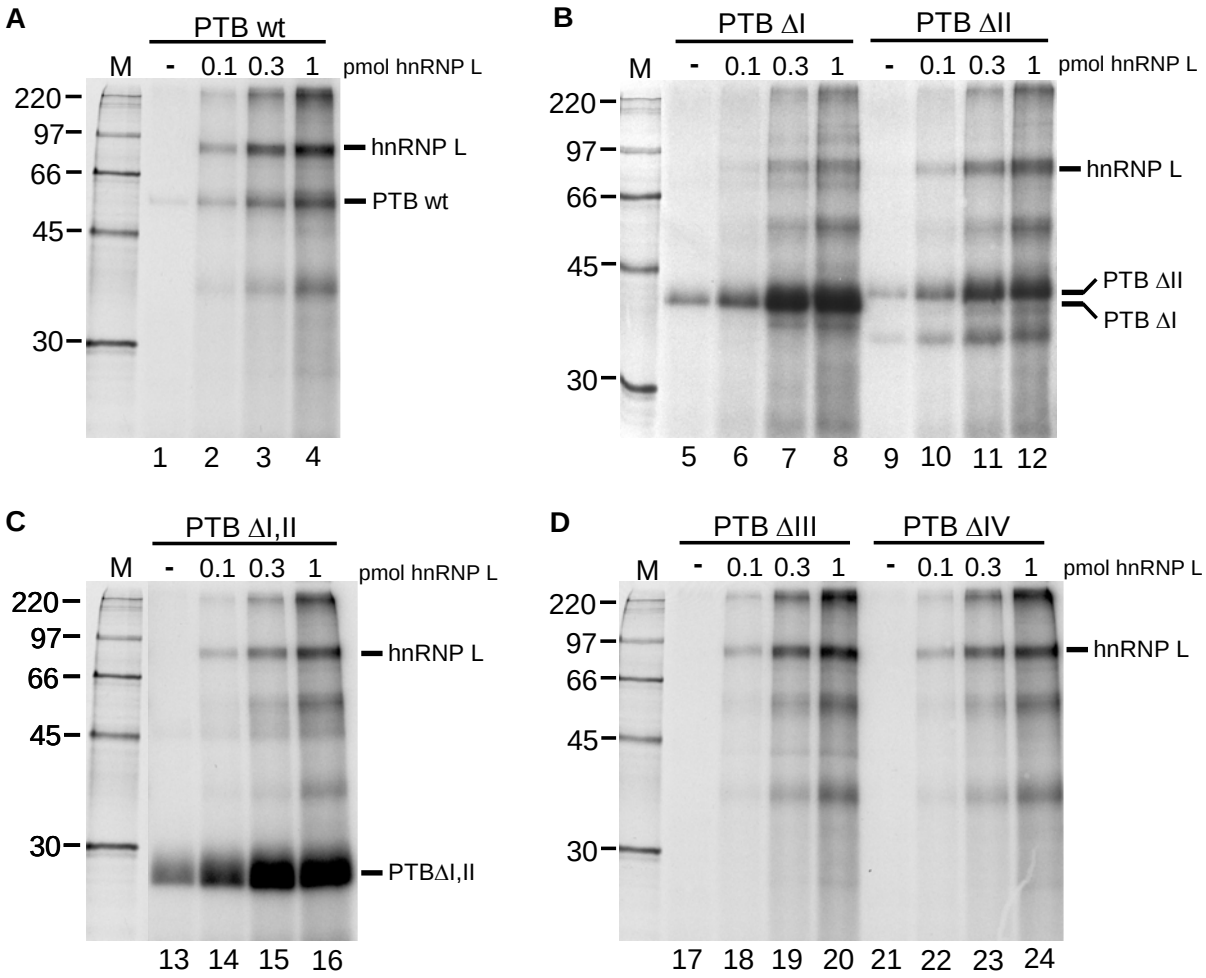

Fig. 39: hnRNP L stimulates the binding of PTB wild-type (A) and PTB domain deletion mutants ΔI and ΔII (B), PTB ΔI,II (C), PTB ΔIII and ΔIV (D) to the HCV RNA analyzed in the UV cross-linking assay. Only HCV IRES plus 3´-UTR RNA labelled with [α-^{32}P]-UTP shown in Fig. 14 was used. Assays were performed in the presence of 1 µg/µl tRNA without any other protein. The amounts of GST-hnRNP L added to the reactions are indicated on the top of the gels. The final concentration of PTB and its mutants present in each reaction is 1 pmol (equivalent to a final concentration of ~100 nM). All samples were separated on 12 % SDS-PAGE and visualized by autoradiography. The molecular masses of ^{14}C labelled proteins marker (M) are given in kDa. The positions of GST-hnRNP L, PTB wild-type (wt) and deletion mutants (except PTB ΔIII and ΔIV) are also indicated.

3.2.4.1.2 Unr and hnRNP L

Next, Unr was included in the same experiment as described above. Using the three HCV RNAs, UV cross-link assays were carried out with a constant amount of recombinant GST-hnRNP L and variable amounts of recombinant Unr, but no other protein present. Unfortunately, no effect of Unr on the binding of hnRNP L to the HCV IRES was observed since there is no interaction of Unr with the HCV IRES RNA. However, the binding of hnRNP L to the HCV IRES including 3´-UTR RNA unexpectedly declines with increasing amounts of Unr added to the reactions (Fig. 40, lanes 5-8). The same effect was observed with the HCV 3´-UTR RNA (Fig. 40, lanes 9-12).

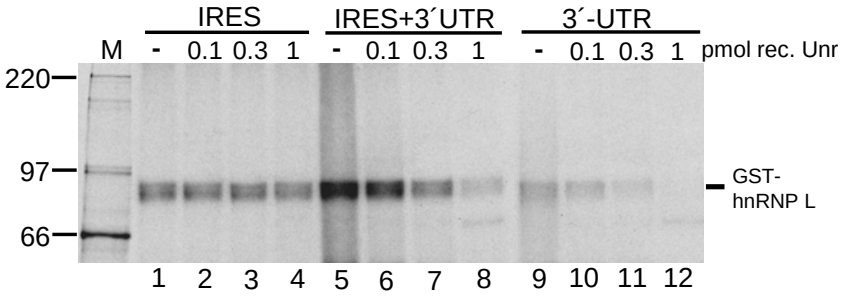

Fig. 40: Binding of hnRNP L to the three HCV RNAs in the presence of Unr analyzed by the UV cross-linking assay. The three HCV RNA constructs labelled with [α-^{32}P]-UTP were shown in Fig. 14. Assays were performed in the presence of a final concentration of 1 µg/µl tRNA without any other protein. The amounts of recombinant His-Unr added to the reactions are indicated on the top of the gel. The final amount of GST-hnRNP L presented in each reaction is 1 pmol (equivalent to a final concentration of ~100 nM). All samples were separated on 8 % SDS-PAGE and visualized by autoradiography. The molecular masses of ^{14}C labelled proteins marker (M) are given in kDa. The position of GST-hnRNP L is indicated.

Thus, Unr appears to compete with the binding of hnRNP L, in contrast to PTB which stimulates the binding of hnRNP L (see above).

3.2.4.1.3 PTB and Unr

In the experiments described above, PTB has been shown to bind to the HCV 3´-UTR (Fig. 21 and 22), and Unr also binds to the HCV RNA containing the 3´-UTR portion (Fig. 34B and 35A). It has been demonstrated that Unr and PTB are able to act in synergy to stimulate Rhinovirus IRES function in RRL (Hunt et al., 1999a). In order to examine the interaction of PTB and Unr together with the HCV RNA, the following experiment was designed. UV cross-linking assays were performed using the HCV 3´-UTR RNA as well as the HCV IRES plus 3´UTR RNA labelled with [α-^{32}P]-UTP in normal RRL supplemented with increasing amounts of recombinant His-Unr protein since Unr and PTB proteins do not interact with HCV IRES only.

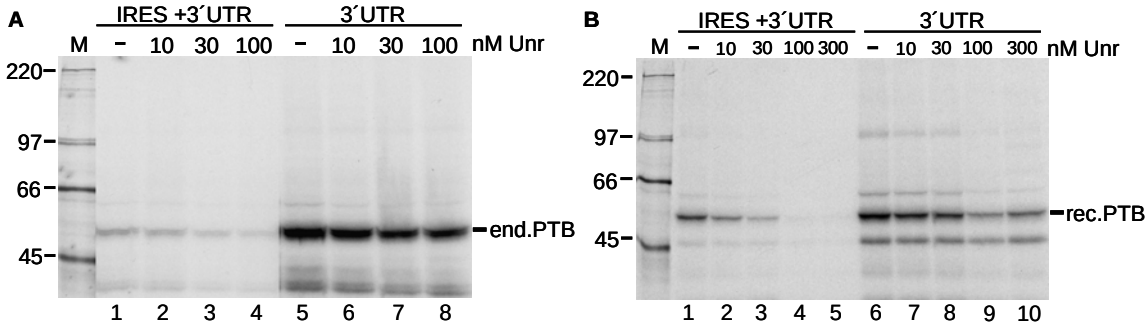

Fig. 41: Binding of PTB to HCV RNAs in the presence of Unr in normal RRL (A) and PTB-depleted RRL (B) analyzed by the UV cross-linking assay. Assays were performed in the presence of final amount of 1 µg/µl. The amounts of recombinant His-Unr added to the reactions are indicated on the top of the gels. The final amount of recombinant PTB (rec. PTB) added to the PTB-depleted RRL **(B)** is 0.3 pmol (equivalent to a final concentration of 30 nM). All samples were separated on 8 % SDS-PAGE and visualized by autoradiography. The molecular masses of ^{14}C labelled proteins marker (M) are given in kDa. The positions of endogenous PTB (end. PTB) and rec. PTB are also indicated.

From the UV cross-linking results (Fig. 41A), it is obvious that the binding of PTB to the HCV RNAs in normal RRL is not enhanced but slightly inhibited by the presence of Unr. A similar inhibitory effect is also detected in PTB-depleted RRL supplemented with recombinant PTB (Fig. 41B). Again, no Unr band was found to bind to HCV RNAs in both cases, confirming that cellular proteins can easily compete for Unr binding.

Taken together, these results suggest that Unr compete binding of PTB to the HCV RNA containing the 3´-UTR. It can be only speculated if a certain fraction of the recombinant Unr protein (which was purified under denaturing conditions and then renatured) which is not in a native state may exert these inhibitory effects.

3.2.4.1.4 PTB, hnRNP L and Unr

The results described above demonstrate the interaction of any two of three proteins with the HCV RNAs in the absence or presence of any lysate by different methods, either shift or UV cross-linking assays. As a last step, the interactions of all these three proteins together with the HCV RNA were examined. Considering the binding of these three proteins to the HCV RNA, only the HCV IRES plus 3´-UTR RNA was used for this experiment. In order to rule out any interference with other cellular proteins, this assay was carried out without any lysate.

When PTB and Unr were present in constant amounts in the reactions, the binding of PTB to the HCV RNA was stimulated by increasing amounts of hnRNP L, which is in accordance with the results obtained in Fig. 38. Similar results are also detected when hnRNP L and Unr are constant parameters and the PTB concentration was varied (Fig. 42, lanes 5-8), indicating that PTB can slightly stimulate binding of hnRNP L to the HCV RNA. In contrast, the binding of hnRNP L and PTB to the HCV IRES + 3´-UTR RNA is inhibited by increasing amounts of Unr (Fig. 42, lanes 9-12), further confirming that the Unr protein used here acts as a competitor of PTB or hnRNP L binding to the HCV RNA.

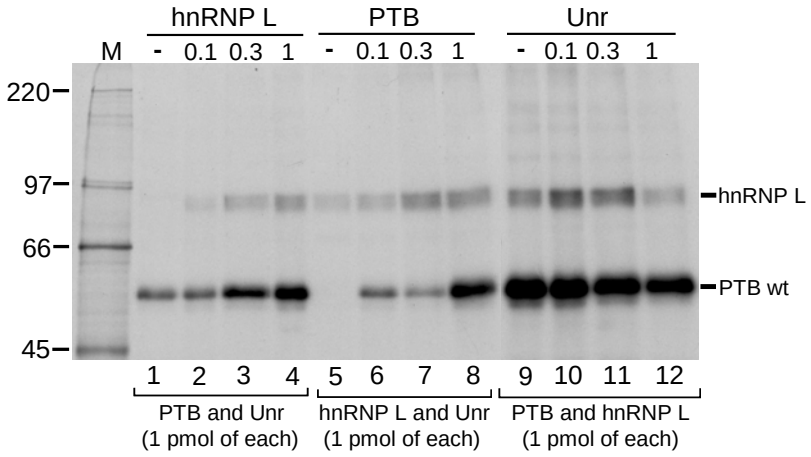

Fig. 42: Interaction of PTB, hnRNP L and Unr with HCV IRES plus 3´-UTR RNA analyzed by UV cross-linking assays. The UV cross-link assays were carried out with the HCV IRES plus 3´-UTR RNA labelled with [α-^{32}P]-UTP in the presence of a final amount of 1 µg/µl tRNA without any other proteins. The amount of each protein added to the reactions is indicated on the top of the gel. The final amounts of the two proteins present in constant amounts in the reactions are 1 pmol each (equivalent to a final concentration of ~100 nM). All samples were separated on 8 % SDS-PAGE and visualized by autoradiography. The molecular masses of ^{14}C labelled proteins marker (M) are given in kDa. The positions of recombinant GST-hnRNP L and PTB wt are indicated.

Taken together, PTB and hnRNP L may play a synergistic role in binding to the HCV RNA including the IRES. In contrast, a possible role of Unr remains unclear from these in vitro-binding assays with the recombinant proteins, mainly due to uncertainties regarding the native state of the Unr preparation used.

3.2.4.2 Effects of PTB, hnRNP L and Unr on the HCV translation

To address the question whether PTB, hnRNP L and Unr play a synergistic role in the translation of HCV RNA, combination of each two of the proteins were chosen in a series of *in vitro*-translation assays which were carried out with two HCV RNA constructs in either normal RRL or PTB-depleted RRL.

First, PTB and hnRNP L were used together to analyze their functional role in HCV translation with HCV RNA constructs with or without 3´-UTR as shown in Fig. 23. In order to use an extract with low concentration of PTB, PTB-depleted RRL was used and supplemented with a constant low amount of recombinant PTB. To this reaction, hnRNP L was added in increasing amounts (Fig. 43). However, no significant influence of hnRNP L on HCV translation could be observed.

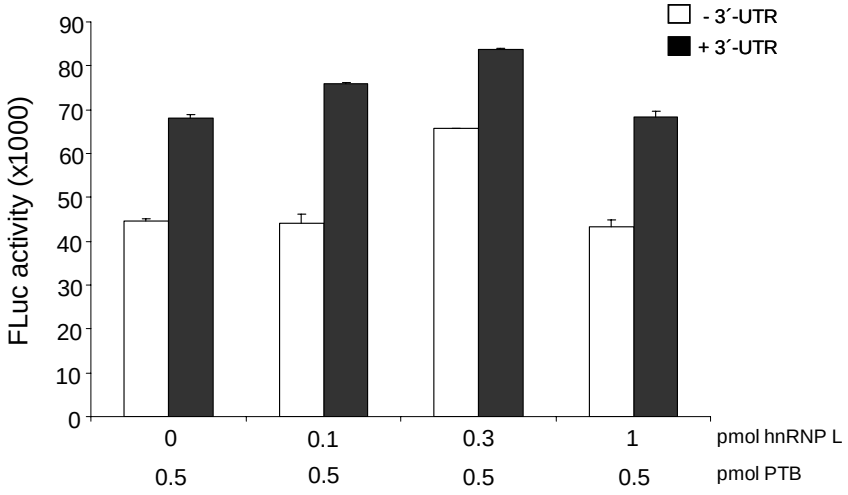

Fig. 43: Effect of hnRNP L and PTB together on HCV translation in PTB-depleted RRL. The amounts of GST-hnRNP L added to each reaction are indicated at the bottom of the graph. Recombinant His_6-PTB was present in a constant amount of 0.5 pmol (equivalent to the final concentration of 50 nM) in each reaction. *Firefly* luciferase (FLuc) activities expressed from the two HCV RNAs were determined. The columns and bars represent the means and standard deviations of duplicate experiments.

Taken together with the results of the experiments above, HCV translation is not significantly affected by PTB and hnRNP L, individually or together, in *in vitro* assays.

Next, PTB and Unr were examined together in *in vitro*-translation assays. As mentioned above, the recombinant Unr protein inhibits the translation efficiency of HCV RNA, but this effect could be relieved to a certain extent by the presence of the HCV 3´UTR region in normal RRL (Fig. 36). Using the same HCV RNAs with or without 3´-UTR, *in vitro*-translation reactions were carried out with different amounts of recombinant PTB and Unr proteins in PTB-depleted RRL. However, HCV translation efficiencies did not change significantly in the presence increasing amounts of PTB (Fig. 44A). This observation is consistent with that obtained from the former *in vitro*-translation assays when recombinant PTB was added to the PTB-depleted RRL (Fig. 28).

Correspondingly, HCV translation was inhibited when increasing amounts of the recombinant Unr protein were added to the PTB-depleted RRL supplemented with exogenous His_6-PTB (Fig. 44B), which is consistent with the result of Fig. 36. Similarly, the same inhibitory effect was also found when increasing amounts of the recombinant Unr were added to the PTB-depleted RRL without exogenous PTB supplemented (data not shown).

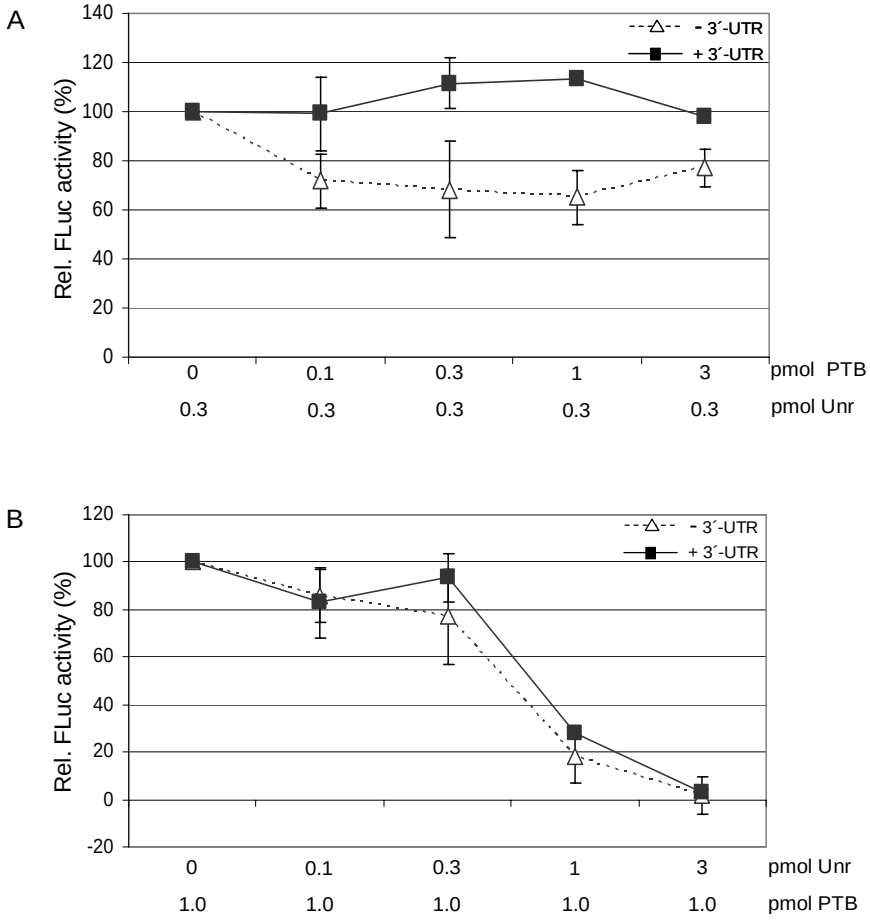

Fig. 44: Effect of PTB and Unr on HCV translation in PTB-depleted RRL. (A) Effect of PTB in the presence of Unr on HCV translation in PTB-depleted RRL. **(B)** Effect of Unr in the presence of PTB on HCV translation in PTB-depleted RRL. The amounts of PTB and Unr added to each reaction are indicated at the bottom of the graphs. Relative *Firefly* luciferase (Rel. FLuc) activities in the reactions were measured after 60 minutes incubation of the reporter RNAs with the indicated recombinant PTB and Unr proteins at 30°C. The FLuc values obtained from HCV RNA with and without 3´-UTR in the absence of PTB are set to 100 %. The bars represent standard deviations of three independent experiments.

3.2.5 Conclusions

PTB binds efficiently to the HCV 3´-UTR but only extremely weakly to the HCV IRES. In contrast, hnRNP L binds to the HCV IRES only. Together, these two proteins mutually promote their binding to the HCV RNA. However, in the *in vitro*-translation with reticulocyte lysate, only a very slightly positive effect of hnRNP L on HCV translation was observed.

The recombinant Unr protein used in this work binds to the HCV 3´-UTR, but no significant effect of Unr on HCV translation could be observed in *in vitro*-translation in reticulocyte lysate.

3.3 Part III: The Hepatitis C Virus RNA 3´-untranslated region strongly enhances translation directed by its internal ribosomal entry site

The main aim of this third part of the study was to investigate the functional influence of the HCV 3´-untranslated region (3´-UTR) on HCV translation directed by its internal ribosome entry site.

3.3.1 The reporter construct used to analyze the possible influence of the HCV 3´-UTR on translation

Several conflicting results have been reported previously on the effect of the HCV 3´-UTR on the IRES-directed translation. Some studies reported a stimulatory role of the viral 3´-X (Ito et al., 1998; Ito & Lai, 1999; Michel et al., 2001), whereas others reported either no detectable or even an inhibitory role of the 3´-end sequences (Fang & Moyer, 2000; Murakami et al., 2001; McCaffrey et al., 2002). The reasons for these discrepancies are not directly evident. Some of researchers discussed that different concentrations of translation factors in the employed translation assay systems, different intracellular mRNA concentrations, and/or mis-folding of *in vitro*-generated RNAs could contribute to the discrepancies (Kong & Sarnow, 2002). However, it was noted that (i) some of these studies concentrated only on a possible role of the HCV 3´-X region but not of the entire viral 3´-UTR, and (ii) the HCV RNA molecules used in most studies did not have precise 3´ termini. It is hypothesized that these experimental variations may have caused the discrepancies between the results obtained in different studies.

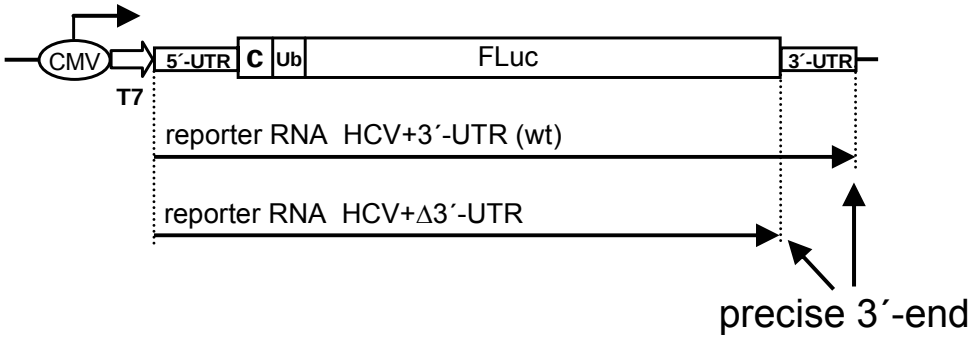

Fig. 45: Schematic representation of the HCV plasmid and reporter RNAs (indicated with arrow lines). CMV, Cytomegalovirus immediate early promoter; T7, T7 RNA polymerase promoter; UTR, untranslated region; C, partial core protein-encoding sequences; Ub, ubiquitin sequences; FLuc, *Firefly* luciferase reporter gene. The precise 3´-ends are also indicated.

In an attempt to clarify the role of the HCV 3´-UTR on HCV IRES activity, different reporter constructs were compared and two different monocistronic reporter mRNAs containing the entire HCV 5´-UTR sequence plus

partial core protein-encoding sequences and the entire *Firefly* luciferase (FLuc) reporter gene, either ending exactly at the 3´-end of the FLuc coding sequence, or additionally including the complete HCV 3´-UTR were designed for the following *in vitro*-translation experiments (Fig. 45). The important point for this monocistronic RNA constructs is that each of them has an exact end at its 3´-terminus, either with or without 3´-UTR, respectively.

3.3.2 Optimization of *in vitro* translation conditions

The templates for *in vitro*-transcription of the reporter RNAs were generated by PCR to obtain run-off transcripts with the precise 3´-ends (see Fig. 45). At the very beginning, the effect of different amounts of RNA on *in vitro*-translation reactions was analyzed. Fig. 46 shows the *Firefly* luciferase (FLuc) activities directed by the HCV IRES expressed in rabbit reticulocyte lysate (RRL) from different amounts of RNA. A high expression level was obtained at 200 ng of the HCV reporter RNA used in the reaction. Interestingly, it was found that increasing amounts of RNA (e.g., 800 ng) did not produce higher expression levels, but led to lower FLuc expression. Therefore, 200 ng HCV RNA was selected for all following *in vitro* translation assays since the amount of 200 ng per reaction appears to represent the upper limit of the dynamic range of expression of FLuc.

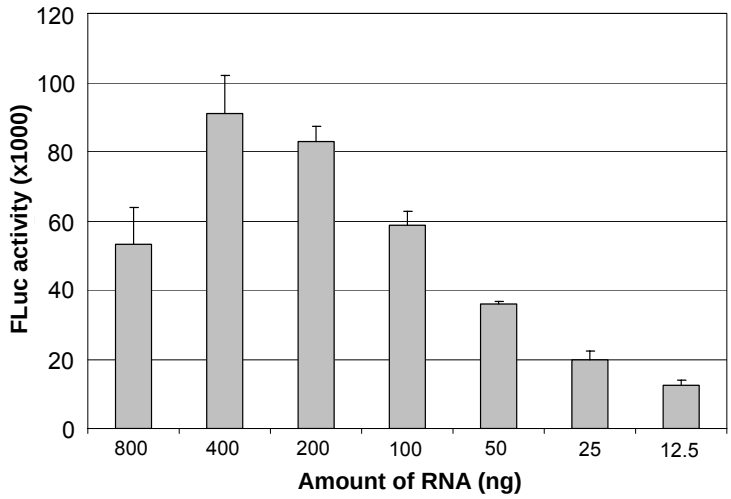

Fig. 46: *In vitro* translation directed by the HCV IRES at different RNA amounts. Amounts of RNA were incubated in 10 µl *in vitro* translation reaction including 4.4 µl RRL. The columns and bars represent the means and standard deviations of four independent experiments, respectively. FLuc, *Firefly* luciferase reporter gene.

In order to analyze the changes in HCV translation at different concentrations of potassium and magnesium, 200 ng of the monocistronic mRNA shown in Fig. 45 were used in this experiment. The concentration of potassium present in the cells is usually about 140 mM. Considering that the endogenous concentration of potassium acetate (KAc) is 113 mM (added by the supplier) in normal rabbit reticulocyte lysate, different concentrations of potassium were adjusted by addition of exogenous potassium in the assays. The monocistronic HCV reporter

RNA was *in vitro*-translated in RRL and FLuc activity was measured. The result showed that the highest FLuc activity was detected near the physiological concentration of potassium, whereas the FLuc expression dropped at further increased potassium concentrations, indicating that too high salt concentrations may somehow inhibit expression of the FLuc reporter gene (Fig. 47A). Based on this result, the physiological concentration of potassium (~150 mM) was selected for all following *in vitro*-translation assays.

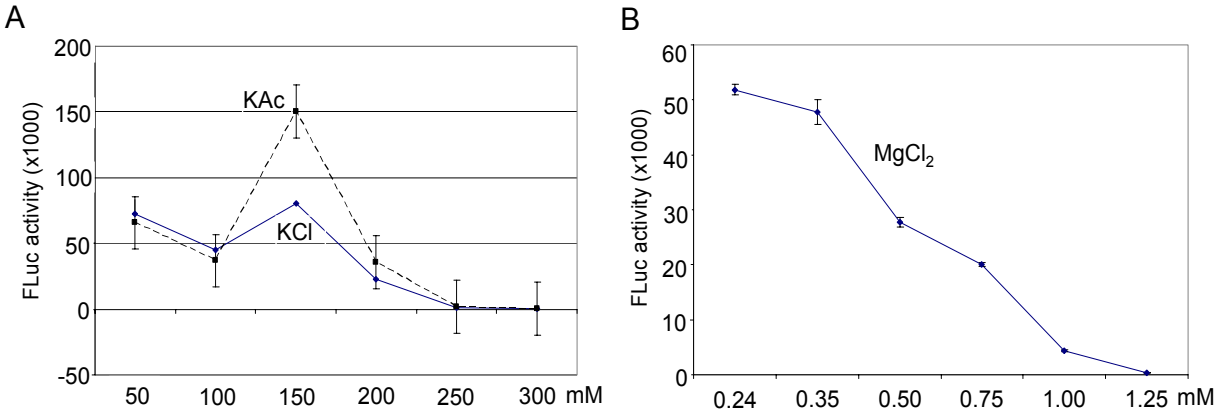

Fig. 47: *In vitro* translation directed by the HCV IRES at different salt concentrations. (A) HCV IRES-dependent translation in the presence of different potassium concentrations (endogenous and added). Translation reactions with monocistronic RNA were performed at 30°C in rabbit reticulocyte lysate. **(B)** HCV IRES-dependent translation in the presence of different magnesium concentrations (endogenous and added). The columns and error bars represent the means and standard deviations of two independent translations, respectively. FLuc, *Firefly* luciferase reporter gene.

In addition, the effect of different concentrations of magnesium (which is about 0.5 mM inside mammalian cells), on the translation driven by the HCV IRES was then examined in the presence of the physiological concentration of potassium (the RRL contains 0.712 mM magnesium added by the supplier). The result shown in Fig. 47B indicates that the highest translation level directed by the HCV IRES in RRL was achieved at low concentrations of magnesium since the highest expression of FLuc was detected at 0.24 mM. The FLuc activity decreases sharply when the concentration of magnesium is ≥ 1 mM in the reaction. This observation means that the concentration of 0.7 mM magnesium contained in the endogenous reticulocyte lysate is sufficient to allow the efficient translation driven by the HCV IRES in RRL when 3-4 µl of RRL are used in a 10 µl reaction, resulting in a final magnesium concentration of about 0.25-0.3 mM.

Based on these observations, the concentrations of both potassium and magnesium were fixed at 140 mM, which is close to the physiological condition, and 0.24 mM, respectively, for all following *in vitro* translation experiments.

3.3.3 Effect of the HCV 3´-UTR on IRES-mediated translation in rabbit reticulocyte lysate

Using the monocistronic HCV constructs shown in Fig. 45, the templates for *in vitro*-transcription of the reporter RNAs were generated by PCR to obtain run-off transcripts with precise 3´-ends. These RNAs were *in vitro*-translated in rabbit reticulocyte lysate (RRL) at a final potassium concentration of 135 mM which is close to physiological conditions. The translation products of these RNAs were examined by measuring FLuc activity (Fig. 48A) and by analyzing Fluc protein amounts by SDS-PAGE and autoradiography (Fig. 48B). However, no significant difference in translation efficiency was detected between these two reporter RNAs, even when using different amounts of RNA to rule out a possible saturation effect in the system. These results indicate that the HCV 3´-UTR has no obvious effect on its IRES-dependent translation in rabbit reticulocyte lysate.

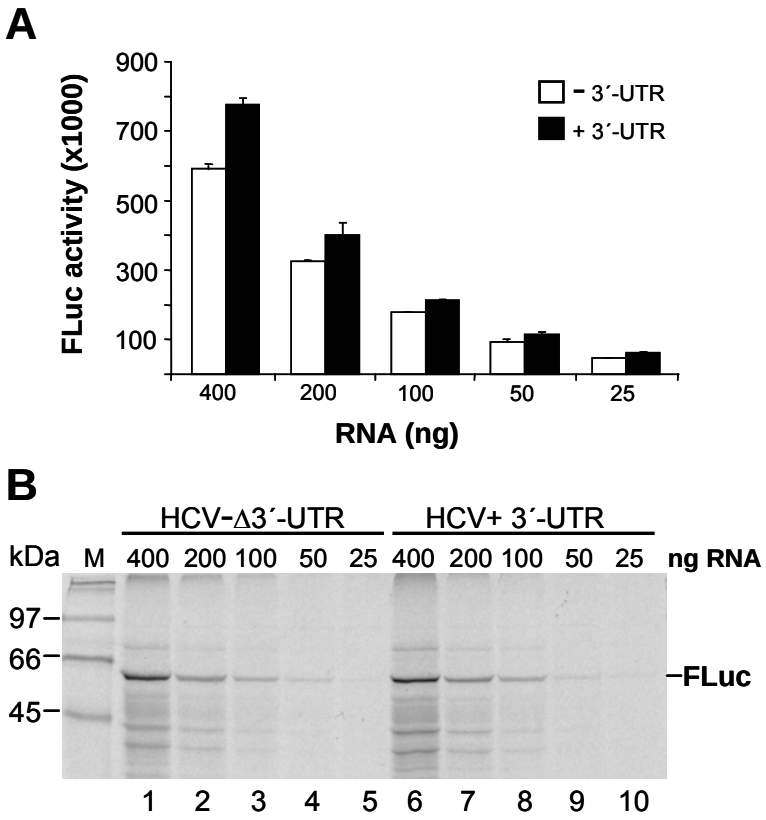

Fig. 48: Functional analysis of the HCV 3´-UTR by *in vitro* translation. (A) *Firefly* luciferase (FLuc) activities from various amounts of RNA expressed in RRL at a physiological potassium concentration (~135 mM KCl). *In vitro*-translation reactions were performed using 4.4 µl standard rabbit reticulocyte lysate (RRL) in a volume of 10 µl. The columns and bars represent the means and standard deviations of at least three independent experiments. **(B)** *In vitro*-translation products of various amounts of RNA separated by 12 % SDS-PAGE and visualized by autoradiography. *Firefly* luciferase (FLuc) protein (62 kDa) is indicated on the right. M, ^{14}C-labelled marker proteins. Molecular masses of marker proteins are indicated in kDa.

3.3.4 Influence of reporter construct design and transfection protocol details on the detection of translation enhancement by the 3´-UTR

Hepatitis C Virus infects specifically human liver cells. Therefore it is an obvious approach to use transfection of human hepatoma cell lines to examine a possible effect of the HCV 3´-UTR on translation. However, the results obtained in several studies using transfection of hepatoma cell lines with reporter constructs including the HCV 5´-UTR and the 3´-UTR are controversial (Ito et al., 1998; Friebe & Bartenschlager, 2002; Kong & Sarnow, 2002; McCaffrey et al., 2002; Imbert et al., 2003; Yi & Lemon, 2003a). Most of these studies used transfection and transient expression of complete circular reporter plasmids or of linearized plasmids. Only in one study, reporter RNAs were transfected into cultured Huh-7 cells, but no enhancement effect of transfection by the HCV 3´-UTR was detected (Friebe & Bartenschlager, 2002). In an attempt to eliminate experimental parameters that hamper a possible enhancing action of the 3´-UTR on HCV IRES-dependent translation, we used a series of reporter constructs and performed different transfection assays.

For this purpose, two types of HCV plasmid DNAs (one with the entire 3´-UTR [named pHCV+3´-UTR], the other without the 3´-UTR [named pHCV+Δ3´-UTR], see Fig. 45 for reference) were transfected into Huh-7 cells. At 40 hrs after transfection, FLuc activities expressed in the cells were determined. However, the translation efficiency obtained with pHCV+3´-UTR was not significantly different from that of pHCV+Δ3´-UTR (Fig. 49A). Also in a time-course experiment (Fig. 49B), no difference in expression of the FLuc from both plasmids was observed.

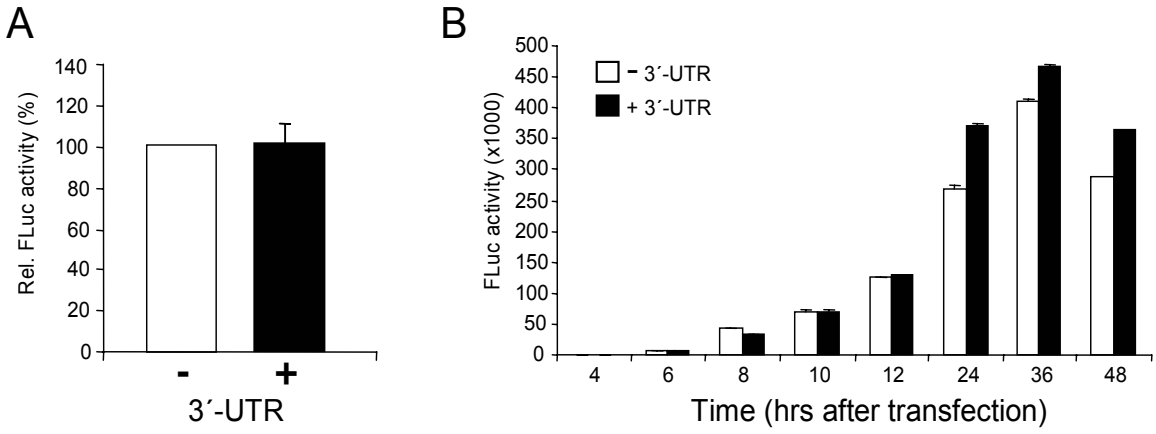

Fig. 49: Effects of the HCV plasmid constructs on HCV translation *in vivo*. (A) HCV plasmids were transfected into Huh-7 cells. Relative *Firefly* luciferase (Rel. FLuc) activities in the lysates were measured at ~40 hrs after transfection. The Fluc activity of the plasmid without 3´-UTR is artificially set to 100 %. **(B)** Effects of HCV plasmids on translation efficiency at different time points after Huh-7 cells were transfected respectively. Cells were harvested at different times and *Firefly* luciferase (FLuc) activities were measured. The columns and bars represent the means and standard deviations of at least three independent experiments, respectively.

To analyze if the presence of an exact 3´-end of the HCV 3´-UTR sequence is required to allow a possible enhancing effect of the 3´-UTR on translation, two types of PCR fragments from the above plasmids were

generated. These PCR fragments include the cytomegalovirus (CMV) promoter and either terminate at the *Firefly* luciferase stop codon, or additionally include the HCV 3´-UTR (Fig. 50A). With these PCR fragments, a slight difference in FLuc expression was observed (Fig. 50B).

When the FLuc activities were measured at different time points after transfection of the PCR fragments into Huh-7 cells, significant differences could be observed (Fig. 50C). Obviously, at early time points after transfection, the FLuc expression from the PCR fragment including the HCV 3´-UTR was up to three-fold higher than that from the PCR fragment without 3´-UTR (Fig. 50C), while this relative difference decreased with increased time after transfection. Thus, assaying reporter gene activity in a time course after transfection may be important for the outcome of experiments testing a possibly enhancing effect of 3´-UTR on HCV IRES-directed translation.

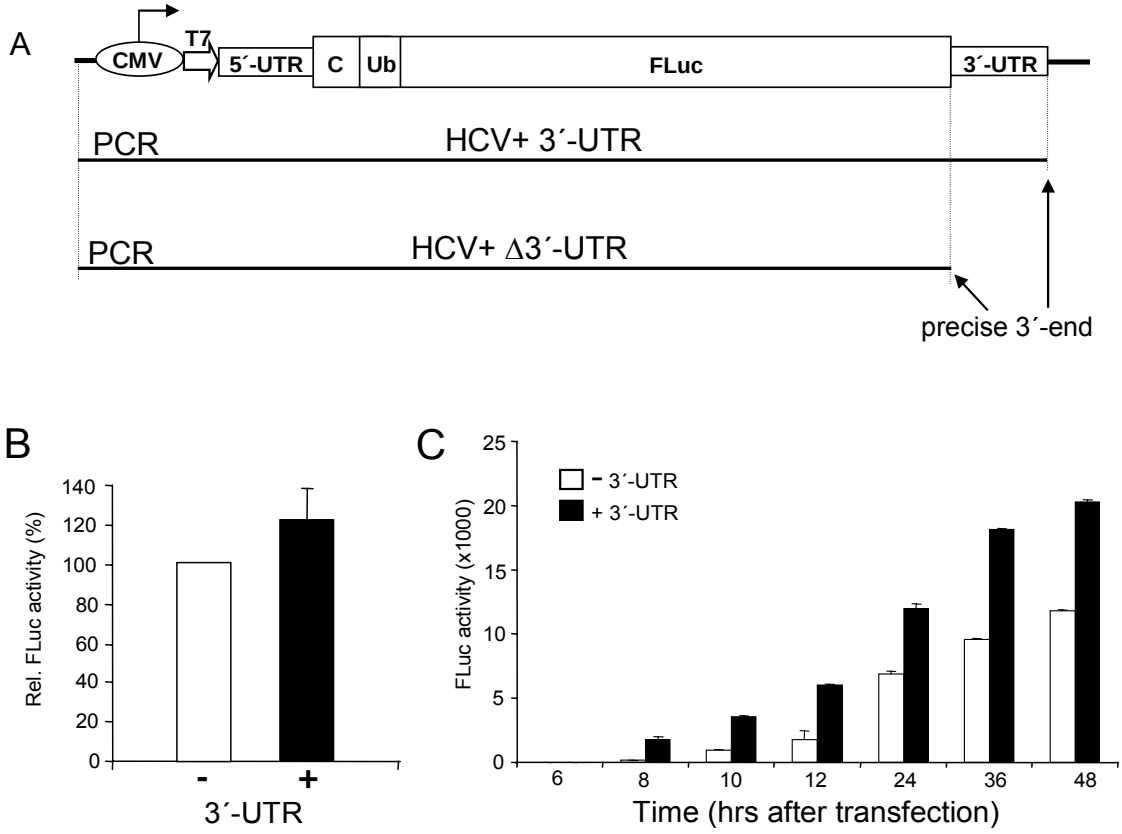

Fig. 50: Effects of the HCV PCR fragments on HCV translation *in vivo*. (A) Schematic representation of the HCV PCR fragments (indicated with lines) with cytomegalovirus (CMV) immediate early promoter upstream of T7 promoter. CMV, Cytomegalovirus immediate early promoter; T7, T7 RNA polymerase promoter; UTR, untranslated region; C, partial core protein-encoding sequences; Ub, ubiquitin sequences; FLuc, *Firefly* luciferase reporter gene. **(B)** HCV PCR fragments were transfected into Huh-7 cells. Relative *Firefly* luciferase (Rel. FLuc) activities in the lysates were measured at ~40 hrs after transfection. The Fluc activity of plasmid without 3´-UTR is artificially set to 100 %. **(C)** Effects of HCV PCR fragments on translation efficiency at different time points after transfection of Huh-7 cells. Cells were harvested at different times and *Firefly* luciferase (FLuc) activities were measured. The columns and bars represent the means and standard deviations of at least three independent experiments, respectively.

In contrast with the above DNA transfection experiments, a strong stimulating effect of the HCV 3´-UTR on translation was found when *in vitro*-transcribed RNAs (see Fig. 45) were transfected into Huh-7 cells (Fig. 51). The translation efficiency of the *in vitro*-transcribed RNA which contains the 3´-UTR (HCV+3´-UTR) was 10 to 20 times higher than that of RNA without 3´-UTR (HCV +Δ3´-UTR). It is important to note that the RNA with 3´-UTR has a precise 3´-end similar to the authentic HCV genome since the RNAs were generated from PCR fragments (Fig. 50A) exactly ending at a position corresponding to the 3´-terminus of genomic HCV RNA. The differences found here are by far larger than those found in previous reports (Ito et al., 1998; Michel et al., 2000) and also those detected in PCR fragment transfection experiments described above (Fig. 50B and C). Thus, the HCV 3´-UTR can strongly enhance translation directed by the HCV IRES when monocistronic reporter RNA with a 3´-end precisely corresponding to the HCV RNA 3´-end is used.

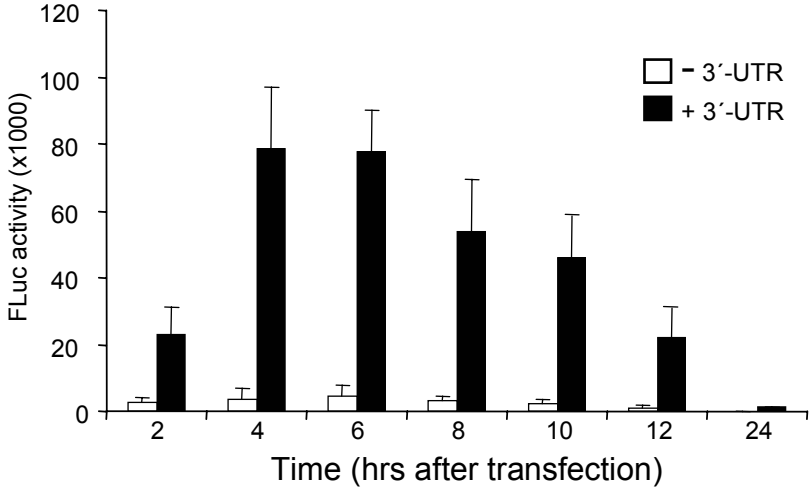

Fig. 51: Translation efficiency of the HCV RNAs transcribed from the corresponding PCR fragments (see Fig. 50A) at different time points after transfection of Huh-7 cells. Cells were harvested at the indicated time points after transfection and *Firefly* luciferase (FLuc) activities were measured. The columns and bars represent the means and standard deviations of at least four independent experiments, respectively.

3.3.5 Expression differences are not due to differences in RNA stability or transfection efficiency

The stem-loop 1 (SL 1) in the 3´-X region forms a stable secondary RNA structure (see Fig. 9, Introduction) that could be argued to protect the 3´-end of the reporter RNA against degradation by exonucleases after transfection, whereas the reporter RNA without HCV 3´-UTR might be degraded more easily. To rule out the possibility that the differences in translation efficiency are due to differences in RNA stability, a specific Fluc anti-sense RNA probe which could hybridize with a 3´ portion of the *Firefly* luciferase-coding sequence in both RNAs was generated (Fig. 52A), and the integrity of the reporter RNAs was tested in an RNase protection assay after re-isolation from the transfected cells. The results showed that with both transfected reporter RNAs, fragments of

the expected length are detected (Fig. 52B), indicating that the 3´-region of the FLuc-encoding sequence was not degraded in both cases. Thus, the differences in translation efficiency are not due to differences in RNA stability.

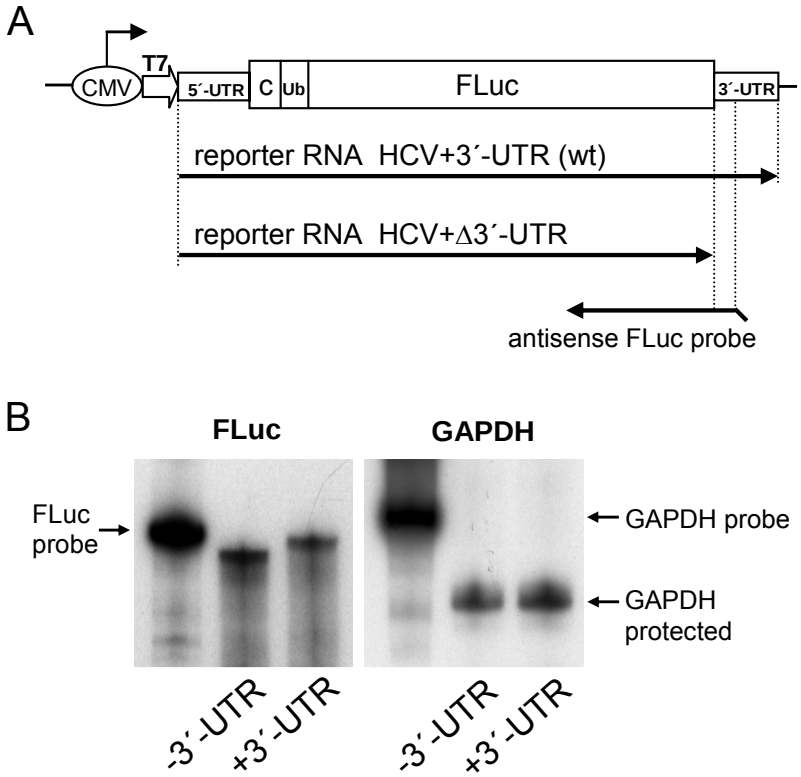

Fig. 52: RNase protection assay. (A) Organization of the anti-sense FLuc RNA probe for the RNase ptotection assay. **(B)** RNA stability control. Cytoplasmic RNA from Huh-7 cells transfected with RNA "HCV - Δ3´-UTR" or RNA "HCV+3´-UTR" was harvested 4 hrs after transfection, purified and analyzed by RNase protection assay using [α-^{32}P]-UTP labelled antisense FLuc RNA probe. As a control, glyceraldehyde-3-phosphate-dehydrogenase (GAPDH) mRNA antisense RNA probe was used. CMV, Cytomegalovirus immediate early promoter; T7, T7 RNA polymerase promoter; UTR, untranslated region; C, partial core protein-encoding sequences; Ub, ubiquitin sequences; FLuc, *Firefly* luciferase reporter gene; wt, wild-type.

To further rule out the possibility that the differences in FLuc expression are due to variations in transfection efficiency, the HCV reporter RNAs were co-transfected together with another reporter RNA construct containing the *Renilla* luciferase gene. For this purpose, *Renilla* luciferase reporter RNA was capped and polyadenylated to allow its efficient translation in eukaryotic cells. Fig. 53 shows how efficiently the processed *Renilla* luciferase RNA was expressed in Huh-7 cells compared with the expression level of unprocessed *Renilla* luciferase reporter RNA.

Then, this modified *Renilla* luciferase reporter RNA was co-transfected together with the HCV reporter RNAs into Huh-7 cells in different amounts. Again, the HCV IRES-directed FLuc expression was much more efficient in the presence of the HCV 3´-UTR (Fig. 54A), while the co-transfected *Renilla* reporter RNA was expressed with similar efficiency in both cases (Fig. 54B). Moreover, the translation stimulation effect by the HCV 3´-UTR

was almost similar after transfection of different amounts of reporter RNA, ruling out any possible saturation effect in the assay.

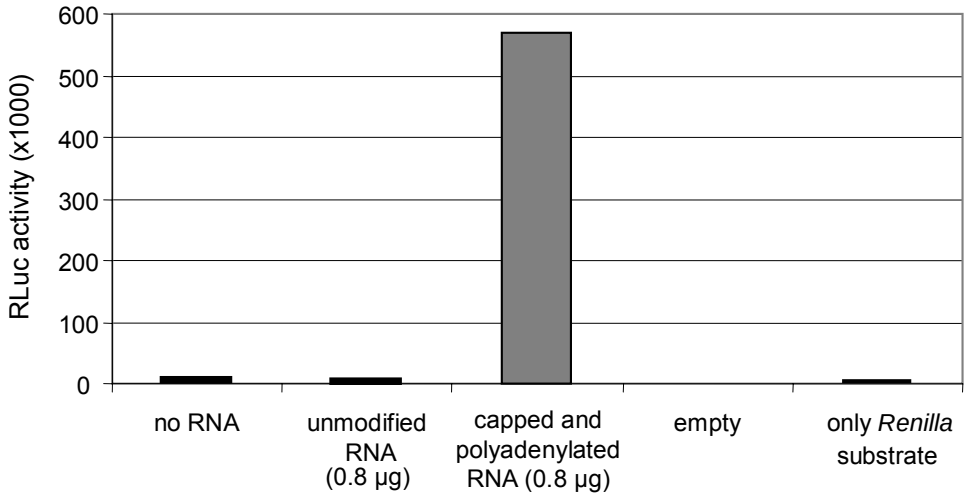

Fig. 53: Comparison of expression levels of different types of *Renilla* luciferase RNA in Huh-7 cells. RLuc, *Renilla* luciferase reporter gene; unmodified RNA, RNA molecule transcribed directly from the corresponding template without modification; capped and polyadenylated RNA, transcribed RNA was processed by capping at the 5´-end and poly (A)-tailing at the 3´-end; empty, only assay tube.

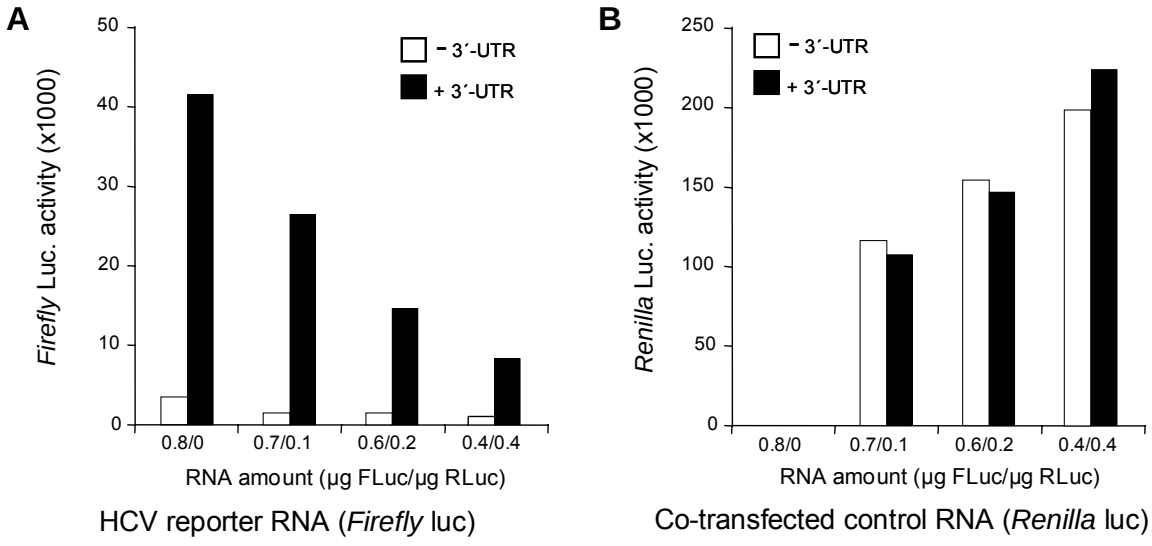

Fig. 54: Co-transfection controls. HCV plus or minus 3´-UTR reporter RNAs (see Fig. 45) were co-transfected together with different amounts of *Renilla* luciferase RNA into Huh-7 cells. Cells were harvested 4 hrs after transfection. *Firefly* luciferase **(A)** and *Renilla* luciferase **(B)** activities were determined according to the manufacturer's instructions.

3.3.6 Additional nucleotides at the 3´ end of 3´-UTR disable stimulation

From the above results, it was concluded that three parameters have impact on the outcome of experiments testing the translation enhancement by the HCV 3´-UTR:

(i) the nature of the 3´-end of the reporter construct plays a role since a PCR fragment providing an exact end of the 3´-UTR resulted in translation stimulation (Fig. 50B and C) whereas transfection of circular plasmid DNA did not (Fig. 49A and B); (ii) the nature of nucleic acid transfected is important since the translation stimulation by the 3´-UTR was more remarkably evident when RNA rather than DNA was used (Fig. 50C); (iii) the time course of measuring reporter gene activity reveals that the stimulatory action of the 3´-UTR is more evident at shorter times after transfection (Fig. 50B and C).

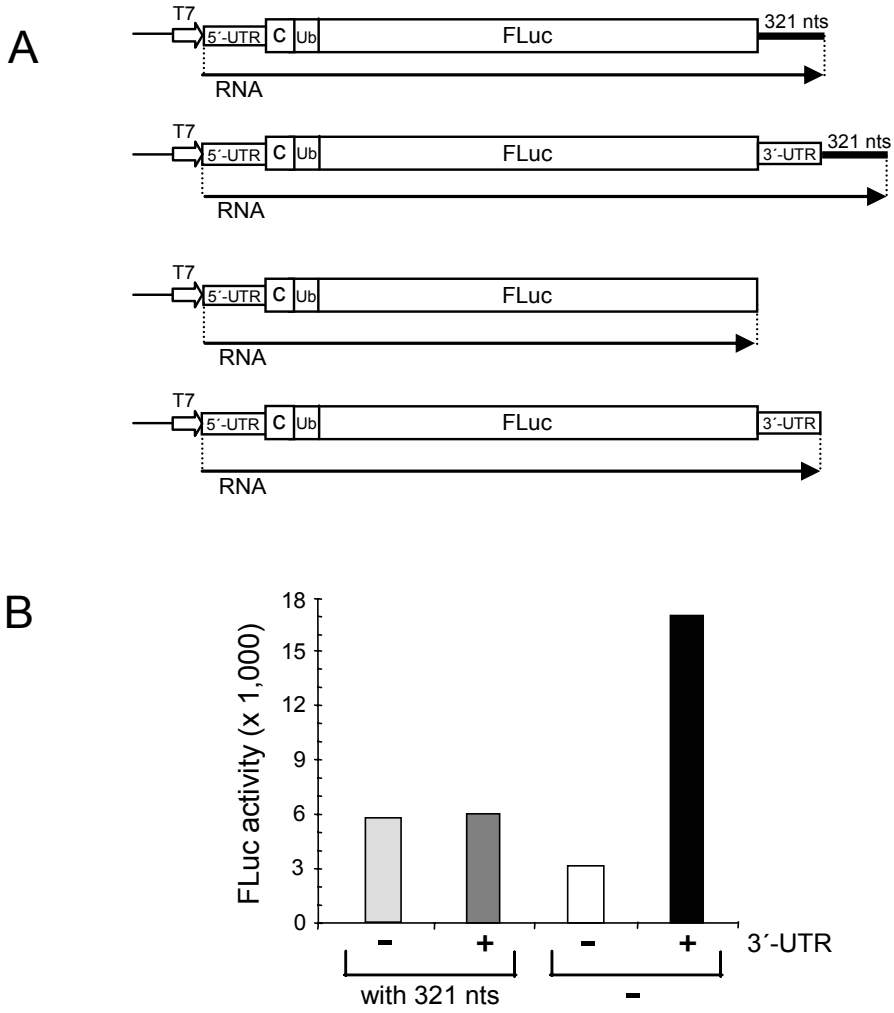

Fig. 55: Additional nucleotides at the 3´ terminal end impair translation enhancement by the 3´UTR. (A) Different RNAs with or without the HCV 3´-UTR followed by 321 nucleotides derived from the plasmid vector sequence, or ending exactly at the FLuc stop codon or the HCV 3´-UTR, respectively. T7, T7 promoter; UTR, untranslated region; C, partial core protein-encoding sequences; Ub, ubiquitin sequences; FLuc, *Firefly* luciferase reporter gene; 321 nts, additional sequences from plasmid vector. The columns and bars represent the means and standard deviations of at least three independent transfections, respectively. **(B)** Activities of *Firefly* luciferase (FLuc) in Huh-7 cell lysates harvested 4 hrs after transfection with the reporter RNAs shown in **(A)**.

To further test if the efficient translation stimulation indeed requires a precise 3´ end of the HCV 3´-UTR, two additional reporter construct templates with artificially extended 3´-ends including 321 nucleotides of unrelated vector sequences were generated by PCR (Fig. 55A). When the corresponding RNAs with artificially extended 3´-ends were compared with the RNA possessing an authentic end of the HCV 3´-UTR, only the RNA with an authentic 3´-UTR terminus gave rise to translation enhancement (Fig. 55B). This observation confirms that a precise 3´-end of the HCV 3´-UTR (corresponding to that of authentic viral RNA genome) is required for efficient translation enhancement.

3.3.7 The HCV 3´-UTR enhances IRES-dependent translation preferentially in human liver-derived cell lines

The above results demonstrated that the HCV 3´-UTR can remarkably enhance its IRES-mediated translation in a human liver cell-based translation system but not in a non-liver system such as rabbit reticulocyte lysate, consistent with the fact that HCV preferentially infects liver cells. Nevertheless, it has been reported that the HCV IRES is also active in non-liver-derived cells (Wang et al., 1993; Reynolds et al., 1995; Kamoshita et al., 1997). Therefore, it was further analyzed whether this stimulatory effect of the 3´-UTR is only restricted to human hepatoma cells such as Huh-7 and Hep G2 cells, or whether also non-hepatoma cells such as HeLa and BHK cells allow translation stimulation by the 3´-UTR.

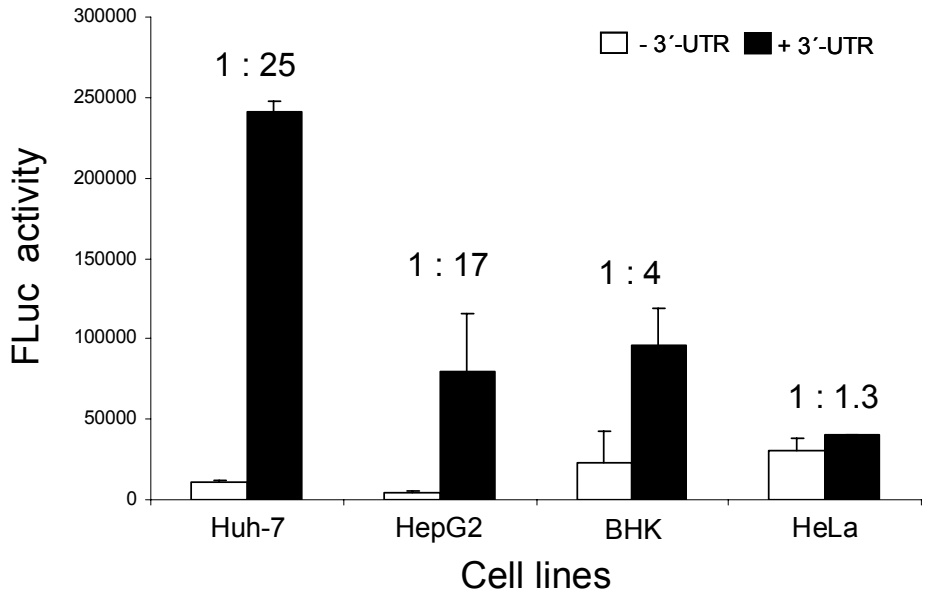

Fig. 56: Effects of the 3´-UTR of on HCV translation in different cell lines. *Firefly* luciferase (FLuc) activities were determined 4 hrs after transfection with HCV plus or minus 3´-UTR RNAs. The columns and bars represent the means and standard deviations of at least three independent experiments, respectively. The ratios shown above the columns represent the FLuc activitiy from the reporter RNA without 3´-UTR relative to the Fluc activity from the reporter RNA with 3´-UTR in different cell lines.

For this purpose, two reporter RNAs, HCV+Δ3´-UTR and HCV+3´-UTR (see Fig. 45), were transfected into four different cell lines: Huh-7, Hep G2, HeLa and BHK cells, and *Firefly* luciferase activities were determined at different time points after transfection. The result shows that the differences in translation efficiency caused by the presence of the 3´-UTR is only two- to four-fold in BHK and HeLa cells but 17- to 25-fold in Hep G2 and Huh-7 cells (Fig. 56). These data indicate that the HCV 3´-UTR preferentially enhances HCV IRES-dependent translation in a cellular environment derived from human liver cells.

3.3.8 Effects of deletions in the 3´-UTR on HCV IRES-mediated translation

To identify the contribution of the three elements of the 3´-UTR, the variable region (VR), the poly (U/C)-tract and the 3´-X region with its three stem-loops, to translation stimulation, a series of deletion mutants in the 3´-UTR sequence was generated (Fig. 57A). The FLuc activities expressed from the corresponding reporter RNAs after transfection into Huh-7 cells were measured over a time range of 2 to 12 hrs post-transfection (data not shown). Since no time specific differences were evident from these data (compare with Fig. 51), the values determined at 4 hrs after transfection are shown here (Fig. 57B).

First, it was tested if efficient reporter translation requires additional sequences downstream of the luciferase gene stop codon. A random sequence of 15 nucleotides was added directly downstream of the luciferase stop codon (HCV+RD15, Fig. 57A). After transfection into Huh-7 cells, both RNAs, the HCV-Δ3´-UTR RNA and the HCV+RD15 RNA, were translated with almost similar efficiencies (Fig. 57B), indicating that the luciferase gene can be correctly translated from the RNA ending exactly at the luciferase stop codon.

Deletion of any of the three sequence elements of the HCV 3´-UTR, the variable region, the poly(U/C)-tract or the 3´-X region (RNAs HCV-Δ3´VR, -UC and -X, respectively), had serious impact on translation efficiencies (which range from 7 % to 11 % of wild-type efficiency). Surprisingly, a combination deletion of the variable region and the pyrimidine tract (HCV-Δ3´VUC RNA) resulted in more efficient translation compared with the single deletions. From these observations, we can only speculate that these sequences might bear not only determinants that enhance translation but also determinants that negatively regulate translation. This idea is supported by the finding that a combination deletion of the poly(U/C)-tract and the 3´-X region (HCV-Δ3´-UCX RNA) also translated slightly more efficiently than the corresponding single deletions. Since the stem-loops within the 3´-X region appear to contribute positively to translation efficiency (see below), we assume that such negatively regulating determinants may be confined to the sequences upstream of the X-region.

When the three predicted stem-loop structures of the 3´-X region were deleted (Fig. 57A), analysis of these RNAs revealed that the involvement of these stem-loops in translation stimulation gradually decreases from 3´ to 5´ (Fig. 57B). Deletion of SL1 allowed only 30 % residual translation activity, whereas deletion of SL2 resulted in 53 % and deletion of SL3 even in 86 % activity.

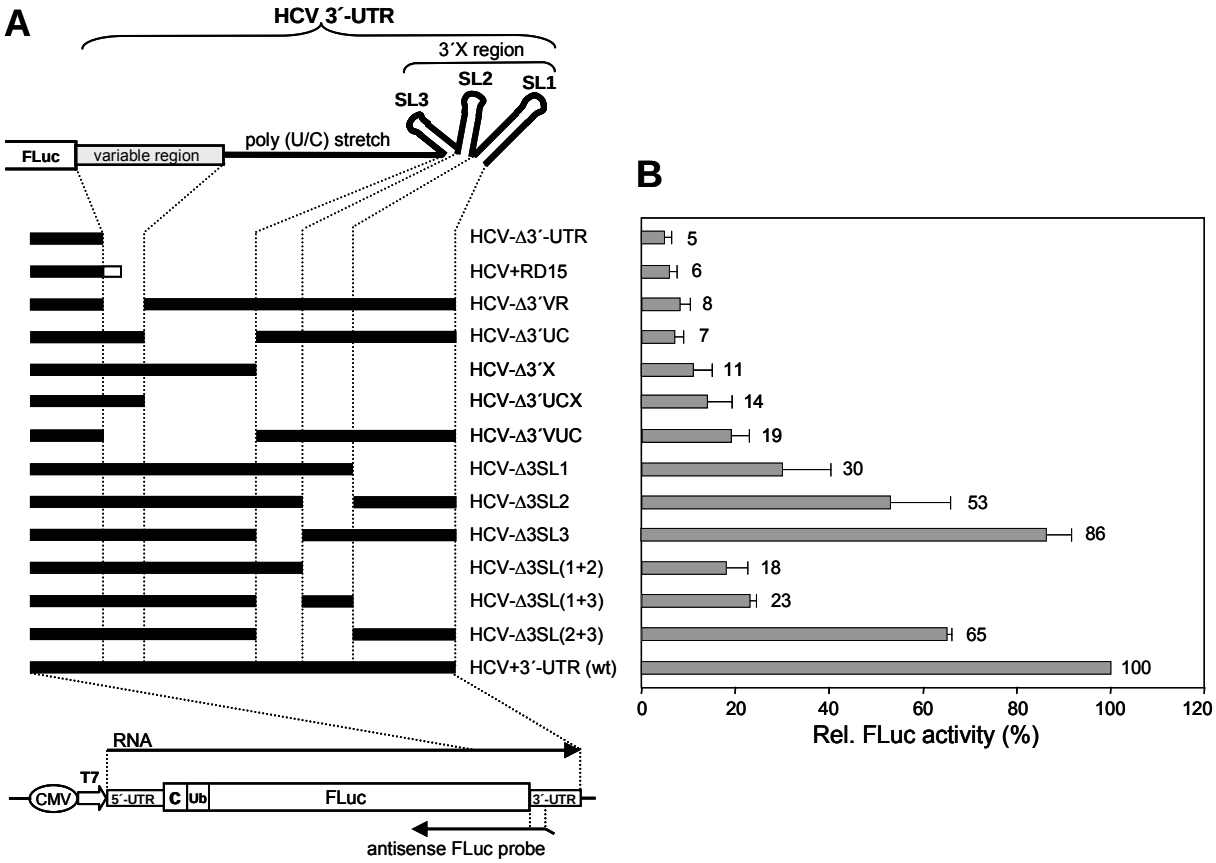

Fig. 57: Effects of deletion mutants within the 3´-UTR on translation efficiency of the HCV RNA. (A) The HCV 3´-UTR and its deletion mutants. The general structure of the reporter construct is shown at the bottom, with the 3´-UTR deletion mutant RNAs and the predicted RNA stem-loop structures of the 3´-X on the top. The HCV 3´-UTR was fused exactly to the luciferase coding sequence. HCV + RD15 includes an artificial sequence of 15 random nucleotides (open bar) immediately downstream of the *Firefly* luciferase (FLuc) coding sequence. SL, stem-loop; wt, wild-type. The Fluc antisense probe used for the RNA stability control (Fig. 58) is shown at the bottom. **(B)** *Firefly* luciferase (FLuc) activities expressed in Huh-7 cells were measured 4 hrs after transfection with all deletion mutants introduced within the HCV 3´-UTR RNAs. Relative *Firefly* luciferase (Rel. FLuc) activities are indicated on the right side of each horizontal column. The FLuc activitiy of HCV+3´-UTR (wt) is artificially set to 100 %. The columns and bars represent the means and standard deviations of two independent experiments.

With combination deletions of the three stem-loops of the 3´-X region an interesting result was obtained. When SL1 was deleted in combination with SL2, the translation efficiency was 18 %. This value is close to the product of the translation efficiencies of both single elements (0.30 × 0.53 = 0.16). Similarly, deletion of SL1 together with SL3 resulted in 23 % activity which is again close to the product of translation efficiencies of both single elements (0.30 × 0.86 = 0.26). These results suggest that the combination of stem-loop 1 together with the other stem-loops contribute to translation stimulation synergistically. With a combination deletion of SL2 and SL3, the translation efficiency was 65 %, which is only roughly in the range of the product of translation efficiency of both single elements (0.86 × 0.53 = 0.46).

According to the different deletions, the predicted secondary structures of the 3´-ends are different among the different RNA variants used in the experiments described above. Only some of these reporter RNAs have very stable RNA secondary structures at the 3´-end which may protect the different RNAs from degradation by exonucleases after transfection.

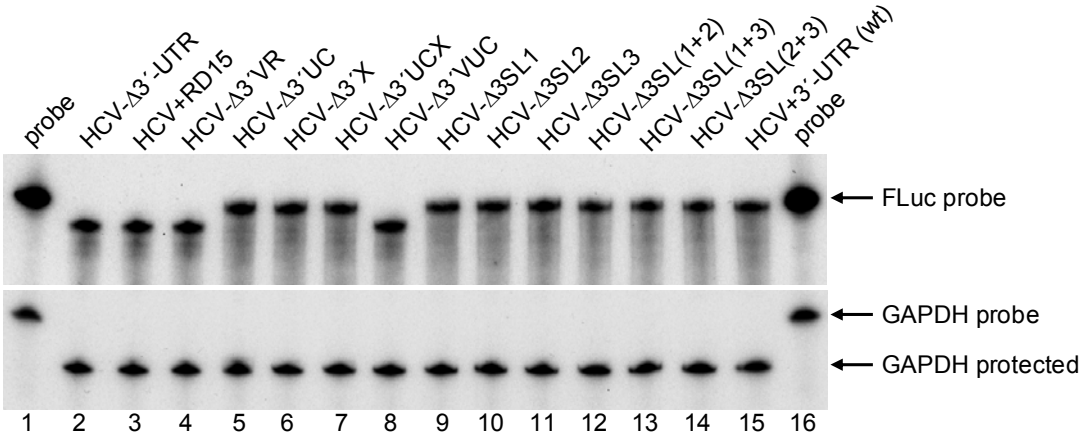

Fig. 58: RNA stability control. Cytoplasmic RNA from Huh-7 cells transfected with the RNAs used in Fig. 57B was harvested 4 hrs after transfection, purified and analyzed by ribonuclease protection assay using the [α-^{32}P]-UTP labelled antisense FLuc RNA probe (see Figs. 57A and 52B). As a control, the same cytoplasmic RNA samples were also analyzed using a glyceraldehyde-3-phosphate-dehydrogenase (GAPDH) mRNA antisense RNA probe (lower panel). In lanes 1 and 16, 5% of the undigested antisense RNA probes were loaded.

To rule out the possibility that the differences in translation efficiency are due to differences in RNA stability, we tested the integrity of the 3´-portion of the *Firefly* luciferase-coding sequence by RNase protection assay (Fig. 22). The result show that all transfected reporter RNAs appear with the expected length (note: the anti-sense probe includes also 29 nucleotides of 3´-UTR sequence) and with similar signal intensity, indicating that differences in RNA stability do not account for the differences in translation efficiency.

3.3.9 Conclusions

The HCV 3´-UTR stimulates translation of a reporter RNA with the HCV IRES at the 5´-end in human hepatoma cell lines. This stimulation requires an exact 3´-end of the 3´-UTR, as well as the use of a monocistronic reporter RNA and activity measurement at short times after transfection.

The variable region, the poly(U/UC)-tract and the 3´-terminal stem-loop 1 of the 3´-X region contribute significantly to the translation enhancement, whereas the stem-loops 2 and 3 of the 3´-X region are less important for this effect.

3.4 Part IV: An unknown protein of about 210 kDa binds to the HCV RNA only in the presence of both 5´-UTR and 3´-UTR

In the previous experiments of this work, no new binding protein was detected by the UV cross-linking assay to interact with the HCV IRES RNA molecules irrespective if the 3´-UTR is present or not. Some extra protein bands were observed only when the HCV 3´-UTR RNA is included, but these bands were found to interact with the 3´-UTR alone as well (Figs. 16, 18 and 19). Also, some proteins interacting only with HCV IRES deletion mutants or detected more evidently with the deletion mutants than with the HCV wild-type IRES were observed (Fig. 12). Taken the above results together, the presence of the HCV 3´-UTR obviously did not augment the binding of protein(s) to the HCV IRES.

However, this conclusion seems to be inconsistent with the fact that the 3´-UTR of HCV is not only responsible for the replication of viral RNA, but is also involved in the stimulation of IRES-directed translation as shown in the third part of the Results section. From the finding that the 3´-UTR stimulates translation, it must be assumed that some factor(s) are involved in an RNA 5´-3´-end interaction so that the translation initiation could be positively regulated by the 3´-UTR. Moreover, the translation stimulation by the HCV 3´-UTR has been reported by other groups (Ito et al., 1998; Michel et al., 2001; McCaffrey et al., 2002), although the degree of stimulation is much lower in those studies than that observed in this work. These arguments gave rise to a reconsideration of the experimental design of the HCV RNA constructs used for the search for new proteins, finally resulting in the discovery of a novel yet unknown protein that binds to the HCV RNA.

3.4.1 Redesigning the HCV RNA constructs used for the protein search

Take into account the above considerations, two inconsistent features were realized in the design of the HCV RNAs used before in the UV cross-linking experiments. The plasmid used for the transfection studies, HCV+3´-UTR (wt), has an in-frame *Firefly* luciferase reporter gene sequence between 5´- and 3´-UTR (Fig. 23), whereas the HCV IRES plus 3´-UTR plasmid used for the UV cross-linking assays, subcloned from the above plasmid by deleting the ubiquitin sequences and the *Firefly* luciferase-coding sequence from the HCV+3´-UTR wt plasmid, has an artificial stretch of sequence between 5´- and 3´-UTR which does not constitute a functional open reading frame (ORF), even if short, but was out-of-frame (due to the restriction sites used for the deletion) (Fig. 14). Another feature is the 3´-end of the 3´-UTR. The former out-of-frame HCV IRES plus 3´-UTR RNA generated from the corresponding plasmid did not have a precise 3´-end (Fig. 14). It could be assumed that always no difference was observed in the previous UV cross-linking assays with both HCV IRES only RNA and HCV IRES plus 3´-UTR RNA (Figs. 15-19) just because of two different reasons: either that additional nucleotides downstream of the 3´-UTR may influence the protein binding to the authentic 3´-UTR sequences, or the ribosomes would not correctly terminate at the authentic stop codon but translate through the variable region and disable protein binding.

In order to allow a decision between these two hypotheses, a new plasmid with an artificial in-frame sequence (96 nucleotides) between the HCV 5´- and 3´-UTR was generated from the HCV + 3´-UTR (wt) construct (Fig. 14A) by double-digestion with *Aat* II and *Eco* NI followed by treatment with *Klenow* fragment and religation. From this plasmid, a PCR fragment with a precise 3´-terminus of the 3´-UTR was generated from which the RNA was then transcribed. Thus, this in-frame RNA also has an exact 3´-end. In contrast, the formerly constructed out-of-frame plasmid was made as described in the first part of the Results section (**3.1.3**), resulting in four additional nucleotides added into the artificial linker between the 5´- and the 3´-UTR due to two subsequent cloning steps including fill-in and removal processes. Therefore, the total number of nucleotides between the 5´- and the 3´-UTR was changed to 100. Fig. 59 shows the difference between the in-frame and out-of-frame HCV RNA constructs.

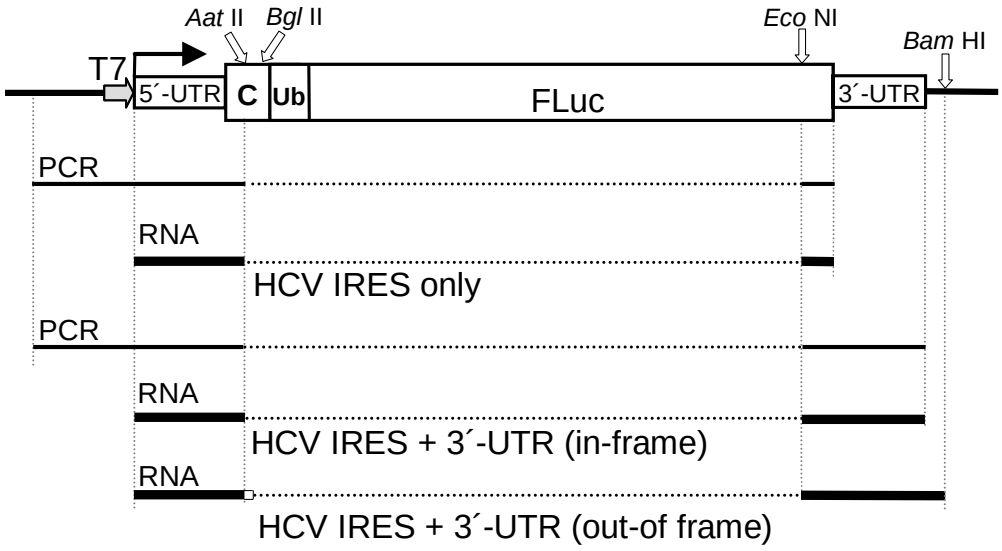

Fig. 59: Schematic diagram of the in-frame and out-of-frame HCV RNA constructs. The very upstream part of the core protein-encoding sequences is present in all HCV RNA constructs. *Bam* HI was used for generating the "HCV 3´-UTR only" RNA template and out-of-frame RNA plus 3´-UTR RNA templates, respectively. *Aat* II and *Eco* NI were used for generating the in-frame HCV IRES plus 3´-UTR clone vector. The in-frame RNAs were all transcribed from the corresponding PCR fragments (indicated with thin lines). T7, T7 RNA polymerase promoter; UTR, untranslated region; C, partial core protein-encoding sequences; Ub, ubiquitin sequences; FLuc, *Firefly* luciferase reporter gene. The solid thick lines represent the HCV RNA molecules and the horizontal dotted lines represent the parts deleted from the original plasmid. The small white box in the out-of-frame RNA construct represents the four additional nucleotides demolishing the open-reading-frame.

3.4.2 Detection of an unknown protein binding to the HCV RNA with a precise end of the 3´-UTR

Then, two [α-^{32}P]-UTP labelled in-frame RNAs (Fig. 59) were *in vitro*-transcribed from the corresponding PCR-generated templates. Using these two new RNAs, UV cross-linking assays were performed in Huh-7 extract, together with the two RNAs used before (compare Fig. 14). Surprisingly, a clearly visible protein band appears

at about 210 kDa in the lane with the in-frame HCV IRES plus 3´UTR RNA (Fig. 60, lane 2), whereas no band is observed at the corresponding position in any other lane, in particular also not in the lane with the out-of-frame RNA (Fig. 60, lane 1).

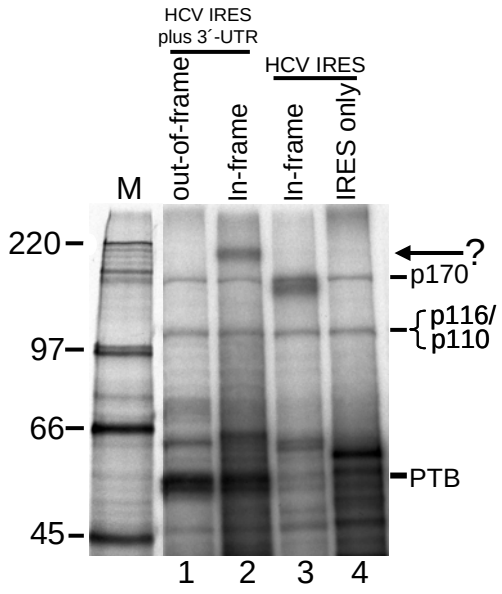

Fig. 60: Interaction of proteins from Huh-7 lysate with HCV RNAs analyzed by the UV cross-linking assay. Four HCV RNAs (see Figs. 14 and 59) were used in 10 µl UV cross-linking reactions including 3 µl cytoplasmic Huh-7 lysate. Proteins were separated on 8 % SDS-PAGE and visualized by autoradiography. The molecular masses of ^{14}C labelled proteins marker (M) are given in kDa. An unknown new protein band is indicated with an arrow and a question mark on the right side of the gel.

In order to further allow a decision whether the exact 3´-end or reading frame is the decisive parameter for binding of the 210 kDa protein, the out-of-frame HCV IRES plus 3´-UTR RNA was *in vitro* transcribed from the PCR-generated template with the exact end of the 3´-UTR (Fig. 61A). UV cross-linking assays were performed in Huh-7 cytoplasmic extract using this [α-^{32}P]-UTP labelled RNA together with another RNA shown in Fig. 61A. Unexpectedly, this about 210 kDa protein band appears in both lanes with the HCV RNAs containing an exact end of the 3´-UTR (Fig. 61B, lanes 2 and 3), whereas no band is observed at the corresponding position in the lane of HCV RNA with an artificial extension of the 3´-UTR due to the linearization of the template by restriction enzyme (Fig. 61B, lane 1). Thus, the existence of a correct 3´-UTR appears to be required for the binding of this 210 kDa protein, irrespective if the sequence between IRES and 3´-UTR is an open-reading-frame or not (Fig. 61B, lanes 2 and 3). No other study has ever reported about a protein of about 210 kDa interacting with the HCV RNA so far. In addition, the eIF3 subunits - p170, p116 and p110 - seem to serve as an internal control for the protein-binding assay. Interestingly, the other two proteins migrating by far more slowly than 220 kDa were also observed to bind to the RNAs with an exact end of the 3´-UTR (Fig. 61B, lanes 2 and 3). However, their binding will need further confirmation.

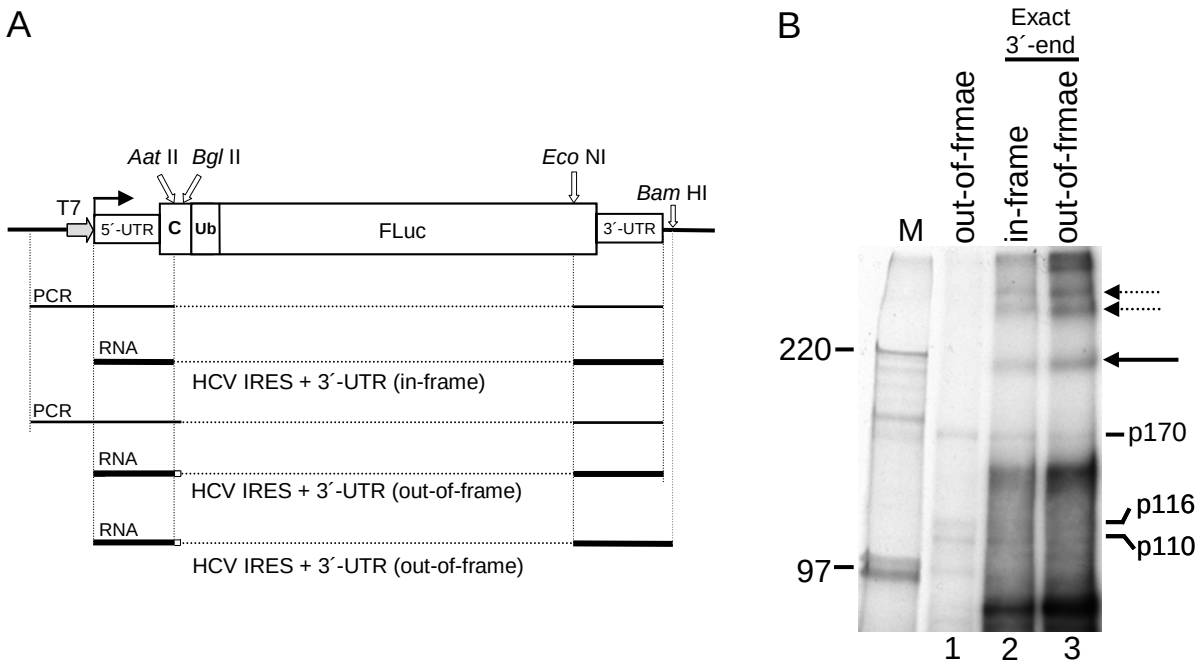

Fig. 61: A precise end of the 3´-UTR is important for the detection of the 210 kDa protein in the UV cross-linking assay. (A) Schematic diagram of the HCV RNAs with or without precise end of the 3´-UTR. The very upstream part of the core protein-encoding sequences is present in all HCV RNA constructs. *Bam* HI was used for generating the HCV RNA template without an authentic 3´-UTR. The RNAs with an exact end of the 3´-UTR were all transcribed from the corresponding PCR fragments (indicated with thin lines). T7, T7 RNA polymerase promoter; UTR, untranslated region; C, partial core protein-encoding sequences; Ub, ubiquitin sequences; FLuc, *Firefly* luciferase reporter gene. The solid thick lines represent the HCV RNA molecules and the horizontal dotted lines represent the parts deleted from the original plasmid. The small white box in the out-of-frame RNA construct represents four additional nucleotides demolishing open-reading-frame. **(B)** Three HCV RNAs shown in (A) were used in 10 µl UV cross-linking reactions including 3 µl Huh-7 lysate, respectively. Proteins were separated on 6 % SDS-PAGE and visualized by autoradiography. The molecular masses of ^{14}C labelled proteins marker (M) are given in kDa and the positions of the subunits of eIF3 (p170, p116 and p110) are indicated. An unknown new protein band is indicated with an arrow on the right side of the gel, as well as two additional bands of more than 220 kDa with dotted arrows.

Since the position of this new unknown protein binding to the in-frame HCV RNA is about 210 kDa, it could have been possible that the new protein detected is identical to eukaryotic initiation factor 4G (eIF4G) which binds to the foot-and-mouth disease virus (FMDV) IRES. eIF4G may act as a multipurpose adaptor connecting the RNA with the ribosome (Hentze, 1997). For example, eIF4G can provide a scaffold for the interaction of eIF4F complexes with poly(A) binding protein (PABP) on most eukaryotic cellular mRNAs during the process of translation initiation (Tarun & Sachs, 1996), and eIF4G has been described to bind to the subdomain 4 of the FMDV IRES initiating cap-independent translation (Saleh et al., 2001).

In order to rule out that this new protein is identical with eIF4G, two kinds of FMDV RNAs, FMDV IRES wild type (wt) and 4M mutant (Bassili et al., 2004) RNA were included in the next UV cross-linking assay. Binding

of eIF4G to FMDV IRES can be abolished by one of the mutants of the FMDV IRES, called FMDV 4M, which was subcloned in our lab (Bassili et al., 2004). In addition, due to the size of this unknown protein, a low percentage acrylamide gel was used in the experiment.

The results show that this protein is most probably not eIF4G since eIF4G interacting with the FMDV wt RNA, although faint in RRL (arrow in Fig. 62, lane 2), migrates faster than the new protein binding to the HCV IRES plus 3´-UTR RNA (Fig. 62, lanes 2 and 3).

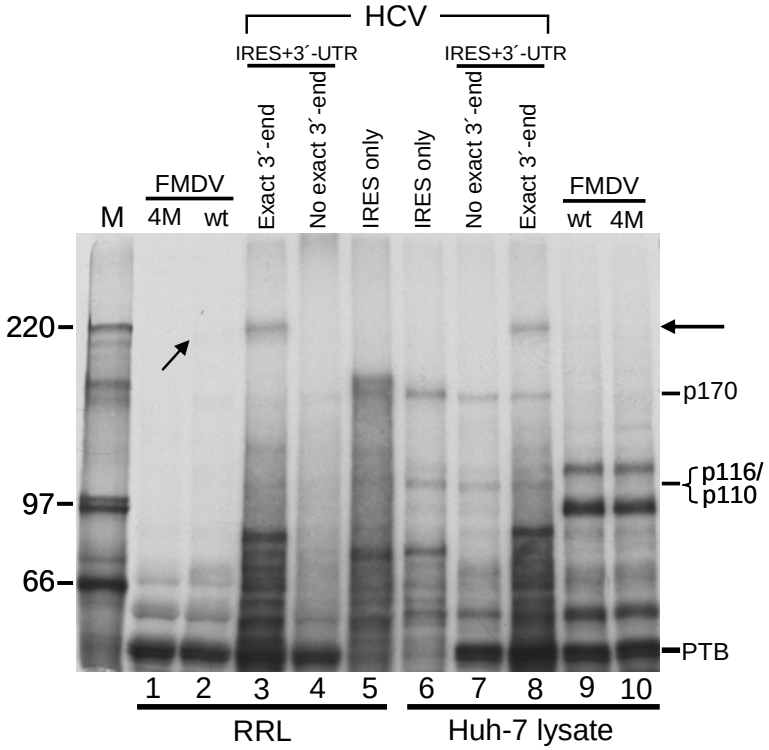

Fig. 62: Interaction of proteins from both RRL and Huh-7 lysate with HCV RNAs analyzed by the UV cross-linking assay. Assays were performed using three HCV RNAs (Fig. 60) in both RRL and Huh-7 lysate. Proteins were separated on 6 % SDS-PAGE and visualized by autoradiography. FMDV, foot-and-mouth disease virus; wt, wild-type; 4M, a mutant of the FMDV IRES which abolishes the binding of eIF4G to the FMDV IRES (Bassili et al., 2004). eIF4G binding to the FMDV wt IRES is indicated with a small arrow (lane 2). The molecular masses of ^{14}C labelled proteins marker (M) are given in kDa and the positions of the subunits of eIF3 (p170, p116/110) are indicated. The unknown new protein band is indicated with an arrow on the right side of the gel.

Moreover, this unknown protein could be cross-linked to the HCV IRES plus an exact end of the 3´-UTR RNA in both RRL and Huh-7 cell lysate. Obviously, it does not bind to the other two types of HCV RNA - HCV IRES only and HCV IRES plus a non-authentic 3´-UTR RNA - in both RRL and Huh-7 lysate (Fig. 62, lanes 4-7). This observation clearly indicates that the unknown protein can interact with the HCV RNA only when the RNA has an exact 3´-end of the 3´-UTR. The reason why negative results were always obtained in all previous experiments of the protein search may be also partially explained by this idea.

3.4.3 The unknown protein interacts with the variable region of the HCV 3´-UTR

The fact that this unknown protein only binds to the RNA containing the IRES plus the authentic 3´-UTR raises the question whether there is a synergistic interaction between the HCV 5´- and 3´-UTR in the presence of this protein during the translation initiation. In order to examine this promising hypothesis, a series of experiments must be considered. The first step is to find out which part in the 3´-UTR region is providing the binding site of this protein. For this purpose, a series of plasmids that meets the demands of the aspect mentioned above was cloned.

First of all, to identify how the three elements of the 3´-UTR, the variable region (VR), the poly (U/C)-tract and the 3´ X-region, individually or in concert, affect the binding of this unknown protein, a series of deletion mutants in the 3´-UTR sequence was generated in the short in-frame construct (96-nucleotide ORF). These mutants included individual deletions of any of the three sequence elements of the HCV 3´-UTR, the variable region, the poly(U/C)-tract or the 3´ X-region (RNAs HCV-ΔVR, -ΔUC and -ΔX, respectively), as well as combination deletions of these elements (Fig. 63).

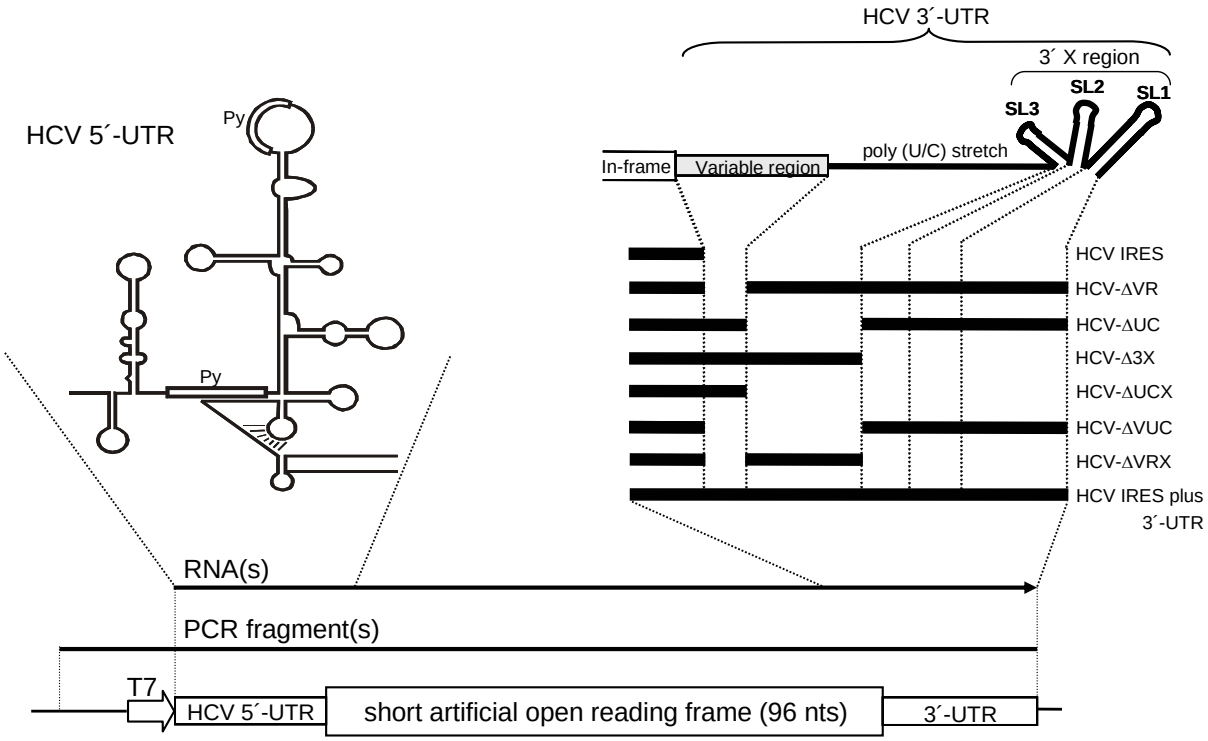

Fig. 63: Schematic diagram of the HCV RNA construct and its deletion mutants. The HCV IRES plus 3´-UTR plasmid was modified from that shown in Fig. 59. The PCR fragment is indicated with a line. The arrow line represents the final HCV RNA molecule. T7, T7 RNA polymerase promoter; Py, polypyrimidine-rich tract; UTR, untranslated region; SL, stem-loop.

From these HCV deletion mutant constructs as shown in Fig. 63, the templates for *in vitro*-transcription of the HCV RNAs were generated by PCR to obtain the corresponding [α-^{32}P]-UTP labelled transcripts with precise

3´-ends. These RNAs were subsequently used in UV cross-linking assays with Huh-7 cytoplasmic lysate. The result shows that the 210 kDa protein appears to bind not only to the HCV IRES plus an authentic 3´-UTR RNA but also to some deletion mutants of the HCV 3´-UTR (Fig. 64). However, the binding of this protein appeared not to be easy to understand. For example, the binding signal vanished in the absence of 3´ X-region (Fig. 64, lane 8), whereas it was still there when the poly-(U/C) stretch of the 3´-UTR was deleted (Fig. 64, lane 7). Interestingly, the 210 kDa protein signal also vanished but another new protein which is migrating slightly slowlier than the protein of interest appeared in the absence of the variable region (Fig. 64, lane 6). Based on the above observations, the variable region plus the 3´-X region of 3´-UTR should be responsible for the binding of this protein. However, the protein was again detected even stronger in the absence of both 3´-X and poly-(U/C) stretch (Fig. 64, lane 11). In contrast, the ΔVRX-mutant also appears to bind the protein (Fig. 64, lane 10), an observation which is completely inconsistent with the results obtained with the other RNAs.

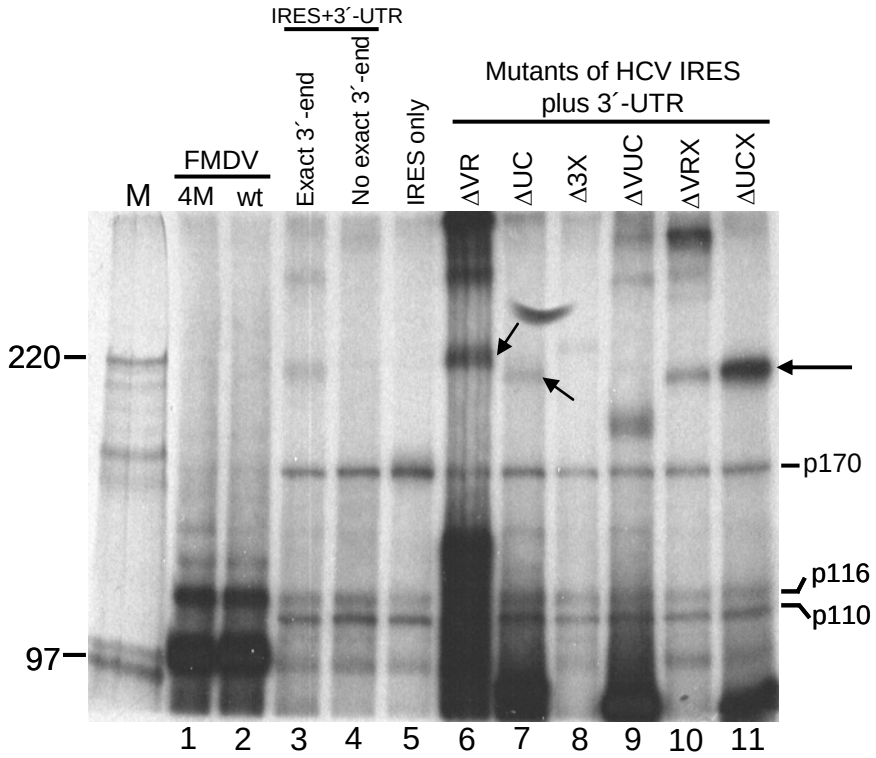

Fig. 64: Effects of deletions within the HCV RNAs containing exact 3´-ends on the binding of the unknown 210 kDa protein in Huh-7 lysate. Proteins were separated on a 6 % SDS-PAGE gel after UV cross-linking with HCV and FMDV RNAs and visualized by autoradiography. The HCV RNA molecules were *in vitro* transcribed from the templates shown in Fig. 63. The unknown new protein band is marked with a horizontal arrow on the right side of the gel. Other new proteins binding to the mutants are indicated with slanted arrows in the gel. FMDV, foot-and-mouth disease virus; wt, wild-type; 4M, one of the mutants of FMDV IRES which can abolish the binding of eIF4G to the FMDV IRES (Bassili et al., 2004). The molecular masses of ^{14}C labelled proteins marker (M) are given in kDa and the positions of the subunits of eIF3 (p170, p116 and p110) are indicated on the right side of the gel.

In addition, the positions of the new proteins migrating in different lanes showed small differences so that it was hard to judge what the actual reason for the conflicting observations was. In order to further analyze the protein(s) in question and to possibly resolve the observed discrepancy, some mutants were selected (ΔVR, ΔVRX, ΔUC, ΔUCX), a new order of the samples was arranged on the gel, and the gels were run extremely long to allow a maximal separation of the proteins to possibly identify differences in their migration (Fig. 65).

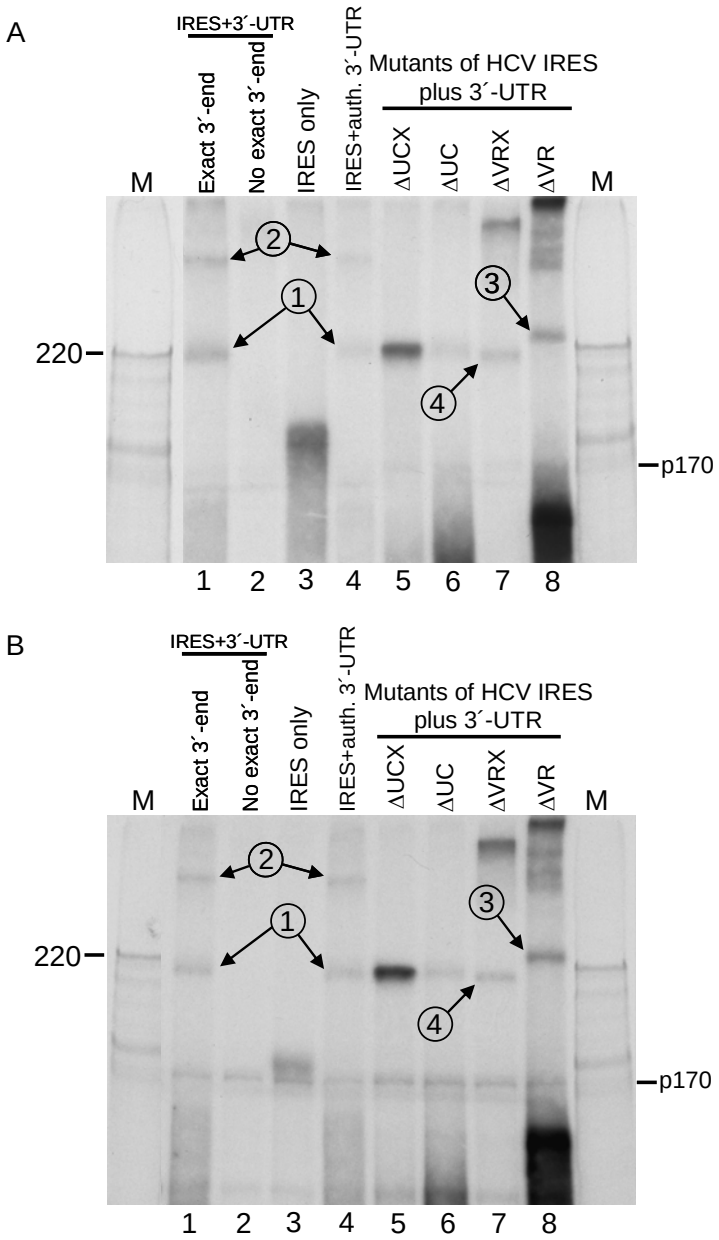

Fig. 65: Effects of deletions within the in-frame HCV RNAs on the binding of the unknown protein analyzed by the UV cross-linking assay in both RRL (A) and Huh-7 lysate (B). The HCV RNA molecules were *in vitro*-transcribed from the templates shown in Fig. 63. The unknown novel protein band of interest is indicated with arrow ①. Three other proteins are marked with arrow ② (largest protein) and ③ (larger protein) and ④ (smaller protein). Proteins were separated on a 6 % SDS-PAGE gel and visualized by autoradiography. auth. 3´-UTR, authentic end of the 3´-UTR. The molecular masses of ^{14}C labelled proteins marker (M) are given in kDa and the position of the p170 subunit of eIF3 is indicated on the right side of the gels.

The results with the high resolution gel shown in Fig. 65 indicate that the proteins binding to the ΔUCX and ΔUC mutants are all below 220 kDa, and their migrating positions are exactly the same as that of the target protein binding to the HCV wild-type RNA (band ① in Fig. 65). Additionally, two other proteins interacting with two different HCV mutants but not with the wild-type RNA are also found. One protein binding to the ΔVR mutant RNA is obviously larger than 220 kDa (band ③ in Fig. 65), whereas the other protein binding to the ΔVRX mutant RNA (band ④ in Fig. 65) is migrating only very slightly faster than the unknown protein bound to the HCV wild-type RNA (band ① in Fig. 65). Thus, the 210 kDa protein binds to the variable region of the 3´-UTR. This protein can be always detected in both RRL and Huh-7 lysate (Figs. 62 and 65), indicating that RRL (which is available in large amounts) can be used in purification steps towards identification of this protein.

Moreover, another protein which migrates even much more slowly than 220 kDa appears with the wild-type 3´-UTR (Fig. 65, band ②). This protein does not appear with any of the deletion mutant RNAs, indicating that it may be involved, in addition to the new 210 kDa protein, in a protein complex that binds to the HCV 3´-UTR only when the 3´-end of the viral RNA is authentic (reference to Figs. 61, 64 and 65).

It is still unclear how these new proteins bind to the HCV IRES plus 3´-UTR RNA. Deletion mutants introduced into the HCV 5´-UTR and a series of 5´-UTR deletions in combination with the 3´-UTR or its mutants can be subsequently used to further answer the following questions:

(1) Is also the 5´-UTR involved in binding of these proteins?

(2) Are these proteins involved in the translation activity mediated by the HCV IRES?

(3) Are these proteins possibly involved in a switch between HCV translation and viral RNA replication?

(4) Are these proteins specific to cell types that share common biochemical features with human liver cells, e.g., also fast growing cells like rapidly dividing reticulocytes; in other words, are these proteins possibly involved in the regulation of lipid metabolism which is required for membrane lipid synthesis in liver cells as well as in quickly growing cells?

3.4.4 Conclusions

A protein of about 210 kDa as well as another high molecular mass protein apparently binds to the 3´-UTR of HCV. Binding of the 210 kDa protein requires the variable region of the 3´-UTR as well as a precise end of the 3´-UTR. In addition, binding of these proteins can be detected with Huh-7 hepatoma cell extract as well as with rabbit reticulocyte lysate.

4 Discussion

In this study, the role of the 5′- and 3′-untranslated region of the RNA genome of Hepatitis C Virus on HCV translation as well as the interaction of cellular RNA-binding proteins with the viral RNA were investigated.

In the first part of the discussion, the interaction of some selected well-known RNA-binding proteins with the HCV IRES and the 3′-UTR as well as the search for new proteins binding to the IRES is discussed. In the second part, the functional role of the HCV 3′-UTR in translation stimulation is discussed in comparison with several other conflicting reports. Finally, the discovery of a novel, yet unknown protein binding to the HCV 3′-UTR and its possible involvement in the HCV life cycle is discussed.

4.1 Interaction of cellular proteins with the HCV RNA untranslated regions and their effects

Since Hepatitis C Virus was discovered in the late 1980s, many studies have focused on mapping structural elements which can function as target sites for RNA-protein interactions. Several kinds of *trans*-acting cellular factors which interact with the HCV IRES, core protein sequences or the 3′-UTR and which possibly affect IRES-mediated translation activity have already been found up to now. As detailed in the introduction, these factors include the 52 kDa human La autoantigen, the 57 kDa polypyrimidine tract-binding protein (PTB), some ribosomal proteins, poly(rC)-binding proteins 1 and 2 (PCBPs), heterogeneous nuclear ribonucleoprotein L (hnRNP L), eukaryotic translation initiation factor eIF3 and NS1-associated protein 1 (NSAP1). Among these factors, the interaction of PTB with the HCV IRES and the exact role of it in HCV IRES-mediated translation are controversial, whereas hnRNP L had been previously reported to interact only with sequences at the beginning of the HCV polyprotein, not with the end of the viral genome, while the interaction of Unr with HCV RNA had not yet been investigated at all.

4.1.1 PTB

For the picornaviruses, it has been clearly reported that PTB binds to the internal ribosome entry site in several viruses, such as poliovirus (PV) (Hellen et al., 1993; Hellen et al., 1994), human rhinovirus (HRV) (Borman et al., 1993), encephalomyocarditis virus (EMCV) (Borovjagin et al., 1994), foot-and-mouth disease virus (FMDV) (Niepmann, 1996) and hepatitis A virus (HAV) (Chang et al., 1993), and is involved in the cap-independent protein translation facilitated by the IRES elements.

In this study, the possible binding of PTB to the HCV RNA, either the 5′-UTR or the 3′-UTR alone, or the two regions in combination has been investigated. The results presented here show that PTB does not bind to the HCV 5′-UTR region, and is also not functionally required for internal initiation of translation when the IRES is used in the absence of the 3′-UTR.

A conserved feature found in all 5′-UTRs of picornavirus RNAs is the presence of a pyrimidine tract followed by an AUG triplet, the so-called Yn-Xm-AUG motif (Beck et al., 1983; Wimmer & Nomoto, 1993). Extensive studies on the pyrimidine tract by deletions and point mutations have demonstrated that this motif is essential for picornavirus IRES function, and the pyrimidine tract must be properly spaced from the AUG triplet for maximal efficiency of translation (Jang & Wimmer, 1990; Kühn et al., 1990; Meerovitch et al., 1991; Pilipenko et al., 1992). As mentioned before, the HCV 5′-UTR contains three independent pyrimidine-rich motifs (see Fig. 66B): site I is located from nucleotide (nt) 40 to 46 (Py-I); site II includes a helical structure encompassing nt 120 to 130 (base-paired partially with nt 318 and 323 located in the vicinity of initiator AUG) (Py-II), and site III resides in nt 191 to 199 in the apical loop of the biggest domain III (Py-III). Additional features around all three polypyrimidine-rich tracts include a stem-loop and a single-stranded region followed by a second stem-loop. However, their exact structural and sequence features do not match the requirements which were found for PTB binding with the EMCV IRES (Witherell et al., 1993; Kolupaeva et al., 1996). Witherell and co-workers suggested, on the basis of their detailed examination of the sites for PTB binding, that a common feature for strong PTB binding includes a helix–ss(single-stranded) RNA–helix motif which contains small U-rich single-stranded bulges or loops linking two helices (Witherell et al., 1993; Witherell & Wimmer, 1994). In the HCV IRES, however, these structural requirements are not fulfilled, a reason why PTB does not bind to the HCV IRES. In contrast, the oligopyrimidine tracts in the HCV IRES have other functions.

Functional studies have shown that deletion of the Py-I may strikingly reduce the functional activity of the HCV IRES (Wang et al., 1993), and an anti-sense oligonucleotide directly against the Py-I sequence blocked HCV RNA translation (Wakita & Wands, 1994). These observations support the functional importance of this 5′ upstream region. In fact, this region has been later verified as the exact 5′-border of the HCV IRES (Honda et al., 1999). The second pyrimidine tract (Py-II) contains a highly-ordered secondary and tertiary structure. Further biochemical and genetic analysis supports evidence for a pseudoknot structure in this region. Disruption of this helical interaction resulted in a dramatic reduction in translation initiation. Compensatory mutants maintaining the base substitutions in this pyrimidine tract and restoring the helical structure regained efficient translation (Wang et al., 1995a), arguing for a more structural role of this sequence. The third pyrimidine-rich motif, Py-III, located in the apical loop of the largest domain III, is somehow characteristic of the pyrimidine-rich sequence motif Yn-Xm-AUG. However, this feature did not coincide with binding of PTB to the HCV IRES in this work, which is consistent with some other observations (Kaminski et al., 1995; Ito & Lai, 1999), but opposite to another report (Ali & Siddiqui, 1995). Accordingly, mutations in this Py-III tract and the relevant downstream AUG do not result in a decrease in translation efficiency (Wang et al., 1994). Most likely, the apical loop of the stem-loop III is involved in binding of eIF3 and thus is not available for binding of PTB.

Fig. 66 is an attempt to explain as far as possible why PTB does not bind to the HCV IRES even though there are three pyrimidine-rich motifs within the HCV 5′-UTR. According to the structure of the sequence-specific RNA-binding domains III and IV of PTB (Yuan et al., 2002), the ideal structure of the RNA to be bound should contain a small apical loop rather than a larger, more flexible structure (Nagai et al., 1995a; Nagai et al., 1995b). The typical motif for PTB-binding is UCUU located in the apical loop of the RNA secondary structure, like in the stem-loops 2 and 4 of FMDV (Fig. 66D) and in the stem-loop 3 within the HCV 3′-UTR (Fig. 66C). These three stem-loops all have a small loop: the number of bases is ≤ 7. Moreover, the base Uracil is predominant in these loops. In contrast, the three polypyrimidine-tracts in the HCV 5′-UTR do not meet these structural requirements. In Py-I and Py-II, the sequences are too long single-stranded regions, and they contain too many Cytosines. Py-III has a typical UCUU sequence in single-strand apical loop (Fig. 66B), but the loop is too large

compared with the other PTB-binding loops of both the FMDV and the 3´-UTR. Presumably, a tight small loop structure is required for the accurate recognition by PTB so that the loop of the RRM domain (Fig. 66A) can properly protrude into the RNA loop, facilitating recognition of bases in the loop by the conserved ribonucleoprotein (RNP) motif amino acid residues in the four- or five-strand β-barrel surface of the RRM domains (Nagai et al., 1995a; Nagai et al., 1995b).

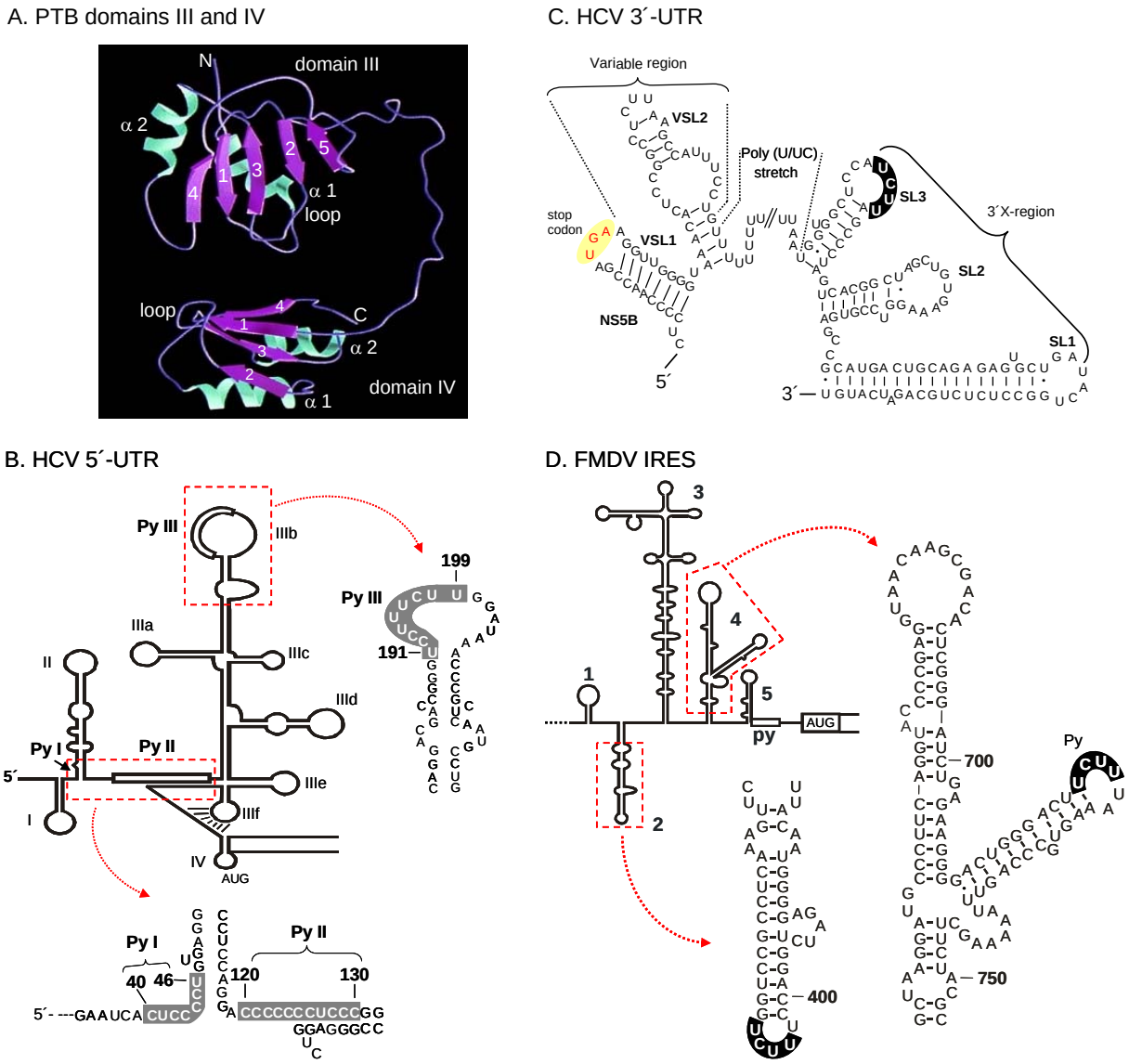

Fig. 66: Proposed structural requirements for the binding of PTB to the viral RNAs. (A) The structure of the PTB domains III and IV (Yuan et al., 2002). The conserved ribonucleoprotein (RNP) β-strand motifs and α-helices are coloured purple and light green, respectively. The loops between the two middle β-strand sheets are supposed to hook into the apical loop of the RNA. **(B)** The locations of the three pyrimidine-tracts within the HCV 5´-UTR. **(C)** The binding sites for PTB in the HCV 3´-UTR. **(D)** The binding sites for PTB within the FMDV IRES.

Although two reports on interaction of PTB with the HCV IRES have produced positive results by either UV cross-linking assay (Ali & Siddiqui, 1995) or electron microscopy with gold-labelled PTB (Beales et al., 2001), several attempts in this work to show binding of PTB to the HCV IRES in different lysates failed, even though various deletion mutants of the 5´-UTR were used (Fig. 12). Initially it was suspected that the failure of detection of PTB binding to the HCV IRES might be just due to a failure in label transfer from RNA to protein. However, negative results were still obtained when different radioactive nucleotides were used for labelling the HCV IRES RNA (Figs. 15 and 16). Thus, it can be concluded that PTB does not directly interact with the HCV IRES of the genotype 1b used in this study.

In addition, potential PTB binding sites have been discovered in the HCV core gene (Ito & Lai, 1999), in the poly (U/C) stretch of the 3´-UTR (Luo, 1999), and in the stem-loops 2 and 3 within the 3´ X-region (Ito & Lai, 1997; Tsuchihara et al., 1997). Among these, the region located in the 3´-end of the core-encoding sequence was found to down-regulate HCV translation by PTB binding (Ito & Lai, 1999). Several conflicting studies demonstrated either stimulating (Ali & Siddiqui, 1995; Anwar et al., 2000; Gosert et al., 2000) or inhibitory (Murakami et al., 2001; Tischendorf, 2004) effects of PTB on HCV IRES-dependent translation *in vitro* or *in vivo*, leaving a possible role of PTB in HCV IRES-dependent translation still controversial. In this work, PTB has been unambiguously shown to bind specifically to the HCV 3´-UTR by the RNA gel shift assay and by the UV cross-linking assay, and in another Ph.D. thesis work in our lab, it was shown that PTB stimulates HCV translation in the presence of the 3´-UTR (E. Tzima, Ph.D. thesis, 2005, Giessen University).

4.1.2 hnRNP L protein

In 1989, an unusual heterogeneous nuclear ribonucleoprotein, named L (hnRNP L), was found (Pinol Roma et al., 1989). UV cross-linking assays in intact HeLa cells showed that hnRNP L is an hnRNA-binding protein. It was shown that hnRNP L binds a *cis*-acting RNA sequence in the pre-mRNA derived from the herpes simplex virus thymidine kinase (HSV-TK) gene, and this RNA-protein interaction enabled proper RNA processing and accumulation of intron-independent pre-mRNAs (Liu & Mertz, 1995). Later, two cytoplasmic functions of hnRNP L were characterized. One study found that hnRNP L binds to the 3´ border region of the HCV IRES, and the binding of hnRNP L to HCV IRES might correlate with the translational efficiency of the HCV RNAs (Hahm et al., 1998b). A stretch of HCV core protein-encoding sequence of at least 33 nucleotides is required for efficient binding of hnRNP L and perhaps for translation activity (Hahm et al., 1998b), consistent with the observation that the 3´ boundary of the HCV IRES reaches into the core protein-encoding region (Reynolds et al., 1995). These additional sequences contain many CA-repeat sequences which have been shown to be specific binding sites for hnRNP L (Hui et al., 2003). However, no direct evidence had been further provided for a possible role of hnRNP L in HCV translation.

In another study, hnRNP L was shown to interact with PTB, an interaction which can be speculated to play a functional role in pre-mRNA splicing and mRNA transport (Hahm et al., 1998a). The interaction of PTB with hnRNP L was first identified by yeast-two-hybrid screening and then confirmed by biological methods. The binding of PTB to hnRNP L was found to be a direct protein-protein interaction in the yeast cell, and the N-terminal half of PTB (Amino Acid 1-329, domain I-II) and most of the hnRNP L protein (AA 141-558, domain II-IV) are involved in the interaction between PTB and hnRNP L (Hahm et al., 1998a). This result implicates that the domain I and II of PTB should be mainly responsible for this protein-protein interaction.

In this work, hnRNP L was found to interact with the HCV IRES but not with the 3´-UTR by RNA gel shifts and UV cross-linking assays (Figs. 30 and 32). At the same time, it was confirmed that hnRNP L is not localized in the cytoplasm but mainly in the nucleoplasm (Fig. 31), rendering cytoplasmic cell extracts suitable for supplementation with recombinant hnRNP L to yield a functional reconstitution system.

Furthermore, it was found that binding of PTB to the HCV IRES plus 3´-UTR RNA or to the 3´-UTR RNA was enhanced by the presence of hnRNP L (Fig. 38), and increasing amounts of hnRNP L resulted in a further increase in PTB binding. Surprisingly, the HCV 3´-UTR, which is supposed to contain no binding site for hnRNP L alone, was also clearly shown to be bound by hnRNP L in the presence of PTB (Fig. 38, lanes 10-12). Correspondingly, a similar effect was also observed with the HCV IRES only RNA. Only in the presence of hnRNP L, PTB binds to the IRES (Fig. 38, lanes 2-4). These results imply that there is a synergistic interaction of PTB and hnRNP L with the HCV RNA when both proteins are present.

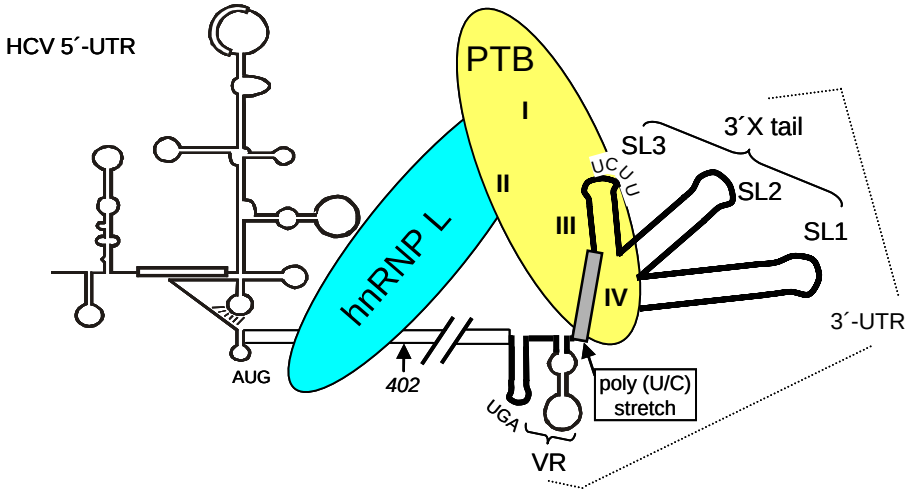

Fig. 67: Hypothetical model of interaction of hnRNP L with PTB in binding to the HCV combination RNA. The typical binding site UCUU for PTB located in stem-loop (SL) 3 of the 3´-X tail is indicated (see also Fig. 66). hnRNP L binds to the HCV core protein-encoding sequences upstream of nucleotide 402. The roman numbers in the PTB protein indicate its four domains. The authentic start and stop codons (AUG and UGA) are also indicated. The interaction of hnRNP L with PTB may stabilize the binding of PTB to the 3´-UTR. VR, variable region of the 3´-UTR.

To better understand which domain of PTB is responsible for a possible interaction of hnRNP L with PTB during their interactions with the HCV RNA, all deletion mutants of PTB (shown in Fig. 26) were included in the assay together with hnRNP L. The results shown in Fig. 39 not only confirm the stimulating effect, but also show different roles of different PTB RRM domains in the interaction with the RNA. Deletion of PTB domain I, II, or I and II together does not affect the strong binding of PTB to the HCV RNA because of the presence of domain III and IV (Figs. 39, lanes 5-16). These results are consistent with the binding of PTB domains to the IRES of FMDV (Song et al., 2005). However, this result obviously is not consistent with the former observation that domains I and II together are required for the interaction of PTB with hnRNP L (Hahm et al., 1998a). This discrepancy may have the reason that the presence of RNA-protein interactions may facilitate the protein-protein

interaction. Therefore, this mutual interaction may stabilize and strengthen the interaction of PTB with the 3´-UTR as illustrated in Fig. 67. Moreover, a PTB-hnRNP L complex may have an RNA-binding specificity different from PTB and/or hnRNP L alone. Nevertheless, the results shown here unambiguously demonstrate that hnRNP L stimulates the binding of PTB to the HCV RNA, suggesting that a PTB-hnRNP L interaction may be somehow involved in HCV translation initiation. Further experiment will be necessary to investigate in more detail the interaction of hnRNP L and PTB with the HCV RNA *in vitro*.

After analyzing the role of PTB and hnRNP L *in vitro*, they were tested together in the HCV IRES-directed translation system using two HCV RNAs with or without 3´-UTR. It was shown that HCV translation efficiency was evidently not affected in the presence of hnRNP L, irrespective if the 3´-UTR was present or not, in either RRL or PTB-depleted RRL (Fig. 33). Under the same experimental conditions, increasing amounts of recombinant PTB were added to the PTB-depleted RRL, but HCV translation efficiency was not altered by the presence of both PTB and hnRNP L (Fig. 43). The FLuc expression from the HCV RNA with 3´-UTR is only slightly higher (maximal ~ 70 %) than that from the HCV RNA minus 3´-UTR in the presence of hnRNP L added. However, this minor difference is also detected only in the absence of hnRNP L. Thus, HCV translation is not significantly affected by PTB and hnRNP L, individually or together, in the *in vitro* assay used here. However, in *in vivo* experiments using transfection of reporter and effector RNAs into Huh-7 cells, it was shown that PTB and hnRNP L act together, resulting in a slight stimulation of HCV IRES-directed translation in the presence of the 3´-UTR (E. Tzima, Ph.D. thesis, 2005, Giessen University).

4.1.3 Unr protein

The Unr gene (upstream of *N-ras*) is defined as a transcription unit encoding a protein with five copies of the cold-shock domain (CSD), located immediately upstream of the *N-ras* gene in several mammalian genomes (Doniger & DiPaolo, 1988; Jeffers et al., 1990; Nicolaiew et al., 1991). Unr has been identified as one of two proteins (the other being PTB) which binds to the human rhinovirus-2 (HRV-2) 5´-UTR and stimulates rhinovirus translation (Hunt et al., 1999a). All five cold-shock domains of Unr have been reported to be required for stimulation of human rhinovirus translation (Brown & Jackson, 2004).

Several of the genes whose protein products are associated with apoptosis contain IRESes, including XIAP (Holcik et al., 1999), DAP5 (Henis-Korenblit et al., 2000), c-*myc* (Stoneley et al., 1998; Stoneley et al., 2000) and Apaf-1 (Coldwell et al., 2000), and can therefore be translated in a cap-independent manner. A former report demonstrates that both Unr and PTB stimulate internal ribosome entry on the Apaf-1 IRES *in vitro* (Mitchell et al., 2001). Moreover, in cell lines that lack these proteins or have reduced levels of them, internal ribosome entry mediated by the Apaf-1 IRES can be stimulated by co-transfection of plasmids encoding these factors.

To address the question whether Unr interacts directly with the HCV RNA, electrophoretic mobility shifting assays and UV cross-linking assays were carried out using purified recombinant His-Unr protein. The shift experiments show that Unr does not bind to HCV IRES at all, but binds well to the HCV 3´-UTR, with a K_d value in the range of 30 nM (Fig. 34B). On the contrary, Unr was detected to bind to the HCV IRES in the absence of other proteins in the UV cross-linking assay (Fig. 35A). Even though tRNA was present in the reaction, the binding signals were clearly detected. In reticulocyte lysate, however, binding of Unr could not be detected. It can only be speculated that Unr binding is easily competed by other proteins. By mass spectrometry-based peptide sequencing, another group has found that as many as 26 proteins can bind to the HCV IRES RNA

but not to a reversed-complementary sequence RNA (Lu et al., 2004). Among these proteins, Unr and Unr-interacting protein (UNRIP) were identified. However, these researchers did not explore functional implications of this binding for translation.

In *in vitro*-translation assays, Unr showed down-regulatory effect on HCV IRES-dependent translation in both normal RRL and PTB-depleted RRL supplemented with recombinant PTB (Figs. 36 and 44B). However, it must be assumed that this inhibitory effect may be due to the fact that this Unr protein was prepared under denaturing conditions from E. coli cells, and it is not known which portion of the protein is in an authentic native state and if remaining denatured protein may unspecifically inhibit translation. Thus, unfortunately, no valid conclusion can be drawn from these *in vitro* experiments using recombinant Unr protein.

However, promising observations were obtained by our cooperation partner in France. Mouse embryonic stem (ES) cells and Unr knock-out ES cells were transfected using two HCV plasmid constructs, either with or without 3´-UTR, respectively (Fig. 45). Their result shows that the FLuc expression levels from the HCV plasmid without 3´-UTR changed only slightly upon Unr knout-out ES cells. However, a larger difference was detected when the HCV plasmid with 3´-UTR was used for the transfection (Table 7). In the presence of the 3´-UTR the FLuc translated activity obtained with the HCV IRES in Unr -/- ES cells is lower (< 50 %) compared with that in Unr +/+ ES cells. Thus, the presence of Unr makes a difference when the HCV 3´-UTR is present.

ES cells	unr +/+	unr -/-
HCV-- 3´UTR	100 %	85 %
HCV-+3´UTR	100 %	49 %

Table 7: Expression levels of HCV reporter constructs with or without 3´-UTR in ES-cells *in vivo*. The values of *Firefly* luciferase activities are set to 100 % in normal ES cells. Unr -/-, Unr knock-out embryonic stem (ES) cells; Unr +/+, normal ES cells (Results from Dr. Hélène Jacquemin-Sablon, Bordeaux, France).

Taken together, purified recombinant Unr protein seems not suitable for functional in vitro studies, and more cell transfection-based experimental approaches may be used to elucidate a possible function. Indeed, transfection studies (E. Tzima, Ph.D. thesis, 2005, Giessen University) support evidence that Unr and PTB may synergistically stimulate HCV translation in the presence of the 3´-UTR to a certain extent, a finding that would be consistent with the Unr knock-out ES cell experiments mentioned above.

4.2 The HCV 3´-UTR strongly enhances the IRES-dependent translation

At least four distinct elements have been suggested to regulate HCV RNA translation:

Firstly, the sequences of the HCV IRES within the 5´-UTR are required for translation. Indeed, some mutations resulted in dramatic changes in IRES activity (Wang et al., 1994; Kamoshita et al., 1997; Collier et al., 1998; Honda et al., 1999; Laporte et al., 2000; Lerat et al., 2000). Actually, it would be better to say that the secondary and tertiary structures are as important as some primary sequences within the 5´-UTR region for IRES activity.

Secondly, *in vitro* studies from several groups suggested that cellular proteins (such as PTB, hnRNP L and La) can slightly stimulate HCV translation (Ali & Siddiqui, 1997; Hahm et al., 1998b; Ito & Lai, 1999; Anwar et al., 2000). One group reported a slight stimulation by PTB *in vivo* system (Gosert et al., 2000). However, it is shown in this work that PTB and hnRNP L do not have positive effect on HCV IRES-directed translation *in vitro*, and PTB does not even bind to the HCV IRES at all.

Thirdly, HCV proteins have been described to affect HCV IRES efficiency. Because of its particularity of promoting persistent infection, HCV has been suggested to possess a self-modulating mechanism to maintain a low level of replication. Therefore, it can be assumed that viral protein(s) might modulate a balance between the three key steps of the viral life cycle: translation, replication, and packaging. Some of these proteins have been proposed to influence HCV IRES activity, such as the core protein and several non-structural proteins. However, the results are rather inconsistent. For example, HCV core protein (HCV-C) was reported to either inhibit or stimulate translation (Shimoike et al., 1999; Zhang et al., 2002; Boni et al., 2005); the non-structural proteins NS4A and NS4B were shown to decrease HCV IRES translation (Kato et al., 2002), whereas others reported a stimulatory effect of translation by NS4B and NS5A (He et al., 2003).

Finally, the 3´-X region of the HCV genome has been shown to enhance IRES-dependent translation weakly (Ito et al., 1998; Michel et al., 2001), although the mechanism for this enhancement has not been elicited yet and remains controversial. From the results presented in this thesis, it must be concluded that the entire 3´-UTR, but not only 3´-X region, is involved in HCV IRES-dependent translation.

Most eukaryotic cellular mRNAs and many viral mRNAs have a cap structure at the 5´ terminus and a poly(A) tail at the 3´-end which play essential roles in the regulation of translation, either individually or in concert (Hentze, 1997; Sachs et al., 1997). Each of them works by associating with specific RNA-binding proteins, and together they function synergistically to stimulate translation. The translation initiation factor eIF4F binds to the 5´-terminal cap structure of cellular mRNA through its subunit eIF4E, and the poly(A) binding protein (PABP) facilitates mRNA 5´-3´ end interaction by binding both to the mRNA poly(A)-tail and to the eIF4G subunit of eIF4F (Tarun & Sachs, 1996). This concept of RNA 5´-3´ end interaction for translation stimulation could be also applied to the HCV RNA genome, even in the absence of the terminal cap and poly(A) structures. Such an interaction of the terminal HCV genome structures, possibly facilitated by yet unknown viral and/or cellular proteins, could play a role in a switch from HCV translation to minus-strand RNA synthesis during the viral life cycle, similar to the switch that has been reported for poliovirus (Gamarnik & Andino, 1998).

As a first step towards testing this hypothesis, it is necessary to explore if the HCV 3´-UTR affects IRES-directed translation at all. Up to present, several groups have investigated a possible modulating effect of the HCV 3´-UTR on translation directed by the HCV IRES either *in vitro*, in cell culture or *in vivo* in transfected livers of mice (Table 8). In some studies, a positive influence of 3´-UTR sequences (sometimes comprising only the 3´-X region) was shown (Ito et al., 1998; Ito & Lai, 1999; Michel et al., 2001; McCaffrey et al., 2002) whereas others showed that the HCV 3´-UTR has no stimulatory influence on HCV IRES-directed translation (Fang & Moyer, 2000; Friebe & Bartenschlager, 2002; Kong & Sarnow, 2002; Imbert et al., 2003; Yi & Lemon, 2003a). One study even reported an inhibitory effect of the 3´-UTR (Murakami et al., 2001).

	in vitro	extract	*in vivo*	cells	nucleic acid transfected	topology	Expression cassette(s)	3´-UTR or 3´X	precise 3´-end?
Ito et al., 1998, J. Virol.	**2-5 x**	RRL	**2-5 x**	Huh-7	DNA	linearized	Mono/dicistronic	X	No
Ito et al., 1999, Virol.	**5 x**	RRL					monocistronic	X	No
Michel et al., 2001, Mol Cell Biol	**3 x**	RRL					monocistronic	X	No
Murakami et al., 2001, Arch. Virol.	**--**	RRL					monocistronic	UTR	No
Fang et al., 2000, J. Hepatol.	0	HeLa, HepG2					monocistronic	UTR	No
McCaffery et al., 2002, Mol. Ther.	0	RRL	**5-10 x**	HeLa, mice	DNA	linearized	monocistronic	UTR	No
Kong et al., 2002, J. Virol.			0	Huh-7, non-liv.	DNA	linearized	monocistronic	UTR	No
Imbert et al., 2003, J. Gen. Virol.			0	Huh7, HepG2, Hep3B, 293	DNA	circular	dicistronic	UTR	No
Friebe et al., 2002, J. Virol.			0	Huh-7	RNA		dicistronic	UTR	√
Yi & Lemon, 2003, J. Virol.			0	Huh-7	RNA		dicistronic	UTR	√
this study	0	RRL	**10-20x**	Huh-7, HepG2	**RNA**		**monocistronic**	**UTR**	√

Table 8: Previous reports on a possible role of the HCV 3´-UTR in IRES-dependent translation. In the table, 0 stands for no influence of 3´-UTR on translation; "--" represents down-regulation of translation by 3´-UTR; RRL, rabbit reticulocyte lysate; non-liver, non-liver cell line.

In an attempt to clarify this confusing situation, it was shown here that reporter construct design is an important parameter in experiments testing 3´-UTR function. By employing transfection of monocistronic reporter RNAs with precise 3´-ends into a human liver-derived cell line, it is shown in this study that all three sequence elements of the HCV 3´-UTR, the variable region, the poly(U/C)-tract and the highly conserved 3´-X region, contribute to efficient translation activity. In particular, efficient translation stimulation depends strictly on a precise 3´-terminus of the HCV 3´-UTR (Fig. 51). The presence of additional nucleotides at the 3´-end of the HCV 3´-UTR disables its translation enhancer function (Fig. 55). This fact may be a reason why many of the previous studies did not detect translation stimulation by the 3´-UTR since they used either circular plasmid DNA or plasmids linearized not exactly at the HCV 3´-end (Fang & Moyer, 2000; Kong & Sarnow, 2002; McCaffrey et al., 2002; Imbert et al., 2003). Moreover, nuclear processing such as capping, splicing and polyadenylation of cellular polymerase II transcripts may have profound effects on their biological activity, consistent with our observation that translation stimulation by the 3´-UTR is much stronger when RNA rather than DNA is used for transfection (Figs. 49-51). The requirement for a precise 3´-end of reporter constructs is also strikingly obvious from the observation of the group of S. Lemon that an *in vitro*-transcribed replicon RNA with additional nucleotides at the 3´-terminus regained the original HCV 3´-end by the loss of these additional nucleotides after transfection into cells and replication passages (Yi & Lemon, 2003a). The second study using precise reporter RNA ends (Friebe & Bartenschlager, 2002) showed that mutations in the 3´-UTR affect replication but not translation. However, these researchers generated a precise 3´-end of the replicon template DNA by introducing a mutation in the 3´-terminal stem-loop sequence to generate a *Sca* I recognition sequence, and we do not know if this mutation may hamper a possible stimulatory effect on translation in the replicon reporter construct used, even if these exchanges maintain stem-loop structure and have been observed in a natural HCV 3b isolate (Yamada et al., 1996). According to the observations that have been previously reported (Fang & Moyer, 2000; Friebe & Bartenschlager, 2002; Yi & Lemon, 2003a) and also here, no evidence was

found that deletions within the 3´-UTR accelerate the degradation of synthetic HCV RNA transcripts by exoribonucleases after transfection (Fig. 58). Thus, the negative impact of deletions within this segment of the viral RNA is likely to result from the loss of an essential RNA signal that participates in translation.

Another common feature of those previous studies reporting a positive enhancement of HCV translation by the 3´-UTR (Ito et al., 1998; Ito & Lai, 1999; Michel et al., 2001; McCaffrey et al., 2002) is that they used monocistronic reporter constructs. In contrast, those studies which did not observe translation stimulation (Friebe & Bartenschlager, 2002; Yi & Lemon, 2003a) used dicistronic reporter constructs employing an additional (picornavirus) IRES element to drive translation of HCV nonstructural proteins. It is known from experiments in our lab (Bassili et al., 2004; C. Jünemann, unpublished results) that a second IRES element in a reporter construct can influence the activity of the first reporter gene in *cis* and by that conceal a modulating effect of the 3´-UTR. In addition, the time at which reporter gene activity is measured may be a relevant parameter. It was found that transfection of PCR fragments resulted in a significant difference (up to 3-fold) early after transfection (8 to 12 hrs), whereas the differences were reduced after longer times. In some other studies (Kong & Sarnow, 2002; Imbert et al., 2003), cells were harvested after longer times, which may be another reason to miss significant differences in expression.

Another important aspect of the involvement of the 3´-UTR in translation stimulation is that it may confer at least a certain degree of tissue specificity. HCV replicates preferentially in human hepatocytes (Lauer & Walker, 2001), and the viral infection often results in chronic diseases such as liver cirrhosis and hepatocellular carcinoma, suggesting that the liver cell may provide factors particularly supporting HCV translation and/or RNA replication. A cell-specific advantage for HCV replication in liver cells could be conferred by *trans*-acting proteins binding to the 3´-UTR, subsequently resulting in translation enhancement mediated by an RNA 3´-5´-end interaction in *cis*. Even though a certain degree of translation stimulation by the 3´-UTR was reported also in non-liver-derived systems like rabbit reticulocyte lysate (Ito et al., 1998; Ito & Lai, 1999; Michel et al., 2001) and HeLa cells (McCaffrey et al., 2002), it was observed in this study that the translation enhancing effect of the 3´-UTR is much stronger in Huh-7 or Hep G2 cells than in HeLa or BHK cells. Thus, it can be assumed that as yet unknown proteins present in human liver-derived cells in higher amounts than in non-human liver-derived cells may be involved in an HCV RNA 3´-5´-end interaction. This notion is consistent with the finding that HCV can replicate in HeLa cells only with very low efficiency, while efficient replication in selected HeLa cell clones requires adaptive mutations in the non-structural protein coding region (Zhu et al., 2003). Therefore, it is of considerable importance to explore the role of possible liver cell-specific factors in HCV translation.

Based on the observation that PTB stimulates translation of several picornaviruses (Borman et al., 1993; Kaminski et al., 1995; Niepmann et al., 1997), it was speculated if PTB is also involved in the regulation of HCV translation. However, the results with the HCV IRES were controversial (Ali & Siddiqui, 1995; Kaminski et al., 1995; Ito & Lai, 1999; Tischendorf, 2004). Furthermore, studies exploring a possible role of the HCV 3´-UTR in HCV translation revealed that PTB binds to the poly(U/C)-tract within the 3´-UTR (Tsuchihara et al., 1997; Chung & Kaplan, 1999; Gontarek et al., 1999; Ito & Lai, 1999; Luo, 1999). However, no clear evidence for a stimulation of 3´-UTR-mediated HCV translation by PTB was found, although Gosert and co-workers (Gosert et al., 2000) reported the stimulatory effect of PTB on HCV translation *in vivo*. PTB is also present in many non-liver tissues like reticulocytes and HeLa cells (Borman et al., 1993; Kaminski et al., 1995), suggesting that the mere presence of PTB is not sufficient to explain tissue-specific expression of HCV.

The *cis*-acting signals in the 3´-UTR were found to be involved in translation regulation partially coincide with the signals required for RNA replication (i.e., the initiation of viral minus-strand synthesis) (Yanagi et al., 1999;

Kolykhalov et al., 2000; Friebe & Bartenschlager, 2002; Yi & Lemon, 2003a, 2003b). All three elements, the variable region, the poly(U/C)-tract and the 3´-X region appear to contribute to both processes, replication and translation stimulation. Oh et al. have shown that the 3´-UTR is required for specific recognition of genome-length RNA by a purified NS5B RNA dependent RNA polymerase *in vitro*. Furthermore, the *de novo* synthesis of genome-length, negative-strand RNA in this *in vitro* system was associated with the binding of NS5B to sequences within the 3´ X-region, the poly(U/UC) tract, and the NS5B-coding sequence (Oh et al., 1999; Oh et al., 2000). However, modifications affecting the variable region have less serious effects on replication efficiency (Yanagi et al., 1999; Friebe & Bartenschlager, 2002; Yi & Lemon, 2003a). Moderate modifications of pyrimidine-tract length are tolerated to a certain extent, but at least a certain minimal length of the poly(U/C)-tract is absolutely required for RNA synthesis. Of the three highly conserved stem-loop structures of the 3´-X region, the stem-loop 2 moderately contributes to translation enhancement, while the stem loop 3 contributes only very slightly. In contrast, for replication (i.e., RNA minus-strand synthesis), both stem-loop 2 and 3 are essential. Also the most 3´-terminal stem-loop 1 is required for RNA synthesis (Friebe & Bartenschlager, 2002; Yi & Lemon, 2003a, 2003b), matching the obvious requirement for a contact of the viral RNA replication machinery with the very 3´-end of the viral RNA genome which is the template for synthesis of the negative strand replicative intermediates.

Furthermore, the 5´-proximal domains I and II of the 5´-UTR have been shown to be essential for replication while sequences lying further downstream within the 5´-UTR and comprising domain III may help to facilitate replication but are not absolutely required (Friebe & Bartenschlager, 2002; Kim et al., 2002). These results suggest an interesting symmetry in the 5´and 3´ terminal RNA signals for both translation and replication. Such a notion is strengthened by the suggestion that the 3´-ends of the negative- and positive-strand RNAs may share common structural features (Schuster et al., 2002).

In many studies on replication, the read-out for monitoring HCV replication after transfection of modified replicon RNAs into cells is the amount of newly synthesized RNA minus strands (or the indirect measurement of their biological activity). Accordingly, this read-out usually also includes the initial translation of the transfected replicon RNA. For future studies, it may be interesting to investigate both aspects in monocistronic reporter systems, using separate read-outs to dissect the effects of mutations in the 3´-UTR on translation and on RNA minus strand synthesis. Nevertheless, the finding in this study that the 3´- terminal stem-loop 1 is an important determinant for translation enhancement points to the idea that this stem-loop may be involved in the regulation of a switch from translation of the viral RNA genome to RNA minus strand synthesis like it was shown for poliovirus (Gamarnik & Andino, 1998). This process may require long-range RNA-RNA interactions and even genome circularization, involving RNA sequences and/or secondary structures not only in the 3´-UTR but also in the NS5B coding region and in the 5´-UTR as well as viral proteins like the NS5A and NS5B polymerase moieties (Luo, 1999; Friebe & Bartenschlager, 2002; Lee et al., 2004; Thurner et al., 2004; You et al., 2004; Friebe et al., 2005).

Very recently, a novel RNA element in the 3´ terminal coding sequence of NS5B that is essential for the viral RNA replication was discovered (Lee et al., 2004; You et al., 2004; Friebe et al., 2005). By using computer-based secondary structure prediction and enzymatic and chemical probing, these groups identified the very same RNA element in the NS5B coding region. Moreover, they also found that only the stem-loops (SLs) in close proximity to the 3´-end of the ORF are essential for RNA replication. The location at the 3´-end of the ORF could facilitate the binding of newly synthesized NS5B in order to initiate negative-strand RNA synthesis which may then interfere with translation. Friebe et al. found that the sequences in NS5BSL3.2, the second loop from

the 3´-end of the viral ORF are critical for viral RNA replication. More importantly, they have discovered that there is a nucleotide sequence complementarity between the stem-loop of 5BSL3.2 and the loop region of stem-loop 2 within the extremely conserved 98-nt X tail, the very 3´-end region of HCV RNA genome. Mismatches introduced into the loops inhibited RNA replication, which could be rescued when complementarity was restored (Friebe et al., 2005). This special interaction stabilizing an RNA conformation within the 3´ terminal region of the viral genome was named a "kissing-loop" structure. Based on their observations, the authors assumed that this kissing-loop interaction could be mediated by viral or host cellular proteins. Some proteins have been reported to bind to the 3´-UTR, including PTB which binds to SL2 and SL3 in the X-tail and to the poly(U/UC) tract (Tsuchihara et al., 1997; Luo, 1999), autoantigen La (Spangberg et al., 1999a), and several ribosomal proteins (Wood et al., 2001). However, the role of these proteins for HCV RNA replication or possibly translation has not been studied. Although they did not analyze in detail the effects of the mutations in NS5BSL3.2 on RNA translation, they found that even altered 5BSL3.2 sequences that disturbed the RNA structure still allowed expression of a functional NS5B, while the insertion of the intact version of 5BSL3.2 into the variable region rescued RNA replication. Consistently also, You and co-workers (You et al., 2004) reported no significant differences in the expression of viral proteins from the wild-type and NS5BSL3.2 mutants *in vitro*.

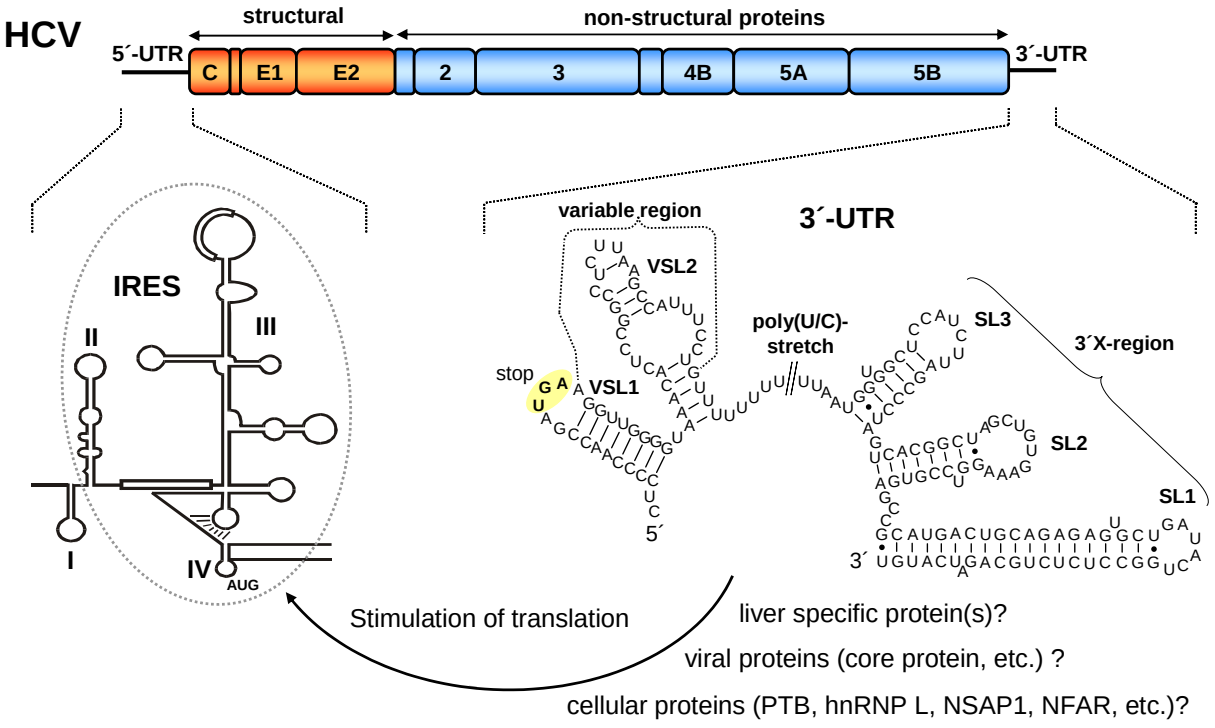

Fig. 68: HCV translation is enhanced by the 3´-UTR. Most likely, viral and/or cellular proteins which remain to be determined are involvement in translation stimulation.

In the closely related bovine viral diarrhoea virus (BVDV), the sequence and secondary structures of the RNA signals in the 3´-UTR are quite different from that in the HCV 3´-UTR. The two conserved stem-loops of BVDV that are located most 3´-terminal are required for RNA minus-strand synthesis (Yu et al., 1999). Cellular proteins binding to the 3´-UTR of the closely related pestivirus BVDV were identified and shown to be required for RNA replication (Isken et al., 2003). These proteins belong to a class of nuclear factors that appear to bring about a

circular conformation of BVDV genome via interactions with the 3′- and the 5′-UTR. In contrast, the upstream variable region binds nuclear factors associated with RNA (NFAR) and may be involved in a switch between translation and replication (Isken et al., 2003; Isken et al., 2004).

Extending this idea to the situation with HCV, it will be interesting to determine whether the NFAR proteins are involved in such a switch through interaction with the kissing-loop in the HCV genome. Consequently, several questions arise: (i) are factors such as the NFAR group proteins involved in HCV translation enhancement by mediating long-range interactions between the 3′- and the 5′-UTR; (ii) are there synergistic interactions of NFAR proteins with other proteins binding to the 3′-UTR or with NSAP1 binding near the 5′-UTR (Kim et al., 2004); and (iii) are there factors in human liver-derived cells that confer at least a certain degree of tissue specificity to HCV translation by interacting preferentially with the 3′-UTR rather with the 5′-UTR? (Fig. 68).

At last, previous reports that have described the 3′-UTR enhancement of HCV translation have generally used short reporter constructs that do not contain the significant RNA structure present with the core or NS5B coding regions. Thus, it is questionable if this stimulatory effect obtained *in vitro* reflects the authentic situation. To demonstrate that the findings shown here are biologically relevant, it should be shown that translation of the HCV genome-length RNA is similarly affected by the presence or absence of the 3′-UTR sequences. Thus, the long-standing debate on this issue may be eventually settled after such studies are done. For that reason, the corresponding work will be continued using the HCV full-length genome of genotype 1b, in collaboration with the research group of Prof. R. Bartenschlager, University of Heidelberg.

4.3 Regulation of HCV translation by a novel, as yet unknown 210 kDa protein?

In an approach using the HCV RNA construct containing both 5′-UTR and the 3′-UTR with a precise end, a novel protein of about 210 kDa (p210) as well as an additional high molecular weight band were detected by the UV cross-linking assay. In contrast, no band was found with HCV RNA containing a non-precise end of the 3′-UTR in both cytoplasmic extract of Huh-7 cells and reticulocyte lysate (Figs. 60, 61B and 62). By comparing the migration of p210 with the migration of eIF4G bound to the FMDV IRES, it was ruled out that this newly detected protein is identical with eIF4G. Furthermore, mutation analysis revealed that the variable region of the 3′-UTR is most important for the binding of p210 (Fig. 65).

The fact that the novel 210 kDa protein binds only to the HCV RNA in the presence of an exact end of the 3′-UTR opens the possibility to study the mechanism by which HCV IRES-mediated translation is regulated. In this context, one important aspect is a possible synergism between the IRES and the 3′-UTR region which is reached by the circularization of the mRNA. Cap-dependent translation initiation is strongly enhanced by poly(A) tails (Gallie, 1991; Sachs, 2000). This synergism is due to the physical interaction between PABP and eIF4G which bind to the ends of the mRNA through their specific recognition of the poly(A) tail and the cap-eIF4E complex, respectively (Preiss & Hentze, 1998). Nevertheless, the evidence for RNA circularization during IRES-dependent initiation is still limited. A slight enhancement of IRES-driven translation by poly(A) tails *in vitro* has been reported (Michel et al., 2000; Michel et al., 2001). Other candidate proteins for a possible circularization of the mRNA are the nuclear factor associated with RNA (NFAR) proteins which were found to bind to both the 5′-UTR and the 3′-UTR of BVDV (Isken et al., 2003). These NFAR proteins might act as a functional bridge between both ends of the viral genome (Isken et al., 2003). The NFAR proteins essentially include three types of proteins, namely NF90 (nuclear factor 90)/NFAR-1, NF45 (nuclear factor 45) and RHA (RNA helicase A or

nuclear DNA helicase II [NDHII]) which form a protein complex (Liao et al., 1998) that considerably augments the interaction of the BVDV genome 5´- and 3´-ends (Isken et al., 2003). The molecular mechanisms underlying this observation remain to be clarified. In addition, there are also interactions among hnRNP proteins such as hnRNP E2, I, K and L which could, in concert with their RNA-binding preferences, possibly mediate interactions between the IRES and the 3´-UTR of mRNA (see discussion above). Protein-protein interactions of hnRNP proteins have been found to be involved in a variety of RNA-related biological processes (Kim et al., 2000).

With the discovery of the 210 kDa protein in this work, a promising new candidate for the stimulation of genome circularization adds to the list of candidates. This novel protein may perhaps stabilize the formation of closed-loop HCV RNA by bridging the 5´- and the 3´-UTR, thereby efficiently promoting ribosome reutilization by the IRES. This hypothesis is illustrated in Fig. 69.

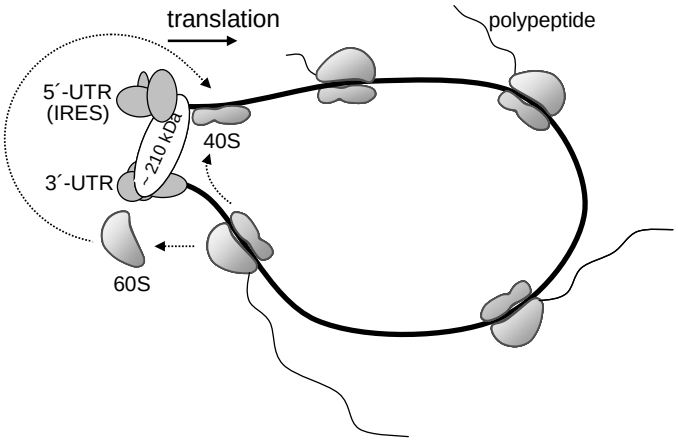

Fig. 69: Hypothetical closed-loop model of the HCV RNA translation complex. The proteins binding to the 5´-UTR are supposed to interact with the 3´-UTR of HCV via the novel ~ 210 kDa protein indicated, and this interaction may then possibly enhance the reutilization of ribosomes detaching at the termination site to start a new round of translation. The gray ovals represent proteins binding to the HCV 5´- and/or 3´-UTR.

The second important aspect is a possible switch between translation and viral minus-strand RNA synthesis. The replication of positive-strand RNA viruses represents an unresolved mystery: how is the negative-strand RNA synthesized in the face of a wave of translating ribosomes moving in the opposite direction? Since each molecule of genomic RNA must be used for translation prior to RNA replication (Kuge et al., 1986; Collis et al., 1992; Novak & Kirkegaard, 1994), the virus should have a mechanism to down-regulate translation to begin RNA synthesis when sufficient amounts of viral replication proteins have been synthesized. Gamarnik and Andino found that an RNA element at the very 5´-end of the poliovirus viral genome, the "cloverleaf" RNA, is involved in a switch from translation to replication (Gamarnik & Andino, 1998). The cellular Poly(rC)-binding protein 2 (PCBP2) binds, on one hand, to the IRES downstream of the 5´-terminal cloverleaf and stimulates the initial rounds of translation of the viral RNA. When sufficient amounts of the viral polymerase precursor 3CD have then accumulated, both 3CD and PCBP2 bind synergistically to two separate stem-loops of the cloverleaf and by that, most likely, promote binding of the viral 3D polymerase to the 3´-terminal sequences of the viral genome. Gamarnik and Andino proposed that these RNA-protein interactions determine the switch from translation to

RNA replication. Interestingly, the RNA phage Qβ uses the interaction of its RNA polymerase with Shine–Dalgarno sequences to control translation of the core protein (Kolakofsky & Weissmann, 1971b; Weber et al., 1972; Meyer et al., 1981), suggesting that animal RNA viruses and bacterial phages might use similar mechanisms to down-regulate translation.

Could this strategy be used by other eukaryotic RNA viruses? Until now, no further relevant report on HCV is available. Nevertheless, the results presented by Gamarnik and Andino bring us an insight into a general strategy by which positive-stranded RNA viruses might use common RNA structures for translation and initiation of RNA replication to coordinate these two opposite processes.

Obviously, with respect to this novel protein detected in this work, some very promising issues are emerging: (i) what is the nature of this new protein? (ii) is this protein possibly involved either in a circularization of the HCV RNA genome by interacting with the 5´- and the 3´-UTR or in a switch between translation and replication during the life cycle of the virus?

5 References

Abastado JP, Miller PF, Hinnebusch AG. 1991. A quantitative model for translational control of the GCN4 gene of Saccharomyces cerevisiae. *New Biol 3*:511-524.

Al RH, Xie Y, Wang Y, Hagedorn CH. 1998. Expression of recombinant hepatitis C virus non-structural protein 5B in Escherichia coli. *Virus Res 53*:141-149.

Alexander L, Lu HH, Gromeier M, Wimmer E. 1994. Dicistronic polioviruses as expression vectors for foreign genes. *AIDS Res Hum Retroviruses 10*:S57-60.

Ali N, Pruijn GJ, Kenan DJ, Keene JD, Siddiqui A. 2000. Human La antigen is required for the hepatitis C virus internal ribosome entry site-mediated translation. *J Biol Chem 275*:27531-27540.

Ali N, Siddiqui A. 1995. Interaction of polypyrimidine tract-binding protein with the 5' noncoding region of the hepatitis C virus RNA genome and its functional requirement in internal initiation of translation. *J Virol 69*:6367-6375.

Ali N, Siddiqui A. 1997. The La antigen binds 5' noncoding region of the hepatitis C virus RNA in the context of the initiator AUG codon and stimulates internal ribosome entry site-mediated translation. *Proc Natl Acad Sci USA 94*:2249-2254.

Alter H, Purcell R, Shih J. 1989. Detection of antibodiy to hepatitis C virus in prospectively followed transfusion recipients with acute and chronic non-A, non-B hepatitis. *N Engl J Med 321*:1494-1500.

Alter HJ, Holland PV, Morrow AG, Purcell RH, Feinstone SM, Moritsugu Y. 1975. Clinical and serological analysis of transfusion-associated hepatitis. *Lancet 2*:838-841.

Alter HJ, Holland PV, Purcell RH, Lander JJ, Feinstone SM, Morrow AG, Schmidt PJ. 1972. Posttransfusion hepatitis after exclusion of commercial and hepatitis-B antigen-positive donors. *Ann Intern Med 77*:691-699.

Alter HJ, Purcell RH, Holland PV, Popper H. 1978. Transmissible agent in non-A, non-B hepatitis. *Lancet 1*:459-463.

Amir-Ahmady B, Boutz PL, Markovtsov V, Phillips ML, Black DL. 2005. Exon repression by polypyrimidine tract binding protein. *RNA 11*:699-716.

Anwar A, Ali N, Tanveer R, Siddiqui A. 2000. Demonstration of functional requirement of polypyrimidine tract-binding protein by SELEX RNA during hepatitis C virus internal ribosome entry site-mediated translation initiation. *J Biol Chem 275*:34231-34235.

Asano K, Kinzy TG, Merrick WC, Hershey JW. 1997. Conservation and diversity of eukaryotic translation initiation factor eIF3. *J Biol Chem 272*:1101-1109.

Asano K, Phan L, Anderson J, Hinnebusch AG. 1998. Complex formation by all five homologues of mammalian translation initiation factor 3 subunits from yeast Saccharomyces cerevisiae. *J Biol Chem 273*:18573-18585.

Bartenschlager R, Ahlborn-Laake L, Mous J, Jacobsen H. 1993b. Nonstructural protein 3 of the hepatitis C virus encodes a serine-type proteinase required for cleavage at the NS3/4 and NS4/5 junctions. *J Virol 67*:3835-3844.

Bartenschlager R, Ahlborn-Laake L, Mous J, Jacobsen H. 1994. Kinetic and structural analyses of hepatitis C virus polyprotein processing. *J Virol 68*:5045-5055.

Bartenschlager R, Frese M, Pietschmann T. 2004. Novel insights into hepatitis C virus replication and persistence. *Adv Virus Res 63*:71-180.

Bartenschlager R, Lohmann V. 2000a. Replication of hepatitis C virus. *J Gen Virol 81 Pt 7*:1631-1648.

Bassili G, Tzima E, Song Y, Saleh L, Ochs K, Niepmann M. 2004. Sequence and secondary structure requirements in a highly conserved element for foot-and-mouth disease virus internal ribosome entry site activity and eIF4G binding. *J Gen Virol 85*:2555-2565.

Bayliss CD, Smith GL. 1996. Vaccinia virion protein I8R has both DNA and RNA helicase activities: implications for vaccinia virus transcription. *J Virol 70*:794-800.

Beales LP, Rowlands DJ, Holzenburg A. 2001. The internal ribosome entry site (IRES) of hepatitis C virus visualized by electron microscopy. *RNA 7*:661-670.

Becher P, Orlich M, Shannon AD, Horner G, Konig M, Thiel HJ. 1997. Phylogenetic analysis of pestiviruses from domestic and wild ruminants. *J Gen Virol 78*:1357-1366.

Becher P, Orlich M, Thiel HJ. 1998. Complete genomic sequence of border disease virus, a pestivirus from sheep. *J Virol 72*:5165-5173.

Beck E, Forss S, Strebel K, Cattaneo R, Feil G. 1983. Structure of the FMDV translation initiation site and of the structural proteins. *Nucleic Acids Res 11*:7873-7885.

Behrens SE, Tomei L, De Francesco R. 1996. Identification and properties of the RNA-dependent RNA polymerase of hepatitis C virus. *EMBO J 15*:12-22.

Belsham GJ, Sonenberg N. 2000. Picornavirus RNA translation: roles for cellular proteins. *Trends Microbiol 8*:330-335.

Benne R, Brown Luedi ML, Hershey JW. 1978. Purification and characterization of protein synthesis initiation factors eIF-1, eIF-4C, eIF-4D, and eIF-5 from rabbit reticulocytes. *J Biol Chem 253*:3070-3077.

Benne R, Hershey JW. 1976. Purification and characterization of initiation factor IF-E3 from rabbit reticulocytes. *Proc Natl Acad Sci USA 73*:3005-3009.

Berlioz C, Darlix JL. 1995. An internal ribosomal entry mechanism promotes translation of murine leukemia virus gag polyprotein precursors. *J Virol 69*:2214-2222.

Bieleski L, Talbot SJ. 2001. Kaposi's sarcoma-associated herpesvirus vCyclin open reading frame contains an internal ribosome entry site. *J Virol 75*:1864-1869.

Blight KJ, Rice CM. 1997. Secondary structure determination of the conserved 98-base sequence at the 3' terminus of hepatitis C virus genome RNA. *J Virol 71*:7345-7352.

Block KL, Vornlocher HP, Hershey JW. 1998. Characterization of cDNAs encoding the p44 and p35 subunits of human translation initiation factor eIF3. *J Biol Chem 273*:31901-31908.

Blumberg BS. 1964. Polymorphisms of the Serum Proteins and the Development of Iso-Precipitins in Transfused Patients. *Bull N Y Acad Med 40*:377-386.

Blyn LB, Swiderek KM, Richards O, Stahl DC, Semler BL, Ehrenfeld E. 1996. Poly(rC) binding protein 2 binds to stem-loop IV of the poliovirus RNA 5' noncoding region: identification by automated liquid chromatography-tandem mass spectrometry. *Proc Natl Acad Sci USA 93*:11115-11120.

Blyn LB, Towner JS, Semler BL, Ehrenfeld E. 1997. Requirement of poly(rC) binding protein 2 for translation of poliovirus RNA. *J Virol 71*:6243-6246.

Boni S, Lavergne JP, Boulant S, Cahour A. 2005. Hepatitis C virus core protein acts as a trans-modulating factor on internal translation initiation of the viral RNA. *J Biol Chem 280*:17737-17748.

Bothwell AL, Ballard DW, Philbrick WM, Lindwall G, Maher SE, Bridgett MM, Jamison SF, Garcia Blanco MA. 1991. Murine polypyrimidine tract binding protein. Purification, cloning, and mapping of the RNA binding domain. *J Biol Chem 266*:24657-24663.

Borman A, Howell MT, Patton JG, Jackson RJ. 1993. The involvement of a spliceosome component in internal initiation of human rhinovirus RNA translation. *J Gen Virol 74*:1775-1788.

Borovjagin A, Pestova T, Shatsky I. 1994. Pyrimidine tract binding protein strongly stimulates in vitro encephalomyocarditis virus RNA translation at the level of preinitiation complex formation. *FEBS Lett 351*:299-302.

Borowski P, Heiland M, Oehlmann K, Becker B, Kornetzky L, Feucht H, Laufs R. 1996a. Non-structural protein 3 of hepatitis C virus inhibits phosphorylation mediated by cAMP-dependent protein kinase. *Eur J Biochem 237*:611-618.

Boulant S, Becchi M, Penin F, Lavergne JP. 2003. Unusual multiple recoding events leading to alternative forms of hepatitis C virus core protein from genotype 1b. *J Biol Chem 278*:45785-45792.

Boussadia O, Amiot F, Cases S, Triqueneaux G, Jacquemin Sablon H, Dautry F. 1997. Transcription of unr (upstream of N-ras) down-modulates N-ras expression in vivo. *FEBS Lett 420*:20-24.

Boussadia O, Jacquemin Sablon H, Dautry F. 1993. Exon skipping in the expression of the gene immediately upstream of N-ras (unr/NRU). *Biochim Biophys Acta 20*:1-2.

Bradley DW, Maynard JE, Popper H, Cook EH, Ebert JW, McCaustland KA, Schable CA, Fields HA. 1983. Posttransfusion non-A, non-B hepatitis: physicochemical properties of two distinct agents. *J Infect Dis 148*:254-265.

Bradley DW, McCaustland KA, Cook EH, Schable CA, Ebert JW, Maynard JE. 1985. Posttransfusion non-A, non-B hepatitis in chimpanzees. Physicochemical evidence that the tubule-forming agent is a small, enveloped virus. *Gastroenterology 88*:773-779.

Bressanelli S, Tomei L, Rey FA, De Francesco R. 2002. Structural analysis of the hepatitis C virus RNA polymerase in complex with ribonucleotides. *J Virol 76*:3482-3492.

Brock KV, Deng R, Riblet SM. 1992. Nucleotide sequencing of 5' and 3' termini of bovine viral diarrhea virus by RNA ligation and PCR. *J Virol Methods 38*:39-46.

Brown EA, Zhang H, Ping LH, Lemon SM. 1992. Secondary structure of the 5' nontranslated regions of hepatitis C virus and pestivirus genomic RNAs. *Nucleic Acids Res 20*:5041-5045.

Brown EC, Jackson RJ. 2004. All five cold-shock domains of unr (upstream of N-ras) are required for stimulation of human rhinovirus RNA translation. *J Gen Virol 85*:2279-2287.

Bruix J, Calvet X, Costa J. 1989. Prevalence of antibodies to hepatitis C virus in Spanish patients with hepatocellular carcinoma and hepatic cirrhosis. *Lancet 334*:1004-1006.

Buck CB, Shen X, Egan MA, Pierson TC, Walker CM, Siliciano RF. 2001. The human immunodeficiency virus type 1 gag gene encodes an internal ribosome entry site. *J Virol 75*:181-191.

Buratti E, Tisminetzky S, Zotti M, Baralle FE. 1998. Functional analysis of the interaction between HCV 5'UTR and putative subunits of eukaryotic translation initiation factor eIF3. *Nucleic Acids Res 26*:3179-3187.

Burnette WN. 1981. "Western blotting": electrophoretic transfer of proteins from sodium dodecyl sulfate--polyacrylamide gels to unmodified nitrocellulose and radiographic detection with antibody and radioiodinated protein A. *Anal Biochem 112*:195-203.

Butcher SJ, Grimes JM, Makeyev EV, Bamford DH, Stuart DI. 2001. A mechanism for initiating RNA-dependent RNA polymerization. *Nature 410*:235-240.

Callis J, Fromm M, Walbot V. 1987. Introns increase gene expression in cultured maize cells. *Genes Dev 1*:1183-1200.

Chambers TJ, Hahn CS, Galler R, Rice CM. 1990. Flavivirus genome organization, expression, and replication. *Annu Rev Microbiol 44*:649-688.

Chang J, Yang SH, Cho YG, Hwang SB, Hahn YS, Sung YC. 1998. Hepatitis C virus core from two different genotypes has an oncogenic potential but is not sufficient for transforming primary rat embryo fibroblasts in cooperation with the H-ras oncogene. *J Virol 72*:3060-3065.

Chang KH, Brown EA, Lemon SM. 1993. Cell type-specific proteins which interact with the 5' nontranslated region of hepatitis A virus RNA. *J Virol 67*:6716-6725.

Chaudhuri J, Chakrabarti A, Maitra U. 1997. Biochemical characterization of mammalian translation initiation factor 3 (eIF3). Molecular cloning reveals that p110 subunit is the mammalian homologue of Saccharomyces cerevisiae protein Prt1. *J Biol Chem 272*:30975-30983.

Chen CM, You LR, Hwang LH, Lee YH. 1997. Direct interaction of hepatitis C virus core protein with the cellular lymphotoxin-beta receptor modulates the signal pathway of the lymphotoxin-beta receptor. *J Virol 71*:9417-9426.

Chen PJ, Lin MH, Tai KF, Liu PC, Lin CJ, Chen DS. 1992. The Taiwanese hepatitis C virus genome: sequence determination and mapping the 5' termini of viral genomic and antigenomic RNA. *Virology 188*:102-113.

Cheng JC, Chang MF, Chang SC. 1999. Specific interaction between the hepatitis C virus NS5B RNA polymerase and the 3' end of the viral RNA. *J Virol 73*:7044-7049.

Choo QL, Kuo G, Weiner AJ, Overby LR, Bradley DW, Houghton M. 1989. Isolation of a cDNA clone derived from a blood-borne non-A, non-B viral hepatitis genome. *Science 244*:359-362.

Choo QL, Richman KH, Han JH, Berger K, Lee C, Dong C, Gallegos C, Coit D, Medina-Selby R, Barr PJ, et al. 1991. Genetic organization and diversity of the hepatitis C virus. *Proc Natl Acad Sci U S A 88*:2451-2455.

Chung RT, Kaplan LM. 1999. Heterogeneous nuclear ribonucleoprotein I (hnRNP-I/PTB) selectively binds the conserved 3' terminus of hepatitis C viral RNA. *Biochem Biophys Res Commun 254*:351-362.

Cocquerel L, Duvet S, Meunier JC, Pillez A, Cacan R, Wychowski C, Dubuisson J. 1999. The transmembrane domain of hepatitis C virus glycoprotein E1 is a signal for static retention in the endoplasmic reticulum. *J Virol 73*:2641-2649.

Coito C, Diamond DL, Neddermann P, Korth MJ, Katze MG. 2004. High-throughput screening of the yeast kinome: identification of human serine/threonine protein kinases that phosphorylate the hepatitis C virus NS5A protein. *J Virol 78*:3502-3513.

Coldwell MJ, Mitchell SA, Stoneley M, MacFarlane M, Willis AE. 2000. Initiation of Apaf-1 translation by internal ribosome entry. *Oncogene 19*:899-905.

Collett MS, Anderson DK, Retzel E. 1988b. Comparisons of the pestivirus bovine viral diarrhoea virus with members of the flaviviridae. *J Gen Virol 69 (Pt 10)*:2637-2643.

Collett MS, Moennig V, Horzinek MC. 1989. Recent advances in pestivirus research. *J Gen Virol 70 (Pt 2)*:253-266.

Collier AJ, Tang S, Elliott RM. 1998. Translation efficiencies of the 5' untranslated region from representatives of the six major genotypes of hepatitis C virus using a novel bicistronic reporter assay system. *J Gen Virol 79*:2359-2366.

Collis PS, O'Donnell BJ, Barton DJ, Rogers JA, Flanegan JB. 1992. Replication of poliovirus RNA and subgenomic RNA transcripts in transfected cells. *J Virol 66*:6480-6488.

Colombo M, Kuo G, Choo QL, Donato MF, Del Ninno E, Tommasini MA, Dioguardi N, Houghton M. 1989. Prevalence of antibodies to hepatitis C virus in Italian patients with hepatocellular carcinoma. *Lancet 2*:1006-1008.

Danaie P, Wittmer B, Altmann M, Trachsel H. 1995. Isolation of a protein complex containing translation initiation factor Prt1 from Saccharomyces cerevisiae. *J Biol Chem 270*:4288-4292.

Deffaud C, Darlix JL. 2000b. Rous sarcoma virus translation revisited: characterization of an internal ribosome entry segment in the 5' leader of the genomic RNA. *J Virol 74*:11581-11588.

Deforges S, Evlashev A, Perret M, Sodoyer M, Pouzol S, Scoazec JY, Bonnaud B, Diaz O, Paranhos-Baccala G, Lotteau V, Andre P. 2004. Expression of hepatitis C virus proteins in epithelial intestinal cells in vivo. *J Gen Virol 85*:2515-2523.

Deleersnyder V, Pillez A, Wychowski C, Blight K, Xu J, Hahn YS, Rice CM, Dubuisson J. 1997. Formation of native hepatitis C virus glycoprotein complexes. *J Virol 71*:697-704.

Dienstag JL. 1983. Non-A, non-B hepatitis. I. Recognition, epidemiology, and clinical features. *Gastroenterology 85*:439-462.

Domier LL, McCoppin NK, D'Arcy CJ. 2000. Sequence requirements for translation initiation of Rhopalosiphum padi virus ORF2. *Virology 268*:264-271.

Doniger J, DiPaolo JA. 1988. Coordinate N-ras mRNA up-regulation with mutational activation in tumorigenic guinea pig cells. *Nucleic Acids Res 16*:969-980.

Doniger J, Landsman D, Gonda MA, Wistow G. 1992. The product of unr, the highly conserved gene upstream of N-ras, contains multiple repeats similar to the cold-shock domain (CSD), a putative DNA-binding motif. *New Biol 4*:389-395.

Dreyfuss G, Matunis MJ, Pinol Roma S, Burd CG. 1993. hnRNP proteins and the biogenesis of mRNA. *Annu Rev Biochem 62*:289-321.

Dubuisson J, Hsu HH, Cheung RC, Greenberg HB, Russell DG, Rice CM. 1994. Formation and intracellular localization of hepatitis C virus envelope glycoprotein complexes expressed by recombinant vaccinia and Sindbis viruses. *J Virol 68*:6147-6160.

Duvet S, Cocquerel L, Pillez A, Cacan R, Verbert A, Moradpour D, Wychowski C, Dubuisson J. 1998. Hepatitis C virus glycoprotein complex localization in the endoplasmic reticulum involves a determinant for retention and not retrieval. *J Biol Chem 273*:32088-32095.

Eckart MR, Selby M, Masiarz F, Lee C, Berger K, Crawford K, Kuo C, Kuo G, Houghton M, Choo QL. 1993. The hepatitis C virus encodes a serine protease involved in processing of the putative nonstructural proteins from the viral polyprotein precursor. *Biochem Biophys Res Commun 192*:399-406.

Egger D, Wolk B, Gosert R, Bianchi L, Blum HE, Moradpour D, Bienz K. 2002. Expression of hepatitis C virus proteins induces distinct membrane alterations including a candidate viral replication complex. *J Virol 76*:5974-5984.

Esteban JI, Cordoba J, Sauleda S. 1998. The clinical picture of acute and chronic hepatitis C. *Curr Stud Hematol Blood Transfus*:102-118.

Failla C, Tomei L, De Francesco R. 1994. Both NS3 and NS4A are required for proteolytic processing of hepatitis C virus nonstructural proteins. *J Virol 68*:3753-3760.

Fang JW, Moyer RW. 2000. The effects of the conserved extreme 3' end sequence of hepatitis C virus (HCV) RNA on the in vitro stabilization and translation of the HCV RNA genome. *J Hepatol 33*:632-639.

Ferrari E, Wright-Minogue J, Fang JW, Baroudy BM, Lau JY, Hong Z. 1999. Characterization of soluble hepatitis C virus RNA-dependent RNA polymerase expressed in Escherichia coli. *J Virol 73*:1649-1654.

Flint M, Thomas JM, Maidens CM, Shotton C, Levy S, Barclay WS, McKeating JA. 1999c. Functional analysis of cell surface-expressed hepatitis C virus E2 glycoprotein. *J Virol 73*:6782-6790.

Forton DM, Karayiannis P, Mahmud N, Taylor-Robinson SD, Thomas HC. 2004. Identification of unique hepatitis C virus quasispecies in the central nervous system and comparative analysis of internal translational efficiency of brain, liver, and serum variants. *J Virol 78*:5170-5183.

Friebe P, Bartenschlager R. 2002. Genetic analysis of sequences in the 3' nontranslated region of hepatitis C virus that are important for RNA replication. *J Virol 76*:5326-5338.

Friebe P, Boudet J, Simorre JP, Bartenschlager R. 2005. Kissing-loop interaction in the 3' end of the hepatitis C virus genome essential for RNA replication. *J Virol 79*:380-392.

Fukushi S, Okada M, Kageyama T, Hoshino FB, Katayama K. 1999. Specific interaction of a 25-kilodalton cellular protein, a 40S ribosomal subunit protein, with the internal ribosome entry site of hepatitis C virus genome. *Virus Genes 19*:153-161.

Fukushi S, Okada M, Stahl J, Kageyama T, Hoshino FB, Katayama K. 2001. Ribosomal protein S5 interacts with the internal ribosomal entry site of hepatitis C virus. *J Biol Chem 276*:20824-20826.

Gale M, Jr., Blakely CM, Kwieciszewski B, Tan SL, Dossett M, Tang NM, Korth MJ, Polyak SJ, Gretch DR, Katze MG. 1998c. Control of PKR protein kinase by hepatitis C virus nonstructural 5A protein: molecular mechanisms of kinase regulation. *Mol Cell Biol 18*:5208-5218.

Gale MJ, Jr., Korth MJ, Tang NM, Tan SL, Hopkins DA, Dever TE, Polyak SJ, Gretch DR, Katze MG. 1997. Evidence that hepatitis C virus resistance to interferon is mediated through repression of the PKR protein kinase by the nonstructural 5A protein. *Virology 230*:217-227.

Gallie DR. 1991. The cap and poly(A) tail function synergistically to regulate mRNA translational efficiency. *Genes Dev 5*:2108-2116.

Gamarnik AV, Andino R. 1997. Two functional complexes formed by KH domain containing proteins with the 5' noncoding region of poliovirus RNA. *RNA 3*:882-892.

Gamarnik AV, Andino R. 1998. Switch from translation to RNA replication in a positive-stranded RNA virus. *Genes Dev 12*:2293-2304.

Garçia-Blanco MA, Jamison SF, Sharp PA. 1989. Identification and purification of a 62,000-dalton protein that binds specifically to the polypyrimidine tract of introns. *Genes Dev 3*:1874-1886.

Gil A, Sharp PA, Jamison SF, Garçia-Blanco MA. 1991. Characterization of cDNAs encoding the polypyrimidine tract-binding protein. *Genes Dev 5*:1224-1236.

Gontarek RR, Gutshall LL, Herold KM, Tsai J, Sathe GM, Mao J, Prescott C, Del Vecchio AM. 1999. hnRNP C and polypyrimidine tract-binding protein specifically interact with the pyrimidine-rich region within the 3 ' NTR of the HCV RNA genome. *Nucleic Acids Res 27*:1457-1463.

Gosert R, Chang KH, Rijnbrand R, Yi M, Sangar DV, Lemon SM. 2000. Transient expression of cellular polypyrimidine-tract binding protein stimulates cap-independent translation directed by both picornaviral and flaviviral internal ribosome entry sites In vivo. *Mol Cell Biol 20*:1583-1595.

Gottlieb E, Steitz JA. 1989. The RNA binding protein La influences both the accuracy and the efficiency of RNA polymerase III transcription in vitro. *EMBO J 8*:841-850.

Graff J, Cha J, Blyn LB, Ehrenfeld E. 1998. Interaction of poly(rC) binding protein 2 with the 5' noncoding region of hepatitis A virus RNA and its effects on translation. *J Virol 72*:9668-9675.

Grakoui A, McCourt DW, Wychowski C, Feinstone SM, Rice CM. 1993a. A second hepatitis C virus-encoded proteinase. *Proc Natl Acad Sci USA 90*:10583-10587.

Grakoui A, McCourt DW, Wychowski C, Feinstone SM, Rice CM. 1993b. Characterization of the hepatitis C virus-encoded serine proteinase: determination of proteinase-dependent polyprotein cleavage sites. *J Virol 67*:2832-2843.

Grakoui A, Wychowski C, Lin C, Feinstone SM, Rice CM. 1993c. Expression and identification of hepatitis C virus polyprotein cleavage products. *J Virol 67*:1385-1395.

Griffin SD, Beales LP, Clarke DS, Worsfold O, Evans SD, Jaeger J, Harris MP, Rowlands DJ. 2003. The p7 protein of hepatitis C virus forms an ion channel that is blocked by the antiviral drug, Amantadine. *FEBS Lett 535*:34-38.

Grifo JA, Tahara SM, Morgan MA, Shatkin AJ, Merrick WC. 1983. New initiation factor activity required for globin mRNA translation. *J Biol Chem 258*:5804-5810.

Grundhoff A, Ganem D. 2001. Mechanisms governing expression of the v-FLIP gene of Kaposi's sarcoma-associated herpesvirus. *J Virol 75*:1857-1863.

Gunnery S, Mathews MB. 1995. Functional mRNA can be generated by RNA polymerase III. *Mol Cell Biol 15*:3597-3607.

Gwack Y, Kim DW, Han JH, Choe J. 1996. Characterization of RNA binding activity and RNA helicase activity of the hepatitis C virus NS3 protein. *Biochem Biophys Res Commun 225*:654-659.

Hahm B, Cho OH, Kim JE, Kim YK, Kim JH, Oh YL, Jang SK. 1998a. Polypyrimidine tract-binding protein interacts with HnRNP L. *FEBS Lett 425*:401-406.

Hahm B, Kim YK, Kim JH, Kim TY, Jang SK. 1998b. Heterogeneous nuclear ribonucleoprotein L interacts with the 3' border of the internal ribosomal entry site of hepatitis C virus. *J Virol 72*:8782-8788.

Han JH, Shyamala V, Richman KH, Brauer MJ, Irvine B, Urdea MS, Tekamp-Olson P, Kuo G, Choo QL, Houghton M. 1991. Characterization of the terminal regions of hepatitis C viral RNA: identification of

conserved sequences in the 5' untranslated region and poly(A) tails at the 3' end. *Proc Natl Acad Sci U S A 88*:1711-1715.

Hanachi P, Hershey JW, Vornlocher HP. 1999. Characterization of the p33 subunit of eukaryotic translation initiation factor-3 from Saccharomyces cerevisiae. *J Biol Chem 274*:8546-8553.

Havens WP, Jr. 1956. Viral hepatitis: multiple attacks in a narcotic addict. *Ann Intern Med 44*:199-203.

He Y, Katze MG. 2002. To interfere and to anti-interfere: the interplay between hepatitis C virus and interferon. *Viral Immunol 15*:95-119.

He Y, Yan W, Coito C, Li Y, Gale M, Jr., Katze MG. 2003. The regulation of hepatitis C virus (HCV) internal ribosome entry site-mediated translation by HCV replicons and nonstructural proteins. *J Gen Virol 84*:535-543.

Hellen CU, Pestova TV, Litterst M, Wimmer E. 1994. The cellular polypeptide p57 (pyrimidine tract-binding protein) binds to multiple sites in the poliovirus 5' nontranslated region. *J Virol 68*:941-950.

Hellen CU, Sarnow P. 2001. Internal ribosome entry sites in eukaryotic mRNA molecules. *Genes Dev 15*:1593-1612.

Hellen CU, Witherell GW, Schmid M, Shin SH, Pestova TV, Gil A, Wimmer E. 1993. A cytoplasmic 57-kDa protein that is required for translation of picornavirus RNA by internal ribosomal entry is identical to the nuclear pyrimidine tract-binding protein. *Proc Natl Acad Sci USA 90*:7642-7646.

Henis-Korenblit S, Strumpf NL, Goldstaub D, Kimchi A. 2000. A novel form of DAP5 protein accumulates in apoptotic cells as a result of caspase cleavage and internal ribosome entry site-mediated translation. *Mol Cell Biol 20*:496-506.

Hentze MW. 1997. eIF4G: a multipurpose ribosome adapter? *Science 275*:500-501.

Hershey JWB, Merrick WC. 2000. Pathway and mechanism of initiation of protein synthesis. In: Sonenberg N, Hershey JWB, Mathews MB, eds. *Translational control of gene expression*. Cold Spring Harbor, NY: Cold Spring Harbor Laboratory Press. pp 33-88.

Hijikata M, Mizushima H, Akagi T, Mori S, Kakiuchi N, Kato N, Tanaka T, Kimura K, Shimotohno K. 1993a. Two distinct proteinase activities required for the processing of a putative nonstructural precursor protein of hepatitis C virus. *J Virol 67*:4665-4675.

Hijikata M, Mizushima H, Tanji Y, Komoda Y, Hirowatari Y, Akagi T, Kato N, Kimura K, Shimotohno K. 1993b. Proteolytic processing and membrane association of putative nonstructural proteins of hepatitis C virus. *Proc Natl Acad Sci U S A 90*:10773-10777.

Hirowatari Y, Hijikata M, Tanji Y, Nyunoya H, Mizushima H, Kimura K, Tanaka T, Kato N, Shimotohno K. 1993. Two proteinase activities in HCV polypeptide expressed in insect cells using baculovirus vector. *Arch Virol 133*:349-356.

Holcik M, Lefebvre C, Yeh C, Chow T, Korneluk RG. 1999. A new internal-ribosome-entry-site motif potentiates XIAP-mediated cytoprotection. *Nat Cell Biol 1*:190-192.

Holland PV, Walsh JH, Morrow AG, Purcell RH. 1969. Failure of Australia antibody to prevent post-transfusion hepatitis. *Lancet 2*:553-555.

Honda M, Beard MR, Ping LH, Lemon SM. 1999. A phylogenetically conserved stem-loop structure at the 5 ' border of the internal ribosome entry site of hepatitis C virus is required for cap-independent viral translation. *J Virol 73*:1165-1174.

Honda M, Brown EA, Lemon SM. 1996a. Stability of a stem-loop involving the initiator AUG controls the efficiency of internal initiation of translation on hepatitis C virus RNA. *RNA 2*:955-968.

Honda M, Kaneko S, Matsushita E, Kobayashi K, Abell GA, Lemon SM. 2000. Cell cycle regulation of hepatitis C virus internal ribosomal entry site-directed translation. *Gastroenterology 118*:152-162.

Honda M, Ping LH, Rijnbrand RC, Amphlett E, Clarke B, Rowlands D, Lemon SM. 1996b. Structural requirements for initiation of translation by internal ribosome entry within genome-length hepatitis C virus RNA. *Virology 222*:31-42.

Hong Z, Ferrari E, Wright Minogue J, Chase R, Risano C, Seelig G, Lee CG, Kwong AD. 1996. Enzymatic characterization of hepatitis C virus NS3/4A complexes expressed in mammalian cells by using the herpes simplex virus amplicon system. *J Virol 70*:4261-4268.

Hui J, Reither G, Bindereif A. 2003. Novel functional role of CA repeats and hnRNP L in RNA stability. *RNA 9*:931-936.

Hunt SL, Hsuan JJ, Totty N, Jackson RJ. 1999a. unr, a cellular cytoplasmic RNA-binding protein with five cold-shock domains, is required for internal initiation of translation of human rhinovirus RNA. *Genes Dev 13*:437-448.

Hunt SL, Jackson RJ. 1999b. Polypyrimidine-tract binding protein (PTB) is necessary, but not sufficient, for efficient internal initiation of translation of human rhinovirus-2 RNA. *RNA 5*:344-359.

Ide Y, Tanimoto A, Sasaguri Y, Padmanabhan R. 1997. Hepatitis C virus NS5A protein is phosphorylated in vitro by a stably bound protein kinase from HeLa cells and by cAMP-dependent protein kinase A-alpha catalytic subunit. *Gene 201*:151-158.

Imbert I, Dimitrova M, Kien F, Kieny MP, Schuster C. 2003. Hepatitis C virus IRES efficiency is unaffected by the genomic RNA 3'NTR even in the presence of viral structural or non-structural proteins. *J Gen Virol 84*:1549-1557.

Inchauspe G, Zebedee S, Lee DH, Sugitani M, Nasoff M, Prince AM. 1991. Genomic structure of the human prototype strain H of hepatitis C virus: comparison with American and Japanese isolates. *Proc Natl Acad Sci U S A 88*:10292-10296.

Inoue Y, Miyazaki M, Ohashi R, Tsuji T, Fukaya K, Kouchi H, Uemura T, Mihara K, Namba M. 1998a. Ubiquitous presence of cellular proteins that specifically bind to the 3' terminal region of hepatitis C virus. *Biochem Biophys Res Commun 245*:198-203.

Ishido S, Fujita T, Hotta H. 1998. Complex formation of NS5B with NS3 and NS4A proteins of hepatitis C virus. *Biochem Biophys Res Commun 244*:35-40.

Isken O, Grassmann CW, Sarisky RT, Kann M, Zhang S, Grosse F, Kao PN, Behrens SE. 2003. Members of the NF90/NFAR protein group are involved in the life cycle of a positive-strand RNA virus. *EMBO J 22*:5655-5665.

Isken O, Grassmann CW, Yu H, Behrens SE. 2004. Complex signals in the genomic 3' nontranslated region of bovine viral diarrhea virus coordinate translation and replication of the viral RNA. *RNA 10*:1637-1652.

Isoyama T, Kamoshita N, Yasui K, Iwai A, Shiroki K, Toyoda H, Yamada A, Takasaki Y, Nomoto A. 1999. Lower concentration of La protein required for internal ribosome entry on hepatitis C virus RNA than on poliovirus RNA. *J Gen Virol 80*:2319-2327.

Ito T, Lai MM. 1997. Determination of the secondary structure of and cellular protein binding to the 3'-untranslated region of the hepatitis C virus RNA genome. *J Virol 71*:8698-8706.

Ito T, Lai MMC. 1999. An internal polypyrimidine-tract-binding protein-binding site in the hepatitis C virus RNA attenuates translation, which is relieved by the 3'-untranslated sequence. *Virology 254*:288-296.

Ito T, Tahara SM, Lai MMC. 1998. The 3'-untranslated region of hepatitis C virus RNA enhances translation from an internal ribosomal entry site. *J Virol 72*:8789-8796.

Iwarson S, Lundin P, Holmgren J, Hermodsson S. 1973. Multiple attacks of hepatitis in drug addicts: biochemical, immunochemical, and morphologic characteristics. *J Infect Dis 127*:544-550.

Izumi RE, Valdez B, Banerjee R, Srivastava M, Dasgupta A. 2001. Nucleolin stimulates viral internal ribosome entry site-mediated translation. *Virus Res 76*:17-29.

Jackson RJ. 2000. Comparative view of initiation site selection mechanisms. In: Sonenberg N, Hershey JWB, Mathews MB, eds. *Translational control of gene expression*. Cold Spring Harbor, NY: Cold Spring Harbor Laboratory Press. pp 127-183.

Jackson RJ, Kaminski A. 1995. Internal initiation of translation in eukaryotes: the picornavirus paradigm and beyond. *RNA 1*:985-1000.

Jacquemin Sablon H, Triqueneaux G, Deschamps S, le Maire M, Doniger J, Dautry F. 1994. Nucleic acid binding and intracellular localization of unr, a protein with five cold shock domains. *Nucleic Acids Res 22*:2643-2650.

Jang SK, Kräusslich HG, Nicklin MJ, Duke GM, Palmenberg AC, Wimmer E. 1988. A segment of the 5' nontranslated region of encephalomyocarditis virus RNA directs internal entry of ribosomes during in vitro translation. *J Virol 62*:2636-2643.

Jang SK, Wimmer E. 1990. Cap-independent translation of encephalomyocarditis virus RNA: structural elements of the internal ribosomal entry site and involvement of a cellular 57-kD RNA-binding protein. *Genes Dev 4*:1560-1572.

Jeffers M, Paciucci R, Pellicer A. 1990. Characterization of unr; a gene closely linked to N-ras. *Nucleic Acids Res 18*:4891-4899.

Ji H, Fraser CS, Yu Y, Leary J, Doudna JA. 2004. Coordinated assembly of human translation initiation complexes by the hepatitis C virus internal ribosome entry site RNA. *Proc Natl Acad Sci U S A 101*:16990-16995.

Johnson KR, Merrick WC, Zoll WL, Zhu Y. 1997. Identification of cDNA clones for the large subunit of eukaryotic translation initiation factor 3. Comparison of homologues from human, Nicotiana tabacum, Caenorhabditis elegans, and Saccharomyces cerevisiae. *J Biol Chem 272*:7106-7113.

Kaito M, Watanabe S, Tsukiyama-Kohara K, Yamaguchi K, Kobayashi Y, Konishi M, Yokoi M, Ishida S, Suzuki S, Kohara M. 1994. Hepatitis C virus particle detected by immunoelectron microscopic study. *J Gen Virol 75 (Pt 7)*:1755-1760.

Kaminski A, Hunt SL, Patton JG, Jackson RJ. 1995. Direct evidence that polypyrimidine tract binding protein (PTB) is essential for internal initiation of translation of encephalomyocarditis virus RNA. *RNA 1*:924-938.

Kaminski A, Jackson RJ. 1998. The polypyrimidine tract binding protein (PTB) requirement for internal initiation of translation of cardiovirus RNAs is conditional rather than absolute. *RNA 4*:626-638.

Kamoshita N, Tsukiyama Kohara K, Kohara M, Nomoto A. 1997. Genetic analysis of internal ribosomal entry site on hepatitis C virus RNA: implication for involvement of the highly ordered structure and cell type-specific transacting factors. *Virology 233*:9-18.

Kannemeier C, Feussner A, Stohr HA, Weisse J, Preissner KT, Romisch J. 2001. Factor VII and single-chain plasminogen activator-activating protease: activation and autoactivation of the proenzyme. *Eur J Biochem 268*:3789-3796.

Kao CC, Del Vecchio AM, Zhong W. 1999. De novo initiation of RNA synthesis by a recombinant flaviviridae RNA-dependent RNA polymerase. *Virology 253*:1-7.

Kato J, Kato N, Yoshida H, Ono-Nita SK, Shiratori Y, Omata M. 2002. Hepatitis C virus NS4A and NS4B proteins suppress translation in vivo. *J Med Virol 66*:187-199.

Kato N, Hijikata M, Ootsuyama Y, Nakagawa M, Ohkoshi S, Sugimura T, Shimotohno K. 1990. Molecular cloning of the human hepatitis C virus genome from Japanese patients with non-A, non-B hepatitis. *Proc Natl Acad Sci U S A 87*:9524-9528.

Katze MG, Kwieciszewski B, Goodlett DR, Blakely CM, Neddermann P, Tan SL, Aebersold R. 2000. Ser(2194) is a highly conserved major phosphorylation site of the hepatitis C virus nonstructural protein NS5A. *Virology 278*:501-513.

Kenan DJ, Query CC, Keene JD. 1991. RNA recognition: towards identifying determinants of specificity. *Trends Biochem Sci 16*:214-220.

Kieft JS, Grech A, Adams P, Doudna JA. 2001. Mechanisms of internal ribosome entry in translation initiation. *Cold Spring Harb Symp Quant Biol 66*:277-283.

Kim DW, Gwack Y, Han JH, Choe J. 1995. C-terminal domain of the hepatitis C virus NS3 protein contains an RNA helicase activity. *Biochem Biophys Res Commun 215*:160-166.

Kim J, Lee D, Choe J. 1999. Hepatitis C virus NS5A protein is phosphorylated by casein kinase II. *Biochem Biophys Res Commun 257*:777-781.

Kim JH, Hahm B, Kim YK, Choi M, Jang SK. 2000. Protein-protein interaction among hnRNPs shuttling between nucleus and cytoplasm. *J Mol Biol 298*:395-405.

Kim JH, Paek KY, Ha SH, Cho S, Choi K, Kim CS, Ryu SH, Jang SK. 2004. A cellular RNA-binding protein enhances internal ribosomal entry site-dependent translation through an interaction downstream of the hepatitis C virus polyprotein initiation codon. *Mol Cell Biol 24*:7878-7890.

Kim YK, Kim CS, Lee SH, Jang SK. 2002. Domains I and II in the 5' nontranslated region of the HCV genome are required for RNA replication. *Biochem Biophys Res Commun 290*:105-112.

Klinck R, Westhof E, Walker S, Afshar M, Collier A, Aboul-Ela F. 2000. A potential RNA drug target in the hepatitis C virus internal ribosomal entry site. *RNA 6*:1423-1431.

Koch JO, Bartenschlager R. 1999. Modulation of hepatitis C virus NS5A hyperphosphorylation by nonstructural proteins NS3, NS4A, and NS4B. *J Virol 73*:7138-7146.

Kolakofsky D, Weissmann C. 1971b. Q replicase as repressor of Q RNA-directed protein synthesis. *Biochim Biophys Acta 246*:596-599.

Kolupaeva VG, Hellen CU, Shatsky IN. 1996. Structural analysis of the interaction of the pyrimidine tract-binding protein with the internal ribosomal entry site of encephalomyocarditis virus and foot-and-mouth disease virus RNAs. *RNA 2*:1199-1212.

Kolupaeva VG, Pestova TV, Hellen CU. 2000a. An enzymatic footprinting analysis of the interaction of 40S ribosomal subunits with the internal ribosomal entry site of hepatitis C virus. *J Virol 74*:6242-6250.

Kolupaeva VG, Pestova TV, Hellen CU. 2000b. Ribosomal binding to the internal ribosomal entry site of classical swine fever virus. *RNA 6*:1791-1807.

Kolykhalov AA, Feinstone SM, Rice CM. 1996. Identification of a highly conserved sequence element at the 3' terminus of hepatitis C virus genome RNA. *J Virol 70*:3363-3371.

Kolykhalov AA, Mihalik K, Feinstone SM, Rice CM. 2000. Hepatitis C virus-encoded enzymatic activities and conserved RNA elements in the 3' nontranslated region are essential for virus replication in vivo. *J Virol 74*:2046-2051.

Konarska M, Filipowicz W, Domdey H, Gross HJ. 1981. Binding of ribosomes to linear and circular forms of the 5'-terminal leader fragment of tobacco-mosaic-virus RNA. *Eur J Biochem 114*:221-227.

Konarska MM, Sharp PA. 1986. Electrophoretic separation of complexes involved in the splicing of precursors to mRNAs. *Cell 46*:845-855.

Kong LK, Sarnow P. 2002. Cytoplasmic expression of mRNAs containing the internal ribosome entry site and 3' noncoding region of hepatitis C virus: effects of the 3' leader on mRNA translation and mRNA stability. *J Virol 76*:12457-12462.

Koonin EV, Dolja VV. 1993. Evolution and taxonomy of positive-strand RNA viruses: implications of comparative analysis of amino acid sequences [published erratum appears in Crit Rev Biochem Mol Biol 1993;28(6):546]. *Crit Rev Biochem Mol Biol 28*:375-430.

Kozak M. 1979. Inability of circular mRNA to attach to eukaryotic ribosomes. *Nature 280*:82-85.

Kozak M. 1989a. Context effects and inefficient initiation at non-AUG codons in eucaryotic cell-free translation systems. *Mol Cell Biol 9*:5073-5080.

Kozak M. 1989b. The scanning model for translation: an update. *J Cell Biol 108*:229-241.

Krüger M, Beger C, Welch PJ, Barber JR, Manns MP, Wong-Staal F. 2001. Involvement of proteasome alpha-subunit PSMA7 in hepatitis C virus internal ribosome entry site-mediated translation. *Mol Cell Biol 21*:8357-8364.

Kuge S, Saito I, Nomoto A. 1986. Primary structure of poliovirus defective-interfering particle genomes and possible generation mechanisms of the particles. *J Mol Biol 192*:473-487.

Kühn R, Luz N, Beck E. 1990. Functional analysis of the internal translation initiation site of foot-and-mouth disease virus. *J Virol 64*:4625-4631.

Kuo G, Choo QL, Alter HJ, Gitnick GL, Redeker AG, Purcell RH, Miyamura T, Dienstag JL, Alter MJ, Stevens CE, et al. 1989. An assay for circulating antibodies to a major etiologic virus of human non-A, non-B hepatitis. *Science 244*:362-364.

Lamphear BJ, Kirchweger R, Skern T, Rhoads RE. 1995. Mapping of functional domains in eukaryotic protein synthesis initiation factor 4G (eIF4G) with picornaviral proteases. Implications for cap-dependent and cap-independent translational initiation. *J Biol Chem 270*:21975-21983.

Laporte J, Malet I, Andrieu T, Thibault V, Toulme JJ, Wychowski C, Pawlotsky JM, Huraux JM, Agut H, Cahour A. 2000. Comparative analysis of translation efficiencies of hepatitis C virus 5' untranslated regions among intraindividual quasispecies present in chronic infection: opposite behaviors depending on cell type. *J Virol 74*:10827-10833.

Lauer GM, Walker BD. 2001. Hepatitis C virus infection. *N Engl J Med 345*:41-52.

Lee H, Shin H, Wimmer E, Paul AV. 2004. cis-acting RNA signals in the NS5B C-terminal coding sequence of the hepatitis C virus genome. *J Virol 78*:10865-10877.

Lemon SM, Honda, M. 1997. Internal ribosome entry sites within the RNA genomes of Hepatitis C virus and other flaviviruses. *Semin Virol 8*:274-288.

Lerat H, Shimizu YK, Lemon SM. 2000. Cell type-specific enhancement of hepatitis C virus internal ribosome entry site-directed translation due to 5' nontranslated region substitutions selected during passage of virus in lymphoblastoid cells. *J Virol 74*:7024-7031.

Liao HJ, Kobayashi R, Mathews MB. 1998. Activities of adenovirus virus-associated RNAs: purification and characterization of RNA binding proteins. *Proc Natl Acad Sci USA 95*:8514-8519.

Lin C, Pragai BM, Grakoui A, Xu J, Rice CM. 1994b. Hepatitis C virus NS3 serine proteinase: trans-cleavage requirements and processing kinetics. *J Virol 68*:8147-8157.

Lin C, Wu JW, Hsiao K, Su MS. 1997. The hepatitis C virus NS4A protein: interactions with the NS4B and NS5A proteins. *J Virol 71*:6465-6471.

Liu X, Mertz JE. 1995. HnRNP L binds a cis-acting RNA sequence element that enables intron-dependent gene expression. *Genes Dev 9*:1766-1780.

Loeffler F, Frosch P. 1964. Report of the commission for research on foot-and-mouth disease virus. *Zentrabl Bacteriol Parasi Infec Krankh 23*:371-391.

Lohmann V, Korner F, Herian U, Bartenschlager R. 1997. Biochemical properties of hepatitis C virus NS5B RNA-dependent RNA polymerase and identification of amino acid sequence motifs essential for enzymatic activity. *J Virol 71*:8416-8428.

Lohmann V, Korner F, Koch J, Herian U, Theilmann L, Bartenschlager R. 1999. Replication of subgenomic hepatitis C virus RNAs in a hepatoma cell line. *Science 285*:110-113.

Lopez Fernandez LA, Lopez Alanon DM, del Mazo J. 1995. Different developmental pattern of N-ras and unr gene expression in mouse gametogenic and somatic tissues. *Biochim Biophys Acta 25*:10-16.

Lu H, Li W, Noble WS, Payan D, Anderson DC. 2004. Riboproteomics of the hepatitis C virus internal ribosomal entry site. *J Proteome Res 3*:949-957.

Lu HH, Wimmer E. 1996. Poliovirus chimeras replicating under the translational control of genetic elements of hepatitis C virus reveal unusual properties of the internal ribosomal entry site of hepatitis C virus. *Proc Natl Acad Sci USA 93*:1412-1417.

Lukavsky PJ, Otto GA, Lancaster AM, Sarnow P, Puglisi JD. 2000. Structures of two RNA domains essential for hepatitis C virus internal ribosome entry site function. *Nat Struct Biol 7*:1105-1110.

Luo G. 1999. Cellular proteins bind to the poly(U) tract of the 3' untranslated region of hepatitis C virus RNA genome. *Virology 256*:105-118.

Luo G, Hamatake RK, Mathis DM, Racela J, Rigat KL, Lemm J, Colonno RJ. 2000. De novo initiation of RNA synthesis by the RNA-dependent RNA polymerase (NS5B) of hepatitis C virus. *J Virol 74*:851-863.

Luz N, Beck E. 1990. A cellular 57 kDa protein binds to two regions of the internal translation initiation site of foot-and-mouth disease virus. *FEBS Lett 269*:311-314.

Macdonald A, Harris M. 2004. Hepatitis C virus NS5A: tales of a promiscuous protein. *J Gen Virol 85*:2485-2502.

Macejak DG, Sarnow P. 1991. Internal initiation of translation mediated by the 5' leader of a cellular mRNA. *Nature 353*:90-94.

Maraia RJ. 1996. Transcription termination factor La is also an initiation factor for RNA polymerase III. *Proc Natl Acad Sci U S A 93*:3383-3387.

Maraia RJ, Kenan DJ, Keene JD. 1994. Eukaryotic transcription termination factor La mediates transcript release and facilitates reinitiation by RNA polymerase III. *Mol Cell Biol 14*:2147-2158.

Martinez-Salas E, Ramos R, Lafuente E, Lopez de Quinto S. 2001. Functional interactions in internal translation initiation directed by viral and cellular IRES elements. *J Gen Virol 82*:973-984.

Matsumoto M, Hsieh TY, Zhu N, VanArsdale T, Hwang SB, Jeng KS, Gorbalenya AE, Lo SY, Ou JH, Ware CF, Lai MM. 1997. Hepatitis C virus core protein interacts with the cytoplasmic tail of lymphotoxin-beta receptor. *J Virol 71*:1301-1309.

Matsumoto M, Hwang SB, Jeng KS, Zhu N, Lai MM. 1996. Homotypic interaction and multimerization of hepatitis C virus core protein. *Virology 218*:43-51.

McCaffrey AP, Ohashi K, Meuse L, Shen S, Lancaster AM, Lukavsky PJ, Sarnow P, Kay MA. 2002. Determinants of hepatitis C translational initiation in vitro, in cultured cells and mice. *Mol Ther 5*:676-684.

Meerovitch K, Nicholson R, Sonenberg N. 1991. In vitro mutational analysis of cis-acting RNA translational elements within the poliovirus type 2 5' untranslated region. *J Virol 65*:5895-5901.

Meerovitch K, Pelletier J, Sonenberg N. 1989. A cellular protein that binds to the 5'-noncoding region of poliovirus RNA: implications for internal translation initiation. *Genes Dev 3*:1026-1034.

Meerovitch K, Svitkin YV, Lee HS, Lejbkowicz F, Kenan DJ, Chan EK, Agol VI, Keene JD, Sonenberg N. 1993. La autoantigen enhances and corrects aberrant translation of poliovirus RNA in reticulocyte lysate. *J Virol 67*:3798-3807.

Melton DA, Krieg PA, Rebagliati MR, Maniatis T, Zinn K, Green MR. 1984. Efficient in vitro synthesis of biologically active RNA and RNA hybridization probes from plasmids containing a bacteriophage SP6 promoter. *Nucleic Acids Res 12*:7035-7056.

Méthot N, Rom E, Olsen H, Sonenberg N. 1997. The human homologue of the yeast Prt1 protein is an integral part of the eukaryotic initiation factor 3 complex and interacts with p170. *J Biol Chem 272*:1110-1116.

Méthot N, Song MS, Sonenberg N. 1996. A region rich in aspartic acid, arginine, tyrosine, and glycine (DRYG) mediates eukaryotic initiation factor 4B (eIF4B) self-association and interaction with eIF3. *Mol Cell Biol 16*:5328-5334.

Meyer F, Weber H, Weissmann C. 1981. Interactions of Q beta replicase with Q beta RNA. *J Mol Biol 153*:631-660.

Michael WM, Choi M, Dreyfuss G. 1995. A nuclear export signal in hnRNP A1: a signal-mediated, temperature-dependent nuclear protein export pathway. *Cell 83*:415-422.

Michel YM, Borman AM, Paulous S, Kean KM. 2001. Eukaryotic initiation factor 4G-poly(A) binding protein interaction is required for poly(A) tail-mediated stimulation of picornavirus internal ribosome entry segment-driven translation but not for X-mediated stimulation of hepatitis C virus translation. *Mol Cell Biol 21*:4097-4109.

Michel YM, Poncet D, Piron M, Kean KM, Borman AM. 2000. Cap-Poly(A) synergy in mammalian cell-free extracts. INVESTIGATION OF THE REQUIREMENTS FOR POLY(A)-MEDIATED STIMULATION OF TRANSLATION INITIATION. *J Biol Chem 275*:32268-32276.

Mitchell SA, Brown EC, Coldwell MJ, Jackson RJ, Willis AE. 2001. Protein factor requirements of the Apaf-1 internal ribosome entry segment: roles of polypyrimidine tract binding protein and upstream of N-ras. *Mol Cell Biol 21*:3364-3374.

Mitchell SA, Spriggs KA, Coldwell MJ, Jackson RJ, Willis AE. 2003. The Apaf-1 internal ribosome entry segment attains the correct structural conformation for function via interactions with PTB and unr. *Mol Cell 11*:757-771.

Monazahian M, Bohme I, Bonk S, Koch A, Scholz C, Grethe S, Thomssen R. 1999. Low density lipoprotein receptor as a candidate receptor for hepatitis C virus. *J Med Virol 57*:223-229.

Morita MT, Tanaka Y, Kodama TS, Kyogoku Y, Yanagi H, Yura T. 1999. Translational induction of heat shock transcription factor sigma(32): evidence for a built-in RNA thermosensor. *Genes Dev 13*:655-665.

Moriya K, Fujie H, Shintani Y, Yotsuyanagi H, Tsutsumi T, Ishibashi K, Matsuura Y, Kimura S, Miyamura T, Koike K. 1998. The core protein of hepatitis C virus induces hepatocellular carcinoma in transgenic mice. *Nat Med 4*:1065-1067.

Morris-Desbois C, Rety S, Ferro M, Garin J, Jalinot P. 2001. The human protein HSPC021 interacts with Int-6 and is associated with eukaryotic translation initiation factor 3. *J Biol Chem 276*:45988-45995.

Mosley JW, Redeker AG, Feinstone SM, Purcell RH. 1977. Mutliple hepatitis viruses in multiple attacks of acute viral hepatitis. *N Engl J Med 296*:75-78.

Murakami K, Abe M, Kageyama T, Kamoshita N, Nomoto A. 2001. Down-regulation of translation driven by hepatitis C virus internal ribosomal entry site by the 3' untranslated region of RNA. *Arch Virol 146*:729-741.

Myers TM, Kolupaeva VG, Mendez E, Baginski SG, Frolov I, Hellen CU, Rice CM. 2001. Efficient translation initiation is required for replication of bovine viral diarrhea virus subgenomic replicons. *J Virol 75*:4226-4238.

Nagai K, Oubridge C, Ito N, Avis J, Evans P. 1995a. The RNP domain: A sequence-specific RNA-binding domain involved in processing and transport of RNA. *Trends Biochem Sci 20*:235-240.

Nagai K, Oubridge C, Ito N, Jessen TH, Avis J, Evans P. 1995b. Crystal structure of the U1A spliceosomal protein complexed with its cognate RNA hairpin. *Nucleic Acids Symp Ser*:1-2.

Neddermann P, Clementi A, De Francesco R. 1999. Hyperphosphorylation of the hepatitis C virus NS5A protein requires an active NS3 protease, NS4A, NS4B, and NS5A encoded on the same polyprotein. *J Virol 73*:9984-9991.

Neumann AU, Lam NP, Dahari H, Gretch DR, Wiley TE, Layden TJ, Perelson AS. 1998. Hepatitis C viral dynamics in vivo and the antiviral efficacy of interferon-alpha therapy. *Science 282*:103-107.

Nicolaiew N, Triqueneaux G, Dautry F. 1991. Organization of the human N-ras locus: characterization of a gene located immediately upstream of N-ras. *Oncogene 6*:721-730.

Niepmann M. 1996. Porcine polypyrimidine tract-binding protein stimulates translation initiation at the internal ribosome entry site of foot-and-mouth-disease virus. *FEBS Lett 388*:39-42.

Niepmann M. 1999. Internal initiation of translation of picornaviruses, hepatitis C virus and pestiviruses. *Recent Res Devel Virol 1*:229-250.

Niepmann M, Petersen A, Meyer K, Beck E. 1997. Functional involvement of polypyrimidine tract-binding protein in translation initiation complexes with the internal ribosome entry site of foot-and-mouth disease virus. *J Virol 71*:8330-8339.

Novak JE, Kirkegaard K. 1994. Coupling between genome translation and replication in an RNA virus. *Genes Dev 8*:1726-1737.

Ochs K, Rust RC, Niepmann M. 1999. Translation initiation factor eIF4B interacts with a picornavirus internal ribosome entry site in both 48S and 80S initiation complexes independently of initiator AUG location. *J Virol 73*:7505-7514.

Ochs K, Saleh L, Bassili G, Sonntag VH, Zeller A, Niepmann M. 2002. Interaction of translation initiation factor eIF4B with the poliovirus internal ribosome entry site. *J Virol 76*:2113-2122.

Ochs K, Zeller A, Saleh L, Bassili G, Song Y, Sonntag A, Niepmann M. 2003. Impaired binding of standard initiation factors mediates poliovirus translation attenuation. *J Virol 77*:115-122.

Odreman-Macchioli FE, Tisminetzky SG, Zotti M, Baralle FE, Buratti E. 2000. Influence of correct secondary and tertiary RNA folding on the binding of cellular factors to the HCV IRES. *Nucleic Acids Res 28*:875-885.

Oh JW, Ito T, Lai MM. 1999. A recombinant hepatitis C virus RNA-dependent RNA polymerase capable of copying the full-length viral RNA. *J Virol 73*:7694-7702.

Oh JW, Sheu GT, Lai MM. 2000. Template requirement and initiation site selection by hepatitis C virus polymerase on a minimal viral RNA template. *J Biol Chem 275*:17710-17717.

Okamoto H, Okada S, Sugiyama Y, Kurai K, Iizuka H, Machida A, Miyakawa Y, Mayumi M. 1991. Nucleotide sequence of the genomic RNA of hepatitis C virus isolated from a human carrier: comparison with reported isolates for conserved and divergent regions. *J Gen Virol 72 (Pt 11)*:2697-2704.

Ostareck DH, Ostareck Lederer A, Wilm M, Thiele BJ, Mann M, Hentze MW. 1997. mRNA silencing in erythroid differentiation: hnRNP K and hnRNP E1 regulate 15-lipoxygenase translation from the 3' end. *Cell 89*:597-606.

Otto GA, Lukavsky PJ, Lancaster AM, Sarnow P, Puglisi JD. 2002. Ribosomal proteins mediate the hepatitis C virus IRES-HeLa 40S interaction. *RNA 8*:913-923.

Palmer TD, Miller AD, Reeder RH, McStay B. 1993. Efficient expression of a protein coding gene under the control of an RNA polymerase I promoter. *Nucleic Acids Res 21*:3451-3457.

Parsley TB, Towner JS, Blyn LB, Ehrenfeld E, Semler BL. 1997. Poly (rC) binding protein 2 forms a ternary complex with the 5'-terminal sequences of poliovirus RNA and the viral 3CD proteinase. *RNA 3*:1124-1134.

Patton JG, Mayer SA, Tempst P, Nadal Ginard B. 1991. Characterization and molecular cloning of polypyrimidine tract-binding protein: a component of a complex necessary for pre-mRNA splicing. *Genes Dev 5*:1237-1251.

Pavlovic D, Neville DC, Argaud O, Blumberg B, Dwek RA, Fischer WB, Zitzmann N. 2003. The hepatitis C virus p7 protein forms an ion channel that is inhibited by long-alkyl-chain iminosugar derivatives. *Proc Natl Acad Sci U S A 100*:6104-6108.

Pelletier J, Sonenberg N. 1988d. Internal initiation of translation of eukaryotic mRNA directed by a sequence derived from poliovirus RNA. *Nature 334*:320-325.

Penin F, Dubuisson J, Rey FA, Moradpour D, Pawlotsky JM. 2004. Structural biology of hepatitis C virus. *Hepatology 39*:5-19.

Pestova TV, Hellen CU. 1999. Internal initiation of translation of bovine viral diarrhea virus RNA. *Virology 258*:249-256.

Pestova TV, Hellen CU, Shatsky IN. 1996. Canonical eukaryotic initiation factors determine initiation of translation by internal ribosomal entry. *Mol Cell Biol 16*:6859-6869.

Pestova TV, Lomakin IB, Lee JH, Choi SK, Dever TE, Hellen CU. 2000. The joining of ribosomal subunits in eukaryotes requires eIF5B. *Nature 403*:332-335.

Pestova TV, Shatsky IN, Fletcher SP, Jackson RJ, Hellen CU. 1998b. A prokaryotic-like mode of cytoplasmic eukaryotic ribosome binding to the initiation codon during internal translation initiation of hepatitis C and classical swine fever virus RNAs. *Genes Dev 12*:67-83.

Petrik J, Parker H, Alexander GJ. 1999. Human hepatic glyceraldehyde-3-phosphate dehydrogenase binds to the poly(U) tract of the 3' non-coding region of hepatitis C virus genomic RNA. *J Gen Virol 80*:3109-3113.

Phan L, Zhang X, Asano K, Anderson J, Vornlocher HP, Greenberg JR, Qin J, Hinnebusch AG. 1998. Identification of a translation initiation factor 3 (eIF3) core complex, conserved in yeast and mammals, that interacts with eIF5. *Mol Cell Biol 18*:4935-4946.

Pileri P, Uematsu Y, Campagnoli S, Galli G, Falugi F, Petracca R, Weiner AJ, Houghton M, Rosa D, Grandi G, Abrignani S. 1998. Binding of hepatitis C virus to CD81. *Science 282*:938-941.

Pilipenko EV, Gmyl AP, Maslova SV, Svitkin YV, Sinyakov AN, Agol VI. 1992. Prokaryotic-like cis elements in the cap-independent internal initiation of translation on picornavirus RNA. *Cell 68*:119-131.

Pinol Roma S, Swanson MS, Gall JG, Dreyfuss G. 1989. A novel heterogeneous nuclear RNP protein with a unique distribution on nascent transcripts. *J Cell Biol 109*:2575-2587.

Pletnev AG, Yamshchikov VF, Blinov VM. 1990. Nucleotide sequence of the genome and complete amino acid sequence of the polyprotein of tick-borne encephalitis virus. *Virology 174*:250-263.

Poole TL, Wang C, Popp RA, Potgieter LN, Siddiqui A, Collett MS. 1995. Pestivirus translation initiation occurs by internal ribosome entry. *Virology 206*:750-754.

Preiss T, Hentze MW. 1998. Dual function of the messenger RNA cap structure in poly(A)-tail-promoted translation in yeast. *Nature 392*:516-520.

Purcell RH, Walsh JH, Holland PV, Morrow AG, Wood S, Chanock RM. 1971. Seroepidemiological studies of transfusion-associated hepatitis. *J Infect Dis 123*:406-413.

Ramratnam B, Bonhoeffer S, Binley J, Hurley A, Zhang L, Mittler JE, Markowitz M, Moore JP, Perelson AS, Ho DD. 1999. Rapid production and clearance of HIV-1 and hepatitis C virus assessed by large volume plasma apheresis. *Lancet 354*:1782-1785.

Realdi G, Alberti A, Rugge M, Rigoli AM, Tremolada F, Schivazappa L, Ruol A. 1982. Long-term follow-up of acute and chronic non-A, non-B post-transfusion hepatitis: evidence of progression to liver cirrhosis. *Gut 23*:270-275.

Reed KE, Rice CM. 1999. Identification of the major phosphorylation site of the hepatitis C virus H strain NS5A protein as serine 2321. *J Biol Chem 274*:28011-28018.

Reed KE, Xu J, Rice CM. 1997. Phosphorylation of the hepatitis C virus NS5A protein in vitro and in vivo: properties of the NS5A-associated kinase. *J Virol 71*:7187-7197.

Reynolds JE, Kaminski A, Carroll AR, Clarke BE, Rowlands DJ, Jackson RJ. 1996. Internal initiation of translation of hepatitis C virus RNA: the ribosome entry site is at the authentic initiation codon. *RNA 2*:867-878.

Reynolds JE, Kaminski A, Kettinen HJ, Grace K, Clarke BE, Carroll AR, Rowlands DJ, Jackson RJ. 1995. Unique features of internal initiation of hepatitis C virus RNA translation. *EMBO J 14*:6010-6020.

Rice CM, Aebersold R, Teplow DB, Pata J, Bell JR, Vorndam AV, Trent DW, Brandriss MW, Schlesinger JJ, Strauss JH. 1986. Partial N-terminal amino acid sequences of three nonstructural proteins of two flaviviruses. *Virology 151*:1-9.

Rijnbrand R, Abell G, Lemon SM. 2000a. Mutational analysis of the GB virus B internal ribosome entry site. *J Virol 74*:773-783.

Rijnbrand R, Bredenbeek PJ, Haasnoot PC, Kieft JS, Spaan WJ, Lemon SM. 2001. The influence of downstream protein-coding sequence on internal ribosome entry on hepatitis C virus and other flavivirus RNAs. *RNA 7*:585-597.

Rijnbrand R, Bredenbeek P, van der Straaten T, Whetter L, Inchauspe G, Lemon S, Spaan W. 1995. Almost the entire 5' non-translated region of hepatitis C virus is required for cap-independent translation. *FEBS Lett 365*:115-119.

Rijnbrand R, van der Straaten T, van Rijn PA, Spaan WJ, Bredenbeek PJ. 1997. Internal entry of ribosomes is directed by the 5' noncoding region of classical swine fever virus and is dependent on the presence of an RNA pseudoknot upstream of the initiation codon. *J Virol 71*:451-457.

Rijnbrand RC, Abbink TE, Haasnoot PC, Spaan WJ, Bredenbeek PJ. 1996. The influence of AUG codons in the hepatitis C virus 5' nontranslated region on translation and mapping of the translation initiation window. *Virology 226*:47-56.

Rogers GW, Richter NJ, Merrick WC. 1999. Biochemical and kinetic characterization of the RNA helicase activity of eukaryotic initiation factor 4A. *J Biol Chem 274*:12236-12244.

Rohll JB, Percy N, Ley R, Evans DJ, Almond JW, Barclay WS. 1994. The 5'-untranslated regions of picornavirus RNAs contain independent functional domains essential for RNA replication and translation. *J Virol 68*:4384-4391.

Rozen F, Edery I, Meerovitch K, Dever TE, Merrick WC, Sonenberg N. 1990. Bidirectional RNA helicase activity of eucaryotic translation initiation factors 4A and 4F. *Mol Cell Biol 10*:1134-1144.

Sachs A. 2000. Physical and functional interactions between mRNA cap structure and the poly(A) tail. In: Sonenberg N, Hershey, J.W.B., and Mathews, M.B., ed. *Translational control of gene expression*. Cold Spring Harbor, NY: Cold Spring Harbor Laboratory Press. pp 447-465.

Sachs AB, Sarnow P, Hentze MW. 1997. Starting at the beginning, middle, and end: translation initiation in eukaryotes. *Cell 89*:831-838.

Safer B, Adams SL, Kemper WM, Berry KW, Lloyd M, Merrick WC. 1976. Purification and characterization of two initiation factors required for maximal activity of a highly fractionated globin mRNA translation system. *Proc Natl Acad Sci USA 73*:2584-2588.

Sakamuro D, Furukawa T, Takegami T. 1995. Hepatitis C virus nonstructural protein NS3 transforms NIH 3T3 cells. *J Virol 69*:3893-3896.

Saleh L, Rust RC, Füllkrug R, Beck E, Bassili G, Ochs K, Niepmann M. 2001. Functional interaction of translation initiation factor eIF4G with the foot-and-mouth-disease virus internal ribosome entry site. *J Gen Virol 82*:757-763.

Sambrook J, Fritsch EF, Maniatis T. 1989. *Molecular cloning. A laboratory manual.* Cold Spring Harbor, NY: Cold Spring Harbor Laboratory Press.

Sasaki J, Nakashima N. 1999. Translation initiation at the CUU codon is mediated by the internal ribosome entry site of an insect picorna-like virus in vitro. *Journal Of Virology Feb 73*:1219-1226.

Sato K, Okamoto H, Aihara S, Hoshi Y, Tanaka T, Mishiro S. 1993. Demonstration of sugar moiety on the surface of hepatitis C virions recovered from the circulation of infected humans. *Virology 196*:354-357.

Schuster C, Isel C, Imbert I, Ehresmann C, Marquet R, Kieny MP. 2002. Secondary structure of the 3' terminus of hepatitis C virus minus-strand RNA. *J Virol 76*:8058-8068.

Selby MJ, Choo QL, Berger K, Kuo G, Glazer E, Eckart M, Lee C, Chien D, Kuo C, Houghton M. 1993. Expression, identification and subcellular localization of the proteins encoded by the hepatitis C viral genome. *J Gen Virol 74 (Pt 6)*:1103-1113.

Shimoike T, Mimori S, Tani H, Matsuura Y, Miyamura T. 1999. Interaction of hepatitis C virus core protein with viral sense RNA and suppression of its translation. *J Virol 73*:9718-9725.

Shine J, Dalgarno L. 1974. The 3'-terminal sequence of Escherichia coli 16S ribosomal RNA: complementarity to nonsense triplets and ribosome binding sites. *Proc Natl Acad Sci U S A 71*:1342-1346.

Simmonds P. 1995. Variability of hepatitis C virus. *Hepatology 21*:570-583.

Simmonds P, Holmes EC, Cha TA, Chan SW, McOmish F, Irvine B, Beall E, Yap PL, Kolberg J, Urdea MS. 1993b. Classification of hepatitis C virus into six major genotypes and a series of subtypes by phylogenetic analysis of the NS-5 region. *J Gen Virol 74 (Pt 11)*:2391-2399.

Simpson PJ, Monie TP, Szendroi A, Davydova N, Tyzack JK, Conte MR, Read CM, Cary PD, Svergun DI, Konarev PV, Curry S, Matthews S. 2004. Structure and RNA interactions of the N-terminal RRM domains of PTB. *Structure (Camb) 12*:1631-1643.

Sizova DV, Kolupaeva VG, Pestova TV, Shatsky IN, Hellen CU. 1998. Specific interaction of eukaryotic translation initiation factor 3 with the 5' nontranslated regions of hepatitis C virus and classical swine fever virus RNAs. *J Virol 72*:4775-4782.

Smith DB, Mellor J, Jarvis LM. 1995. Variation of the hepatitis C virus 5′ non-coding region: implications for secondary structure, virus detection and typing. *J Gen Virol 76*:1749-1761.

Smith KC. 1976. The radiation-induced addition of proteins and other molecules to nucleic acids. In: Wang SY, ed. *Photochemistry and photobiology of nucleic acids*. New York, San Francisco, London: Academic Press. pp 187-218.

Song Y, Tzima E, Ochs K, Bassili G, Trusheim H, Linder M, Preissner KT, Niepmann M. 2005. Evidence for an RNA chaperone function of polypyrimidine tract-binding protein in picornavirus translation. *RNA 11*:1809-1824.

Spahn CM, Kieft JS, Grassucci RA, Penczek PA, Zhou K, Doudna JA, Frank J. 2001. Hepatitis C virus IRES RNA-induced changes in the conformation of the 40s ribosomal subunit. *Science 291*:1959-1962.

Spangberg K, Goobar-Larsson L, Wahren-Herlenius M, Schwartz S. 1999a. The La protein from human liver cells interacts specifically with the U-rich region in the hepatitis C virus 3' untranslated region. *J Hum Virol 2*:296-307.

Spangberg K, Schwartz S. 1999b. Poly(C)-binding protein interacts with the hepatitis C virus 5' untranslated region. *J Gen Virol 80*:1371-1376.

Srivastava S, Verschoor A, Frank J. 1992. Eukaryotic initiation factor 3 does not prevent association through physical blockage of the ribosomal subunit-subunit interface. *J Mol Biol 226*:301-304.

Stoneley M, Chappell SA, Jopling CL, Dickens M, MacFarlane M, Willis AE. 2000. c-Myc protein synthesis is initiated from the internal ribosome entry segment during apoptosis. *Mol Cell Biol 20*:1162-1169.

Stoneley M, Paulin FE, Le Quesne JP, Chappell SA, Willis AE. 1998. C-Myc 5' untranslated region contains an internal ribosome entry segment. *Oncogene 16*:423-428.

Sugawara Y, Makuuchi M, Kato N, Shimotohno K, Takada K. 1999. Enhancement of hepatitis C virus replication by Epstein-Barr virus-encoded nuclear antigen 1. *EMBO J 18*:5755-5760.

Sundkvist IC, Staehelin T. 1975. Structure and function of free 40 S ribosome subunits: Characterization of initiation factors. *J Mol Biol 99*:401-418.

Suzich JA, Tamura JK, Palmer-Hill F, Warrener P, Grakoui A, Rice CM, Feinstone SM, Collett MS. 1993. Hepatitis C virus NS3 protein polynucleotide-stimulated nucleoside triphosphatase and comparison with the related pestivirus and flavivirus enzymes. *J Virol 67*:6152-6158.

Svitkin YV, Pause A, Sonenberg N. 1994. La autoantigen alleviates translational repression by the 5' leader sequence of the human immunodeficiency virus type 1 mRNA. *J Virol 68*:7001-7007.

Tabor E, Gerety RJ, Drucker JA, Seeff LB, Hoofnagle JH, Jackson DR, April M, Barker LF, Pineda-Tamondong G. 1978. Transmission of non-A, non-B hepatitis from man to chimpanzee. *Lancet 1*:463-466.

Tai CL, Chi WK, Chen DS, Hwang LH. 1996. The helicase activity associated with hepatitis C virus nonstructural protein 3 (NS3). *J Virol 70*:8477-8484.

Takamizawa A, Mori C, Fuke I. 1991. Structure and organization of the hepatitis C virus genome isolated from human carriers. *J Virol 65*:1105-1113.

Tanaka T, Kato N, Cho MJ, Shimotohno K. 1995. A novel sequence found at the 3' terminus of hepatitis C virus genome. *Biochem Biophys Res Commun 215*:744-749.

Tanaka T, Kato N, Cho MJ, Sugiyama K, Shimotohno K. 1996. Structure of the 3' terminus of the hepatitis C virus genome. *J Virol 70*:3307-3312.

Tanaka T, Kato N, Nakagawa M, Ootsuyama Y, Cho MJ, Nakazawa T, Hijikata M, Ishimura Y, Shimotohno K. 1992. Molecular cloning of hepatitis C virus genome from a single Japanese carrier: sequence variation within the same individual and among infected individuals. *Virus Res 23*:39-53.

Tanji Y, Hijikata M, Satoh S, Kaneko T, Shimotohno K. 1995a. Hepatitis C virus-encoded nonstructural protein NS4A has versatile functions in viral protein processing. *J Virol 69*:1575-1581.

Tarun SZ, Jr., Sachs AB. 1996. Association of the yeast poly(A) tail binding protein with translation initiation factor eIF-4G. *EMBO J 15*:7168-7177.

Taylor DR, Shi ST, Romano PR, Barber GN, Lai MM. 1999. Inhibition of the interferon-inducible protein kinase PKR by HCV E2 protein [see comments]. *Science 285*:107-110.

Teerink H, Voorma HO, Thomas AA. 1995. The human insulin-like growth factor II leader 1 contains an internal ribosomal entry site. *Biochim Biophys Acta 27*:403-408.

Tellinghuisen TL, Rice CM. 2002. Interaction between hepatitis C virus proteins and host cell factors. *Curr Opin Microbiol 5*:419-427.

Thurner C, Witwer C, Hofacker IL, Stadler PF. 2004. Conserved RNA secondary structures in Flaviviridae genomes. *J Gen Virol 85*:1113-1124.

Tischendorf JJW. 2004. Polypyrimidine tract-binding protein (PTB) inhibits Hepatitis C virus internal ribosome entry site (HCV IRES)-mediated translation, but does not affect HCV replication. *Arch Virol 149*:1955-1970.

Tomei L, Failla C, Santolini E, De Francesco R, La Monica N. 1993. NS3 is a serine protease required for processing of hepatitis C virus polyprotein. *J Virol 67*:4017-4026.

Tsuchihara K, Tanaka T, Hijikata M, Kuge S, Toyoda H, Nomoto A, Yamamoto N, Shimotohno K. 1997. Specific interaction of polypyrimidine tract-binding protein with the extreme 3'-terminal structure of the hepatitis C virus genome, the 3'X. *J Virol 71*:6720-6726.

Tsukiyama-Kohara K, Iizuka N, Kohara M, Nomoto A. 1992. Internal ribosome entry site within hepatitis C virus RNA. *J Virol 66*:1476-1483.

Vagner S, Gensac MC, Maret A, Bayard F, Amalric F, Prats H, Prats AC. 1995. Alternative translation of human fibroblast growth factor 2 mRNA occurs by internal entry of ribosomes. *Mol Cell Biol 15*:35-44.

Valcárcel J, Gebauer F. 1997. Post-transcriptional regulation: the dawn of PTB. *Curr Biol 7*:705-708.

Varaklioti A, Vassilaki N, Georgopoulou U, Mavromara P. 2002. Alternate translation occurs within the core coding region of the hepatitis C viral genome. *J Biol Chem 277*:17713-17721.

Vornlocher HP, Hanachi P, Ribeiro S, Hershey JW. 1999. A 110-kilodalton subunit of translation initiation factor eIF3 and an associated 135-kilodalton protein are encoded by the Saccharomyces cerevisiae TIF32 and TIF31 genes. *J Biol Chem 274*:16802-16812.

Wakita T, Wands JR. 1994. Specific inhibition of hepatitis C virus expression by antisense oligodeoxynucleotides. In vitro model for selection of target sequence. *J Biol Chem 269*:14205-14210.

Walewski JL, Keller TR, Stump DD, Branch AD. 2001. Evidence for a new hepatitis C virus antigen encoded in an overlapping reading frame. *RNA 7*:710-721.

Walsh JH, Purcell RH, Morrow AG, Chanock RM, Schmidt PJ. 1970. Posttransfusion hepatitis after open-heart operations. Incidence after the administration of blood from commercial and volunteer donor populations. *JAMA 211*:261-265.

Walter BL, Nguyen JH, Ehrenfeld E, Semler BL. 1999. Differential utilization of poly(rC) binding protein 2 in translation directed by picornavirus IRES elements. *RNA 5*:1570-1585.

Wang C, Le SY, Ali N, Siddiqui A. 1995a. An RNA pseudoknot is an essential structural element of the internal ribosome entry site located within the hepatitis C virus 5' noncoding region. *RNA 1*:526-537.

Wang C, Sarnow P, Siddiqui A. 1993. Translation of human hepatitis C virus RNA in cultured cells is mediated by an internal ribosome-binding mechanism. *J Virol 67*:3338-3344.

Wang C, Sarnow P, Siddiqui A. 1994. A conserved helical element is essential for internal initiation of translation of hepatitis C virus RNA. *J Virol 68*:7301-7307.

Wang C, Siddiqui A. 1995b. Structure and function of the hepatitis C virus internal ribosome entry site. *Curr Top Microbiol Immunol 203*:99-115.

Weber H, Billeter MA, Kahane S, Weissmann C, Hindley J, Porter A. 1972. Molecular basis for repressor activity of Q replicase. *Nat New Biol 237*:166-170.

Wilson JE, Powell MJ, Hoover SE, Sarnow P. 2000b. Naturally occurring dicistronic cricket paralysis virus RNA is regulated by two internal ribosome entry sites. *Mol Cell Biol 20*:4990-4999.

Wimmer E, Nomoto A. 1993. Molecular biology and cell-free synthesis of poliovirus. *Biologicals 21*:349-356.

Witherell GW, Gil A, Wimmer E. 1993. Interaction of polypyrimidine tract binding protein with the encephalomyocarditis virus mRNA internal ribosomal entry site. *Biochemistry 32*:8268-8275.

Witherell GW, Wimmer E. 1994. Encephalomyocarditis virus internal ribosomal entry site RNA-protein interactions. *J Virol 68*:3183-3192.

Wölk B, Sansonno D, Krausslich HG, Dammacco F, Rice CM, Blum HE, Moradpour D. 2000. Subcellular localization, stability, and trans-cleavage competence of the hepatitis C virus NS3-NS4A complex expressed in tetracycline- regulated cell lines. *J Virol 74*:2293-2304.

Wood J, Frederickson RM, Fields S, Patel AH. 2001. Hepatitis C virus 3'X region interacts with human ribosomal proteins. *J Virol 75*:1348-1358.

Xu Z, Choi J, Yen TS, Lu W, Strohecker A, Govindarajan S, Chien D, Selby MJ, Ou J. 2001. Synthesis of a novel hepatitis C virus protein by ribosomal frameshift. *EMBO J 20*:3840-3848.

Yamada N, Tanihara K, Takada A, Yorihuzi T, Tsutsumi M, Shimomura H, Tsuji T, Date T. 1996. Genetic organization and diversity of the 3' noncoding region of the hepatitis C virus genome. *Virology 223*:255-261.

Yamashita T, Kaneko S, Shirota Y, Qin W, Nomura T, Kobayashi K, Murakami S. 1998. RNA-dependent RNA polymerase activity of the soluble recombinant hepatitis C virus NS5B protein truncated at the C-terminal region. *J Biol Chem 273*:15479-15486.

Yanagi M, Claire MS, Emerson SU, Prurcell RH, Bukh J. 1999. In vivo analysis of the 3´ untranslated region of the hepatitis C virus after in vitro mutagenasis of an infectious cDNA clone. *Proc Natl Acad Sci U S A 96*:2291-2295.

Yasui K, Okanoue T, Murakami Y, Itoh Y, Minami M, Sakamoto S, Sakamoto M, Nishioji K. 1998. Dynamics of hepatitis C viremia following interferon-alpha administration. *J Infect Dis 177*:1475-1479.

Yi M, Lemon SM. 2003a. 3' nontranslated RNA signals required for replication of hepatitis C virus RNA. *J Virol 77*:3557-3568.

Yi M, Lemon SM. 2003b. Structure-function analysis of the 3' stem-loop of hepatitis C virus genomic RNA and its role in viral RNA replication. *RNA 9*:331-345.

You S, Stump DD, Branch AD, Rice CM. 2004. A cis-acting replication element in the sequence encoding the NS5B RNA-dependent RNA polymerase is required for hepatitis C virus RNA replication. *J Virol 78*:1352-1366.

Yu H, Grassmann CW, Behrens SE. 1999. Sequence and structural elements at the 3´ terminus of bovine viral diarrhea virus genomic RNA: functional role during RNA replication. *J Virol 73*:3638-3648.

Yuan X, Davydova N, Conte MR, Curry S, Matthews S. 2002. Chemical shift mapping of RNA interactions with the polypyrimidine tract binding protein. *Nucleic Acids Res 30*:456-462.

Yuan ZH, Kumar U, Thomas HC, Wen YM, Monjardino J. 1997. Expression, purification, and partial characterization of HCV RNA polymerase. *Biochem Biophys Res Commun 232*:231-235.

Zeuzem S, Schmidt JM, Lee JH, von Wagner M, Teuber G, Roth WK. 1998. Hepatitis C virus dynamics in vivo: effect of ribavirin and interferon alfa on viral turnover. *Hepatology 28*:245-252.

Zhang J, Yamada O, Yoshida H, Iwai T, Araki H. 2002. Autogenous translational inhibition of core protein: implication for switch from translation to RNA replication in hepatitis C virus. *Virology 293*:141-150.

Zhong W, Uss AS, Ferrari E, Lau JY, Hong Z. 2000a. De novo initiation of RNA synthesis by hepatitis C virus nonstructural protein 5B polymerase. *J Virol 74*:2017-2022.

Zhu Q, Guo JT, Seeger C. 2003. Replication of hepatitis C virus subgenomes in nonhepatic epithelial and mouse hepatoma cells. *J Virol 77*:9204-9210.

Appendices

pHCV wt clone map

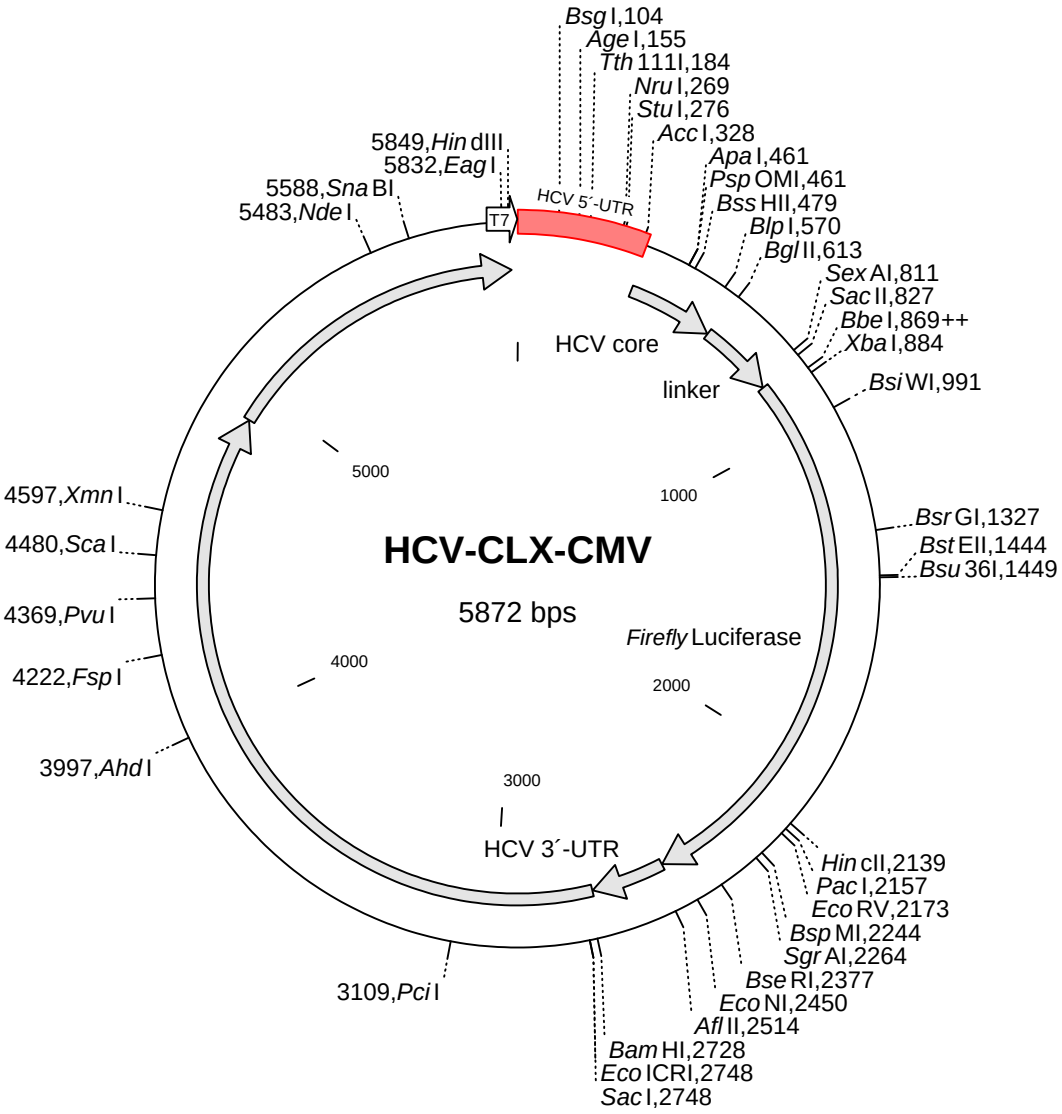

Molecule Features:

Type	Start	End	Name	Description
REGION	1	341	HCV 5´-UTR	341 bps
GENE	342	344	Initiator	3 bps
GENE	345	606	HCV core	262 bps
GENE	607	836	linker	230 bp (608-823: ubiquitin, 216 bps)
GENE	837	2489	*Firefly* Luciferase	1653 bps
GENE	2490	2710	HCV 3´-UTR	221 bps
GENE	2711	4917	pBSII 698#	2207 bps
GENE	4918	5855	p352	938 bps (5249-5829 is CMV-IE promoter, 581 bps)

Interaction of FSAP with HCV RNA

Biochem. J. (2005) **385**, 831–838 (Printed in Great Britain) **831**

Extracellular RNA is a natural cofactor for the (auto-)activation of Factor VII-activating protease (FSAP)

Fumie NAKAZAWA*[1], Christian KANNEMEIER†[1,2], Aya SHIBAMIYA‡, Yutong SONG‡, Eleni TZIMA‡, Uwe SCHUBERT‡, Takatoshi KOYAMA*, Michael NIEPMANN‡, Heidi TRUSHEIM‡, Bernd ENGELMANN§ and Klaus T. PREISSNER‡[3]

*Graduate School of Allied Health Sciences, Tokyo Medical and Dental University, Bunkyo-ku, Tokyo 113-8519, Japan, †Research Laboratories, Aventis Behring GmbH, D-35002 Marburg, Germany, ‡Institute for Biochemistry, Medical Faculty, Justus-Liebig-Universität, D-35392 Giessen, Germany, and §Institute of Clinical Chemistry, Ludwig-Maximilians-Universität, D-81377 München, Germany

FSAP (Factor VII-activating protease) is a new plasma-derived serine protease with putative dual functions in haemostasis, including activation of coagulation Factor VII and generation of urinary-type plasminogen activator (urokinase). The (auto-)activation of FSAP is facilitated by polyanionic glycosaminoglycans, such as heparin or dextran sulphate, whereas calcium ions stabilize the active form of FSAP. In the present study, extracellular RNA was identified and characterized as a novel FSAP cofactor. The conditioned medium derived from various cell types such as smooth muscle cells, endothelial cells, osteosarcoma cells or CHO (Chinese-hamster ovary) cells contained an acidic factor that initiated (auto-)activation of FSAP. RNase A, but not other hydrolytic enzymes (proteases, glycanases and DNase), abolished the FSAP cofactor activity, which was subsequently isolated by anion-exchange chromatography and unequivocally identified as RNA. In purified systems, as well as in plasma, different forms of natural RNA (rRNA, tRNA, viral RNA and artificial RNA) were able to (auto-)activate FSAP into the two-chain enzyme form. The specific binding of FSAP to RNA (but not to DNA) was shown by mobility-shift assays and UV crosslinking, thereby identifying FSAP as a new extracellular RNA-binding protein, the K_D estimated to be 170–350 nM. Activation of FSAP occurred through an RNA-dependent template mechanism involving a nucleic acid size of at least 100 nt. In a purified system, natural RNA augmented the FSAP-dependent Factor VII activation several-fold (as shown by subsequent Factor Xa generation), as well as the FSAP-mediated generation of urokinase. Our results provide evidence for the first time that extracellular RNA, present at sites of cell damage or vascular injury, can serve an important as yet unrecognized cofactor function in haemostasis by inducing (auto-)activation of FSAP through a novel surface-dependent mechanism.

Key words: blood coagulation, extracellular RNA, Factor VII-activating protease (FSAP), haemostasis, plasma hyaluronan-binding protease.

RNA–protein complexes

HCV (Hepatitis C Virus) RNA (nt 1–402) was transcribed *in vitro* from plasmid pHCV-CUL, linearized with *Aat* II, in the presence of [α-^{32}P] UTP using T7 RNA polymerase. The resulting RNA contains the HCV internal ribosome entry site (nt 1–342) plus the first 60 nt of the HCV core-protein-coding sequence. For obtaining a control DNA fragment using PCR, two DNA oligonucleotides were used to generate an amplified fragment with exactly the same limits (HCV nt 1–402). This fragment was internally labelled using [α-^{32}P] dCTP. Binding and UV-cross-linking reactions, as described previously (Ochs et al., 2003), were performed in the absence or presence of 10 pmol of FSAP (unless otherwise indicated) with 0.7 pmol of RNA in binding buffer (10 mM Tris/HCl, pH 7.5, containing 100 mM NaCl, 0.3 mM $MgCl_2$, 2 % glycerol and 1 mM dithiothreitol) in a 10-μl reaction volume. Protease inhibitors (50 units/ml aprotinin, 10 mM PMSF and 0.05 mM $ZnCl_2$) were added as indicated. Reaction mixtures were incubated for 10 min at 30°C, irradiated with UV light (254 nm) for 30 min at 0°C and treated with 2 mg/ml RNase for 60 min at 37◦C. After addition of one-third volume of loading buffer (125 mM Tris/HCl, pH 6.8, containing 4 % SDS, 10 % 2-mercaptoethanol, 20 % glycerol, 0.02 % Bromophenol Blue and 7 M urea), samples were boiled and subjected to SDS/PAGE (12 % gel) followed by autoradiography. Alternatively, FSAP was UV cross-linked to [α-^{32}P] UTP-labelled HCV RNA as described above, with the difference that samples were not treated with RNase A after UV cross-linking, but incubated in the absence or presence of proteinase K. After addition of loading buffer, samples were analysed by SDS/PAGE (6 % gel) followed by autoradiography.

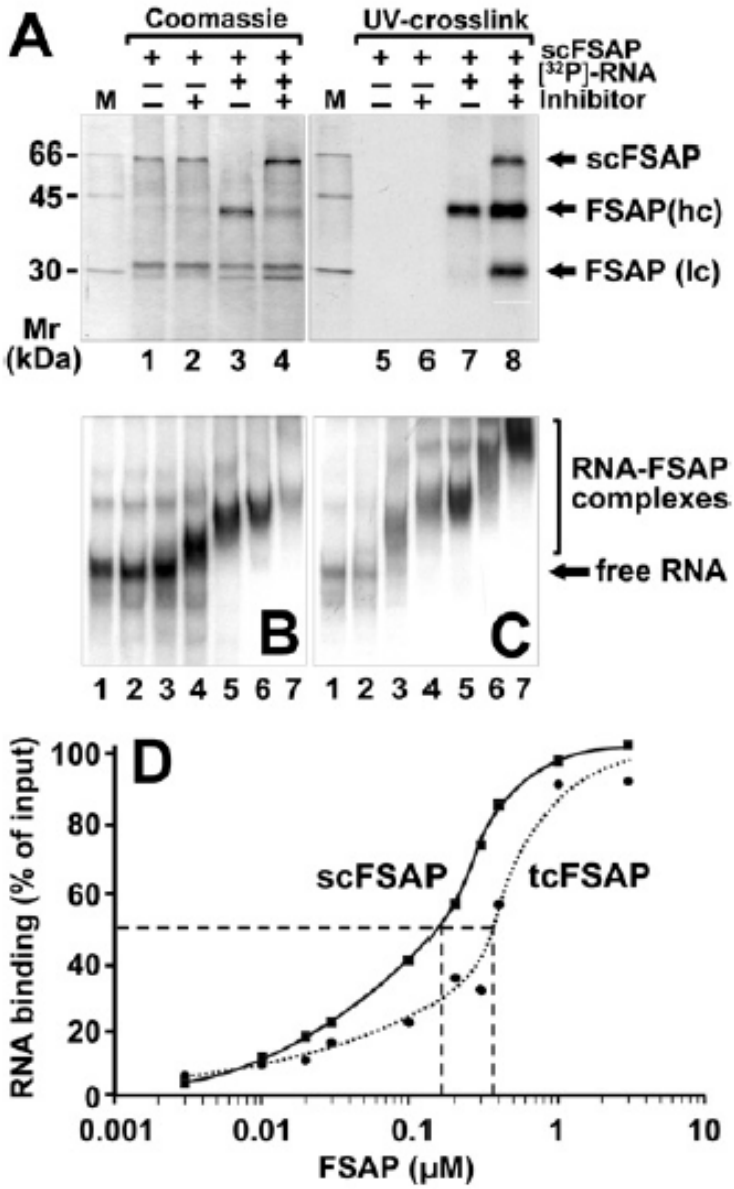

Figure 5: Binding interactions between FSAP and RNA. (**A**) Purified human single-chain FSAP (scFSAP) was incubated at 30°C for 10 min in the absence or presence of [α-^{32}P] UTP-labelled HCV RNA and in the absence or presence of protease inhibitors as indicated. Samples were irradiated with UV light (254 nm), treated with 2 mg/ml RNase A at 37°C for 60 min, denatured and separated by denaturing SDS/PAGE (12 % gel) which was stained with Coomassie Brilliant Blue (left-hand panel). For detection of protein bound to radioactive RNA, X-ray film was exposed overnight (right-hand panel). Size markers indicate positions of ^{14}C-labelled marker proteins at the left margin. Binding of RNA to two-chain FSAP (**B**) or single-chain FSAP (**C**) was analysed in an electrophoretic mobility shift assay. [α-^{32}P] UTP-labelled HCV RNA (15 nM) was incubated in the absence (lane 1) or presence of FSAP at the following concentrations: 0.03 μM (lane 2), 0.1 μM (lane 3), 0.2 μM (lane 4), 0.3 μM (lane 5), 1 μM (lane 6), 2 μM (lane 7), and RNA–two-chain FSAP (**B**) or RNA–single-chain FSAP complexes (**C**) were separated on a non-denaturing 6 % polyacrylamide gel followed by exposure of the dried gel to visualize the RNA-containing bands. (**D**) Filter-binding assay with FSAP and HCV RNA in the presence (continuous curve) or absence (broken curve) of protease inhibitor. The K_D values obtained from the binding curves at 50 % maximal binding are indicated (broken lines).

To analyse FSAP–RNA complexes by electrophoretic mobility shift assay, binding reactions contained 0.15 pmol of [α-^{32}P] UTP-labelled HCV RNA in 5 mM HEPES buffer, pH 7.4, containing 145 mM NaCl, 5 mM KCl, 1.5 mM $MgCl_2$, 3.8 % glycerol, 2 mM dithiothreitol and 0.1 mM EDTA, in a volume of 10 μl. Protease inhibitors (50 units/ml aprotinin, 10 mM PMSF and 0.05 mM $ZnCl_2$) were added as indicated. Reaction mixtures were incubated for 20 min at 30°C. After addition of 5 μl of 20 % glycerol, samples were resolved on a non-denaturing 6 % polyacrylamide gel (Konarska et al., 1986). In control experiments, a DNA fragment instead of RNA was used, which was generated by asymmetric PCR from the same sequence as the RNA transcript and labelled internally during the PCR reaction using [α-^{32}P] dCTP.

To analyse FSAP–RNA complexes by filter-binding assays, nitrocellulose filters were soaked with washing buffer (20 mM Tris/HCl, pH 7.25, 2 mM $MgCl_2$ and 1 mM dithiothreitol) and fixed into a slot-blot apparatus. The indicated FSAP concentrations were incubated on the filters in 100 μl of wash buffer for 15 min and then aspirated through the filters, followed by incubation with 3 % BSA for 20 min. Binding buffer (100 μl; 10 mM Tris/HCl, pH 7.25, 145 mM NaCl, 5 mM KCl, 1.5 mM $MgCl_2$, 3.8 % glycerol, 2 mM dithiothreitol and 0.1 mM EDTA) containing 0.15 pmol of [α-^{32}P] UTP-labelled HCV RNA was incubated with each filter well for 15 min, and 1 mM PPACK was present for binding assay of single-chain FSAP. The reaction mixtures were aspirated through the filters, followed by four wash cycles, and after drying filter pieces corresponding to the slots were excised, added to 2 ml of scintillation fluid and radioactivity measured in a scintillation counter. The values shown represent means +/- S.D. from 3–5 measurements. For estimation of the dissociation constant K_D for the reaction

FSAP + RNA_{free} ↔ FSAP–RNA equation (1) was used:

$$K_D = ([FSAP] \times [RNA_{free}])/[FSAP–RNA] \quad (1)$$

Equation (2) is fulfilled if 50 % binding of RNA to FSAP is achieved, thus obtaining K_D =[FSAP].

$$[RNA_{free}] = [FSAP–RNA] \quad (2)$$

The respective dissociation constants for single- and two-chain FSAP were derived from the sigmoidal binding curves at 50 % RNA–FSAP complex formation (see Figure 5D).

Conclusions

At plasma concentrations of FSAP of 0.2 μM (Kannemeier et al., 2001), all RNA was bound within FSAP–RNA complexes, indicating that FSAP may bind RNA at a threshold close to the FSAP plasma concentration.

More than one molecule of FSAP may bind to a single RNA template. The dissociation contant K_D of the binding of RNA to single-chain FSAP (performed in the presence of protease inhibitors to prevent activation) (Figure 5D, continuous curve) is 170 nM, whereas the K_D for the two-chain FSAP–RNA interaction is 350 nM (Figure 5D, broken curve). These values correspond well with the FSAP concentrations required for binding of RNA in the shift assays and are compatible with a template mechanism of activation as well.

Single-chain FSAP provides multiple contacts with RNA, whereas the active two-chain enzyme binds to RNA exclusively via its heavy-chain (with approx. 50 % affinity as compared with the single-chain protein), indicative of the fact that both forms of FSAP can interact with RNA in a complex that leads to (auto-)- activation of the proenzyme.

Publications

Original publications in peer-reviewed journals:

Song Y, Tzima E, Ochs K, Bassili G, Trusheim H, Linder M, Preissner KT, Niepmann M. 2005. Evidence for an RNA chaperone function of polypyrimidine tract-binding protein in picornavirus translation. *RNA 11*:1809-1824.

Nakazawa F, Kannemeier C, Shibamiya A, Song Y, Tzima E, Schubert U, Koyama T, Niepmann M, Trusheim H, Engelmann B, Preissner KT. 2005. Extracellular RNA is a natural cofactor for the (auto-) activation of Factor VII-activating protease (FSAP). *Biochem. J. 385*:831-838.

Bassili G, Tzima E, Song Y, Saleh L, Ochs K, Niepmann M. 2004. Sequence and secondary structure requirements in a highly conserved element for foot-and-mouth disease virus internal ribosome entry site activity and eIF4G binding. *J. Gen. Virol. 85*:2555-2565.

Ochs K, Zeller A, Saleh L, Bassili G, Song Y, Sonntag A, Niepmann M. 2003. Impaired binding of standard initiation factors mediates poliovirus translation attenuation. *J. Virol. 77*:115-122.

Song X and Hong H. 1992, Research progresses of *in vitro* bioassay of parasporal crystal toxin of *Bacillus thuringiensis*. *Chinese Journal of Biological Control. No.2*:

Manuscripts submitted or in preparation:

Song Y, Tzima E, Jünemann C, Niepmann M. The Hepatitis C Virus RNA 3´-Untranslated Region strongly enhances Translation directed by the Internal Ribosome Entry Site (Revised version resubmitted).

Kannermeier C, Nakazawa F, Trusheim H, Shibamiya A, Ruppert C, Markart P, Grimminger F, Song Y, Tzima E, Kennerknecht E, Niepmann M, Massberg S, Guenther A, Engelmann B, Preissner KT. Extracellular RNA is a novel procoagulant factor in the initiation of blood coagulation. 2005 (Submitted).

Tzima E, Song Y, Jünemann C, Bindereif A, Jacquemin-Salblon H, Niepmann M. Cellular proteins enhance translation directed by the internal ribosome entry site of Hepatitis C virus in the presence of the viral 3´-untranslated region (Manuscript in preparation).

Meeting Abstracts:

Song Y, Friebe P, Tzima E, Jünemann C, Niepmann M. The Hepatitis C Virus RNA 3´-Untranslated Region strongly enhances Translation directed by the Internal Ribosome Entry Site.
Yearly conference of the Society of Virology, 15-18 March 2006, München, Germany.

Tzima E, Song Y, Jünemann C, Bindereif A, Jacquemin-Salblon H, Niepmann M. Cellular proteins enhance translation directed by the internal ribosome entry site of Hepatitis C virus in the presence of the viral 3´-untranslated region.
Yearly conference of the Society of Virology, 15-18 March 2006, München, Germany.

Jünemann C, Bassili G, Song Y, Tzima E, Niepmann M. Translation enhancement: picornavirus IRES elements stimulate translation of upstream genes in dicistronic vectors.
Yearly conference of the Society of Virology, 15-18 March 2006, München, Germany.

Niepmann M, Zheng J, Tzima E, Ochs K, Song Y. The polyprimidine tract-binding protein PTB is a monomer introducing a novel system for forcusing native gel electrophoresis of basic proteins.
Yearly conference of the Society of Virology, 15-18 March 2006, München, Germany.

Song Y, Tzima E, Jünemann C, Niepmann M. The Hepatitis C Virus RNA 3´-Untranslated Region strongly enhances Translation directed by the Internal Ribosome Entry Site.
Yearly conference of the Society of Virology, 16-19 March 2005, Hannover, Germany (Oral presentation).

Niepmann M, Tzima E, Ochs K, Bassili G, Trusheim H, Linder M, Preissner KT, Song Y. Evidence for an RNA chaperone function of polypyrimidine tract-binding protein in picornavirus translation.
Program and abstracts -- Yearly conference of the Society of Virology, 17-19 March 2004, Tuebingen, Germany.

Bassili G, Song Y, Tzima E and Niepmann M. A highly conserved sequence element of the foot-and-mouth disease virus internal ribosome entry site is essential for interaction with eIF4G and for translation.
Program and abstracts -- Yearly conference of the Society of Virology, 26-29 March 2003, Berlin, Germany.

Kerstin Ochs, Zeller A, Saleh L, Bassili G, Song Y, Sonntag A and Niepmann M. Impaired binding of standard initiation factors mediates poliovirus translation attenuation.
Programand abstracts --Yearly conference of the Society of Virology, 26-29 March 2003, Berlin, Germany.

Hong H, Song X and Chen Q. An elementary study on cytotocicity of *Bacillus thuringiensis* var. *israelensis* 187 (Chinese strain) crystal to cultured mosquito cells-II.
Program and abstracts -- XIX International Congress of Entomology. Jun. 28 th-Jul. 4 th 1992, Beijing, China

Song X, Hong H and Chen Q. An elementary study on cytotocicity of *Bacillus thuringiensis* var. *israelensis* 187 (Chinese strain) crystal to cultured mosquito cells.
Program and abstracts of SIP XXIV Meeting. 1991, Arizona, USA.

Erklärung

Hiermit erkläre ich, dass ich die vorliegende Arbeit selbstständig verfasst und keine anderen Hilfsmittel als die angegeben benutzt habe. Die Stellen, die ich anderen Untersuchungen dem Wortlaut oder Sinn entsprechend entnommen habe, sind durch Quellenangaben gekennzeichnet.

Gießen, den 24. 01.2006